Inflammasome regulation and activation in the intestinal epithelium



Andrea Lei

St. Peter's College, University of Oxford

A thesis submitted for the degree of Doctor of Philosophy, Trinity Term 2017

Acknowledgments

This thesis would have not been possible without the continuous support and encouragement from my family, especially my parents and brother. They have been my inspiration throughout these years and the reason why all the hard work is completely worth it. A very special thank you to Gytis for being my rock in Oxford and giving me unquantifiable support and happiness. Also thank you to my buddy Sonia, for always being there no matter what and providing some "next level" encouragement and energy.

Another special thank you to Dr. Kevin Maloy. I am grateful for the opportunity he has given me to work in his lab, as well as his encouragements and support.

I would like to thank the very special people I met during my life at Oxford. Firstly, the great Maloy Lab, which has been full of wonderful people throughout the years. I would like to give a special thank you to:

- Alison Murphy, the FACS and T-cell Master, for her help, support (including proof-reading this entire thesis) and advice throughout the whole journey of this thesis. In fact, we not only shared a bench and a project but also underwent serious Irish-Spanish cultural crossover, including expressions of triumph and tragedy. Oh! And not to forget our really empty swear jar, go us!
- Johanna Pott for her continuous advice, support, encouragement, brain-storming, laughter…and for introducing me to the organoid magic.
- Belen and her family for providing a great environment for everyone and being the source of happiness in the lab, whenever and wherever needed.
- Luara and her "sporozoitos" for providing great advice and help when I most needed it early in my PhD, as well as a great amount of memorable moments and laughter.
- Theo, Aga, Cristina, Cornelia, Sandra, Sarah, Sandrine, Paola, George, Sofia and Gökçen for making the lab a much better place to work and becoming great friends.

A hugely special thank you to my lovely housemates Julia, Sam, Harald and Andra. Thanks for the yummy meals and late-night teas, or stronger beverages when required. They were so necessary to survive the PhD madness, along with the long rants and home therapy sessions. My life at Oxford would have not been the same without you, my Oxford surrogate family.

A GREAT component of my live at Oxford was the Oxford University Volleyball Club. There are too many wonderful people to thank in my Blues and NVL teams that I won't name them all. But people that will always stay very close to my heart are:

- Jansie and Gareth who created so many good memories. Thanks for spending an entire summer with me traveling across the whole of England to play beach volleyball. Thanks for always being there and providing a support and a great partner during, rain, hail, storm, injury, snowmen, Skegness… and always with a huge smile!
- Megan, a genuinely great person besides a great player, that just made everything seem so easy and fun (such a Canadian!). Thanks for providing so much entertainment and laughter.
- Monika, my career, science, and volleyball counsellor. Thanks for all the help and advice during these years. Thanks also for hosting so many yummy pick-me-up events!
- Martina, Erin, Zi, Marina, Flora, Fabio, Ceci, Nicki, Ana, Maria K, Natalie, Ania, T-Ania, and many other team mates that made Oxford so memorable.

Last, but not least, I would like to thank Richard Stillion for preparing fantastic, and very missed, histological sections and stainings. Also thank you to all the PSB staff (especially Linda Randall and Nicky Hamp) for all their support with "carrot" work.

Abstract

Inflammasome regulation and activation in the intestinal epithelium

Andrea Lei, St. Peter's College, University of Oxford

A thesis submitted for the degree of Doctor of Philosophy, Trinity Term 2017

Microbiota colonisation of the intestinal tract makes it difficult for pattern recognition receptors (PRR) to discriminate between beneficial microbes and harmful pathogens. We aim to define the roles of cytosolic Nod-like receptors (NLR) in intestinal immunity and homeostasis. Upon activation, some NLR form inflammasomes that mediate the release of inflammatory cytokines and pyroptosis, an inflammatory form of cell death. NLR activation in the non-hematopoietic compartment was shown to be protective during acute intestinal infection. To identify the cell type responsible for this protection, we generated transgenic mice in which the key inflammasome adaptor molecule Asc is selectively ablated in intestinal epithelial cells (IEC) ($Asc^{\Delta IEC}$) and observed that inflammasomes are important for controlling *Citrobacter rodentium* clearance in these mice. To further dissect the importance of pathogen clearance by IEC inflammasome, *ex vivo* cultures of primary IEC organoids were established. Thus far this system has revealed profound differences in inflammasome regulation between IEC organoids and bone marrow-derived macrophages (BMDM). This research will inform our understanding of cell type-specific regulation of inflammasomes.

Declaration of Authorship

Data presented in the thesis are all from the authors' own experiments, other than FACS data which was acquired by Dr. Alison Murphy, Mucosal Immunology Group, Sir William Dunn School of Pathology, University of Oxford. Furthermore, *in vivo* experiments and tissue isolations presented in Chapter 3 were performed in collaboration with Dr. Alison Murphy.

Parts of the introduction of this thesis were submitted for authors' own publication and remain largely unaltered from the published material (1). Published contents are clearly highlighted in the relevant sections. Co-authors (Dr. Kevin Maloy and Dr. Alison Murphy) were notified and agreed with the reproduction of the mentioned published material in this thesis.

Table of Contents

Acknowledgments ... 2
Abstract ... 3
Declaration of Authorship ... 4
Table of Contents ... 5
List of Figures ... 9
List of Tables ... 12
Abbreviations ... 13
Chapter 1: General Introduction ... 18
1.1. The intestine: a unique challenge to the immune system ... 18
1.1.1. The microbiota ... 18
1.1.2. Intestinal epithelium ... 19
1.1.3. Intestinal stromal cells ... 24
1.1.4. Hematopoietic cells ... 24
1.1.4.1. Innate myeloid cells ... 26
1.1.4.2. Intestinal lymphocytes ... 28
1.2. Inflammatory Bowel Disease. A breakdown in intestinal homeostasis ... 32
1.3. Innate immunity and pattern recognition receptors ... 33
1.3.1. Toll-like receptors ... 34
1.3.2. NLR ... 39
1.4. The inflammasome ... 42
1.4.1. Nlrp3 ... 45
1.4.2. Nlrc4 ... 47
1.4.3. Consequences of inflammasome activation ... 49
1.4.3.1. Asc speck formation ... 49
1.4.3.2. Soluble mediators and inflammasome-associated IL-1 family cytokines ... 49
1.4.3.3. Inflammasomes and cell death: pyroptosis and apoptosis ... 55
1.4.4. Linking inflammasome effector mechanisms ... 63
1.5. Models of intestinal inflammation ... 68
1.5.1. *Citrobacter rodentium* infection- a model of acute intestinal inflammation ... 68
1.5.2. *Salmonella* Typhimurium ... 73
1.6. *Ex vivo* study of intestinal epithelial biology: organoids ... 74
1.7. Aims of the thesis ... 78
Chapter 2: Materials and Methods ... 80
2.1. Mice ... 80

2.2. Antibodies 83
2.3. Cytokines and PAMP 84
2.4. Primer list 85
2.5. Bacterial culture and infection 86
2.5.1. *Citrobacter rodentium* culture 86
2.5.2. *Salmonella* Typhimurium culture 86
2.5.3. *Salmonella* Typhimurium and *Citrobacter rodentium in vitro* infections 87
2.5.4. *Citrobacter rodentium in vivo* infection 87
2.6. Assessment of intestinal and systemic inflammation 87
2.6.1. Isolation of tissues from *C. rodentium* infected mice 87
2.6.2. Quantification of *C. rodentium* colonization 89
2.6.3. Histopathology analysis 90
2.7. Isolation of cell subsets 92
2.7.1. Cell isolation from spleen 92
2.7.2. Cell isolation from lamina propria leukocytes and stroma cells 92
2.7.3. *Ex vivo* culture of primary intestinal epithelial cells into 3D organoids and monolayers 94
2.7.4. Isolation of bone marrow derived macrophages (BMDM) 96
2.8. *Ex vivo* culture of organ explants 97
2.9. Flow cytometry 97
2.9.1. Surface FACS staining 97
2.10. Cytokine secretion and inflammasome activation assays 98
2.10.1. Quantification of cytokine levels 98
2.10.2. Caspase-1 activation assays 99
2.11. Gene expression analyses 99
2.11.1. Tissue processing for RNA isolation 99
2.11.2. RNA isolation and quantitative PCR (qPCR) 99
2.12. Western Blot 100
2.12.1. Preparation of colon and cecum tissue pieces 100
2.12.2. Preparation of 3D organoids and IEC monolayers samples 101
2.12.3. Protein quantification 101
2.12.4. Protein precipitation 101
2.12.5. Western Blots 102
2.13. Cell death measurements 102
2.13.1. LDH release 102
2.13.2. ApoTox-Glo Triplex Assay 103

2.14. Fluorescence microscopy 103
2.14.1. IEC monolayer staining 103
2.14.2. Immunohistochemistry in *in vivo* tissue 104
2.15. Genotyping 104
2.16. Cloning of ler gene and transformation into *C. rodentium* 105
2.16.1. *C. rodentium* chemically competent protocol 105
2.16.2. Gene amplification and cloning 105
2.17. Statistics 109
Chapter 3: Protective role of epithelial Asc expression during intestinal infection with *Citrobacter rodentium* 110
3.1. Introduction 110
3.2. Results 113
3.2.1. Asc deficiency within the intestinal epithelium of $Asc^{\Delta VC}$ mice .. 113
3.2.2. Asc in the intestinal epithelium is involved in protection against *C. rodentium* infection 120
3.2.3. $Asc^{\Delta VC}$ mice have an impaired ability to control tissue-adherent *C. rodentium* colonization 123
3.2.4. Comparable systemic immune activation and neutrophil tissue infiltration in $Asc^{\Delta VC}$ and $Asc^{fl/fl}$ mice following *C. rodentium* infection.. 127
3.2.5. Reduced levels of inflammasome activation in intestinal tissues of $Asc^{\Delta VC}$ mice following *C. rodentium* infection 130
3.2.5.1. Other inflammasome-associated cytokine responses are unaffected in $Asc^{\Delta VC}$ mice 134
3.2.6. Asc deficiency within the epithelium does not affect the IL-22/AMP axis 136
3.2.7. Reduced caspase-8 activation in intestinal tissues of $Asc^{\Delta VC}$ mice. 139
3.2.8. Asc speck formation in IEC during *C. rodentium* infection. 145
3.3. Discussion 147
Chapter 4: Regulation of inflammasome components in the intestinal epithelium - an organoid approach. 153
4.1. Introduction 153
4.2. Results 155
4.2.1. Inflammasome signal 1 in the epithelium: IL-22 upregulates the expression of IL-18 155
4.2.2. Nlrp3 activating DAMP fail to activate the inflammasome in IEC ... 157
4.2.3. Differential expression of Nlrp3 and Nlrc4 in IEC, stromal cells and myeloid cells 159
4.2.4. Epithelial responses to challenge with enteric pathogens 163

4.2.4.1. Epithelial inflammasomes are not primed upon challenge with *C. rodentium* or *S.* Typhimurium 163

4.2.4.2. *Salmonella* Typhimurium elicits more powerful inflammasome responses in IEC compared to *Citrobacter rodentium* 166

4.2.4.3. IEC death upon challenge with enteric pathogens 175

4.2.4.4. Circumventing the absence of virulence in LB-grown *C. rodentium* 179

4.2.4.5. Increased attachment of *C. rodentium* to Asc-deficient IEC 185

4.2.4.6. Antimicrobial activity and signalling of Asc vs WT 189

4.3. Discussion 191

Chapter 5: General Discussion 200

5.1. Cell type-specific regulation of PRR is key to understanding the discrimination between commensals and pathogens 200

5.2. The response of IEC inflammasomes to pathogenic invasion 201

5.3. Host microbiota sculpts host-pathogen interactions: Challenges of *in vitro* studies. 203

5.4. Epithelial inflammasomes and cell death 205

5.5. Interconnected circuits of inflammasome effector functions 209

5.6. Concluding remarks 211

References 214

List of Figures

Figure 1.1. Intestinal epithelium structural organisation 22

Figure 1.2. The canonical Wnt pathway. 23

Figure 1.3. Overview of Hematopoietic Stem Cells 25

Figure 1.4. Schematic representation of human NLR domain architecture 41

Figure 1.5. The two-signal model of NLR-mediated inflammasome activation 44

Figure 1.6. The caspase-11 non-canonical inflammasome pathway in myeloid cells... 61

Figure 1.7. Inflammasomes in intestinal epithelial cells 67

Figure 1.8. Schematic representation of an intestinal epithelial organoid and polarised monolayer. 77

Figure 2.1. Schematic of epithelial-specific Asc knock-out mice, $Asc^{\Delta VC}$, and their littermate controls $Asc^{fl/fl}$ 82

Figure 2.2. Intestinal tissue isolation map. Tissue pieces cut from each intestinal part and their purpose 89

Figure 2.3. Summary of cell isolation from lamina propria leukocytes and stroma cells 94

Figure 2.4. *Ex vivo* IEC 3D organoids and monolayers. 96

Figure 2.5. Map of pBAD33 vector containing the *ler* gene of *C. rodentium* under an arabinose inducible promoter 108

Figure 3.1. Asc deficiency in intestinal epithelial cells from $Asc^{\Delta VC}$ mice. 115

Figure 3.2. Colonic intestinal epithelial cells from $Asc^{\Delta VC}$ mice are deficient in Asc. 116

Figure 3.3. Cecal intestinal epithelial cells from $Asc^{\Delta VC}$ mice are deficient in Asc..... 117

Figure 3.4. Rare Asc-positive cecal crypts were present in a minority of $Asc^{\Delta VC}$ mice. 118

Figure 3.5. *C. rodentium*-infected $Asc^{\Delta VC}$ mice harbour Asc-sufficient cells in their lamina propria 119

Figure 3.6. *C. rodentium* infected $Asc^{\Delta VC}$ mice exhibit increased weight loss compared to $Asc^{fl/fl}$ littermates. 121

Figure 3.7. *C. rodentium*-infected $Asc^{\Delta VC}$ mice exhibit increased pathology compared to $Asc^{fl/fl}$ littermates 122

Figure 3.8. *C. rodentium* infected *Asc*$^{\Delta VC}$ mice display increased tissue adherent bacteria in intestinal tissues 124

Figure 3.9. *C. rodentium* infected *Asc*$^{\Delta VC}$ mice display increased planktonic bacteria in the cecal contents 125

Figure 3.10. *C. rodentium* infected *Asc*$^{\Delta VC}$ and *Asc*$^{fl/fl}$ mice have comparable systemic *C. rodentium* spread 126

Figure 3.11. *Asc*$^{\Delta VC}$ and *Asc*$^{fl/fl}$ mice have comparable systemic immune activation upon C. rodentium infection 128

Figure 3.12. Asc deficiency is associated with a trend towards increased neutrophil recruitment during *C. rodentium* infection 129

Figure 3.13. Reduced intestinal Caspase-1 and IL-18 activation in *Asc*$^{\Delta VC}$ mice during C. rodentium infection 132

Figure 3.14. Reduced IL-18 secretion in intestinal tissues of *Asc*$^{\Delta VC}$ mice upon *C. rodentium* infection 133

Figure 3.15. IL-1β or IL-1α secretion is not induced in intestinal tissues during *C. rodentium* infection 135

Figure 3.16. Comparable, low levels of IL-22 secretion in intestinal tissues of *Asc*$^{fl/fl}$, *Asc*$^{\Delta VC}$ and *Asc*$^{-/-}$ mice upon *C. rodentium* infection 137

Figure 3.17. Comparable AMP responses in colonic IEC from *Asc*$^{fl/fl}$ and *Asc*$^{\Delta VC}$ mice upon *C. rodentium* infection 138

Figure 3.18. Reduced caspase-8 activation in the cecum of *Asc*$^{\Delta VC}$ mice at day 8 p.i. with *C. rodentium* 141

Figure 3.19. Reduced caspase-8 activation in the colon of *Asc*$^{\Delta VC}$ mice at day 8 p.i. with *C. rodentium* 142

Figure 3.20. Reduced caspase-8, caspase-1 and IL-18 activation in the colons of *Asc*$^{-/-}$ mice during *C. rodentium* infection 143

Figure 3.21. Colonic IEC from *Asc*$^{\Delta VC}$ mice show reduced expression of *caspase-8* and *Ki67* during *C. rodentium* infection 144

Figure 3.22. Asc speck formation in the epithelium of *Asc*$^{fl/fl}$ mice upon *C. rodentium* infection 146

Figure 4.1. IL-22 induces pro-IL-18 expression in primary IEC 156

Figure 4.2. Nlrp3 inflammasomes are not classically activated in primary IEC 158

Figure 4.3 Differential expression of inflammasome components by primary IEC and BMDM 161

Figure 4.4. Differential expression of inflammasome components by stroma and BMDM. 162

Figure 4.5. *C. rodentium* infection does not alter expression of inflammasome components by primary IEC monolayers. 164

Figure 4.6. *Salmonella* Typhimurium infection does not alter expression of inflammasome components by primary IEC monolayers. 165

Figure 4.7. *S.* Typhimurium activates the inflammasome in primary IEC monolayers in an Nlrc4-dependent manner 169

Figure 4.8. Stimulation with *S.* Typhimurium, but not *C. rodentium*, leads to IL-18 release from IEC monolayers. 170

Figure 4.9. Asc speck formation in *S.* Typhimurium treated IEC monolayers 171

Figure 4.10. Asc speck formation in *S.* Typhimurium treated IEC monolayers 172

Figure 4.11. Kinetics of IL-18 release from IEC monolayers infected with *S.* Typhimurium or *C. rodentium* 173

Figure 4.12. *C. rodentium* is unable to drive inflammasome activation in IEC monolayers 174

Figure 4.13. LDH release upon *C. rodentium* or *S.* Typhimurium infection of cecal IEC monolayers 177

Figure 4.14. Cell viability and cytotoxicity upon *C. rodentium* or *S.* Typhimurium infection of cecal IEC monolayers 178

Figure 4.15. Lack of IL-18 release by IEC challenged with fecal host-adapted *C. rodentium*..... 182

Figure 4.16. Modulation of virulence genes expression in *C. rodentium*..... 183

Figure 4.17. Increased attachment of *Citrobacter rodentium* to Asc-deficient IEC monolayers 187

Figure 4.18. Quantification of *C. rodentium* attachment to IEC monolayers 188

Figure 4.19. Culture supernatants from primary cecal IEC monolayers do not exhibit antibacterial activity against *C. rodentium*..... 190

Figure 4.20. Inflammasome activation in *C. rodentium* and *S.* Typhimurium in macrophages (phagocytic) versus IEC (non-phagocytic)..... 199

Figure 5.1. Reduced cell death in infected tissues in $Asc^{\Delta VC}$ mice may explain the increased pathogen burden compared to $Asc^{fl/fl}$ 208

Figure 5.2. Summary figure..... 213

List of Tables

Table 1.1. Toll-like receptors (TLR): Location and ligands 37

Table 1.2. NLR family members & other inflammasome components 40

Table 1.3. Proposed mechanisms of Nlrp3 inflammasome activation..... 46

Table 1.4. Soluble mediators of inflammasome activation and intestinal inflammation 54

Table 1.5. Characteristic features of different cell death pathways 62

Table 1.6. Inflammasome components and intestinal inflammation. 71

Table 1.7. Supplements to support intestinal epithelial organoid growth *ex vivo*. 76

Table 1.8. Example of host-pathogen interactions studied with the aid of intestinal epithelial organoids. 76

Table 2.1. Mouse strains used in this thesis. 81

Table 2.2. List of antibodies used in this study and their purpose. 83

Table 2.3. List of cytokines and PAMP used in this study for *in vitro* stimulation of epithelial organoids and monolayers 84

Table 2.4. List of primers used in this study 85

Table 2.5. Summary of histological scoring for *C. rodentium*-induced colitis. 91

Abbreviations

A/E	Attaching and effacing
ACK	Ammonium chloride potassium
AhR	Aryl hydrocarbon receptor
AIM2	Absent in melanoma 2
Amp	Ampicillin
AMP	Antimicrobial peptide
AP1	Activator protein 1
Apaf1	Apoptotic protease activating factor 1
APC	Adenomatous polyposis coli
APC	Antigen presenting cell
Asc	Apoptosis-associated speck-like protein containing a CARD
ATG16L1	Autophagy- related protein 16- 1
ATP	Adenosine triphospate
BIR	Baculovirus inhibitor domain
BM	Bone marrow
BMDM	Bone marrow-derived macrophages
BSA	Bovine serum albumin
C.rod	*Citrobacter rodentium*
CAPS	Cryopyrin- associated periodic syndromes
CARD	Caspase activation and recruitment domains
CD	Cluster of differentiation
CD	Crohn's disease
CF	Cystic fibrosis
CFTR	Cystic fibrosis transmembrane conductor receptor
CFU	Colony forming units
CK1α	Casein kinase 1 alpha
cl	Cleaved
CL	Colon
CLR	C-type lectin receptor
CM	Cecum
CMP	Common myeloid precursor
CRISPR	Clustered regularly interspaced palindromic repeats
CSR	Chain class-switch recombination
CTB	Cholera toxin subunit B
CTL	Cytotoxic T lymphocyte
DAMP	Danger associated molecular pattern
DC	Dendritic cell
DMEM	Dulbecco's modified eagle medium
DNA	Deoxyribonucleic acid
DSS	Dextran sodium sulphate
EDTA	Ethylenediaminetetraacetic acid
EGF	Epidermal growth factor

EHEC	Enterohemorrhagic E. Coli
EPEC	Enteropathogenic E. Coli
ER	Endoplasmic reticulum
ERK	Extracellular signal–regulated kinases
Fabpi	Fatty acid binding protein gene
FACS	Fluorescence activated cell sorting
FCAS	Familial cold autoinflammatory syndrome
FCS	Foetal calf serum
FIIND	Function to find domain
FlaTox	*Legionella pneumophila* flagellin fused to the N-terminal domain of *Bacillus anthracis* lethal factor
Foxp3	Forkhead box P3
GALT	Gut-associated lymphoid tissue
Gata3	GATA binding protein 3
GBP	Guanylate-binding proteins
GF	Germ free
GlrA	Global Regulator of LEE-Activator)
GsdmD	Gasdermin D
GSK3	Glycogen synthase kinase 3
GWAS	Genome wide association studies
H&E	Haematoxylin and eosin
HEPES	4-(2-hydroxyethyl)-1-piperazineethanesulfonic acid
HMGB1	High-mobility group box 1
Hprt	Hypoxanthine phosphoribosyl transferase
HRP	Horseradish peroxidase
HSC	Hematopoietic stem cells
IBD	Inflammatory bowel disease
IEC	Intestinal epithelial cell
IEL	Intraepithelial lymphocyte
IFI16	Interferon-inducible protein 16
IFN	Interferon
Ig	Immunoglobulin
Igif	IFNγ inducing factor
IHC	Immunohistochemistry
IL	Interleukin
IL-18bp	IL-18 binding protein
IL-1RA	IL-1 receptor antagonist
ILC	Innate lymphoid cell
IRAK	IL-1 receptor-associated kinase
JNK	C-Jun N-terminal kinases
Kb	Kilo base pair
kDa	Kilodalton
KO	Knock out
LA	Localised adherence

LDH	Lactate dehydrogenase
LEE	Locus of enterocyte effacement
Ler	LEE encoded regulator
Lgr5	Leu-rich repeat-containing G protein-coupled receptor 5
LP	Lamina propria
LPL	Lamina propria leukocyte
LPS	Lipopolysaccharide
LRR	Leucine-rich Repeat
LT	Lymphotoxin
LV	Liver
M cells	Microfold cells
mAb	Monoclonal antibody
MAP	Mitogen associated protein
MAVS	Mitochondrial antiviral-signalling protein
MDP	Muramyl dipeptide
MHCI/II	Major histocompatibility complex type I/II
MLN	Mesenteric lymph node
MOI	Multiplicity of infection
MPO	Myeloperoxidase
mtDNA	Mitochondrial DNA
MWS	Muckle–Wells syndrome
MYD88	Myeloid differentiation primary response gene 88
NA	Not available
NAC	N-acetylcysteine
NACHT	Nucleotide- binding and oligomerization. Naip, ciita, het-e, and tp-2
Naip	Nlr family apoptosis inhibitory protein
NBD	Nucleotide-binding domain
ND	Not detectable/not determined
NEK	NIMA-related kinases
NEMO	(NF-kB) essential modulator
NET	Neutrophil extracellular traps
NF-κB	Nuclear factor kappa-light-chain-enhancer of activated B cells
NGS	Normal goat serum
NK	Natural killer
NLR	NOD-like receptor/ nucleotide-binding domain and leucine-rich repeat
NOD	Nucleotide binding and oligomerization domain
NOMID	Neonatal onset multisystem inflammatory disease
OD	Optical density
ON	Overnight
oxPAPC	oxidized phospholipids
p.i.	Post infection
P/S	Penicillin-streptomycin

PAGE	Polyacrylamide gel electrophoresis
PAI	Pathogenicity island
PAMP	Pathogen associated molecular pattern
PBS	Phosphate buffered saline
PCR	Polymerase chain reaction
PFA	Paraformaldehyde
pIgR	Polymeric Ig receptor
PMA	Phorbol 12-myristate 13-acetate
PMN	Polymorphonuclear
PPL	Project license
PVDF	Polyvinylidene difluoride
PYD	Pyrin domain
PYHIN	PYD and HIN domain-containing
qPCR	Quantitative polymerase chain reaction
R	Receptor
RA	Receptor antagonist
RAG	Recombinase activating gene
RAP	Receptor accessory protein
RBS	Ribosome binding site
REGIIIγ	Regenerating islet-derived protein iiiγ
RLR	Retinoic acid- inducible gene- I- like receptors
ROCK	Coiled-coil containing protein kinase
RORγt	Retinoic acid- related orphan nuclear hormone receptor
ROS	Reactive oxygen species
RPMI	Roswell Park Memorial Institute medium
RT	Room temperature
***S*. Tm**	*Salmonella enterica* serovar Typhimurium/*S.* Typhimurium
SAA	Serum amyloid A
SCFA	Short-chain fatty acids
SDS	Sodium dodecyl sulfate
SFB	Segmented filamentous bacteria
SI	Small intestine
SP	Spleen
SPF	Specific pathogen-free
SPI	*Salmonella* pathogenicity island
T3SS	Type 3 secretion system
T4SS	Type 4 secretion system
TA cells	Transient amplifying cells
TAK1	Transforming growth factor β-activated kinase 1
Tcf/Lef	T-cell factor/lymphoid enhancer-binding factor
TCR	T cell receptor
TFF3	Trefoil factor 3
TGF	Transforming growth factor
Th	T helper

TIR	Toll/Interleukin-1 receptor
TLR	Toll-like receptors
TMB	3,3’,5,5’-tetramethylbenzidine
TMCH	Transmissible murine colonic hyperplasia
TNF	Tumour necrosis factor
TRAF6	Tumour necrosis factor [TNF] receptor-associated factor 6
TRAM	TIR-domain-containing adaptor molecule
Treg	Regulatory T cell
TRIF	TIR-domain-containing adaptor protein inducing beta interferon [IFN-β]
TSLP	Thymic stromal lymphopoietin
TXNIP	Thioredoxin-interacting protein
UC	Ulcerative colitis
WT	Wild type

Chapter 1: General Introduction

1.1.The intestine: a unique challenge to the immune system

The gut is a potentially hostile world filled with a bewildering array of microbes, some of which have the potential to cause disease under specific conditions. The host has developed effective defence mechanisms against potential infections. The large surface area of the gut and the intricate complexity of host-microbe interactions within, make the intestinal mucosa an exciting site to study in the field of immunology.

1.1.1. The microbiota

The microbiota is a general term that refers to the whole collection of microbes that reside in harmony within the body of a host. The group of microbes that constitute the symbiotic microbiota are commonly referred to as commensals. The human intestinal microflora is estimated to contain 500 to 1000 species and about 10^{14} bacteria (2-4). Appropriate immune responses help maintain the delicate balance between the host and the microbiota. The breakdown of this dialogue can result in chronic inflammation of the gut known as inflammatory bowel disease (IBD) (5), highlighting the importance of intestinal homeostasis.

The microbes of a healthy gut provide us with several benefits including the ability to metabolise certain nutrients, like complex plant polysaccharides, otherwise indigestible for the host (6). The gut microbiota has been shown to generate metabolites, like short-chain fatty acids (SCFA) that contribute to several host functions, such as the regulation of colonic regulatory T (Treg) cells that maintain homeostasis (7). The vast presence of commensals in the gut constitutes an extra barrier against invading organisms in the intestine by providing competition for diverse intestinal niches (8). Competition normally favours commensals that have evolved to survive in the harsh intestinal environment, and this provides colonisation resistance against invading pathogens (9-12). However, when protective commensals are disturbed for example by antibiotic treatment or during active IBD, the resulting dysbiosis can increase susceptibility to opportunistic pathogenic infections (8, 13, 14). Nevertheless, the effects of antibiotics on the intestinal microflora are poorly understood beyond the induction of antibiotic resistance following treatment

(13). Therefore, the complex microbiota–pathogen–host interactions in the intestine require further investigation to develop effective treatments against infection and chronic inflammation.

1.1.2. Intestinal epithelium

The largest line of defence in the human gut is the intestinal epithelium, with a reported surface area ranging from $100m^2$ to $400m^2$ (3, 15). When intact, this barrier is impermeable to most infectious agents. The intestinal epithelium is composed of a single layer of simple columnar IEC that separate the external environment from the sterile tissues of the body. In the small intestine (SI), the epithelium is organised into crypts and villi with constant proliferation and migration along the crypt-villus axis, whereas in the colon the crypts open into a flat epithelium (Figure 1.1). These cells are adapted to constitutive colonisation by the gut microbiota. However, if intestinal homeostasis is disrupted infection and inflammation become major risks and disrupted epithelial barrier function is associated with IBD (15).

The intestinal epithelium is constantly replenished by Leu-rich repeat-containing G protein-coupled receptor 5-expressing ($Lgr5^+$) intestinal epithelial stem cells located at the bottom of the intestinal crypt (16, 17). The stem cell niche is supported by subepithelial myofibroblasts and in the SI by Paneth cells. These cells maintain and regulate this microenvironment by secreting an array of local factors (15, 18). Wnt signalling is instrumental in maintaining the stem cell niche and it instructs IEC to adopt a proliferative progenitor phenotype (19).

The canonical Wnt signalling pathway triggers β-catenin-mediated cell type-specific gene expression programs (20). In the absence of Wnt signalling, β-catenin remains in the cytosol associated with serine/threonine kinases casein kinase 1 alpha (CK1α), a glycogen synthase kinase 3 (GSK3), and the tumour suppressors: axin inhibition protein (Axin) and adenomatous polyposis coli (APC) (21, 22). GSK3 and CK1α-mediated phosphorylation of the β-catenin amino-terminus targets it for proteasomal degradation (21, 23). Under these circumstances, β-catenin is unable to associate with DNA-binding proteins of the T-cell factor/lymphoid enhancer-binding factor (Tcf/Lef) family (23, 24). However, in the presence of Wnt signalling, Wnt engagement to its receptor Frizzled leads to the

accumulation of β-catenin in the cytosol and subsequent translocation into the nucleus through a poorly understood signalling cascade (19, 25) (Figure 1.2). Nuclear β-catenin relieves the repression of Tcf/Lef-dependent genes and drives the expression of Wnt-responsive genes (21). R-spondin-1 potently amplifies Wnt responses by stabilising Frizzled and inhibiting its turnover (22, 26).

$Lgr5^+$ stem cells can proliferate, migrate (they are named transient amplifying (TA) cells at this stage) and differentiate into mature IEC. Approximately 3 days after becoming terminally differentiated IEC and after reaching the top of the crypt/villi, they undergo spontaneous apoptosis, termed anoikis, and are shed into the intestinal lumen (27). The epithelial barrier is always sealed during normal IEC turnover and dying cells are pushed out of the epithelial layer by the neighbouring cells that will replace them (28, 29). The intestinal epithelium has a high turnover and it replenishes itself approximately every 5 days in the mouse (16, 30). The majority of cells lining the intestinal epithelium are absorptive enterocytes (~80% of all IEC) (21), specialised in nutrient absorption and transport across the epithelial barrier. In addition, there are other specialised cells in charge of maintaining intestinal barrier function and homeostasis. Six differentiated epithelial cell types are reported thus far: goblet cells, Paneth cells, enteroendocrine cells, enterocytes, tuft cells and M cells (31) (Figure 1.1).

Most invading bacteria fail to survive for long in the gut because of the harsh intestinal environment. Enterocytes are capable of secreting antimicrobial peptides (AMP) like the C-type lectin regenerating islet-derived protein IIIγ (REGIIIγ) throughout the SI and the colon that keep the threat from intestinal bacteria in check (15, 32). However, specialised IEC in the SI, Paneth cells can secrete additional AMP including defensins (cryptdins in mice), cathelicidins and lysozyme (32, 33). C-type lectins and lysozyme target peptidoglycans in the cell wall of Gram-positive bacteria whilst defensins and cathelicidins are pore-forming AMP (15). Paneth cells are located at the bottom of the SI crypts interspersed with LGR^+ cells (Figure 1.1), and were shown to provide essential signals for supporting the intestinal stem cell niche, such as EGF (epidermal growth factor), Wnt3 and Notch (16). Furthermore, Paneth cells are the only type of IEC that resides fully differentiated at the bottom crypt for ~3-6 weeks (30). This is much longer than TA cells that only reside in the crypts for ~48-72h and through ~6 rounds of divisions move upwards in the crypt (30) (Figure 1.1).

Goblet cells, another secretory IEC, are responsible for the secretion of highly glycosylated mucins, as well as other factors regulating the mucus barrier integrity including the mucin crosslinking agent trefoil factor 3 (TFF3) (15, 34). The most abundant mucin in the intestinal epithelium mucus layer is Muc2. Indeed, Muc2-deficient mice develop spontaneous colitis and display higher propensity for tumour formation (35, 36). The proportion of goblet cells, amongst the other IEC, increases from the start of the SI, the duodenum (4%) to the colon (16%) (21, 37). The mucus layer acts as a protective barrier to block the adherence of bacteria to epithelial cells (34, 38-40). This matrix is loaded with AMP and Immunoglobulin A (IgA) that further reinforce IEC defences (15, 41, 42). IgA is a dimeric antibody that is translocated into the lumen with the aid of polymeric Ig receptor (pIgR). In the intestinal lumen, it can interact with intestinal commensal, dietary and self-antigens (43, 44).

Enteroendocrine cells are specialised in the production of hormone regulators of digestive function. There are ~15 subtypes of enteroendocrine cells depending on the specific hormones they secrete (21). They represent 1% of the IEC population lining the intestinal lumen and are the link between the central and enteric nervous systems (15, 21). Another specialised IEC called microfold cells (M cells) constitute part of the gut associated lymphoid tissue (GALT) and are enriched in the SI Peyer's patches and colonic isolated lymphoid follicles (21, 45, 46). M cells are able to sample luminal antigens and present them to cells of the immune system (47). Tuft cells are yet another IEC type thought to be involved in sensing luminal contents. They are very rare but can occur anywhere in the crypt-villus axis (48) (49). Recently, tuft cells were described to contribute to innate immunity against helminths and protozoa through triggering type 2 immune responses (50-52).

The epithelium can communicate with the immune cell compartment and mediate the cross talk between the microbiota and the lamina propria (LP) immune cells. For instance, besides mucus production, goblet cells may also regulate lymphocyte activation by delivering luminal antigens to the lamina propria $CD103^+$ Dendritic cell (DC), which in turn promote lymphocyte migration, IgA production and Treg differentiation (53, 54). Furthermore, segmented filamentous bacteria (SFB) can attach to the IEC leading to IL-22 production by innate like lymphoid cells (ILC). This IL-22 secretion can then trigger the production of AMP and serum amyloid A (SAA) by the IEC, and induce T helper (Th)17 cell differentiation and IgA production (55, 56)

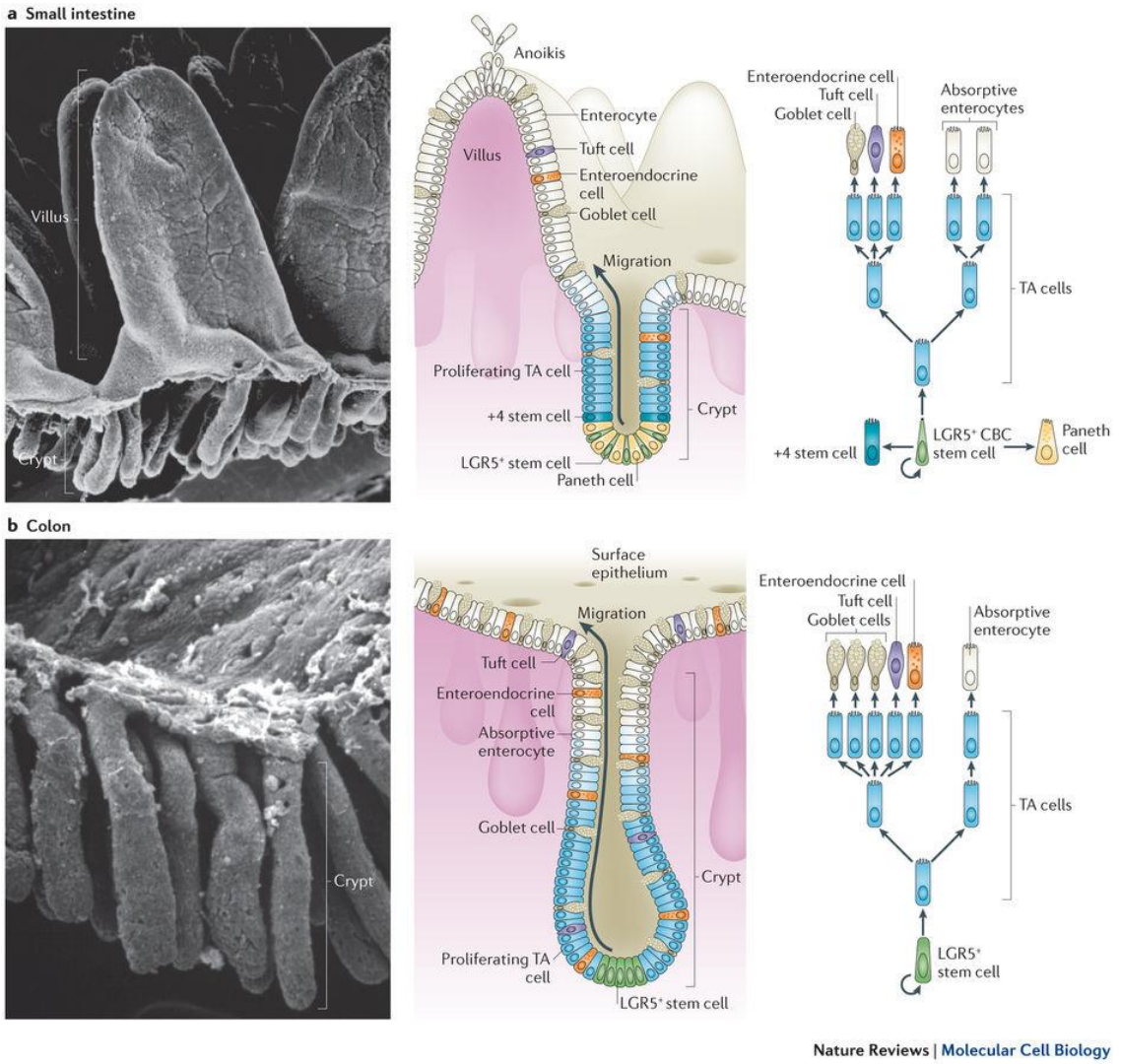
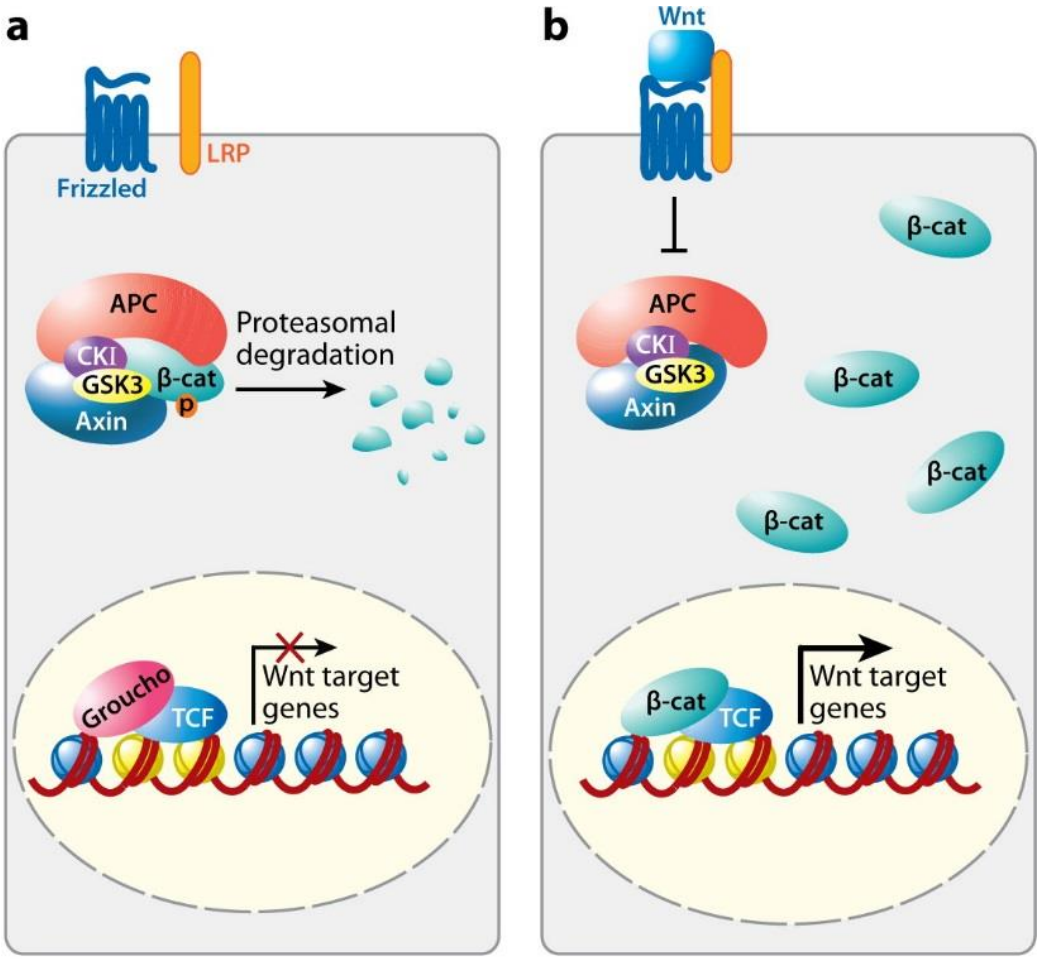


Figure 1.1. Intestinal epithelium structural organisation. A) Structural organisation of small intestinal epithelium (scanning electron micrograph in the left panel). $Lgr5^+$ cells intercalated by Paneth cells at the bottom of the intestinal crypts. +4 stem cells restore the $Lgr5^+$ cells in case of necessity. $Lgr5^+$ cells generate TA cells that proliferate and migrate upwards in the crypts of Lieberkühn towards the tip of the villi. TA cells can differentiate into various kinds of mature IEC: goblet cells, Paneth cells, enterocytes, tuft cells and enteroendocrine cells. Once cells reach the tip of the villi they are pushed out by neighbouring cells and die by anoikis, a spontaneous form of apoptosis in IEC. The hierarchy of stem cells and differentiated IEC are represented in the right panel. B) Structural organisation of colonic epithelium (scanning electron micrograph in the left panel). $Lgr5^+$ cells generate TA cells that proliferate and migrate upwards in the colonic crypts and towards the surface of the epithelium. TA cells can differentiate into different lineages of mature IEC, as represented in the hierarchy tree in the rightmost panel. Figure taken from (27). Reprinted by permission from Copyright Clearance Center: Springer Nature; Nature Reviews Molecular Cell Biology; Adult intestinal stem cells: critical drivers of epithelial homeostasis and regeneration; Barker, Nick (2013).



van der Flier LG, Clevers H. 2009.
Annu. Rev. Physiol. 71:241–60

Figure 1.2. The canonical Wnt pathway. The canonical Wnt pathway transcriptionally regulates its target genes through TCF target sites. Wnt engagement to Frizzled leads to β-catenin stabilisation and accumulation into the cytosol and eventual nuclear translocation where it can relieve TCF target gene inhibition and activate their transcription. Figure taken from (21). Reprinted by permission from Copyright Clearance Center: American Physiological Society; Annual review of physiology; Stem Cells, Self-Renewal, and Differentiation in the Intestinal Epithelium; Van Der Flier, Laurens (2009).

1.1.3. Intestinal stromal cells

A thin layer of loose connective tissue named lamina propria supports intestinal epithelial cells. The LP is composed of stromal cells (also referred to as mesenchymal cells) which consist of endothelial cells, fibroblasts, myofibroblasts, pericytes and smooth muscle cells (57-59). Together, IEC and stromal cells plus the haematopoietic cells of the LP constitute the intestinal mucosa. The most abundant type of stromal cells in the intestinal mucosa are myofibroblasts which reside beneath the epithelium in direct contact with IEC (58). Stroma provide growth factors that modulate epithelial maintenance and proliferation, including members of the Wnt signalling family (60). Furthermore, stromal cells, have been shown to actively participate in many immunological axes through the production of cytokines and other mediators (57). Indeed, stromal cells express PRR that may promote the recruitment of inflammatory mediators upon infection (61).

1.1.4. Hematopoietic cells

All cellular elements of the blood, including erythrocytes, platelets and white blood cells of the immune system, derive from the same progenitor; the hematopoietic stem cells (HSC) of the bone marrow. As HSC undergo differentiation they give rise to intermediate progenitors, which further differentiate into the various blood cells. White blood cell progenitors are divided into two lineages, the common myeloid progenitor and the common lymphoid progenitor, which give rise to myeloid cell and lymphoid cell lineages, respectively (62) (Figure 1.3).

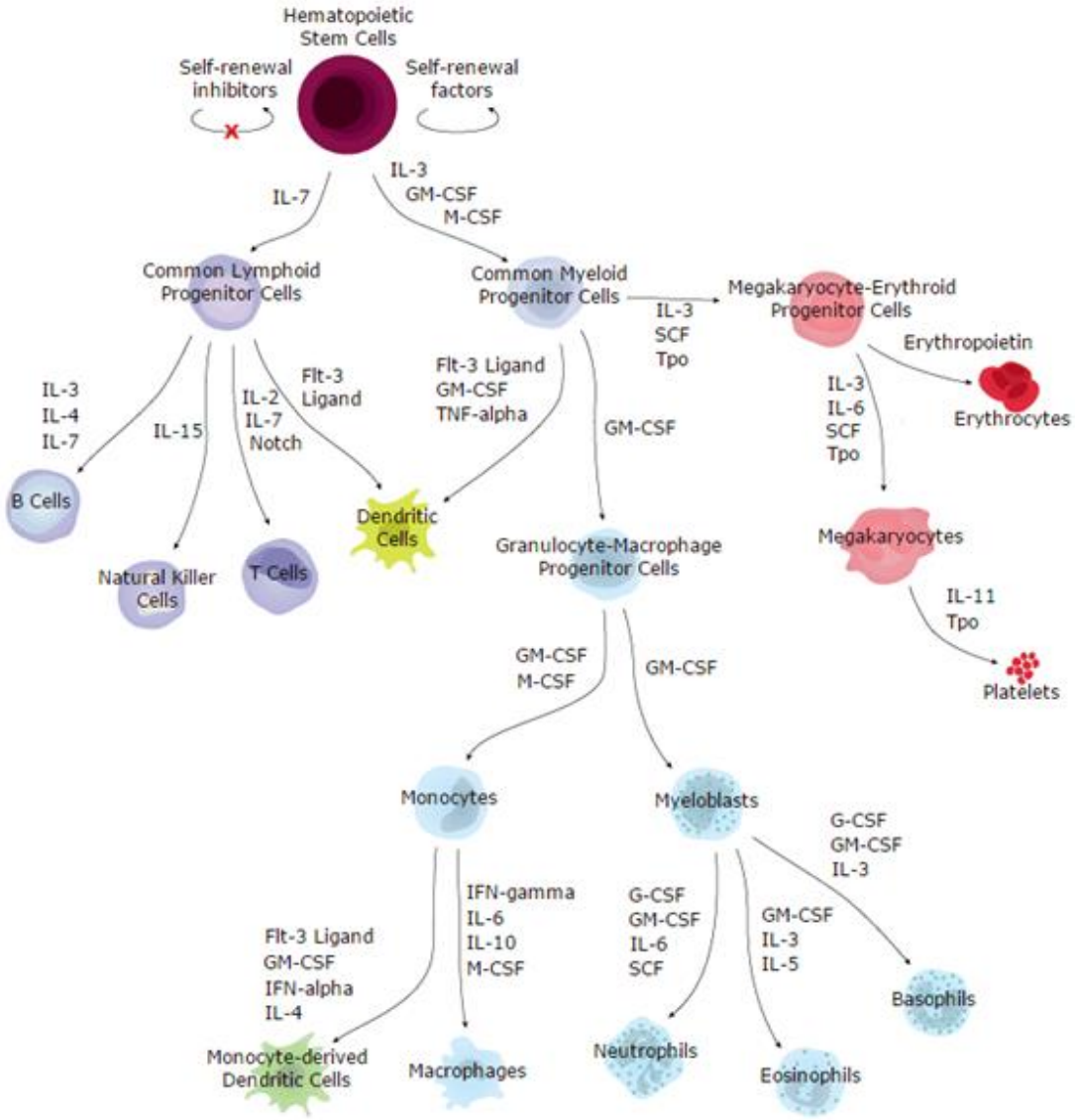


Figure 1.3. Overview of Hematopoietic Stem Cells. Figure taken from Bio-Techne (R&D Systems). Reprinted by permission from Bio-Techne: R&D Systems, Interactive Pathways & Processes; Hematopoietic Stem Cell Differentiation Pathways & Lineage-specific Markers; R&D Systems (2018).

1.1.4.1. Innate myeloid cells

When microorganisms bypass the mechanical barriers to penetrate the body, several non-specific antimicrobial systems are in place; these are referred to as innate. The innate immune system is the first line of defence against invading pathogens (63). The name illustrates that they are not intrinsically dependent on prior contact with the invading agent. Once activated, the innate immune system orchestrates the onset of a signalling cascade targeted at clearing the invading pathogen. This chain of events is known as inflammation, a rapid non-specific process that can initiate the adaptive immune response (64).

The different cells of the immune system can be classified by various overlapping parameters, such as function, morphology, and developmental origin. The term myeloid refers to the classification of cells according to their developmental origin. Myeloid cells originate from a common myeloid precursor (CMP) during hematopoiesis (65). These cells include neutrophils, macrophages, DC, basophils, eosinophils and mast cells.

Granulocytes

Granulocytes or polymorphonuclear (PMN) cells are a group of myeloid cell types that are classed apart due to their characteristic morphology. They are named granulocytes due to the presence of granules in their cytoplasm, and polymorphonuclear because of their multi-lobulated nuclei. They are the major population of blood leukocytes and are normally circulating in the blood but can be selectively recruited to sites of inflammation. Granulocytes are divided into three groups: neutrophils, eosinophils and basophils (62).

Neutrophils, although short-lived, are the dominant white blood cell in the bloodstream. They are important phagocytes whose killing mechanisms largely reside within their cytosolic granules. These granules contain myeloperoxidase (MPO) as well as antimicrobial effectors, such as defensins and cathepsin G (66-68). In addition to antimicrobial agents, neutrophil granules contain proteolytic enzymes that breakdown the surrounding tissues. Furthermore, neutrophils may also kill the invading pathogen extracellularly by neutrophil extracellular traps or NET (69). Notably, these effector mechanisms are non-selective and can lead to host-tissue damage (70, 71).

Eosinophils play an important role in dealing with pathogens that cannot be phagocytosed such as large parasites and helminths. The contents of their cytosolic granules allow

eosinophils to launch an extracellular attack damaging the membranes of parasites through proteases that are released upon degranulation, like eosinophil basic protein, that kill parasites (72). In addition, another type of granulocyte is often recruited, the basophil, which mediate vasodilation and blood clotting prevention through histamine and heparin production, respectively. These two granulocytes in conjunction are potent stimulators of inflammation (62, 73).

Antigen presenting cells: dendritic cells and macrophages

Signalling by the innate immune system is also required to initiate specific adaptive immune responses. Antigen presenting cells (APC) are the bridge between innate and adaptive immunity (74). For antigen presentation to occur, APC take up certain antigens, process them and display immunogenic fragments in complex with major histocompatibility complex (MHC) molecules, which, together with the expression of co-stimulatory molecules, delivers an activation signal to antigen-specific T lymphocytes (75). APC can also produce a vast number of cytokines and alarmins that are important in the activation and shaping of adaptive responses (76, 77). Professional APC comprise macrophages and DC and their different subsets (62).

Macrophages can constitutively reside within tissues (tissue resident macrophages) or can develop from blood monocytes that are recruited upon inflammation or infection (elicited macrophages) (78-80). Tissue resident macrophages are present in almost every tissue of the body and in most tissues early precursors generated in the yolk sac seed a self-renewing population of tissue macrophages. However, the intestine is one notable exception, as the tissue resident intestinal macrophages are derived from circulating blood monocytes (81-83). Under normal physiological conditions, they filter off foreign or waste material and promote tissue homeostasis (84, 85). Macrophages patrol the diverse tissue environments acting as sentinels that can raise the alarm upon pathogen invasion by triggering inflammation (86). Elicited macrophages possess a vast range of effector functions that help clear the infection. They are much more phagocytic than tissue resident macrophages and secrete an enormous array of molecules like interleukin-6 (IL-6) and tumour necrosis factor α (TNFα) that amplify the inflammatory response and aid the recruitment of other effector cells (80, 86, 87).

DC, similarly to tissue resident macrophages, are constantly sampling material at the tissue boundaries (88). In the gut, some DC can sample luminal contents and migrate

from the lamina propria to the mesenteric lymph nodes (MLN), and promote tolerogenic responses by enhancing the differentiation of forkhead box P3-expressing ($Foxp3^+$) Treg cells (84, 85, 89, 90). However, upon pathogenic invasion and inflammation, DC, like macrophages, adopt a more pro-inflammatory phenotype characterised by the production of pro-inflammatory mediators like IL-6, TNFα and interferon γ (IFNγ) that rapidly trigger the host immune response (91).

1.1.4.2. Intestinal lymphocytes

The mucosal lymphoid tissues lining the gut are collectively referred to as gut-associated lymphoid tissue or GALT. Principal sites for the induction of immune responses within the GALT are the Peyer's patches of the SI and the isolated lymphoid follicles of the large intestine and rectum (62). Instead of microvilli, Peyer's patches have a smooth surface containing specialized epithelial M cells that are in direct contact with luminal antigens as these structures are devoid of mucus. M cells deliver luminal material to APC of the lamina propria through transcytosis, leading to the induction of mucosal immune responses (62).

Naïve lymphocytes emerge from the primary lymphoid tissue, bone marrow (BM) and thymus, and enter the GALT (secondary lymphoid organs) through the bloodstream. Lymphocytes are divided into B cells that originate and mature in the BM and T cells that originate in the BM but mature in the thymus (62). In the GALT and LP, foreign antigens are presented to naïve lymphocytes, triggering their activation and migration to the systemic circulation and through the lymphatics draining the intestine, the MLN and spleen for further activation. Eventually, lymphocytes circulate in the blood through the entire body and/or return to the LP to exert their local effector functions (15, 62). Thus, besides several populations of myeloid cells, the LP also contains many activated T lymphocytes and plasma cells (62).

<u>T cells</u>

Antigen specific T lymphocytes are at the centre of adaptive immunity. Antigen presentation by APC, accompanied by co-stimulatory signals and cytokines, induces T cell clonal expansion and differentiation into effector T cells. These responses are key for mucosal barrier defence and protection against future challenges. Depending on the

signal, T cells can exert tolerogenic or inflammatory effects on the local environment through the secretion of cytokines that tailor the immune response (77).

The LP T cells consist primarily of the so called conventional T cells that bear αβ T-cell receptors in conjunction with either cluster of differentiation 4 or 8 (CD4 or CD8) for T helper or T cytotoxic cells, respectively (92, 93). Conversely, the T cells belonging to the intraepithelial lymphocyte family (IEL), which are located within the epithelial layer adjacent to IEC, often display unconventional surface phenotypes, such as TCRγδ receptors and expression of CD8αα homodimers (92-94).

$CD8^+$T cells or cytotoxic T lymphocyte (CTL) recognise peptides bound to the MHC class I present in all nucleated cells and are important for antiviral immunity (95). $CD4^+$T cells recognize fragments of antigens degraded within intracellular vesicles, displayed at the cell surface by MHC class II molecules. Upon activation, they can differentiate into several Th effector subsets (62). The cytokines delivered by APC play an important role in this cellular decision.

IFN-γ and IL-12 signalling leads to up-regulation of the T-bet transcription factor, which drives Th1 responses that promote cellular immunity (96, 97). Th1 cells are characterised by the production of IFN-γ, the main macrophage-activating cytokine, but can also secrete TNF-α, GM-CSF, IL-2 and lymphotoxin (LT-α or TNF-β), which activates macrophages, inhibits B cells and is directly cytotoxic for some cells (98, 99). Th1 cells generally express the chemokine receptors CXCR3 and CCR5 (99). As potent macrophage activators, Th1 cells are key in the defence against intracellular pathogens like *Leishmania* and *Toxoplasma* (100-102). However, aberrant Th1 type responses have been associated with a number of chronic inflammatory disorders, including multiple sclerosis (103), Type I diabetes (104), and IBD (105).

Th2 cells differentiate in response to IL-4, which drives expression of the key transcription factor Gata binding protein 3 (Gata-3), and are characterised by the production of amphiregulin, IL-4, IL-5, IL-9, and IL-13 (98). Other factors shown to promote Th2 responses are TSLP, IL-25 and IL-33, which are secreted by epithelial cells upon tissue injury and prime DC and basophils to drive a Th2 type response (106, 107). The Th2 program is actively suppressed when cells are committed to a Th1 lineage since T-bet suppresses the expression of Gata-3 (108). Th2 immunity has been shown to ameliorate Th1 or Th17 driven inflammation and promote tissue repair (109, 110). Th2

responses have been attributed several functions thanks to the vast array of cytokines they secrete. To name a few: IL-4 facilitates the IgE switch in B cells; IL-5 drives the generation and activation of eosinophils and thus defence against parasites like helminths; IL-19 can activate mast cells and ILC2; amphiregulin promotes epithelial repair; IL-13 drives mucus production, goblet cell metaplasia and type 2 macrophage differentiation among other functions (107, 110, 111). Disproportionate Th2 responses can lead to several adverse reactions including allergic diseases, like food allergies and asthma and antagonism of antitumor defence through inhibition of Th1 and cytotoxic T cell responses (99, 107, 108, 112, 113).

The inflammatory cytokines IL-6, IL-23, and IL-1β, when elaborated in the presence of transforming growth factor β (TGFβ), stimulate the expression of the retinoic acid-related orphan nuclear hormone receptor (RORγt) transcription factor that drives the differentiation of Th17 cells. This subset is characterised by the production of IL-17, IL-17F and IL-22 (114, 115). Due to the broad distribution of the receptors for these cytokines, Th17 activation leads to neutrophil influx and activation that is often associated with tissue inflammation. Th17 responses are important for combating extracellular bacterial and fungal infections but are also associated with autoimmunity, cancers, and have a potential role in the development of IBD (116-119).

Another $CD4^+$ T cell that can produce IL-22 is the Th22 subset that is dependent on IL-6 and the aryl hydrocarbon receptor (AhR) transcription factor for its differentiation. Th22 cells are characterised by the production of IL-22 and have been shown to provide effective antibacterial defence against mucosal pathogens by promoting AMP production and barrier repair (120, 121). Finally, an essential cell type for the maintenance of tolerogenic responses in the gut are the $CD4^+$ Treg cells which are induced upon TGF-β signalling that drives expression of their key transcription factor Foxp3 (122). Treg cells are abundant in the intestine where they control potentially deleterious responses towards dietary and microbial stimuli by exerting anti-inflammatory effects through the release of immune suppressive factors such as IL-10 and TGF-β (117, 123, 124).

IEL

The intestinal epithelium is heavily populated by specialised T cells known as IEL (125). These cells are anchored to epithelium through the expression of CD103 or αEβ7 integrin which binds E-cadherin on IEC (126). Unlike other T cells, IEL do not need priming for

activation and reside in close association with IEC in an activated phenotype (15). Indeed, irrespective of their MHC restriction and T cell receptor (TCR) lineage specification, both $CD4^+$ and $CD8^+$ IEL progressively acquire CD8αα homodimer expression, an absent phenotype from circulating T cells that is associated with decreased sensitivity to antigen (tolerised state)(127-129). Notably, CD8αα TCRαβ IEL have only been characterised in mice and are believed to recognise non-polymorphic MHC class IB molecules (15). IEL are functionally heterogeneous and include both TCRαβ and TCRγδ populations. IEL γδ T cells recognize class-I like molecules on stressed IEC, produce IL-17 upon infection, and are thought to promote resolution and repair through secretion of keratinocyte growth factor (TGFβ) (130-135). Interestingly, γδ T cells are specially enriched in the gut mucosa compared to other lymphoid tissues (94). Due to IEL's close contact with the intestinal epithelium, it is believed that their maintenance and function is modulated by IEC (15). Although their functions are unclear, suggested roles are cytotoxicity, cytokine secretion, regulation of intestinal epithelium replenishment and tolerance (136).

ILC

An additional cell type of emerging interest are innate lymphoid cells. They are believed to play important roles in intestinal immune homeostasis (137). ILC are classed as innate cells as they lack properties of adaptive cells, like the recombined antigen-specific receptors (138). They are found at barrier surfaces including the intestine and are partially regulated by epithelial-derived signals (15, 139). ILC are classified into three groups (ILC1, ILC2 and ILC3) according to their differential cytokine expression patterns and their developmental requirements.

ILC1, phenotypically similar to natural killer (NK) cells, are characterised by Th1 type cytokine production (IFNγ and TNF) in response to IL-12 and/or IL-15 (140). Although ILC1 are limited to cytokine production, NK cells can kill target cells through cytotoxic activity (perforin and granzymes), especially virus-infected cells (141, 142). NK cells were originally classed as ILC1 but further analyses of the ILC family members indicated that NK cells and ILC1 are separate lineages (141). ILC2 produce Th2 type cytokines (IL-5 and IL-13) and are responsive to IL-25, IL-33 and thymic stromal lymphopoietin (TSLP) (15, 140, 143-146). Finally, ILC3 produce Th17 and Th22-associated cytokines, including IL-17A and IL-22 in response to IL-23 (15, 140). IL-22 has tissue protective and repair functions in the intestine (121, 147). Conversely, IL-17 has pro-inflammatory

effects and has been implicated in mouse colitis models and human IBD (15, 148-150). Although ILC have been attributed functional roles in mouse models of intestinal disease and inflammation, the relevance of ILC to human disease is poorly understood (15).

B cells

Antigen presentation at the intestinal mucosa is also important for IgA secretion. Indeed, antigen presentation to naïve B cells by intestinal DC carrying antigens from the intestinal epithelium promotes heavy chain class-switch recombination (CSR) in activated B cells, turning them into mature IgA producing plasma cells (151). Secretory IgA is the dominant antibody isotype of the mucosal immune system. Secretory IgA is a dimer that is released into the luminal surface of the gut by transcytosis through IEC with the aid of pIgR in the basolateral surface of IEC (152, 153). Once released into the lumen, secretory IgA remains embedded in the mucus layer and is able to neutralise pathogens or toxic luminal products. Low numbers of IgM and IgG secreting plasma cells are also present in the LP (62, 154, 155).

1.2. Inflammatory Bowel Disease. A breakdown in intestinal homeostasis

During normal physiological conditions, intestinal homeostasis relies on the ability of gut-associated DC and macrophages to preferentially induce the differentiation of Tregs and thus the release of anti-inflammatory cytokines such as IL-10 (76, 156). These cytokines prevent aberrant responses against the commensal microbiota. Conversely, pathogens activate DC to promote the differentiation of naive $CD4^+$ T-cells into Th1, Th2, or Th17 lineages (150, 157). Together with macrophages and DC, Th cells secrete pro-inflammatory cytokines in order to recruit and activate the appropriate cells and factors required to eliminate the pathogen (158). Deregulation and over-stimulation of the immune system results in the breakdown of homeostasis, leading to increased T-cell responses against intestinal microflora that Tregs are unable to suppress (76, 159). This disproportionate reaction induces chronic inflammation and tissue damage that is characteristic of disorders like IBD, including Crohn's disease (CD) and ulcerative colitis (UC). Genome-wide association studies (GWAS) have identified many genetic loci that are related with intestinal inflammation. Many of these genes play a role in inflammation

and immunity, including: *IL-1R* (160), *IL-18R1-IL-18RAP* locus (161, 162), *IL-23*, and PRR such as *NOD2* and *NLRP3* (160).

1.3.Innate immunity and pattern recognition receptors

Innate immune responses are a vital first line of defence against invading pathogens. Discrimination between self and foreign antigens is required for the innate immune system to mount an adequate immune response (163). However, deregulated innate immune responses can contribute to the development of pathological inflammation. Pathological inflammatory responses can occur when an immune response is targeted against self-antigens or beneficial symbionts such as the gut microbiota. To date, it is not clear what initiates the deregulation of innate immunity causing it to mount an unnecessarily strong inflammatory response (164).

To rapidly respond to threats the innate immune system relies on a set of PRR (165). PRR can recognise conserved pathogen-associated molecular patterns (PAMP) that are present in microbial proteins, nucleic acids, lipids, and carbohydrates, or danger associated molecular patterns (DAMP) released from damaged or dying cells (64). There are different families of PRR, including membrane-associated Toll-like receptors (TLR) and C-type lectin receptors (CLR), as well as cytoplasmic Nucleotide-binding domain (NBD) and a Leucine-rich Repeat (LRR) domain receptors (NLR) and retinoic acid inducible gene I-like helicase receptors (RLR). These receptors are able to recognize a wide variety of signals associated with infection by different types of pathogens (166-168).

The TLR and NLR families are characterized by a variable number of ligand-sensing LRR at their N-terminal (TLR), or C-terminal (NLR) regions, and at least one domain for protein-protein interactions (Toll/Interleukin-1 receptor (TIR); Caspase activation and recruitment domains (CARD); pyrin domain (PYD)), or oligomerisation (NACHT). Mutations modifying the function of PRR are associated with auto-inflammatory diseases (NLR) and autoimmune disorders (TLR and NLR), and/or increased susceptibility to infection (169, 170).

1.3.1. Toll-like receptors

Ten functional TLR have been identified in humans (12 in mice). TLR1-9 are conserved between human and mouse. However, TLR10 is non-functional in mice due to a retro-viral insertion and TLR11-13 are not present in humans (171). TLR1, 2, 4, 5 and 6 are located on the cell surface, while TLR 3, 7, 8 and 9 are found in intracellular compartments, particularly endosomes, where they are activated by microbial nucleic acid recognition (168, 172) (Table 1.1). TLR expression is not restricted to innate immune cells, as they are also expressed by lymphocytes and various non-hematopoietic cell types (15).

All TLR have a common extracellular LRR domain, a transmembrane helix, and a cytoplasmic TIR domain. The TIR domain allows them to interact with intracellular adaptor molecules that also contain a TIR domain. Most TLR signal through the adaptor molecule Myeloid differentiation primary response gene 88 (MYD88). However, other adaptor molecules such as TIR-domain-containing adaptor molecule (TRAM) and TIR-domain-containing adaptor protein inducing IFN-β (TRIF) can signal downstream of TLR3 and/or 4 in a MYD88-independent maner (173).

The MYD88-dependent pathway signals through IL-1 receptor-associated kinase 1/4 (IRAK1/4) and TNF receptor-associated factor 6 (TRAF6), to drive mitogen-associated protein kinase MAPKKK signalling and TGFβ-activated kinase 1 (TAK1) activation. In the MYD88-independent pathway, TRIF can interact with TRAF6 and again activate the TAK1 complex (173). TLR signalling ultimately leads to the activation of multiple pro-inflammatory signalling cascades including nuclear factor kappa-light-chain-enhancer of activated B cells (NF-κB), c-Jun N-terminal kinases /Activator protein 1 (JNK/AP1), Extracellular signal–regulated kinases (ERK) and p38, and as well as the IFN pathway (174). NF-κB is considered the master switch of inflammation. Its activation and translocation into the nucleus, where it functions as a transcription factor, regulates over 100 pro-inflammatory mediators (168, 175). The activation of this pathway prompts the recruitment of other cells of the immune system, thus acting as a bridge between innate and adaptive immunity (176).

Despite the thought that microbiota would somehow avoid being recognized by PRR, TLR-microbiota dialogue occurs during steady-state conditions. In the intestinal epithelium, microbial sensing by IEC ensures intestinal homeostasis (15, 177). Indeed,

the treatment of TLR-2 and -4 and MYD88-deficient mice with broad-spectrum antibiotics demonstrated that microbiota-derived signals contribute to intestinal homeostasis and repair upon chemically induced colitis with dextran sodium sulphate (DSS) (178). TLR signalling in IEC was shown to regulate IEC proliferation, expression of AMP and IgA secretion into the intestinal lumen, among other functions (178-180). However, due to the proximity of IEC to the variety of microbial signals in the intestinal lumen, certain systems are in place to maintain epithelial hypo-responsiveness to commensal stimulus (181-183). Nevertheless, the microbial signals that TLR can sense are not unique to pathogens. Therefore, in addition to maintaining IEC hypo-responsiveness, innate immune pathways must discern between pathogenic and commensal microbes (15). Negative regulation of TLR signalling pathways involves a complex network of complementary mechanisms, including; subcellular localization, degradation, deubiquitination, and competition (reviewed in (184, 185)).

The polarised nature of IEC allows for compartmentalisation of TLR to the basolateral or apical membranes of IEC. TLR5 expression was found to be restricted to the basolateral surface of IEC, thereby preventing activation of this receptor by luminal flagellin (186). Conversely, TLR2, TLR4, and TLR9 were found at both the apical and the basolateral surfaces (187, 188) (Table 1.1). Nevertheless, expression of the TLR does not mean that they signal equally or with the same downstream consequences when activated at different sites. For instance, basolateral exposure of an IEC line (polarised Caco-2) to various TLR9 ligands resulted in NF-κB activation, whereas apical exposure led to IκB stabilisation and thus NF-κB inhibition, and inducing tolerance to subsequent TLR stimulation (15, 188).

Notably, the complexity of studying epithelial cells in isolation has hampered the temporal-space mapping of TLR expression and activation in primary IEC (189). Therefore, TLR expression and functional studies on IEC ought to be interpreted with caution.

To add to the complex landscape of TLR signalling in the intestinal epithelium, the ways by which IEC override their relative hypo-responsiveness and respond to a pathogenic threat remain ill defined. In addition, microbial signals can activate multiple PRR, including NLR, that are localised in the cell cytosol and can rapidly respond to pathogen

invasion (190). The simultaneous activation of more than one PRR may hold the key to understand the breakdown in IEC tolerance during infection and inflammation.

Table 1.1. Toll-like receptors (TLR): Location and ligands. Adapted from (189, 191).

TLR	Subcellular location	Location within IEC	Adapter	Ligand	Effector responses by professional immune cells	Ref
1	Cell surface	ND	MYD88	Triacylated lipoproteins. Acting in conjunction with TLR2.	IL-6, TNF-α	(192)
2	Cell surface	Apical and basolateral	MYD88, TIRAP	Di/tri-acylated lipoproteins. Gram-positive derived bacterial lipopeptides, peptidoglycans, lipoteichoic acids, zymosan, and mannan.	IL-6, TNF-α, IL-8, MCP-1, RANTES	(193)
3	Endosome	ND	TRIF	Viral dsRNA and self RNAs derived from damaged cells	IFN-β	(194-196)
4	Cell surface	Apical and basolateral	MYD88, TRIF, TIRAP,TRAM	lipopolysaccharide (LPS) derived from Gram-negative bacteria	IL-6, TNF-α, IFNβ, IP-10	(173)
5	Cell surface	Basolateral	MYD88	Flagellin	TNF-α	(168, 197)
6	Cell surface	ND	MYD88, TIRAP	Diacylated lipopeptides. Acting in conjunction with TLR2.	TNF-α, IL-6, IL-8, MCP-1, RANTES	(198)
7	Endosome	ND	MYD88	Single stranded viral RNAs or guanosine-related analogues such as loxoribine and imidazoquinoline	IFN-α	(168, 197, 199)
8	Endosome	ND	MYD88	Single stranded viral RNAs or guanosine-related analogues such as loxoribine and imidazoquinoline	IFN-α	(172)

TLR	Subcellular location	Location within IEC	Adapter	Ligand	Effector responses by professional immune cells	Ref
9	Endosome	Apical and basolateral	MYD88	Bacterial and viral unmethylated CpG-DNA motifs (common to prokaryotic genomes and DNA viruses)	IFN-α	(168, 197, 200)
10	Cell surface. Not in mice	ND	MYD88	ND	ND	ND
11	Endosome Not in humans	ND	MYD88	Flagellin and profillin	IL-12, TNF-α	(201)
12	Endosome Not in humans	ND	MYD88	Combines with TLR11 to recognise flagellin and profillin	IL-12p40, IFN-α	(202)
13	Endosome Not in humans	ND	MYD88	23S rRNA	IL-6, IL-12p40	(203-205)

1.3.2. NLR

In contrast to TLR, NLR are located intracellularly and thus recognise PAMP and DAMP that cross cellular membranes. Their activation initiates diverse signalling pathways that allow cells to mount an appropriate defensive response. NLR are highly conserved throughout evolution and are expressed by both hematopoietic and non-hematopoietic cells, attesting to their important role in host innate immunity (206). NLR proteins have a common domain organization with a central NBD named NACHT domain (Naip, CIITA, HET-E, and TP-2), an N-terminal effector domain, and a C-terminal LRR (207). The central domain is involved in dNTPase activity and oligomerisation (208), the C-terminal LRR is presumably involved in ligand sensing and binding (209), as well as having an autoinhibitory role (210), and the N-terminal domain interacts with effector proteins or signalling adaptors (169).

The way in which NLR recognise their ligand is under scrutiny in the inflammasome field (211). The function of ligand sensing and binding has long been attributed to the LRR domain by analogy to the LRR sensing domain of TLR (212). Tenthorey *et al.* mapped the domain in Naip proteins that is responsible for specific ligand detection (213). Conflicting with previous assumptions, the LRR domain was not involved in ligand specificity. Instead, several α-helical domains associated with the NBD were responsible for this (213).

NLR subfamilies are classified according to two systems: one based on their type of N-terminal domain (NLRA, B, C and P) and the other one based on their phylogenetic relationship (Nlrc3, Nlrc5, and Nlrx1 are commonly classed as Nlrc despite their unclassified N-terminal domains) (214). Classification according to their N-terminus denotes four NLR subgroups: the acidic transactivation domain (NLRA), the baculoviral inhibitory repeat (BIR)-like domain (NLRB), the CARD (NLRC), and the PYD (NLRP) (214). The different NLR can perform very diverse functions that reflect the vast number of ligands they can recognise and the nature of their downstream signalling adaptors (Table 1.2, Figure 1.4).

Table 1.2. NLR family members & other inflammasome components. Abbreviations: SCFA (small chain fatty acids), ND (not determined), NA (Not applicable), T3SS (type three secretion system). Adapted from (1).

NLR component		Ligand/Agonist	Expression in IEC
NLRA (Acidic transactivation domain)	CIITA	Unknown	+ (215, 216)
NLRB1 (BIR domain)	Naip1, Naip2	T3SS needle (Naip1) and rod (Naip2) (209, 217)	+ (218-220)
	Naip5, Naip6	Flagellin (209, 217)	+ (218-220)
NLRC (CARD domain)	Nlrc1 (NOD1)	iE-DAP (221)	+ (222)
	Nlrc2 (NOD2)	MDP (223, 224)	+ (222, 225, 226)
	Nlrc4	Flagellin, T3SS rod proteins (via Naip) (227-229)	+ (230-232)
NLRC (unclassified domain)	Nlrc3 + 5	Unknown	ND
	Nlrx1	ssRNA, dsRNA, poly (I:C) (233)	+ (234)
NLRP (PYRIN domain)	Nlrp1	Anthrax lethal toxin ATP, MDP (235, 236)	+ (237)
	Nlrp3	ATP, MSU, Toxins, oxidised mitochondrial DNA, alum, silica, UV radiation, amyloid β (169, 238), SCFA (Acetate) (239)	+/- (1, 232, 240)
	Nlrp6	Metabolites (e.g. Taurine, Spermine, Histamine) (241)	+ (242-244)
	Nlrp7	Microbial lipopeptides (245)	ND
	Nlrp9b	dsRNA (246)	+ (246)
	Nlrp12	*Yersinia pestis* (247)	ND
	Nlrp2, 4, 5, 8, 10, 11, 13 + 14	Unknown	ND
Other inflammasome components		**Ligand/Agonist**	**Expression in IEC**
AIM2		dsDNA	+ (248)
Asc		PYD or CARD domains	+ (219, 249)
Caspase-1		CARD domains	+ (232, 250, 251)
Caspase-11		LPS + CARD domains	+ (251-254)
Caspase-8		CARD domains	+ (230)
IL-1β		NA	+ (251)
IL-18		NA	+ (251, 255-258)
Gasdermin D		NA	+ (230, 246, 259)

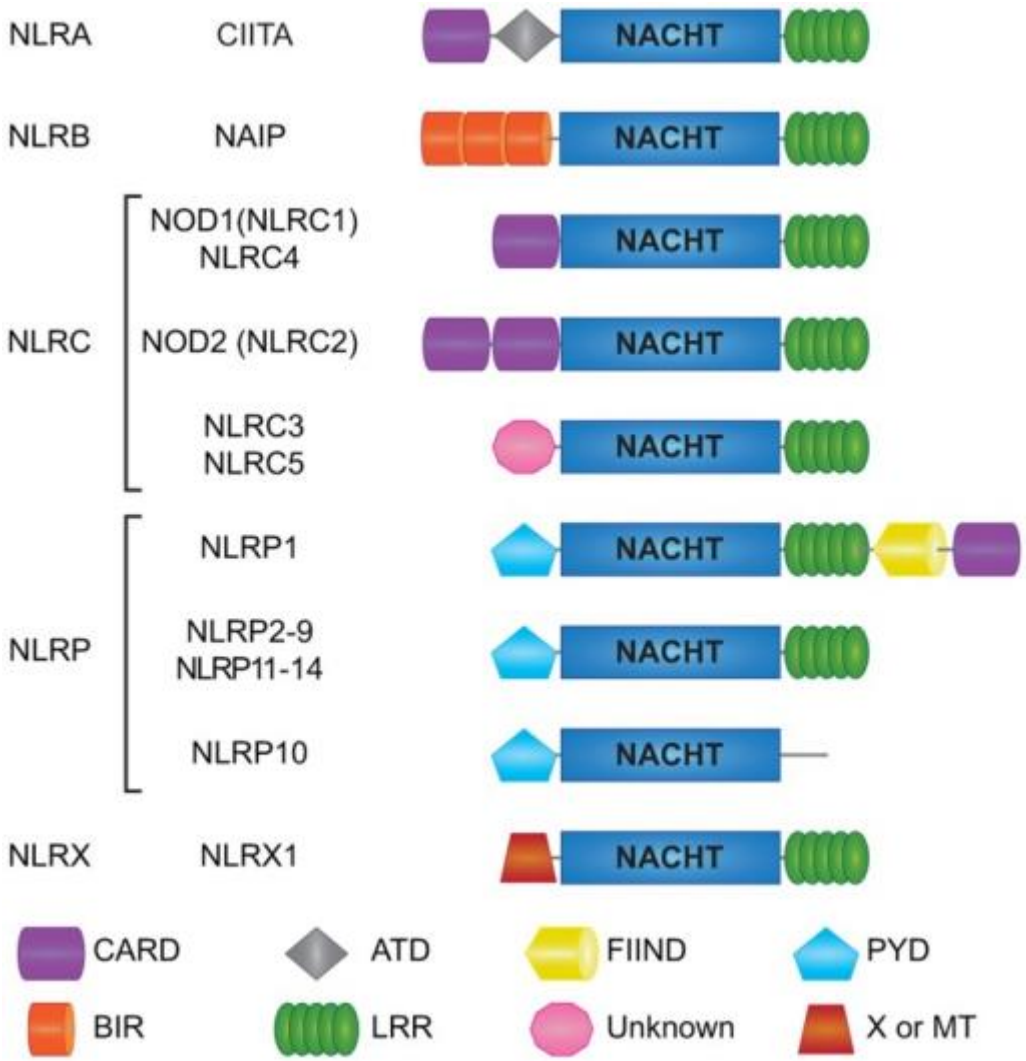


Figure 1.4. Schematic representation of human NLR domain architecture. Human NLR are sub-classified into five categories: NLRA, NLRB, NLRC, NLRP, and NLRX. All 22 human NLR contain a central NACHT domain and a C-terminal ligand sensing LRR domain, except for NLRP10. Functional characteristics of the NLR are assigned through their N-terminal domains. The functions of some NLR domains remain elusive, including the N-terminal domain of NLRC3 and NLRC5, as well as the C-terminal FIIND (function to find domain) in NLRP1. MT; targets NLRX1 to the mitochondria but no sequence homology with traditional mitochondrial targeting sequence has been reported. Figure taken from (260).

1.4.The inflammasome

Two different forms of inflammasomes have been described; those that are formed from a member of the NLR family and those containing members of the PYD domain and HIN domain containing family (PYHIN) (261). The activation of PYHIN inflammasomes such as absent in melanoma 2 (AIM2) and interferon-inducible protein 16 (IFI16) is better understood than NLR inflammasomes, as AIM2 and IFI16 contain DNA-binding HIN domains that act as receptors for dsDNA (248, 262). Inflammasome forming NLR to date include Nlrc4 and its associated NLR Family Apoptosis Inhibitory Protein (Naip) adaptors, Nlrp1, 2, 3, 6, 7, 9b, and 12 (263, 264).

Inflammasome activation in myeloid cells requires two signals: a priming signal (lipopolysaccharide (LPS), for example) sensed by TLR to drive transcription of some NLR and pro-IL-1β/-IL-18 and a second signal (DAMP for instance) for the activation of NLR (265)(Figure 1.5). Nevertheless, there is evidence suggesting that signal 1 is dispensable for the priming of IL-18 as the pro-form of this cytokine is constitutively expressed in both myeloid and epithelial cells (266, 267).

Upon sensing of endogenous or exogenous cytosolic danger signals, NLR form oligomers through their NACHT domains. Activated NLR facilitate the recruitment of pro-caspase-1 and the formation of the inflammasome. The recruitment of caspase-1 can be mediated through direct interaction between the CARD domains of some NLR such as Nlrc4 and that of caspase-1 (190). However, for NLR lacking a CARD domain, a bridging adaptor molecule named apoptosis-associated speck-like protein containing a CARD (Asc) is needed to form inflammasomes. This occurs by facilitating the interaction between the PYD domains of Asc and NLR and the CARD domains of Asc and caspase-1 (268-270). Asc is present in the cytosol of resting cells and contains both PYD and CARD domains that are brought together by a flexible linker region. Analogous to apoptotic protease activating factor 1 (Apaf1) in the apoptosome, Asc oligomerises into disk-like structures ("Asc-specks") that contribute to the formation of a macromolecular platform for inflammasome activation.

The main result of inflammasome activation is the auto-cleavage of pro-caspase-1 (45 kilodalton (kDa)) into 35 kDa and 10 kDa fragments. Then, the CARD containing p35 fragment is cleaved into the CARD domain and a further p20 fragment that heterodimerises with two p10 subunits to form active caspase-1 (271). This is an

aspartate-specific cysteine protease that cleaves pro-IL-1β (31 kDa) and pro-IL-18 (24 kDa), at recognition sites adjacent to aspartate residues (268). The cleavage of these two pro-inflammatory cytokines is required for their secretion from the cell. Furthermore, caspase-1 activation can also lead to pyroptosis, an inflammatory form of programmed cell death (Figure 1.5; discussed later).

Genetic mutations in NLR inflammasome components associated with constitutive activation of the inflammasome and over-secretion of active IL-1β (17 kDa) and IL-18 (22 kDa), have been causally linked to certain rare auto-inflammatory disorders (272). For instance, mutations in Nlrp3 lead to the development of cryopyrin-associated periodic syndromes (CAPS) including neonatal onset multisystem inflammatory disease (NOMID) and Muckle–Wells syndrome (MWS) (273-275). Further research is necessary to identify factors that regulate inflammasome activation, to characterize the cell type-specific effects of NLR/inflammasome dependent signalling and to determine how defects in these pathways contribute to the development and progression of inflammation-related pathological conditions.

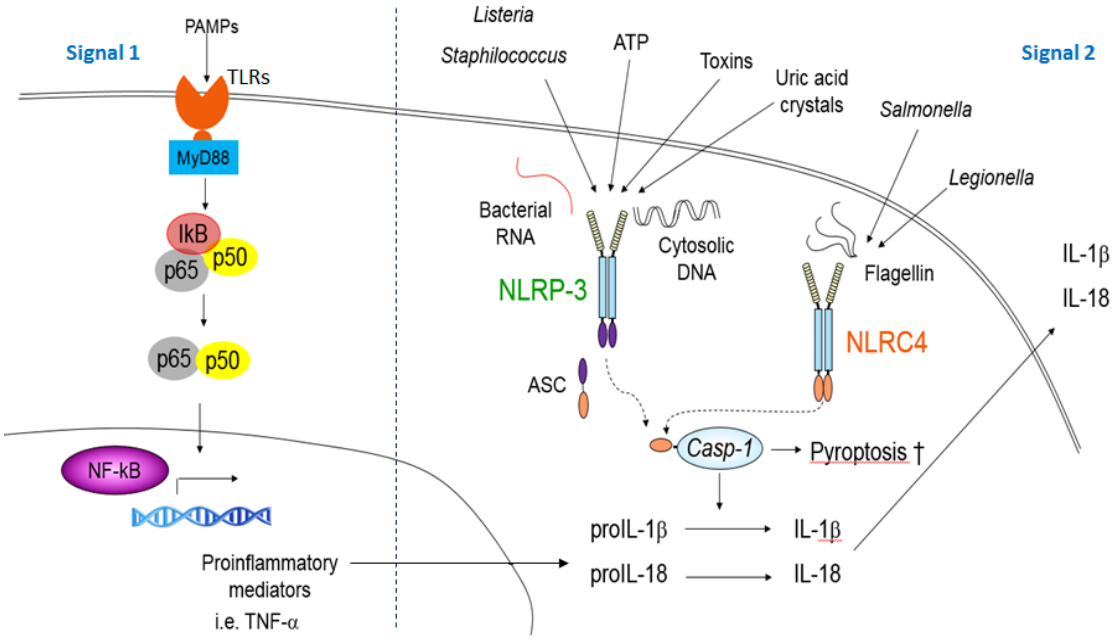


Figure 1.5. The two-signal model of NLR-mediated inflammasome activation. Optimal inflammasome activation is believed to require two signals. Signal 1 mediates the transcription of inflammasome components and substrates, such as Nlrp3, proIL-1β and pro-IL-18, and is typically provided by TLR signalling, via MyD88 and NFκB. TLR signalling leads to phosphorylation, polyubiquitination and degradation of the inhibitor of NFκB, IκB. The degradation of IκB releases repression of NFκB, allowing it to move into the nucleus and drive transcription of a multitude of inflammatory genes e.g. IL-6, TNF-α and CXCL2 (276). Signal 2 promotes activation of the cytosolic NLR sensors and, depending on the NLR, may be delivered by a wide variety of PAMP or DAMP. NLR have a characteristic three domain structure: an N-terminus LRR; a central NACHT domain; and C-terminus PYD or CARD (207, 277). Following activation by signal 2, auto-repression by the LRR domain is relieved, allowing the NLR to form oligomers through their NACHT domains. Recruitment of pro-caspase-1 can be mediated through direct CARD-CARD interactions between the CARD domains of some NLR, such as Nlrc4, with that of pro-caspase-1. However, for the PYD-containing Nlrp subset (including Nlrp3), a bridging adaptor molecule named Asc is needed. Asc contains a PYD and CARD domain, using the former to associate with the NLR and the latter to recruit pro-caspase-1. Once assembled, inflammasomes facilitate the autocatalytic cleavage of pro-caspase-1, leading to the release of active capase-1, resulting in cleavage and secretion of the inflammatory cytokines IL-1β and IL-18, and an inflammatory form of cell death termed pyroptosis (190, 207, 265). It should be noted that these pathways have been deduced from studies in myeloid cells and whether inflammasome activation pathways and effector responses are conserved in non-haematopoietic cells, such as IEC, remains to be established.

1.4.1. Nlrp3

The Nlrp3 or cryopyrin inflammasome is the most widely studied inflammasome. It contains a PYD domain thus requiring Asc for inflammasome formation and recruitment of caspase-1. Nlrp3 responds to a wide range of ligands and/or stimuli (265) (Table 1.2). Since Nlrp3 is unlikely to recognise such diverse motifs, much work has focussed on identifying the common mechanism by which Nlrp3 senses this vast variety of stimuli. Although there is no consensus on a common mechanism for Nlrp3 activation, Nlrp3 is likely to sense the disturbance of cellular homeostasis (265, 278). The most widely reported mechanisms leading the activation of this inflammasome include changes in redox status or cellular ion concentration (207, 279). These likely occur through the formation of membrane/pores or channels coupled with K^+ efflux and lysosomal and mitochondrial damage (Table 1.3)(279). The latter two mechanisms result in release of lysosomal and mitochondrial mediators and reactive oxygen species (ROS) production that can signal to various mediators capable of interacting with Nlrp3 (Table 1.3). The nature and full spectra of these mediators however, remains poorly understood.

Given the vast array of stimuli that can activate the Nlrp3 inflammasome, its activation is tightly regulated. In quiescent state Nlrp3 is expressed at low levels and TLR stimulation is essential for NF-κB-dependent production of Nlrp3 and pro-IL-1β (280, 281) (as outlined in Figure 1.5). Furthermore, activation of the Nlrp3 inflammasome is further regulated by post-transcriptional mechanisms, such as ubiquitination and de-ubiquitination of Nlrp3, and its downstream effector molecules (265, 282-286).

Disruption of Nlrp3 inhibition (272) or gain-of-function mutations in the *Nlrp3* gene (287), are associated with autoinflammatory diseases grouped under the name of CAPS. CAPS include familial cold autoinflammatory syndrome (FCAS), MWS, and NOMID. These rare diseases result in systemic inflammation and are characterised by an overproduction of IL-1β (288, 289).

Table 1.3. Proposed mechanisms of Nlrp3 inflammasome activation. Non-exhaustive list. Abbreviations: (NEK) NIMA-related kinases, (TXNIP) Thioredoxin-interacting protein, Mitochondrial antiviral-signalling protein (MAVS), mitochondrial DNA (mtDNA), endoplasmic reticulum (ER).

Mechanism of Nlrp3 activation	Triggers	Downstream consequences
Pore/channel formation	P_2X_7 activation triggers the opening of pannexin-1 channel. Triggered by ATP and pore forming toxins i.e. nigericin (290-292).	**1)** K^+ efflux, implicated in caspase-1 activation (293).
		2) PAMP and DAMP gain access to the cell cytosol and directly engage Nlrp3 (294).
		3) K^+ efflux leads to NEK7 to create an Nlrp3–NEK7 complex and Nlrp3 oligomerization and activation (295).
Lysosomal destabilization	Frustrated phagocytosis leads to lysosomal rupture. Triggered by sterile particulate and crystalline matter (296).	**1)** Cytosolic release of lysosomal cathepsins which bind and activate Nlrp3 (297).
		2) Rising ROS concentrations leads to ER stress and TXNIP release from thioredoxin and binds to the LRR domain of Nlrp3 and triggers its activation (298-300).
Mitochondrial damage	Mitochondria proposed as a platform for assembly of the Nlrp3. MAVS directly bound Nlrp3 and co-localized to the mitochondria (301).	**1)** mtDNA (302, 303), and phospholipid cardiolipin(304) release.
		2) Rising ROS concentrations (298).
		3) $Ca2^+$ signalling coupled with mitochondrial damage (305-307).

1.4.2. Nlrc4

The Nlrc4 or Ipaf inflammasome is activated upon cytosolic invasion by intracellular bacteria and components of active bacterial type III (T3SS) and IV (T4SS) secretion systems (229, 308). Nlrc4 is unique amongst other inflammasomes in that it requires another member of the NLR family as an adaptor. The Naip proteins are the sensors of the Nlrc4 inflammasome, facilitating the interaction between Nlrc4 and the different ligands recognised by this inflammasome (309). However, the precise mechanism by which Naip and Nlrc4 interact with each other remains unknown (310). C57BL/6 mice possess four Naip: Naip1 detects the needle of the T3SS (311, 312), Naip2 detects the T3SS rod, and Naip5 and Naip6 detect flagellin (T4SS) (209, 313). On the other hand, humans appear to possess only one Naip that senses the needle protein and does not seem to respond to flagellin (311, 313).

The specificity of Naip-Nlrc4 for flagellin was confirmed by the observation that flagellin-deficient bacteria are unable to activate the inflammasome and lead to caspase-1 secretion (314, 315). Furthermore, purified recombinant flagellin delivered directly into the cytosol is enough to activate the inflammasome (227). Like the rest of inflammasomes, Nlrc4 engages caspase-1 to drive its effector responses. In contrast with other inflammasomes, the presence of a CARD domain in Nlrc4 allows the Nlrc4 inflammasomes (and the Nlrp1 inflammasome) to recruit and activate caspase-1 directly, independent of Asc (217, 316). However, the consequences of Asc-independent inflammasome activation and their *in vivo* relevance are not fully understood (1).

Nlrc4 inflammasome plays a central role in innate immune defence against invading pathogens. Indeed, Nlrc4 has been shown to severely restrict intracellular pathogen replication in several cell types (317-319). Naip specific deletion in IEC revealed their importance in the extrusion of infected IEC into the intestinal lumen following *Salmonella enterica* serovar Typhimurium (*S.* Tm) challenge of streptomycin-treated mice (220). Pyroptosis seems to be at the heart of Nlrc4 effector responses by inducing a rapid lytic cell death that leads to the expulsion of bacteria from their intracellular niche and exposing them to detection by the immune system (320, 321). However, it is unclear if the mechanisms leading to pathogen clearance fully overlap from one cell type to another. Several reports indicate that IEC bear a functional Nlrc4 inflammasome, and

current effort is directed at understanding the consequences of Nlrc4 activation in IEC (220, 230, 231).

Gain-of-function mutations in Nlrc4 has been shown to lead to serious auto-inflammatory conditions (322). These mutations appear to alter the auto-inhibition on Nlrc4 and lead to spontaneous caspase-1 activation and associated with increased levels of IL-18 (323, 324). The conditions are characterised by fever, diarrhoea, splenomegaly and duodenal inflammation, among other symptoms (217, 323). Nevertheless, there is an indication that these conditions have variable clinical symptoms, much like Nlrp3 gain-of-function mutations (217).

1.4.3. Consequences of inflammasome activation

1.4.3.1. Asc speck formation

The release of pro-inflammatory cytokines and alarmins are regarded as the major contribution of inflammasome towards inflammatory responses (325). However, pyroptotic BMDM have been shown to release parts of the inflammasome complex as particulate danger signals that can activate immune cells once phagocytosed leading to amplification of inflammasome signalling (326). Both agglomerations of Asc (termed Asc specks) and Nlrp3 have been reported to have so called 'prionoid' activities *in vitro* (326-328). Although there are instances where Asc specks have been observed *in vitro*, the occurrence and relevance of these structures *in vivo* remain poorly understood and their research is limited by a dearth of tools (326, 329).

Besides acting as an inflammasome amplifying/perpetuating signal, Asc specks are considered a platform for efficient inflammasome activation. Indeed, inflammasomes containing Asc form specks where caspase-1 undergoes autoproteolysis leading to cytokine maturation and cell death (316, 330). In contrast, inflammasomes lacking Asc can activate caspase-1 in the absence of autoproteolysis and speck formation, leading to cell death but inefficient cleavage of IL-1β and IL-18 (316). However, the occurrences of Asc speck formation and completely Asc-independent processes *in vivo* remain to be shown (331).

1.4.3.2. Soluble mediators and inflammasome-associated IL-1 family cytokines

One of the most widely studied downstream consequences of inflammasome formation is the cleavage and activation of the inflammatory cytokines IL-1β and IL-18. The release of these cytokines is the final consequence of the inflammasome activation cascade. Thus, dysregulation of any component of the inflammasome signalling cascade is likely to affect IL-1β and IL-18 levels. As previously mentioned, deregulation of this pathway is linked to a range of inflammatory disorders (275).

These cytokines play an important role in immune signalling and have a wide range of target cells and functions. IL-1β is a pleiotropic cytokine that is responsible for increasing

the recruitment of granulocytes, activating and accumulating ILC and promoting Th17 responses from $CD4^+$ T cells (150, 255, 332, 333). The IL-1β signalling cascade is further amplified by its ability to induce adhesion molecules and chemoattractants from DC, macrophages, and neutrophils (334-336).

Inflammatory conditions, including IBD, have often been associated with increased levels of IL-1β production (337-339). The role of inflammasomes and IL-1β in the development of chronic intestinal inflammation has been studied in mouse models. Increased levels of mature IL-1β were reported in the colon of IL-10 KO mice that developed chronic colitis resembling human IBD (340). Furthermore, IL-1β has been shown to be essential for promoting the recruitment of granulocytes to the colon thus driving innate immune inflammation in response to *Helicobacter hepaticus* (150). In addition, T cell transfer models of colitis have identified this cytokine to be important for promoting the accumulation and survival of $CD4^+$T cells in the colon (150). Thus, not surprisingly, treatment with IL-1 receptor agonists (IL-Ra) or caspase-1 inhibitors or anti-IL-1β antibodies, suppressed IL-1β production from inflamed colon explants and ameliorated spontaneous colitis in IL-10 KO mice models (340). Furthermore, there have been reports of successful treatments with IL-1 signalling blocking agents (including IL-Ra) in reversing auto-inflammatory diseases associated with elevated levels of IL-1β, such as chronic granulomatous disease and rheumatoid arthritis (341, 342). Together, these studies suggest that inflammasomes drive the development of chronic intestinal inflammation through uncontrolled IL-1β secretion (150, 340).

In the context of infection, blocking IL-1β was also beneficial in ameliorating pathology in *Clostridium difficile*–associated colitis and *S.* Typhimurium–induced enteritis (343, 344). The importance of this cytokine lies in the fact that it mediates both local and systemic effects and can drive innate and adaptive immune responses in hematopoietic and non-hematopoietic cells (150). However, the effects of IL-1β are not only deleterious, and this cytokine is important in protective immunity against *C. rodentium.* This is supported by the observations that IL-$1R1^{-/-}$ and IL-$1\beta^{-/-}$ animals suffered from increased bacterial burden and pathology upon *C. rodentium*-induced colitis (345, 346).

The vast array of roles for IL-1β in inflammation and immunity may lie in the cell of origin of this cytokine and thus the different conditions promoting its secretion. In the gut, the primary source of IL-1β during intestinal inflammation appears to be the LP

phagocytes (150, 251, 347). Conversely, intestinal epithelial cells do not produce significant levels of IL-1β themselves (251, 348). This compartmentalisation may limit unnecessary inflammation by IL-1β. For instance, the LP leukocytes ought to be engaged in IL-1β for the onset of antimicrobial responses during barrier disruption and active pathogen invasion.

IL-18 is structurally very similar to IL-1β and both belong to the IL-1 family of cytokines. Unlike IL-1β which requires transcriptional priming, IL-18 is constitutively expressed in activated macrophages and DC, and in barrier cell types like keratinocytes and mucosal epithelial cells of the gut and lung (231, 257, 267, 349). Furthermore, IEC are the main source of IL-18 in the intestine and are involved in inflammatory responses as well as in homeostasis maintenance (231, 255). IL-18 was originally named IFNγ inducing factor (Igif) given its role in promoting Th1 responses and IFNγ production aimed at activating macrophages and neutrophils for intracellular pathogen killing (350, 351). IL-18 produced by IEC can also drive perforin production by NK cells during *S.* Tm infection (352). Moreover, in the context of specific co-stimulation, IL-18 has been shown to drive Th2 cytokine production (353), and IL-17 production by γδ T cells (354). These examples display the diverse consequences of IL-18 activation and release.

GWAS associated mutations within the *IL-18R1-IL-18 receptor accessory protein (RAP)* locus with increased susceptibility to IBD (161, 162, 355). Furthermore, increased levels of IL-18 production have been detected in colonic epithelial cells from Crohn's disease patients (257, 349). Curiously, IL-18 binding protein (IL-18bp), a negative regulator of active IL-18, was also reported to be elevated in CD patients (356, 357). Thus, the precise contribution of IL-18 to intestinal inflammation and pathology remains unclear.

Much effort has been concentrated in the role of IL-18 in intestinal pathology and homeostasis. However, murine models have yielded conflicting results that attribute IL-18 signalling with both protection and exacerbation of intestinal inflammation. Chemically induced intestinal damage and inflammation by DSS have revealed detrimental roles for IL-18 (358) (359). Indeed, biochemical inhibition of IL-18 or over-expression of IL-18 in IL-18 transgenic mice led to increased severity of DSS-induced colitis (358) (359). Conversely, IL-18 and IL-18R deficient mice also exhibited exacerbated colitis upon DSS, suggesting that under certain conditions IL-18 is beneficial during DSS-induced inflammation (242, 360). In support of a beneficial role for IL-18,

caspase-1 deficiency leading to reduced IL-18 was detrimental for DSS-induced pathology (361). Administration of recombinant IL-18 rescued this exacerbated phenotype (361). Interestingly, adoptive transfer of myeloid cells did not confer protection, suggesting that IL-18 from the non-hematopoietic compartment was important for mediating this protection (258).

More recent reports suggest that impaired IL-18 production due to Nlrp6 deletion leads to increased susceptibility to DSS injury, possibly due to a dysbiotic microflora (241, 242). This phenotype was ameliorated by rIL-18 treatment whose positive effects were attributed to increased AMP production by IEC (241). Asc and Nlrp6 deletion have been reported to lead to a dominant dysbiosis when compared to non-littermate wild-type C57BL/6 animals (241, 242). However, a recent report demonstrated, with the use of littermate controls and replicate experiments in different animal facilities, that Nlrp6 and Asc do not regulate the intestinal microbiota (362). Furthermore, in this study, Asc and Nlrp6-deficiency did not influence susceptibility to DSS (362).

The complicated landscape of IL-18 effects during DSS colitis could be explained by the dependency of this model on the composition of the microbiota. Indeed, microbiota do shape epithelial-immune responses at the host-microbe interphase (2, 363). In fact, DSS colitis is exacerbated in germ-free (GF) (364) and Myd88$^{-/-}$ mice (178) but ameliorated in antibiotic-treated genetically susceptible mice (242, 248, 365-368). This argues for a role of microbial signals in regulating host immune responses. In support of this notion, there is an indication that microbiota derived metabolites can modulate inflammasome activation and IL-18 secretion (241). Collectively these studies highlight the need to employ appropriate co-housing and/or littermate-controlled experimental design in studies aimed at understanding the immune responses at the host-microbe interface.

IL-18 has also been implicated in protection against infection induced intestinal inflammation. Decreased IL-18 secretion has been linked with increased susceptibility to *C. rodentium* colonisation and inflammation in *IL-18*$^{-/-}$ or *IL-18R*$^{-/-}$ mice. Deletion of individual inflammasome components, including *Casp-1*$^{-/-}$, *Asc*$^{-/-}$, *Nlrp3*$^{-/-}$, Nlrp6$^{-/-}$ or *Nlrc4*$^{-/-}$ were also associated with increased pathogen burden, possibly through decreased IL-18 secretion (231, 243, 249, 345, 369). In several of these studies, non-hematopoietic cells were deemed responsible for the protective effects of Asc, Nlrp3 and Nlrc4 against

C. rodentium (231, 249). Nevertheless, IL-18 was shown to be dispensable for the Nlrc4-mediated protection against *S*. Typhimurium, another enteric pathogen (220).

Epithelial protective responses of IL-18 during infection may be dependent on the nature of the threat and the level of damage induced to cells. Intestinal IL-18 signalling has been suggested to be important in maintaining homeostasis by mediating epithelial barrier repair and promoting AMP production via the IL-22 circuit (369-372). During infection, IL-18 was shown to drive IL-22 production, which in turn induced IL-18 secretion (369). Interestingly, IL-22 co-administration with IL-18 was associated with protection against rotavirus infection (373). Co-administration induced IEC transcriptional changes not observed with either cytokine alone (1, 373). Thus, the wide variety of roles associated with IL-18 may be explained by its ability to act in concert with other cytokines resulting in diverse context and tissue-dependent effects. Therefore, tissue-specific analysis of IL-18 signalling will help dissect the various roles of this cytokine in the immune system (1).

In addition to IL-18 and IL-1β, inflammasome activation leads to the release of other soluble mediators including alarmins like IL-1α and cytotoxic DAMP. IL-1α is another member of the IL-1 family that also lacks a signal peptide and is therefore not released through the conventional pathway of cytokine secretion. However, unlike IL-18 and IL-1β, IL-1α does not rely on post-translational processing for activation and is thus synthesised in its bioactive form (18 kDa) (374). IL-1α is considered an alarmin due to its release from cells that are damaged or undergoing a lytic form of cell death, including pyroptosis (375). Upon pyroptosis, many other inflammatory mediators are released alongside IL-1α. For instance, the alarmin High-mobility group box 1 (HMGB1), a nuclear non-histone DNA-binding protein that can trigger inflammation upon release (376, 377). Furthermore, inflammasome activation can also lead to the release of lipid inflammatory mediators, like eicosanoids (378, 379). Recently, Rauch *et al.* described the release of the prostaglandin eicosanoid PGE_2 from IEC upon Nlrc4 inflammasome activation with FlaTox (230). A comprehensive analysis of alarmins and other inflammatory mediators released upon inflammasome activation by different stimuli is currently unavailable. Proteomics studies on the secretome profile of different cell types undergoing various inflammasome activating stimuli will aid the understanding of the downstream consequences of inflammasome-related responses (1, 380).

Table 1.4. Soluble mediators of inflammasome activation and intestinal inflammation. Abbreviations: *C. rod* (*C. rodentium*), *S.* Tm (*S.* Typhimurium), Treg (T regulatory cells). Mutant strain abbreviations: *IL-18Tg* (IL-18 Transgenic: over expression of *IL-18*), *IL-18$^{\Delta IEC}$* (*IL-18*-deficient IEC), *IL-18$^{\Delta/HE}$* (IL-18-deficient haematopoietic cells), *IL-18r$^{\Delta IEC}$* (*IL-18R*-deficient IEC), *IL-18r $^{\Delta/HE}$* (*IL-18R*-deficient haematopoietic cells), *IL-18bp$^{-/-}$* (*IL-18* binding protein-deficient), *IL-18bp$^{-/-}$ IL-18r$^{\Delta/HE}$* (*IL-18bp$^{-/-}$* with *IL-18R*-deficient haematopoietic cells). Table adapted from (1).

Mutant Strain	Phenotype		Proposed mechanism
	Pathogen	**DSS**	
IL-1R1 signalling pathway			
IL-1αβ$^{-/-}$	↔ *S.* Tm load (220)		
IL-1β$^{-/-}$	↑ *C. rod* load and pathology (345)	↓ pathology (365)	
IL-1R1$^{-/-}$	↑ *C. rod* pathology (346)	↑ pathology (346)	
IL-18R signalling pathway			
IL-18$^{-/-}$	↔ *C. rod* load (346) ↑ *C. rod* load and pathology (345) ↔ *S.* Tm load (220) ↔ rotavirus load (246)	↑ pathology (242, 360)	
IL-18Tg		↑ pathology (359)	
IL-18$^{\Delta IEC}$		↓ pathology (358)	
IL-18$^{\Delta/HE}$		↓ pathology (358)	
IL-18R$^{-/-}$	↑ *C. rod* load and pathology (249)	↑ pathology (360)	
IL-18r$^{\Delta IEC}$		↓ pathology (358)	
IL-18r $^{\Delta/HE}$		↔ pathology (358)	
IL-18bp$^{-/-}$		↑ pathology (358)	↑ goblet cell loss (358)
IL-18bp$^{-/-}$ IL-18r$^{\Delta/HE}$		↔ pathology (358)	

1.4.3.3. Inflammasomes and cell death: pyroptosis and apoptosis

This section is my own work and has been submitted for publication (1).

Inflammasome functional studies to date have largely focused on the secretion of downstream soluble mediators. However, there is much emerging interest in the role of inflammasome-dependent cell death, termed pyroptosis (320, 381). Pyroptosis takes place following engagement of 'canonical' (caspase-1) or 'non-canonical' (caspase-11) inflammasomes. The 'non-canonical' triggering of pyroptosis occurs by intracellular LPS engagement with caspase-11 and has mainly been described in macrophages (382, 383).

Identification of the 'non-canonical' pathway followed from the finding that 129SvEv mice carried a passenger mutation that truncated the *Casp-11* gene (271), meaning that the original *Casp-1* knockout mice, which were generated on a 129SvEv background, were deficient in both *Casp-1* and *Casp-11*. Using caspase-11 complementation, Kayagaki *et al.* showed that macrophages underwent caspase-1-independent 'non-canonical' cell death in response to several inflammasome activating stimuli, including Gram-negative bacteria such as *Escherichia coli*, *Vibrio cholerae* and *C. rodentium*, as well as LPS co-treatment with cholera toxin subunit B (CTB) (271). Subsequently, it was found that macrophages that were loaded with intracellular LPS activated caspase-11 and died by pyroptosis, and that mice lacking caspase-11 were protected from LPS induced endotoxemia and pyroptosis (271, 384, 385). Finally, two independent studies identified caspase-11 as the key intracellular receptor for LPS (252, 386) (Figure 1.6).

Caspase-11-driven pyroptosis has been shown to be key for protection against intracellular pathogens, particularly those that can escape from phagocytic vacuoles, such as *S.* Tm (382, 387, 388). However, studies with phagocytes and embryonic fibroblasts reported that caspase-1 'canonical' inflammasomes were required for efficient processing of IL-1β and IL-18, even in the context of direct caspase-11 activation, which was only able to lead to cytokine cleavage via indirect activation of caspase-1 (314, 316, 389, 390). Nevertheless, caspase-11-dependent activation of IL-18 has also been reported, for instance, cecal tissue explants from *S.* Tm-infected *Casp-11*-deficient mice were also defective in IL-18 but not IL-1β secretion (251). Furthermore, colonic tissue explants from *C. rodentium*-infected *Casp-11*-deficient mice also had decreased IL-18 secretion (391). This caspase-11-dependent IL-18 processing was proposed to occur in IEC,

contrary to the caspase-1-dependent cleavage of IL-18 and IL-1β observed in myeloid cells (315).

The importance of 'canonical' and 'non-canonical' inflammasomes may vary depending on the nature and characteristics of the pathogenic threat and the cell types involved. For example, upon challenge with flagellin-deficient *Salmonella,* caspase-1-deficient macrophages died in a similar manner to WT macrophages, whereas caspase-11-deficient macrophages were resistant to cell death (314, 315). In contrast, both caspase-1 and caspase-11 were required for cell death in macrophages infected with WT *Salmonella* (314). This highlights the fact that *Salmonella* can activate both the 'canonical' inflammasome, through flagellin-Naip-Nlrc4 interactions, and the 'non-canonical' inflammasome, through direct LPS-caspase-11 interactions (Figure 1.7).

The complementary roles of 'canonical' and 'non-canonical' inflammasomes are especially important in the context of bacterial infections. Bacterial evasion strategies can counteract inflammasome responses, such as inhibition of epithelial caspase-11 via NleF, a T3SS effector protein produced by *E. coli* and *C. rodentium* (391). In a caspase-11-deficient scenario however, pyroptosis may still proceed due to intact caspase-1 activation, highlighting potential redundancy of these two caspases (392). Although, caspase-11 is transcriptionally regulated by LPS and Type I IFN in mouse myeloid cells (271, 314), it is constitutively expressed at high levels in intestinal epithelial cells (251, 254, 393). It seems logical that the intestinal epithelium, as a first line of defence, would have intrinsic mechanisms to warn the immune system of an invading threat. Indeed, as noted above, caspase-11 in mice (an orthologue of human caspases-4/5) is important for the recognition and clearance of *S.* Tm, and mice lacking caspase-11 harbour increased loads of *S.* Tm in the intestinal epithelium (220, 251). Furthermore, siRNA knock-down of caspase-4 in human colonic IEC led to reduced cell death upon *E. coli*, *S.* Tm and *Shigella flexneri* infection (251, 394), and this was accompanied by increased *S.* Tm intracellular load, and reduced IEC shedding (251, 315).

Recent studies, in addition to highlighting the importance of 'non-canonical' inflammasomes in innate immune defence in IEC, have also shed some light on the mechanisms involved in IEC-intrinsic restriction of *S.* Tm invasion. The innate immune sensor Nlrc4 and its Naip adaptors were shown to be essential for the extrusion of infected IEC into the intestinal lumen following *S.* Tm challenge of streptomycin-treated mice

(220). IEC extrusion may represent a cell-intrinsic defence mechanism that serves to limit the rate of pathogen colonization of the intestinal epithelium. In this study, it was unclear whether IEC extrusion was linked to pyroptosis, as plasma membrane integrity of extruded enterocytes seemed to be maintained (220). However, by using an inducible construct to drive the expression of Nlrc4 specifically in the intestinal epithelium, Rauch *et al.* showed that IEC-specific Nlrc4 activation by FlaTox (*Legionella pneumophila* flagellin fused to the N-terminal domain of *Bacillus anthracis* lethal factor to drive cytosolic delivery) was sufficient to drive pathology, IEC death and IL-18 release (230).

Moreover, in agreement with the findings of Sellin *et al.*, activation of Nlrc4 in IEC also limited *S.* Tm colonization of intestinal tissues and drove IEC death and extrusion (230). However, FlaTox-induced expulsion of IEC was accompanied by lytic cell death with plasma membrane permeabilization, resembling pyroptosis (230) (See Table 1.5 for morphological features of pyroptosis). From these studies, it becomes clear that, upon Nlrc4 activation, IEC can undergo cell death and expulsion from the intestinal epithelium. In parallel, experiments in which caspase-1 expression was selectively induced in IEC, it was found that caspase-1 could drive pyroptosis in response to Nlrc4 activation by FlaTox. On the contrary, caspase-1-deficient IEC did not undergo lytic cell death but were expelled from the epithelial layer with intact plasma membranes, indicating that caspase-1 was required for pyroptosis but not for IEC extrusion (230). Furthermore, they also observed that caspase-1-independent IEC extrusion following Nlrc4 activation was dependent on both Asc and caspase-8 (230).

Taken together, these studies show that a variety of inflammasome-dependent responses are triggered in IEC during *S.* Tm infection, and these encompass activation of Nlrc4, caspase-1, caspase-11 and possibly caspase-8 (220, 230, 251) (see Figure 1.7). However, it is unclear how the different inflammasome responses are regulated in IEC and if they are redundant, complementary, or interdependent. In addition, further studies are required to better define the precise kinetics and interconnections between downstream responses, such as IEC expulsion and cell death.

The detailed role of pyroptosis *in vivo* remains largely unexplored due to limited knowledge of the downstream targets of caspase-1 and caspase-11 culminating in cell death. Recently, however, Gasdermin D (GsdmD) was identified as a direct downstream

target of caspase-1 and caspase-11 and was shown to be required for pyroptosis upon 'canonical' and 'non-canonical' inflammasome engagement (381, 395-398). Indeed, upon GsdmD cleavage by caspase-1 or capase-11, its ~30 kDa N-terminus embeds itself in the plasma membrane, forming 10-14nm pores and ultimately leading to lytic cell death (397, 399, 400). Interestingly, GsdmD is highly expressed in the intestinal epithelium, suggesting that GsdmD may also be involved in pyroptosis in IEC (399, 401). Consistent with this hypothesis, IEC pyroptosis in response to *in vivo* administration FlaTox did not proceed in GsdmD -deficient mice (230). A very recent study using a mouse model of rotavirus infection reported that activation of a novel Nlrp9b inflammasome that recognises viral dsRNA contributed to the restriction of rotavirus replication in IEC organoids, at least partly through GsdmD-induced pyroptosis (246). Furthermore, mice deficient in either GsdmD or Nlrp9b displayed increased susceptibility to rotavirus infection *in vivo* (246). Collectively, these reports suggest that different IEC inflammasomes converge on GsdmD-induced pyroptosis to restrict pathogen load in infected IEC.

Pyroptosis shares a number of morphological features with both apoptotic and necrotic forms of cell death (Table 1.5). Akin to necrosis, in pyroptosis, nuclear integrity is maintained and the cell undergoes cytoplasmic swelling due to membrane permeabilization that ultimately terminates in cell lysis (402, 403). Akin to apoptosis, pyroptotic cells exhibit DNA fragmentation and are TUNEL positive, as well as presenting nuclear condensation (402-405). Before the acknowledgement of pyroptosis as a new form of cell death (406), its similarities to necrosis and apoptosis led researchers to attribute inflammasome driven cell death to only apoptosis and/or necrosis (402, 403, 405). It is partly for this reason that the interconnections between the different types of cell death upon inflammasome activating stimuli remains poorly understood. The discovery of GsdmD as a key player in pyroptosis should help elucidate the molecular pathways involved (381, 398, 399).

In addition to pyroptosis, inflammasome responses in various cell types have also been linked to apoptotic cell death. For instance, ectopic expression of Nlrc4 and Asc in HEK293T cells (which lack caspase-1), showed that these molecules can engage with caspase-8 to drive apoptosis (407). Furthermore, both apoptosis and pyroptosis have been observed in macrophages following Nlrp3 or AIM2 activation (407, 408). Interestingly, macrophages lacking GsdmD were reported to undergo cell death upon LPS plus *S.* Tm

or nigericin treatment, through a poorly defined mechanism that was independent of caspase-1, was delayed compared to pyroptosis, and had some features of apoptosis (399).

The literature also suggests some cross-regulation between pyroptosis and apoptosis as THP-1 cells treated with etoposide, an apoptosis inducing drug, resulted in the cleavage of GsdmD into a ~43 kDa fragment (different from the 30 kDa fragment observed in pyroptosis) that occurred independently of caspase-1 (409). The generation of the 43 kDa fragment was observed upon caspase-3 and -7 activation during apoptosis. This suggests that the apoptosis and pyroptosis pathways may compete for the same substrate and that cells may not be able to simultaneously undergo both forms of cell death. The authors speculated that the alternative cleavage of GsdmD by apoptotic caspases-3 and -7 may prevent apoptotic cells from becoming pyroptotic, thus maintaining and immunologically silent cell death (409).

Other studies suggest that differing thresholds may operate between the two cell death pathways following inflammasome activation. For example, in macrophages, for caspase-8 dependent apoptosis to occur upon AIM2 activation, the concentrations of DNA required were much lower than for pyroptosis (408). Under low stress levels, it would be desirable to deal with the invading threat in an immunologically silent way to avoid hyper inflammation, thus apoptosis would be favoured. However, when the threat is high, an inflammatory response could help deal with the microbial insult, therefore pyroptosis may be beneficial. However, it is important to stress that it remains to be demonstrated if this threshold-dependent decision controls differential cell death pathways following inflammasome activation *in vivo* and in cells other than macrophages.

The importance of having several caspase-mediated cell death pathways downstream of the inflammasome can be explained by the ability of some pathogens to inhibit the activation of inflammasome caspases or to avoid detection. For instance, NleB1 and NleF in *E. coli* and *C. rodentium* are known to inhibit caspase-8 and -4/11 signalling, respectively (391, 410). Caspase-4 may also be inhibited by *Shigella* OspC3 (411, 412). Furthermore, NleA from EPEC and EHEC is able to bind Nlrp3 and avoid its activation and consequent Caspase-1 cleavage (411). Likewise, *Shigella* IpgD can block the release of extracellular ATP, a potent Nlrp3 activator (411, 412). In addition to actively inhibiting inflammasome pathways, microbes also possess strategies to evade detection. For instance, Gram-negative bacteria, like *Francisella novicida* can modify their LPS to avoid

detection by caspase-11 (385). Similarly, *Yersinia* uses Yopk to evade detection of its T3SS and consequent inflammasome activation in macrophages (413). Thus, the ability to activate inflammasome-mediated cell death through different pathways may be beneficial for the host to counteract pathogen evasion strategies.

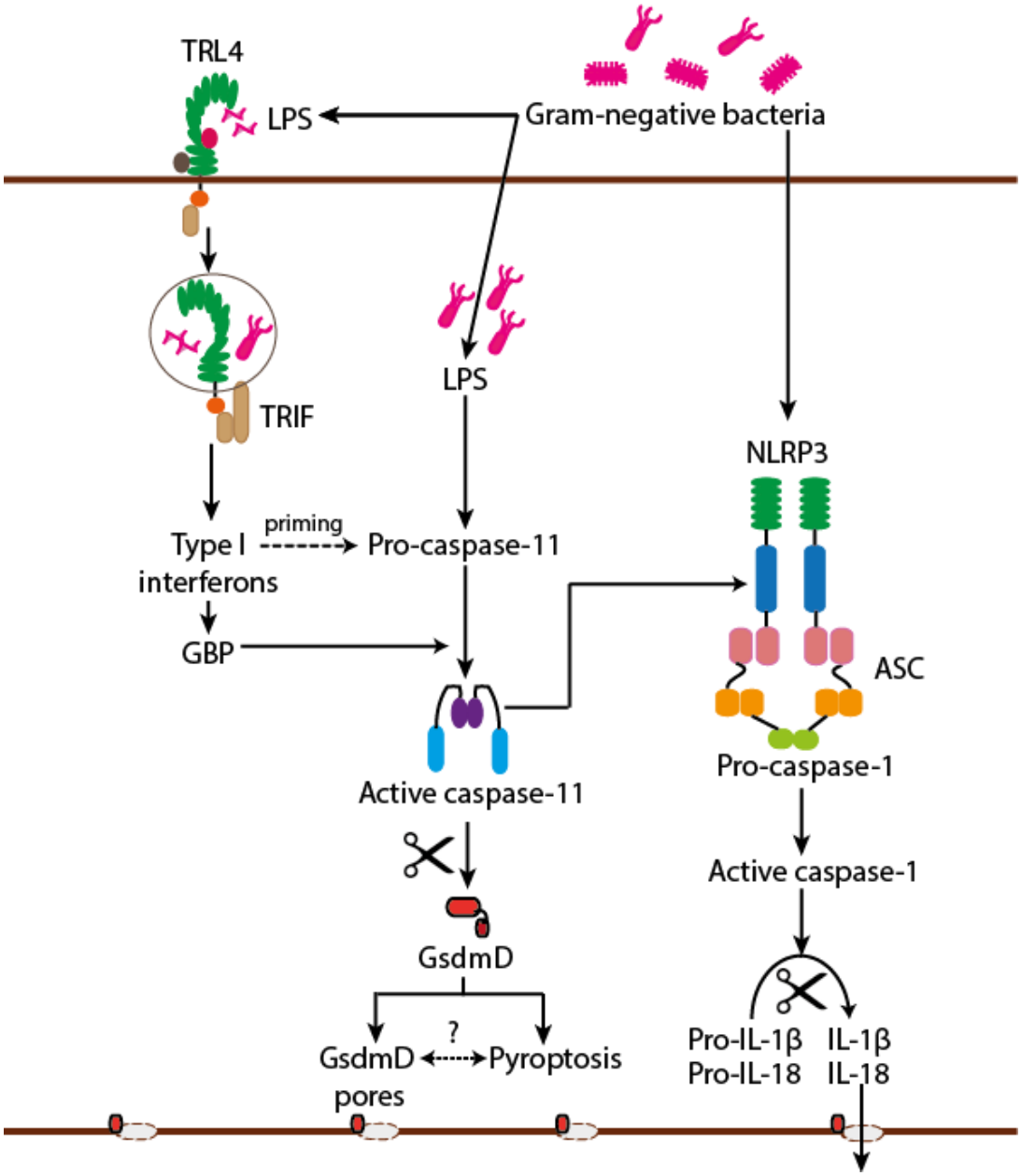


Figure 1.6. The caspase-11 non-canonical inflammasome pathway in myeloid cells. During an inflammatory response, extracellular LPS is sensed by TLR4 and its adaptor TRIF which lead to the transcriptional upregulation of inflammatory mediators. TLR4-TRIF engagement can induce the expression of pro-caspase-11 through Type I IFN signalling (414, 415). Cytosolic localisation of LPS results from the active invasion of intracellular Gram-negative bacteria, or from the release of LPS from Gram-negative bacterium-containing vacuoles by small IFN-inducible guanylate-binding proteins (GBP)-mediated lysis of the vacuoles (414, 416). Direct recognition of LPS by Caspase-11 (intracellular LPS sensor) leads to its oligomerisation and auto-cleavage. This results in the cleavage of GsdmD, whose N-terminal fragment is able to embed itself in the membrane of activated cells leading to pore formation (252, 271, 384-386). GsdmD pores allow the leakage of proteins like IL-1β, IL-18 and IL-1α. The activation of the Caspase-11 and GsdmD ultimately lead to cell death by Pyroptosis. However, it is unclear whether GsdmD pore formation is reversible or if it inevitably leads to cell lysis and Pyroptosis. Active caspase-11 also induces the non-canonical activation of NLRP3 inflammasome possibly by processing pannexin 1 and causing potassium efflux (not shown) (417). This results in the activation of caspase-1 and cleavage of IL-1β and IL-18 (389, 417).

Table 1.5. Characteristic features of different cell death pathways. (+) present; (-) absent; (+/-) present to a limited degree; (?) not yet assessed. Abbreviations: gasdermin D (Gsdmd). *This table is my own work and has been submitted for publication (1).*

Characteristic of the dying cell	Apoptosis	Necrosis	Pyroptosis	Necroptosis
DNA fragmentation	+ (418-420)	+/- (418, 419)	+ (403-405, 421)	? (see necrosis)
Nuclear condensation	+ (418-420)	- (419, 422)	+ (402)	- (419, 423)
Nuclear integrity maintained	- (418-420)	+ (418, 419)	+ (424)	+ (419, 423)
Cell Swelling	- (418-420)	+ (418, 419)	+ (404)	+ (419, 423)
Lysis/membrane permeability	- (418-420)	+ (418, 419)	+ (404)	+ (422)
Membrane blebbing and shedding	+ (418-420)	- (418, 419)	- (425)	? (see necrosis)
Membrane pore formation	-	-	+ (395, 397, 400)	+ (426, 427)
DAMP release	-	+ (428)	+ (402)	+ (422)
IL-1β and IL-18 release	-	-	+ (402)	-
Main caspases	casp-3 and casp-7	Non-caspase mediated	casp-1 and casp-11 (mouse) casp4 and casp-5 (humans)	Non-caspase mediated (429).

1.4.4. Linking inflammasome effector mechanisms

This section is my own work and has been submitted for publication (1).

Both IL-1β and IL-18 lack signal peptides and therefore are not secreted through the conventional ER-Golgi pathway (430-432). For IL-1β, the better described cytokine of the two, several routes of release have been proposed, including secretory lysosomes, exosomes and microvesicles (433-437). The secretory exosome pathway was proposed through the observation that IL-1β in monocytes was localised in endosomal-like vesicles that are normally targeted for degradation, but can be redirected to the extracellular space (435, 438). In addition, microvesicle-mediated rapid secretion was proposed after observing vesicles associated with bioactive IL-1β as early as 2 minutes post-ATP stimulation in activated monocytes (436). However, studies on these secretory routes were often contradictory and employed different cell systems, thus these models of secretion remain controversial (439). The mechanisms of secretion of IL-18 are generally assumed to follow the mechanisms of IL-1β secretion, but are much less investigated.

However, pyroptosis has now been proposed to be responsible for the release of IL-1β and IL-18 to alert the immune cells of the imminent danger, leading to the onset of inflammatory responses (325). This was first suggested by the observation of caspase-1 dependent pores in the plasma membrane of *Salmonella*-infected macrophages, ultimately leading to cell swelling and osmotic lysis (404). This was supported by more recent studies of ATP-stimulated BMDM, in which pharmacological inhibition of membrane permeabilization - a hallmark of pyroptosis - abolished IL-1β secretion, but not processing (433). The recent discovery of GsdmD and its requirement for pyroptosis offers a potential mechanistic explanation linking pyroptosis and cytokine secretion. Both caspase-1 and -11 can cleave GsdmD, releasing the active N-terminus that mediates pore formation and lytic cell death (397-400). Consistent with the concept that pyroptosis facilitates cytokine secretion, macrophages lacking GsdmD exhibit defective IL-1β secretion in response to various ‘canonical’ and ‘non-canonical’ inflammasome activators, including intracellular LPS, Gram-negative bacteria and nigericin (381, 398-400).

However, there is also evidence in the literature of IL-1β release in the absence of cell death in peritoneal macrophages, human monocytes and neutrophils (291, 440). In particular, neutrophils could secrete IL-1β in response to *Salmonella* infection through a

mechanism that was dependent on Nlrc4 and caspase-1, but was independent of cell lysis (441). Furthermore, treatment with the cytoprotective agent glycine protected *S.* Typhimurium- infected macrophages from cell swelling and lysis but did not prevent the release of processed IL-18 and IL-1β (404). In DC, caspase-11 activation with LPS and self-encoded oxidized phospholipids (oxPAPC) led to IL-1β release but only LPS-induced DC activation led to pyroptosis. This non-pyroptotic DC activation with oxPAPC was referred to as hyperactive DC (442). This research suggests that the mechanisms of secretion of inflammasome-processed cytokines is context dependent and can occur without the lysis of the host cell. The mode of release may thus depend on the cell type and the nature of the activatory signals.

More recent evidence supports pyroptosis-independent IL-1β release and shone light on the mechanism of secretion (443). Evavold *et al.* observed IL-1β release from living macrophages upon inflammasome activation in a GsdmD-dependent manner (443). Cytokine release across an intact lipid bilayer occurred from GsdmD pores. This evidence was obtained by utilising the cytoprotective glycine to maintain membrane integrity. The generation of liposomes containing different sizes' dextrans revealed that only dextrans with a smaller diameter than the GsdmD pores (4 kDa and 20 kDa with hydrodynamic radii of less than 4 nm) were secreted upon GsdmD and caspase-11 co-treatment (443).

This research supports the notion that proteins can be secreted from GsdmD pores without compromising the integrity of the lipid membrane. The authors proposed dual functionality for GsdmD in the context of cell-fate decisions (443). One function would be to execute cell death by pyroptosis whilst amplifying the inflammatory cascade. The other function would be to promote a state of cellular hyperativation resulting in continuous release of inflammasome cytokines from living cells. However, if this cellular fate decision occurs *in vivo* remains to be identified. It would be important to investigate if GsdmD pore formation is reversible or if it ultimately leads to cell death by pyroptosis, thus refuting the idea of a two-way cellular fate decision.

It is again important to emphasise that inflammasome effector responses have largely been studied in leukocytes, particularly phagocytic cells. Whether the discoveries made in these cell types are applicable to tissue cells, including IEC, remains to be determined. For instance, classical activation of the inflammasome has long been viewed as a two-step process, starting with the transcriptional regulation of the inflammasome

components. Thus, caspase-11 induced cell death in macrophages was dependent on priming by TLR4 ligands through TRIF, but not on Myd88 signals (314, 389, 415). Indeed, LPS administration in mice, rapidly induced *Casp-11* expression in various tissues including thymus, spleen and lung (315, 444). Conversely, IL-1β release in phagocytic cells depended on Myd88-mediated transcriptional priming (207, 281). These requirements appear to be somewhat different in the intestinal epithelium, for example, although TLR4 signalling is downregulated in IEC (445), caspase-11-dependent responses still occur. This suggests that *Casp-11* is constitutively expressed in the intestinal epithelium and can be rapidly activated upon pathogen invasion (254). This 'ready-to-go' phenotype of IEC inflammasome components is further supported by the observations that *Nlrc4* and *pro-IL-18* are constitutively expressed by IEC and may not require priming (231, 255). Furthermore, the constitutive colonisation of commensal Gram-negative bacteria in the intestine could explain the constitutive elevated expression of *Casp-11* and *IL-18* in the gut compared to other tissues (www.proteinatlas.org) (315).

It is also worth noting that during homeostatic conditions, and thus in the absence of inflammation, the inflammasome-dependent cytokine IL-18 is released from IEC and is believed to have functions in epithelial repair, proliferation and maturation (242, 243). The mechanisms of secretion of IL-18 by IEC during homeostatic conditions are not well understood and whether pyroptosis occurs in IEC under physiological conditions *in vivo* remains to be determined (446). Although there is increasing evidence that IEC-intrinsic inflammasome activation plays a key role in early innate defence against pathogens that target the intestinal epithelium (220, 230, 231, 249, 251), much remains to be learned on how inflammasomes and their downstream effector responses are regulated in IEC.

Due to IEC constitutive exposure to microbial PAMP, inflammasome circuits and thresholds in IEC may be quite different to those primarily identified in macrophages and DC. Nevertheless, the constitutive secretion of IL-18 by IEC indicates that inflammasomes are active under homeostatic conditions in the intestinal epithelium. However, the precise signals or thresholds that determine when this may be superseded by the induction of pyroptosis or alternative cell death pathways remain to be determined. For example, it will be important to assess the role of GsdmD in IL-18 secretion and IEC turnover during steady-state conditions. Furthermore, it will also be vital to understand how inflammasome responses in IEC are modulated during pathogenic attack or during

inflammatory conditions, where an optimal balance between apoptosis, pyroptosis and cytokine release may be required to control potential pathogens and restore homeostasis.

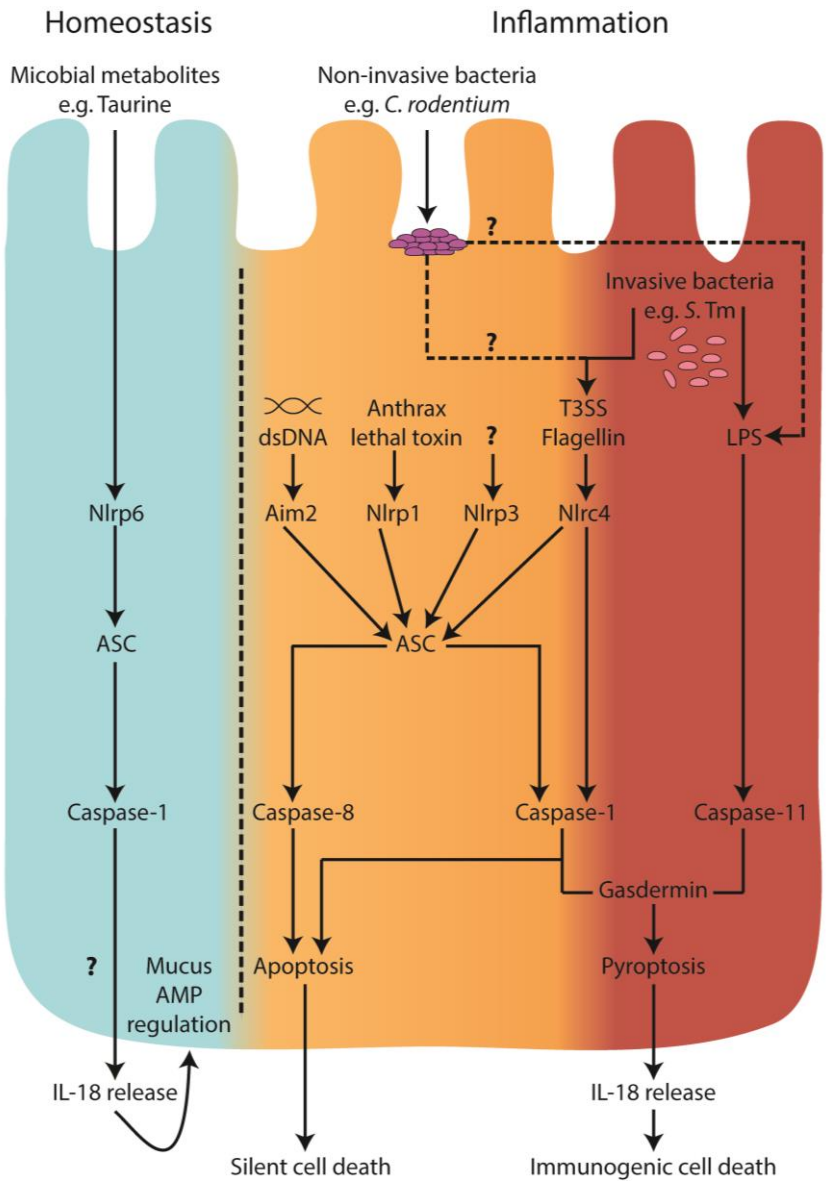


Figure 1.7. Inflammasomes in intestinal epithelial cells. During homeostatic conditions, in the absence of inflammation, IL-18 is released from IEC and is involved in epithelial repair, proliferation and maturation (242, 243). A metabolomics screen identified microbiome-derived metabolites, including taurine, that are capable of modulating Nlrp6 inflammasome activation and subsequent IL-18 secretion (241). However, the mechanisms of release of IL-18 during homeostatic conditions are undefined. In the context of microbial invasion and PAMP stimulation, inflammasome activation in IEC has been described to engage both 'canonical', caspase-1 mediated and 'non-canonical', caspase-11 pathways (220, 230, 251). Recently, caspase-8 was also shown to be involved in inflammasome responses downstream of Nlrc4 engagement with intracellular flagellin (230). Both caspase-1 and caspase-11 can lead to cell death by pyroptosis accompanied by IL-18 secretion, however, caspase-1 and caspase-8 were shown to lead to a non-lytic form of cell death upon Nlrc4 sensing of intracellular flagellin (230). These observations raise the possibility of a distinction between a pro-immunogenic cell death signal driven by caspase-11 and Gsdmd, a silent cell death driven by caspase-8, and perhaps a threshold dependent cellular decision between non-lytic, and lytic forms of cell death involving caspase-1. Under low stress levels, it would be desirable to deal with the invading threat in an immunologically silent way. However, when the threat is high, an immunogenic cell death could recruit inflammatory cells to help clear the microbial insult. *This figure is my own work and has been submitted for publication (1).*

1.5.Models of intestinal inflammation

1.5.1. Citrobacter rodentium infection- a model of acute intestinal inflammation

C. rodentium is a Gram-negative enteric attaching and effacing (A/E) murine pathogen. It is transmitted via the fecal-oral route and causes a transient colitis, also known as transmissible murine colonic hyperplasia (TMCH) (447). *C. rodentium* infection is characterised by intimate bacterial adherence to host IEC, effacement of microvilli and reorganisation of the host actin cytoskeleton to form pedestal-like extensions of IEC beneath the adhesion foci, called A/E lesions (448, 449). The formation of A/E lesions causes excessive epithelial regeneration and repair mechanisms that lead to thickening of the colonic mucosa and thus hyperplasia (449, 450).

C. rodentium adhesion to IEC and formation of A/E lesions are mediated by the locus of enterocyte effacement (LEE), a pathogenicity island that is well conserved among A/E bacteria (451), encoding multiple virulence factors, such as components of a T3SS (452). *C. rodentium* is the only A/E pathogen known to infect mice and is regarded as the mouse equivalent of human pathogenic *E. Coli* infection. Thus, *C. rodentium* is used as the gold standard mouse model of infections with enteropathogenic and enterohaemorrhagic *E. coli* (EPEC and EHEC) (453). In addition, *C. rodentium* is used to model intestinal inflammatory disorders, like Crohn's disease, ulcerative colitis, and colon tumorigenesis (448, 454, 455).

Susceptibility to *C. rodentium*-induced colitis varies greatly according to genotype. The severity of the disease varies from self-limiting colitis and sterilising immunity to severe inflammation and potentially lethal dehydration (448). The microbiota is another important factor influencing the susceptibility to *C. rodentium* infection (456). Indeed, *C. rodentium*-induced colitis leads to a profound dysbiosis and outgrowth of the pathogen (456, 457).

Most studies rely on the inoculation of *C. rodentium* by oral gavage with laboratory cultured bacteria (458), which results in a highly reproducible cycle of infection (448, 459-461). Initially *C. rodentium* colonises the cecal patch which is the major cecal lymphoid structure (459). Adherent bacteria adapt to the intestinal environment and

undergo a virulence switch that allows them to colonise the distal colon and rectum (462-464). The peak of infection is observed between days 7-9 post infection (p.i.) After this, *C. rodentium* begins to be cleared from the cecum and then from the colon as infected enterocytes are expelled from the epithelial lining (448, 465). Resolution of infection is after ~21 days and is associated with the onset of adaptive immunity (463, 465).

The host-adapted *C. rodentium* being shed at the peak of infection are hyper-infectious and able to infect co-housed mice by coprophagy with 1000-fold fewer CFU than that of LB-grown *C. rodentium* (448, 466). Currently, the mechanisms regulating *C. rodentium* virulence switch are poorly understood. Nevertheless, the fecal host-adapted *C. rodentium* displays higher expression of T3SS genes and is hyper-adherent to *in vitro* cultured epithelial cells compared to LB-grown *C. rodentium* (467). It is suggested that signals from the microbiota or from the host may be able to regulate *C. rodentium* pathogenesis and ability to colonise the intestinal mucosa (448). Indeed, germ free mice do not develop pathology despite being unable to clear *C. rodentium* infection (468). Furthermore, during the later stages of infection, *C. rodentium* displays a less virulent phenotype and is no longer able to outcompete the host microbiota or remain tissue adherent, thus becoming planktonic bacteria in the intestinal lumen (468, 469).

Clearance of *C. rodentium* is achieved by robust inflammation that encompasses effector responses mediated by both the innate and adaptive immune systems. These include the recruitment of neutrophils, Th22 and Th17 $CD4^+$T cells and B cells, as well as production of AMP and microbiota competition (459). At the initial stage of infection, *C. rodentium* and its associated PAMP (i.e. LPS) are sensed primarily by TLR2/4 and their adaptor MYD88 on the surface of IEC and myeloid cells (470-472). These events trigger the activation of the NFκB and initiation of a transcriptional cascade leading to the release of pro-inflammatory cytokines IL-6, IL-12, IL-23 and TNF by innate immune cells (189, 389, 470). Mice deficient in MYD88 have an impaired ability to control bacterial replication (471). TLR2-deficient mice display severe colonic pathology, rapid weight loss and mortality that could be rescued by IL-11 administration and STAT3 signalling restoration (473, 474). Although TLR4 is dispensable for *C. rodentium* clearance, it does contribute to the development of colitis via recruitment of inflammatory cells (475).

When *C. rodentium* associated PAMP and/or DAMP reach the cellular cytosol, NLR within hematopoietic and non-hematopoietic cells become activated and form

inflammasomes (231, 249, 345). Inflammasomes are also important in the immunity against *C. rodentium* possibly by promoting AMP responses, mediating the death of infected cells, and promoting the release of pro-inflammatory mediators, including IL-1α, -β and -18 (1, 190). Indeed, deficiency in several inflammasome components and effectors leads to increased pathogen burden and/or pathology (Table 1.6 and Table 1.4).

During the later stages of infection adaptive responses are initiated. IL-23 secretion from innate immune cells has a central role in immunity against *C. rodentium* by orchestrating Th17 and Th22-mediated immunity (120, 448). This is demonstrated by the high rate of mortality observed in *IL-23*$^{-/-}$ mice (476). IL-23 together with TGFβ induce potent Th17 responses from around ~1-week p.i. (476). Th17 derived IL-17 promotes neutrophil recruitment to the site of infection by inducing secretion of chemokines such as CXCL1 and 2 from activated DC, macrophages and IEC (477). Another cell type contributing to the production of IL-17 are the ILC3 (478). ILC3 require priming from the microbiota and are also able to secrete IL-22 (478) which is regarded as an anti-inflammatory cytokine that induces the secretion of AMP from IEC, as well as leading to IL-18 transcriptional up-regulation in IEC and epithelial cell regeneration (121, 369, 479, 480). Early IL-22 production is associated with ILC3, whilst during later stages of infection Th22 are more proactive in the secretion of IL-22 (120). Both these sources of IL-22 are required for the resolution of *C. rodentium* infection (480). Th1 responses are also necessary for the production of IFNγ and TNF and controlling *C. rodentium* systemic spread (455).

Finally, B cells are also required for the resolution of *C. rodentium* infection (481). Indeed, *RAG1*$^{-/-}$ mice, as well as mice that lack B cells or CD4^{+}T cells, displayed severe colitis and increased bacterial burden. This was accompanied by systemic dissemination of the bacterium often leading to fatal infection (481, 482). B cell deficient mice suffer from severe *C. rodentium* infection due to lack of IgG antibodies that play a key role in mediating clearance of *C. rodentium* (483, 484).

Table 1.6. Inflammasome components and intestinal inflammation. Abbreviations: AMP (antimicrobial peptides), *C. rod* (*C. rodentium*), FlaTox (*Legionella pneumophila* flagellin fused to the N-terminal domain of *Bacillus anthracis* lethal factor; Naip5 ligand delivered to cytosol), IEC (intestinal epithelial cells), *S.* Tm (*S.* Typhimurium). Mutant strain abbreviations: *Casp1*$^{\Delta IEC}$ (*caspase*-1-deficient IEC), *Naip1-6*$^{\Delta/\Delta IEC}$ (*Naip1-6*-deficient IEC), *iNlrc4+ Vil-Cre+ (Nlrc4* only expressed in IEC), *Nlrp9*$^{\Delta IEC}$ (*Nlrp9b*-deficient IEC), *Nlrx1*$^{\Delta IEC}$ (*Nlrx1*-deficient IEC). Table adapted from (1).

Mutant Strain	Phenotype		Proposed mechanism
	Pathogen	DSS	
NLR			
Naip1-6$^{\Delta/\Delta}$	↑ *S.* Tm load (220)		↓ IEC expulsion
Naip1-6$^{\Delta/\Delta IEC}$	↑ *S.* Tm load (220)		↓ IEC expulsion
Nlrc4$^{-/-}$	↑ *C. rod* load and pathology (231) ↑ *S.* Tm load (220)	↑ pathology (239)	↓ IEC expulsion (*S.* Tm) ↓ IL-18 (*C. rod*)
iNlrc4^{+} ***Vil-Cre***$^{+}$	↔ *S.* Tm load (230)		↓ IEC death
Nlrp1$^{-/-}$		↑ pathology (367)	↓ IL-18 and IL-1β
Nlrp3$^{-/-}$	↑ *C. rod* load and pathology (249, 345)	↑ pathology (239, 248, 256, 485) ↓ pathology (486)	**DSS**: ↓ IL-1β (486)
Nlrp6$^{-/-}$	↑ *C. rod* load (243)	↑ pathology (241, 242)	**DSS** and ***C. rod*****:** ↓ IL-18 (242, 256) and ↓ AMP (241) ***C. rod*****:** ↓ mucus secretion (243)
Nlrp9b$^{-/-}$	↑ rotavirus load (246)		
Nlrp9b$^{\Delta IEC}$	↑ rotavirus load (246)		
Nlrp12$^{-/-}$		↑ pathology (487-489)	
Nlrx1$^{\Delta IEC}$		↔ pathology ↑ Tumour formation (234)	↑ proliferation factors ↑ IEC proliferation
Caspases			
Casp1$^{-/-}$***Casp11***$^{-/-}$	↑ *C. rod* load (243)	↑ pathology (242, 256, 258, 485)	**DSS:** ↓ IL-18 (256, 258)
Casp-1$^{-/-}$	↑ rotavirus load (246)	↓ pathology (361)	**DSS**: ↓ IL-18
Casp1$^{\Delta IEC}$	↑ rotavirus load (246)	↓ pathology (361)	**DSS**: ↓ IL-18
Casp-11$^{-/-}$	↑ *S.* Tm load but decreased pathology (251)	↑ pathology (253, 254)	**DSS:** ↑ IL-18 (254) **DSS and *S.* Tm*:*** ↓ IL-18 (253) ***S.* Tm:** ↓ IEC expulsion (251)
Casp1$^{-/-}$***Casp8***$^{-/-}$ ***Ripk3***$^{-/-}$	↑ *S.* Tm load		↓ IEC expulsion (230)
Other inflammasome components			
Asc$^{-/-}$	↑ *C. rod* load and pathology (243, 249, 345) ↑ rotavirus load (246)	↑ pathology (242, 248, 256, 367, 485)	**DSS and *C. rod*****:** ↓ IL-18 (242, 256) and ↓ AMP (241) ***C. rod*****:** ↓ mucus secretion (243)
Gasdermin D$^{-/-}$	↑ rotavirus load		↓ IEC death (246)

Mutant Strain	Phenotype		Proposed mechanism
	Pathogen	DSS	
AIM2$^{-/-}$		↑ pathology (248, 368)	↓ IL-18 and IL-1β (248, 368), ↓ IL-22BP (248) and ↓ AMP (248, 368)

1.5.2. Salmonella Typhimurium

S. Typhimurium is a Gram-negative facultative aerobic rod-shaped bacterium that causes gastroenteritis in humans and other mammals (490, 491). It actively invades its host through IEC. *S.* Tm can colonise the Peyer's patches through M cells, as well as the lamina propria via uptake by LP cells such as macrophages and DC (492). Under certain circumstances, *S.* Tm can spread systemically (to MLN, spleen and liver) through the bloodstream or lymphatics, or through trafficking by immune cells carrying the bacteria (493, 494). However, in healthy individuals *S.* Tm is normally self-limiting and restricted to the gastrointestinal tract (490, 491).

Propulsive flagella allow *S.* Tm to come in close proximity to the epithelial layer. Then, it can attach to IEC through fimbriae and adhesins that bind to glycoproteins present on the host cell surface (495-497). Following bacterial adhesion to IEC, *S.* Tm can promote its uptake through endocytosis mediated by a T3SS which is encoded on the *Salmonella* pathogenicity island 1 (SPI-1). *S.* Tm uses its T3SS to inject effector proteins that can manipulate the hosts cytoskeleton and facilitate bacterial uptake by the host cell (498). The *S.* Tm SPI-1 major effector proteins are SipA, SopB, SopE and SopE2 (499). These factors mediate the assembly and stabilisation of actin filaments, which induces membrane ruffling and extension outwards from the site of bacterial attachment (499, 500). These processes lead to the engulfment of S. Tm which thus gains access to the host cell.

Once inside, *S.* Tm is protected by the vacuole formed upon engulfment. At this vacuolar stage, *S.* Tm assembles a second T3SS (encoded in SPI-2) to inject another set of effector molecules across the vacuolar membrane (501). These molecules manipulate host biological processes to protect the invading bacteria from vacuole acidification and rupture, thus aiding intracellular S. Tm survival and replication (502). Intracellular *S.* Tm rapidly (~18-24h) induces host cell death (503), leading to the release of intact bacteria for further infection.

In this thesis *S.* Tm was used as a model organism to infect intestinal epithelial organoids *ex vivo*. This pathogen was chosen for its ability to actively invade epithelial cells, including epithelial organoids (504) (Table 1.8).

1.6.*Ex vivo* study of intestinal epithelial biology: organoids

Intestinal epithelial cells have a very rapid turnover. Within 5-7 days, they have differentiated from epithelial stem cells to mature IEC, and finally undergone death by anoikis once cell-cell contact is lost (27). The rapid death of differentiated IEC has hindered the study of IEC in isolation *in vitro* due to the inability to keep them in culture. However, recently developed methods have enabled the culture, propagation and differentiation of $Lgr5^+$ intestinal epithelial stem cells *ex vivo*. The IEC stem cell microenvironment is replicated *in vitro* through supplementation of the culture media with key stem cell supporting factors and the provision of a 3D matrix (Table 1.7). These *ex vivo* cultured IEC generate crypt-like epithelial domains, termed organoids, which harbour multiple differentiated IEC lineages and can be propagated for extended periods (16, 505, 506).

Until the development of organoids, long-term cultures from adult primary epithelial tissue was unfeasible. However, organoids have now been grown from various adult human and mouse tissues (507, 508), including stomach (509, 510), small intestine (16), colon (505, 511), pancreas (512) and liver (513, 514).

$Lgr5^+$ intestinal epithelial stem cells isolated from the adult gut can be grown in culture in the presence of EGF, Noggin, R-spondin and Wnt-3A (505) (Table 1.7). Initially, the epithelial stem cells form symmetric spheres enriched in stem cells. As the organoid grows, crypt-like structures begin to appear containing Lgr5+ cells flanked by their differentiated progeny (16). Indeed, small intestinal organoids display distinctive crypt and villus domains that are arranged around a luminal cavity which fills with apoptotic cells as the organoids proliferate, much like in the *in vivo* intestinal epithelium (16) (Figure 1.8).

Small intestinal organoids do not require Wnt3A supplementation since Paneth cells, neighbouring the $Lgr5^+$ cells, can provide this signal and support stem cell replenishment. Conversely, colonic epithelial organoids are devoid of Paneth cells thus need supplementation with Wnt3A for their self-renewal (505). In the presence of the optimal growth factors and the support of a growth matrix (laminin-rich Matrigel), the organoids can be indefinitely passaged. For this purpose, organoids are dissociated and re-seeded every 3-5 days to reinitiate new organoid formation from $Lgr5^+$ intestinal epithelial stem

cells (515). To differentiate organoids, Wnt3A is removed from the media leading to induction of the epithelial cell differentiation (505).

Before the development of the organoid system, the *in vitro* study of epithelial biology was restricted to the use of immortalised or cancerous cell lines. Organoids are a valuable tool for studying epithelial responses in a way that is closer to the *in vivo* intestinal physiology. Furthermore, organoids can be propagated long-term and enclose the different cell types that constitute the intestinal epithelium (16, 516). The use of organoids is becoming common practice for the modelling of diseases, including the development of cancer, hereditary diseases and study of host-pathogen interactions (517). Furthermore, genetic modification of organoids was also successfully applied to repair a mutation in the cystic fibrosis (CF) transmembrane conductor receptor (CFTR) leading to CF by homologous recombination in cultured IEC organoids derived from CF patients (511).

Due to the closed 3D structure of organoids, the apical side of IEC is not accessible for stimulation. Host-pathogen interactions in the gut normally initiate at the apical site of the epithelium. Currently, studies employ various techniques to gain access to the apical side of organoids. The most commonly used method is luminal microinjection (504, 518-522). However, pathogens can also be delivered to dissociated organoids, which are then embedded into Matrigel and allowed to reform (504, 522). More recently, direct pathogen/substance administration to polarised, collagen-supported 2D IEC monolayers has been implemented to access the apical side of IEC (517, 523)(Table 1.8) (Figure 1.8). The continuous development of research techniques employing the use of organoids will allow us to complement the *in vivo* studies of epithelial biology. This will be key to improving our understanding of host-pathogen interactions at the barrier site in a functionally and physiologically relevant *ex vivo* model.

Table 1.7. Supplements to support intestinal epithelial organoid growth *ex vivo*.

Supplements	Purpose
Matrigel (laminin-rich)	Laminin (α1 and α2) is enriched at the crypt base. Provides 3D matrix (524).
Epidermal growth factor (EGF)	Supports intestinal proliferation (525).
Noggin	Induces an expansion of crypt numbers. Negative regulator of Bone morphogenetic protein (BMP). BMP pathway functions as a negative regulator of crypts (526, 527).
Wnt-3A	Required for crypt proliferation and stem cell maintenance (528, 529).
R-spondin	Wnt agonist. Potentiates Wnt signalling (530).
Rock-inhibitor (Y27632)	Prevent dissociation-induced apoptosis (531).
N-acetyl-l-cysteine (NAC) (dispensable)	ROS quencher
B27	Antioxidant cocktail, vitamin A, insulin (505).
N2 (dispensable)	Human transferrin, (holo), insulin recombinant full chain, progesterone, putrescine, selenite (505).

Table 1.8. Example of host-pathogen interactions studied with the aid of intestinal epithelial organoids.

Pathogen	Mode of administration
Clostridium difficile	• Microinjection into the lumen of human small intestinal organoids (519).
Shigella flexneri	• Microinjection into the lumen of organoids (518)
Salmonella enterica serovar Typhimurium	• Bacteria delivered to the basolateral side of mouse small intestinal organoids (522). • Microinjection into the lumen of human intestinal organoids (504, 520, 521). • Infection of dissociated cells (trypsinised) before the 3D structure is reformed (504, 522).
Enterohemorrhagic and enteropathogenic *Escherichia coli*	• Direct addition into the culture media of human intestinal 2D monolayer cultures derived from colonic organoids (523, 532).
Noroviruses	• Direct addition into the culture media of human intestinal 2D monolayer cultures derived from small intestinal organoids (533)
Rotaviruses	• Infection of dissociated human and mouse small intestinal organoid cells (trypsinised) before the 3D structure is reformed (534, 535)

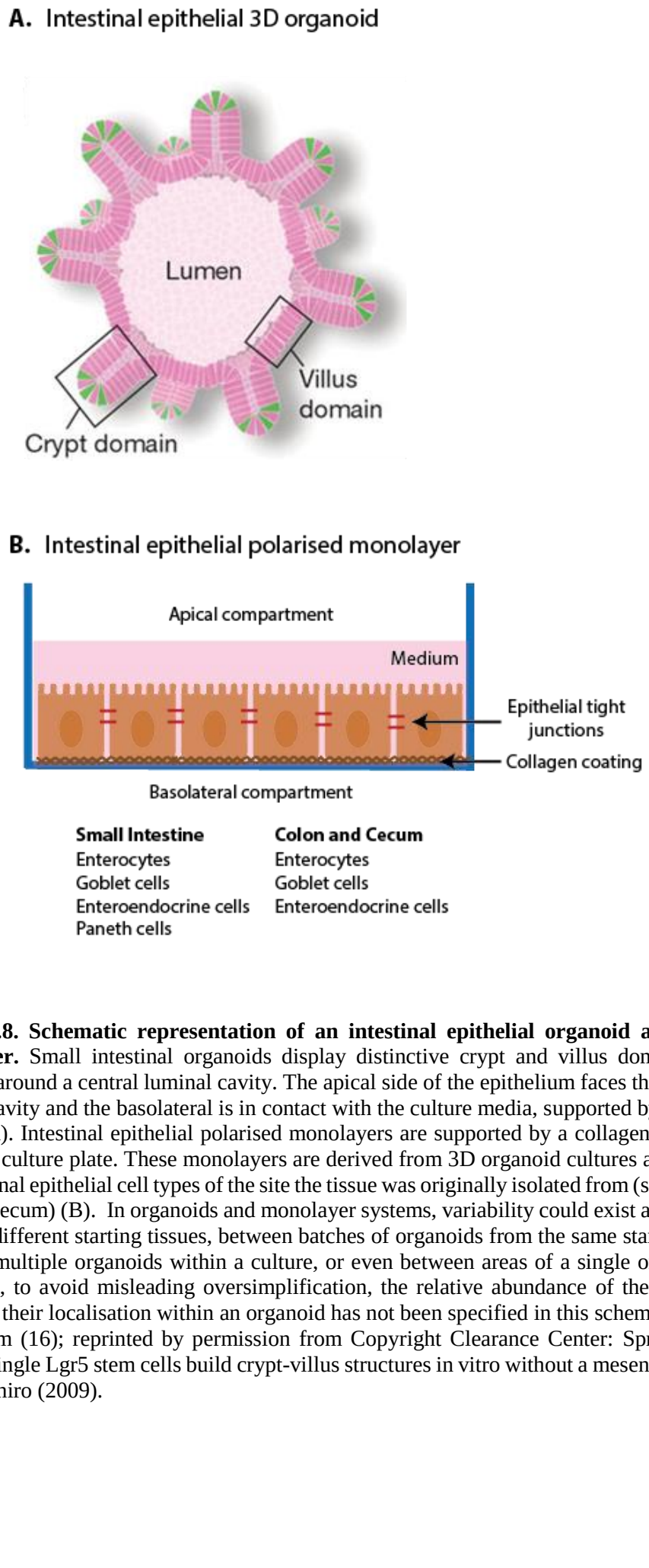


Figure 1.8. Schematic representation of an intestinal epithelial organoid and polarised monolayer. Small intestinal organoids display distinctive crypt and villus domains that are arranged around a central luminal cavity. The apical side of the epithelium faces the inside of the luminal cavity and the basolateral is in contact with the culture media, supported by the Matrigel matrix (A). Intestinal epithelial polarised monolayers are supported by a collagen layer coating the tissue culture plate. These monolayers are derived from 3D organoid cultures and contain all the intestinal epithelial cell types of the site the tissue was originally isolated from (small intestine, colon or cecum) (B). In organoids and monolayer systems, variability could exist at many levels: between different starting tissues, between batches of organoids from the same starting material, between multiple organoids within a culture, or even between areas of a single organoid itself. Therefore, to avoid misleading oversimplification, the relative abundance of the different cell types and their localisation within an organoid has not been specified in this schematic. Figure A taken from (16); reprinted by permission from Copyright Clearance Center: Springer Nature; Nature; Single Lgr5 stem cells build crypt-villus structures in vitro without a mesenchymal niche; Sato, Toshiro (2009).

1.7.Aims of the thesis

How do inflammasome signals in IEC confer protection against intestinal infection and inflammation?

Recent studies by our group have implicated a protective role for Nlrp3 and Nlrc4 activation within IEC against an enteric pathogen (231, 249). Indeed, *in vivo* models of acute infection with *C. rodentium* revealed exacerbated pathology in mice lacking Nlrp3, Nlrc4 or Asc compared to co-housed WT mice. Furthermore, bone marrow chimera experiments revealed that protection from disease was mediated through Nlrp3, Nlrc4 and Asc activation in non-hematopoietic cells (231, 249), implicating multiple inflammasomes in protection from infection. Fluorescent microscopy revealed that Asc localised to the intestinal epithelium following infection, suggesting that this Asc/inflammasome dependent protection is mediated by IEC (249). Immunofluorescence localization of IL-18 confirmed expression in IEC that was mainly observed towards the top of the intestinal crypt in steady state (255). We hypothesise that this localization may be due to the close proximity to intestinal microbes or to involvement of IL-18 in IEC differentiation in intestinal crypts. Although the protective mechanism of inflammasome activation in IEC is not defined, previous studies suggest that IEC can secrete IL-18 and this has been associated with protection against *C. rodentium* infection (345, 536).

We aim to verify the involvement of IEC inflammasomes in protection against enteric pathogens and establish the basis of this protection. We also wish to characterize the production of IL-18, and whether inflammasome activation in IEC is constitutive or activated in response to pathogenic stimuli. These analyses will be carried out by parallel *in vivo* and *in vitro* models of infection, initially with the *C. rodentium* model of acute inflammation. To fully understand what triggers inflammasome activation we established an *in vitro* IEC screening platform for challenging IEC with both microbes and microbial compounds and characterising effector responses.

Technical aspects of the project:

Mice will be generated in which the inflammasome pathway is selectively ablated in IEC ($Asc^{\Delta VC}$). This will be done by crossing a transgenic strain in which Asc is flanked by loxP recombination sites ($Asc^{fl/fl}$) (537) with another transgenic strain expressing the Cre recombinase under the control of the epithelial cell-specific promoter Villin (Villin-Cre).

Intestinal morphology, physiology and local and systemic immune compartments will be characterised in inflammasome-deficient strains. They will also be assessed using models of intestinal bacterial infection that are already established within the lab, based on acute infection with *C. rodentium*.

In parallel, intestinal epithelial organoid culture has already been established in the group and will be utilised to generate primary IEC that can be analysed *in vitro* (16, 505). We aim to optimise the organoid culture system to generate primary IEC 2D monolayers enabling the examination of NLR activation circuits in polarized IEC. This overcomes the current difficulty of accessing the luminal surface of the closed 3D organoids and allows for *ex vivo* primary IEC infection assays, as well as the potential addition of selected leukocytes (or cytokines) to the basolateral surface of the epithelium. In first instance, organoid monolayers will be screened against different intestinal pathogens and their derived compounds.

Together these techniques will help further the understanding into the molecular mechanisms orchestrating epithelial inflammasome activation. This will inform potential new therapies against a variety of infectious and/or autoinflammatory diseases such as infection with enteric pathogens and IBD.

Chapter 2: Materials and Methods

2.1.Mice

Mice are maintained under specific pathogen-free (SPF) conditions in accredited animal facilities at the University of Oxford, UK. Experiments are performed in accordance with the UK Scientific Procedures Act of 1986 and under a Project License (PPL) authorised by the UK Home Office Animal Procedures Committee and approved by the Sir William Dunn School of Pathology Local Ethical Review Committee. Mice are routinely screened for *Helicobacter spp.* and other pathogens. Mice used were 8-12 weeks of age at the start of experiments.

Throughout this thesis, epithelial-specific Asc deficient mice will be referred to as $Asc^{\Delta VC}$ and their littermate controls as $Asc^{fl/fl}$ mice (Table 2.1 and Figure 2.1). Fully deficient Asc, Nlrp3 and Nlrc4 knock out (KO) mice were also used in this study and will be referred to as $Asc^{-/-}$, $Nlrp3^{-/-}$ and $Nlrc4^{-/-}$ mice, respectively. These mice are derived from different, individual mouse colonies and are compared to control C57/BL6 mice referred to as wild type (WT) B6 mice. $Asc^{\Delta VC}$ and $Asc^{fl/fl}$ mice were infected in parallel to $Asc^{-/-}$ mice. Given that $Asc^{-/-}$ mice originate from a different colony to the $Asc^{\Delta VC}$ and $Asc^{fl/fl}$ mice, all genotypes were cohoused for at least 21 days to normalise microbiota composition between the strains. Furthermore, in each individual experiment, mice were simultaneously infected with the same bacterial inoculum.

Table 2.1. Mouse strains used in this thesis.

Mouse colony	Referred to as	Origin
C57/BL6 (B6),	WT B6	Sir William Dunn School of Pathology
B6 *Nlrp3*$^{-/-}$	*Nlrp3*$^{-/-}$	Generated by George Xiaoxi Song-Zhao as described before (249, 538).
B6 *Nlrc4*$^{-/-}$,	*Nlrc4*$^{-/-}$	Professor Vishva Dixit (Genentech Inc., USA).
B6 *Asc*$^{-/-}$	*Asc*$^{-/-}$	Professor Vishva Dixit (Genentech Inc., USA).
B6 *Atg16l1*$^{\Delta villin}$	Not referred to. Only used for *Asc*$^{\Delta VC}$ generation	Transgenic strain in which Atg16l1 is flanked by loxP recombination sites; *Atg16l1*$^{Flox/Flox}$. Generated as described in (539).Crossed with Tg(*Vil1-cre*) mice obtained from Jackson Laboratories to express Cre recombinase under the control of the *Villin 1* promoter. Mice generated, crossed and provided by the H. Virgin laboratory (Washington University, Saint Louis, MO, USA).
B6 *Asc*$^{Flox/Flox}$	*Asc*$^{fl/fl}$	Transgenic strain in which Asc is flanked by loxP recombination sites (*Asc*$^{Flox/Flox}$). Mice generated and provided by Dr. Stefan Drexler, University of Lausanne, Switzerland, as previously described (264).
B6 *Asc*$^{\Delta Villin}$	*Asc*$^{\Delta VC}$	Generated by initially crossing *Atg16l1*$^{\Delta villin}$ with *Asc* $^{Flox/Flox}$ and selecting for: *1)* homozygous mice for the non-floxed Atg16l1 locus; *Atg16l1*$^{WT/WT}$. Outbreeding *Atg16l1*$^{Flox/Flox}$ *2)* homozygous for floxed *Asc* $^{Flox/Flox}$ locus. *3)* heterozygous Tg(*Vil1-cre*) locus Selective ablation of *Asc* in IEC.

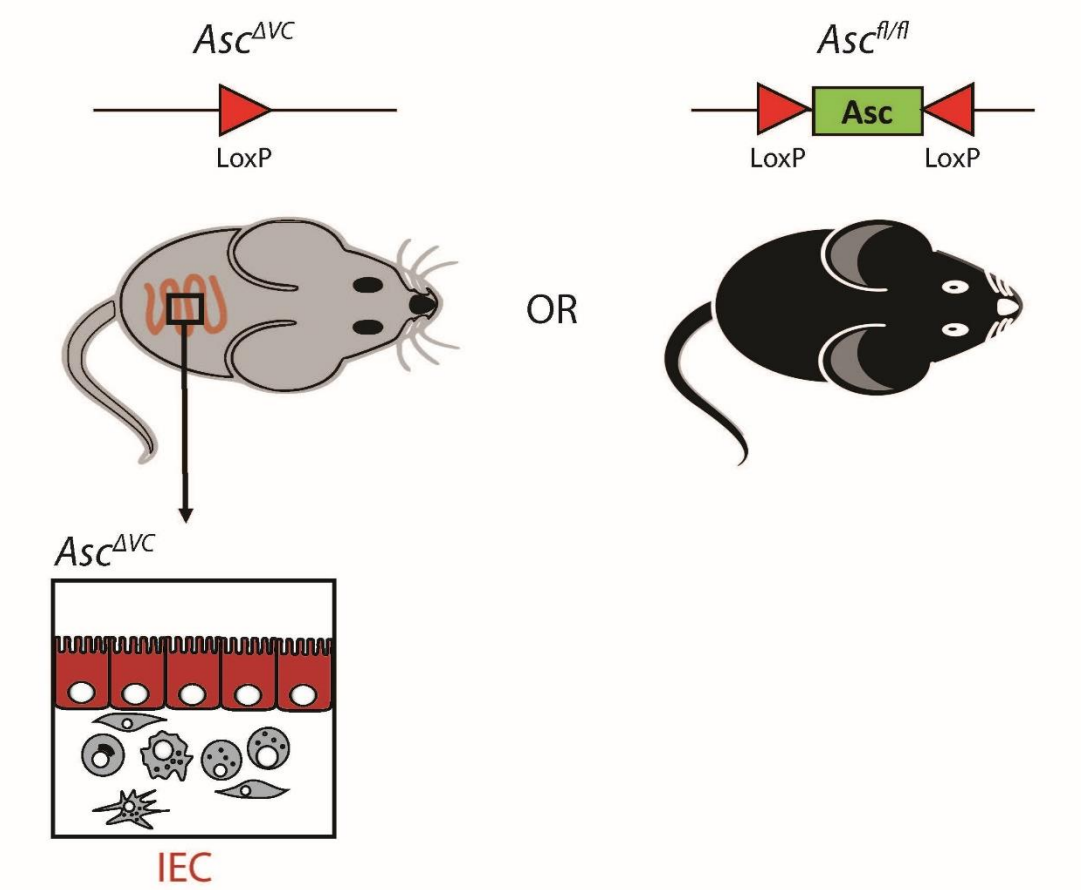


Figure 2.1. Schematic of epithelial-specific *Asc* knock-out mice, $Asc^{\Delta VC}$, and their littermate controls $Asc^{fl/fl}$**.** $Asc^{\Delta VC}$ mice denote mice that are homozygous for the *Asc* locus flanked by LoxP sites, and heterozygous for the Cre recombinase gene insertion preceded by the *Villin-1* gene promoter. $Asc^{fl/fl}$ mice denote mice that are homozygous for the *Asc* locus flanked by LoxP sites but lack the Cre recombinase gene.

2.2.Antibodies

Table 2.2. List of antibodies used in this study and their purpose.

Antibody	Dilution	Supplier/Clone	2ary antibody	Assay
Immunoblotting				
Caspase-1 (p10; M-20)	1:2000	Santa Cruz Biotech (sc-514)	Cell Signalling. Anti-rabbit IgG HRP-linked #7074S 1:3000	WB Lysates and supernatants
Caspase-1 p10	1:1000	Adipogen (AG20B0042-C100)	Cell Signalling. Anti-mouse IgG, HRP-linked Antibody #7076 1:3000	WB Lysates and supernatants
Caspase-1 p20	1:1000	Adipogen (AG20B004-C100)	Cell Signalling. Anti-mouse IgG, HRP-linked Antibody #7076 1:3000	WB Lysates and supernatants
IL-1β (mouse specific)	1:1000	Cell signalling (2022)	Cell Signalling. Anti-rabbit IgG HRP-linked #7074S 1:3000	WB Lysates and supernatants
IL-18	1:1000	Abcam (ab71495)	Cell Signalling. Anti-rabbit IgG HRP-linked #7074S 1:3000	WB Supernatants
Cleaved caspase-8 (Asp387) (D5B2)	1:2000	Cell Signalling (8592S)	Cell Signalling. Anti-rabbit IgG HRP-linked #7074S 1:3000	WB Lysates
Cleaved Caspase-3 (Asp175)	1:2000	Cell Signalling (9661S)	Cell Signalling. Anti-rabbit IgG HRP-linked #7074S 1:3000	WB Lysates
Caspase-11	1:2000	Cell Signalling (143405)	Cell Signalling. Anti-rat IgG HRP-linked #7077 1:3000	WB Lysates and supernatants
Tubulin	1:1000	Santa Cruz Biotech (sc5286)	Cell Signalling. Anti-rabbit IgG HRP-linked #7074S 1:3000	WB Lysates
FACS				
MHCII	1:200	Ebioscience (M5/114.15)	NA	FACS PMN
CD11b	1:200	Ebioscience (M1/70)	NA	FACS PMN
CD11C	1:300	Ebioscience (N418)	NA	FACS PMN
F4/80	1:100	BioLegend (BMB)	NA	FACS PMN
Ly6C	1:100	BD Biosciences (AL-21)	NA	FACS PMN

Antibody	Dilution	Supplier/Clone	2ary antibody	Assay
Ly6G	1:400	BD Biosciences (1A8)	NA	FACS PMN
Siglec-F	1:200	Ebioscience (E50-2440)	NA	FACS PMN
GR1	1:100	Ebioscience (RB6-8C5)	NA	FACS PMN
Aqua (live/dead)	1:1000	Ebioscience	NA	FACS PMN
Immunofluorescence				
rabbit anti-Asc	1:200	Santa Cruz Biotech (sc22514R)	Life Technologies Goat antibodies conjugated to AlexaFluor 488 or 555	Immunofluorescence staining of IEC monolayers and histology slides
mouse anti-E-cadherin	1:500	BD Bioscience (610182)	Life Technologies Goat antibodies conjugated to AlexaFluor 488 or 555	Immunofluorescence staining of IEC monolayers and histology slides
rabbit anti-*C. rodentium* antiserum	1:2000	Gift from Professor Gad Frankel (Imperial College London)	Life Technologies Goat antibodies conjugated to AlexaFluor 488 or 555	Immunofluorescence staining of IEC monolayers and histology slides
Phalloidin	1:50	Conjugated to AlexaFluor 647 (8940S)	NA	Immunofluorescence staining of IEC monolayers
DAPI	1:50000	Sigma D9542-5 mg	NA	Immunofluorescence staining of IEC monolayers and histology slides

2.3.Cytokines and PAMP

Table 2.3. List of cytokines and PAMP used in this study for *in vitro* stimulation of epithelial organoids and monolayers

Condition	Supplier	Final Concentration
IFN-y	InVivogen	100 ng/ml
TGF-b	R&D	100 ng/ml

Condition	Supplier	Final Concentration
IL-6	MBL	100 ng/ml
IL-13	R&D	100 ng/ml
IL-21	Peprotech	100 ng/ml
IL-22	R&D	100 ng/ml
IL-23	R&D	100 ng/ml
IL-25	eBiosciences	100 ng/ml
IL-27	eBiosciences	100 ng/ml
LPS	Alexis Biochemicals ultra-pure (isolated and purified from *E. coli* EH100 (Ra-mutant))	100 ng-2 µg/ml
Flagellin	InVivogen	2 µg/ml
MDP	InVivogen	2 µg/ml
ODN	InVivogen	2 µM
Pam3Cys	InVivogen	2 µg/ml
Poly I:C	InVivogen	2 µg/ml
Zymosan	NA	2 µg/ml

2.4. Primer list

Table 2.4. List of primers used in this study. Abbreviations: ribosome binding site (RBS).

Gene	Forward	Reverse	Supplier
Genotyping			
Atg16l1 *Flox/Flox*	ctttctcaacagaaccagcagtac	gtagaaagactggtgatggtaaacc	Sigma
Asc *Flox/Flox*	ggcttagtgttctagctgtt	accaggaagtcagctgctta	Sigma
Cre	aggttcgttcactcatgga **fabpi internal control F:** cctccggagagcagcgattaaaagtgtcag	tcgaccagtttagttaccc **fabpi internal control R:** tagagctttgccacatcacaggtcattcag	Sigma
Sybr Green qPCR			
ler	aatatacctgatggtgctcttg	ttcttccattcaataatgcttctt	Sigma (540)
tir	tacacattcggttattcagcag	gacatccaaccttcagcata	Sigma (468)
rrsA (16S rRNA gene)	aggccttcgggttgtaaagt	attccgattaacgcttgcac	Sigma(540)
Taqman probes for qPCR			
All Taqman primer and probe mixes were predesigned by the supplier (Life Technologies). Probes with best coverage were selected.			

Gene	Forward	Reverse	Supplier
Primers for cloning			
ler	gatcggtaccatatcttaatatataaaagtatgaggagattattta	gatcctgcagttaaatgttattcagagatgttacttc	Sigma. Designed for this thesis
ler+RBS	gatcggtaccgggaggcgatatgaggagattatttattatgaatatg	gatcctgcagttaaatgttattcagagatgttacttc	Sigma. Designed for this thesis
glrA	gatcggtaccaaataaaaagaacatggaaaatgg	gatcctgcagctaactctccttttttcgtctc	Sigma. Designed for this thesis
glrA+RBS	gatcggtaccggagggacggatggaatctaaaaatagtgactatgta	gatcctgcagctaactctccttttttcgtctc	Sigma. Designed for this thesis
pBAD	atgccatagcatttttatcc	ctgatttaatctgtatcagg	Sigma

2.5.Bacterial culture and infection

2.5.1. Citrobacter rodentium culture

A single colony of a nalidixic acid resistant strain of *Citrobacter rodentium* (ICC169) was transferred to nalidixic acid (BD-Biosciences)-supplemented Luria-Bertani broth and grown overnight (ON) at 37^0 C shaking to stationary phase. The next day, the culture was diluted to an optical density of 0.1 at OD_{600} and grown to log phase (OD_{600} 1-1.5), before harvesting by centrifugation. Harvested bacteria were suspended in sterile PBS for *in vivo* infection and in sterile cell culture media for *in vitro* infections.

2.5.2. Salmonella Typhimurium culture

A single colony of ampicillin resistant strain of *S.* Typhimurium (NCTC12023; Amp^R) was transferred to ampicillin-supplemented (Sigma) LB broth and grown ON at 37^0 C shaking to stationary phase. The next day, the culture was diluted to an optical density of 0.1 at OD_{600} and grown to log phase (OD_{600} 1), before harvesting by centrifugation. Harvested bacteria were suspended in sterile cell culture media for *in vitro* infections.

2.5.3. Salmonella Typhimurium and Citrobacter rodentium in vitro infections

Epithelial monolayers were infected with multiplicity of infection (MOI) ranging from 1 to 100 with *C. rodentium* or *S.* Typhimurium for different stipulated time points. Following the incubation period, the culture supernatants were collected, centrifuged at 13000rpm at 4^0 C for 15 min to dispose of cells in suspension in the supernatants and then frozen at -20^0 C. Furthermore, cells were lysed in RIPA buffer or RLT+β-mercaptoethanol buffer (as indicated below) and stored at -80^0 C for subsequent preparation for immunoblotting or qPCR.

2.5.4. Citrobacter rodentium in vivo infection

Mice were orally gavaged with 200µl of bacterial solution at a concentration of ~10^9 CFU per mouse. Thereafter, mice were weighed every day during infection and euthanized if weight loss exceeded 20% of their initial body weight. Mice were culled at various time points post infection (3, 8, 14 and 21 days p.i.), and different tissues were dissected for further assessment of intestinal inflammation (isolate tissues stated in Figure 2.2).

2.6.Assessment of intestinal and systemic inflammation

2.6.1. Isolation of tissues from C. rodentium infected mice

Mice were sacrificed at the indicated time points during *C. rodentium* infection. At the time of sacrifice, intestinal tissues were dissected from the mouse and cleaned in sterile phosphate buffered saline (PBS), kept moist and on ice during tissue collection and until further processing in this order (Figure 2.2):

1. **Spleen (SP)**: whole spleens were isolated and stored in PBS-bovine serum albumin (BSA). The weight of the whole spleen was recorded and then spleens were cut into 3 pieces that were individually weighted and stored in PBS (for CFU counting), PBS-0.1% BSA (for fluorescence activated cell sorting (FACS)) and PBS-1%Penicillin-Strptamycin (P/S; Gibco) (for organ explants).

2. **Liver (LV):** ~2 cm pieces from a liver lobe were cut and stored in PBS for subsequent quantification of CFU

3. **Colon (CL)**: the last 0.5-1 cm from the colon (distal colon) was sectioned and fixed in 10% formaldehyde for histology analysis. Next, colon was cut open and several pieces were cut and stored for different purposes: for CFU counts (PBS), RNA and protein analysis (snap-frozen in liquid nitrogen), organ explants (PBS-1% P/S). The remaining tissue was also cut in 0.5-1 cm pieces that were stored in PBS-0.1% BSA for subsequent tissue processing and digestion with the purpose of isolating IEC, IEL, stroma cells and lamina propria leukocytes (LPL) (Figure 2.2 and Figure 2.3). These cells were then subsequently processed for different analyses such as RNA, immunoblotting and FACS.

4. **Cecum (CM)**: the cecum was cut open and cecal contents were collected and kept in PBS for further processing. Two longitudinal 0.2-0.5 cm pieces of cecum were cut and kept in PBS-0.1% BSA (for CFU count) and in PBS-1% P/S (for organ explants). Another two 0.5-1 cm of cecum were cut and snap-frozen for subsequent protein and RNA analysis. The remaining cecal tissue was laid on a piece of blotting paper and fixed in 10% formaldehyde in PBS.

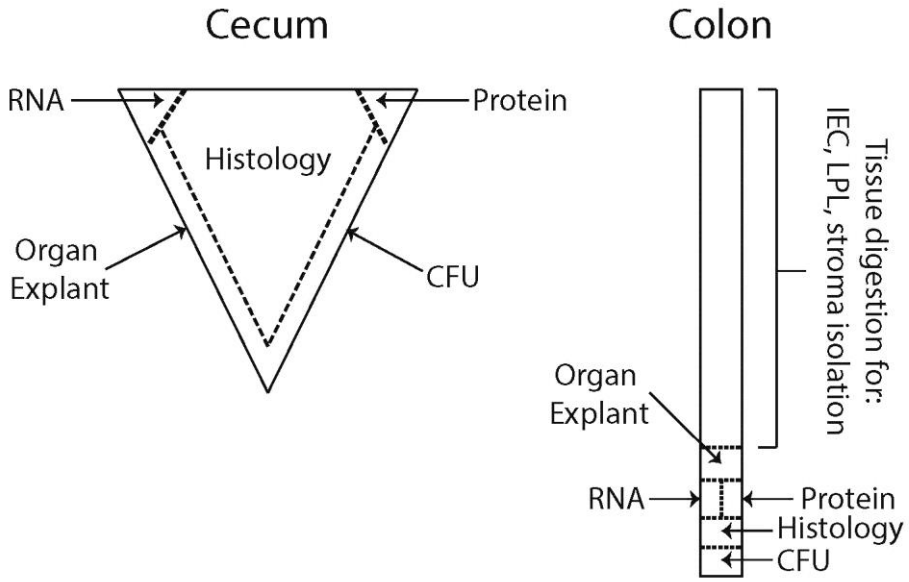


Figure 2.2. Intestinal tissue isolation map. Tissue pieces cut from each intestinal part and their purpose

2.6.2. Quantification of C. rodentium colonization

To measure the tissue adherent *C. rodentium* levels in the different tissues (spleen, liver, colon, cecum) and cecal contents of infected mice, tissues were first weighed and then homogenized using glass beads in a FASTPREP-24 (MP) in 600µl of sterile PBS for 40 s at 6.5 m/s. Cecal contents, in turn, were vortexed and centrifuged at 1000 g for 1 min. The tissue lysate and cecal content supernatants were then serially diluted in PBS. Dilutions were subsequently plated on nalidixic acid (50µg/ml) LB agar plates and incubated at 37^0 C ON before counting colony forming units (CFU) the following day. *C. rodentium* (ICC169) harbours a spontaneous mutation that makes it resistant against nalidixic acid. Therefore, this plating method allows for the selection of *C. rodentium*. The number of colonies were normalised to the weight of the tissue/cecal content used for homogenization to generate CFU/g.

2.6.3. Histopathology analysis

Mice were euthanized at indicated time points and tissue sections were rinsed in PBS-0.1% BSA and isolated as explained above. Tissue sections of 0.5-1 cm from cecum and distal colon were isolated as previously mentioned and fixed in PBS containing 10% formaldehyde for at least 24h at room temperature (RT). Tissue that designated for immunohistochemistry (IHC) was transferred to 70% Ethanol following the 24h in 10% formaldehyde and stored at 4^0 C until processed.

Fixed tissue was paraffin-embedded and cut into ~5μm sections using a microtome for subsequent staining with haematoxylin and eosin (H&E). Sections of cecum and distal colon were then scored by two researchers in a blinded fashion in accordance with the criteria for *C. rodentium*-induced intestinal pathology (Table 2.5). Scores for colon sections were averaged together to give the total histopathology score. The average scores for the two sites were then calculated to generate the combined histopathology score. Only cecum and distal colon were scored as minimal inflammation developed in other regions (final score 0-15). Micrographs were acquired on a CoolScope Microscope (Nikon, Tokyo, Japan).

Table 2.5. Summary of histological scoring for *C. rodentium*-induced colitis.

A	Epithelium	Hyperplasia	and/or	Goblet Cell Depletion	and/or	Damage
	0	None		None		None
	1	Mild (1.5X)		Mild (25%)		Mild
	2	Moderate (2-3X)		Marked (25-50%)		Marked
	3	Severe (>3X)		Substantial (>50%)		Substantial
B	Inflammation in lamina propria					
	0	None - few leucocytes				
	1	Mild - some increase in leukocytes at tips of crypts OR many lymphoid follicles				
	2	Moderate - marked infiltrate (notable broadening of crypt)				
	3	Severe - dense infiltrate throughout				
C	Submucosal	Edema		Infiltration		Follicle
	0	None	and/or	None	and/or	None
	1	Mild	and/or	Mild	and/or	Enlarged
	2	Marked	OR	Marked		-
	3	Marked	AND	Marked		-
D	Area affected (% of section)					
	0	None				
	1	Up to 25%				
	2	25-50%				
	3	>50%				
E	Markers of severe inflammation	Bleeding	and/or	Crypt abscesses	and/or	Necrosis/ulceration
	0	None		None		None
	1	Some		Few		None
	2	Marked		Many		Few/small
	3	-		-		Large/many

2.7.Isolation of cell subsets

2.7.1. Cell isolation from spleen

Spleens were collected in PBS-0.1% BSA and stored on ice. To obtain a single cell suspension, spleen cells were disrupted using 70-100 µm cell strainers.

Any red blood cells present in samples were lysed using ACK buffer (Ammonium Chloride Potassium; 150 mM NH4CL, 10 mM, KHCO3, 0.1 mM NA2EDTA, pH 7.2-7.4). All cell samples were then resuspended in Roswell Park Memorial Institute medium 1640 (RPMI 1640)/BSA-PBS.

2.7.2. Cell isolation from lamina propria leukocytes and stroma cells

Colons were cut open and washed in PBS. The part of the colon destined for tissue processing (see Figure 2.2) was cut into ~0.5 cm pieces and collected in a 50 ml tube containing 10 ml of ice cold PBS-0.1% BSA. Next, colon pieces were washed again and resuspended in ~20 ml of warm (37^0 C) RPMI 1640/10% foetal calf serum (FCS) containing 5 mM ethylenediaminetetraacetic acid (EDTA) and subjected to orbital shaking at 180 rpm for 10 min. The supernatants from this first EDTA digestion contained the IEC fraction. This IEC fraction was centrifuged at 1500 rpm to collect IEC pellets which were then stored at -80^0 C for further processing or directly lysed in RLT buffer with β-mercaptoethanol (for RNA isolation), or in RIPA buffer for immunoblotting sample preparation as indicated below. The remaining tissue pieces were washed once more in RPMI/FCS/EDTA (2 washes in total), and supernatants were discarded. Next, ~10 ml of RPMI 1640 10%FCS containing 15 mM 4-(2-hydroxyethyl)-1-piperazineethanesulfonic acid (HEPES) was added to all samples to neutralize the EDTA activity at RT.

After discarding the supernatants from the HEPES wash, 10 ml of RPMI/10%FCS/15 mM HEPES containing 0.4 mg/ml type VIII collagenase (Sigma Aldrich, UK) and 40µg/ml DNase I (Roche, UK) was added and samples incubated for ~40 min-1h at 37^0 C with orbital shaking (180 rpm), until tissue pieces were fully digested. At this point, supernatants were collected and filtered through a cell strainer (100µm) into PBS/0.1% BSA; EDTA 5 mM was added to neutralise collagenase activity. Digestion was

centrifuged and resuspended in 3 ml 30% Percoll (GE, Amersham, UK) solution (P30; diluted in PBS). The cell suspension in P30 was overlaid over a gradient comprising 3 ml 75% Percoll solution (P75; diluted in PBS) overlaid with 4 ml of 40% Percoll solution (P40; diluted in RPMI 1640), creating a discontinuous gradient of P30(+cells)/P40/P75. Gradients were centrifuged without the brake for 20 min at RT and 1800 rpm. Leukocytes were isolated from the P40/P75 interface. Finally, LPL were washed with PBS/0.1% BSA and resuspended in ice cold PBS-0.1% BSA and stained for FACS (Figure 2.3).

To isolate stroma cells, cells in the P30 gradient and ¾ of the P40 gradient were combined and washed in PBS-0.1% BSA (supplemented with P/S). Cells were washed twice in this media by centrifuging at 500 g for 5 min, and resuspending in the same media. Then, cell pellet was resuspended in RPMI 1640+10%FCS+P/S and plated in 6-well plates (1 well per colon). Media was changed the following day and every other day thereafter. When cells reached confluency, they were transferred onto T75 flaks and expanded until fibroblasts-like cells are visible (~10 days). After 10 days, all cells other than stroma cells should die, leaving a pure population of stroma cells. Cells were expanded as needed (at a ratio of 1:2) by short trypsin treatment.

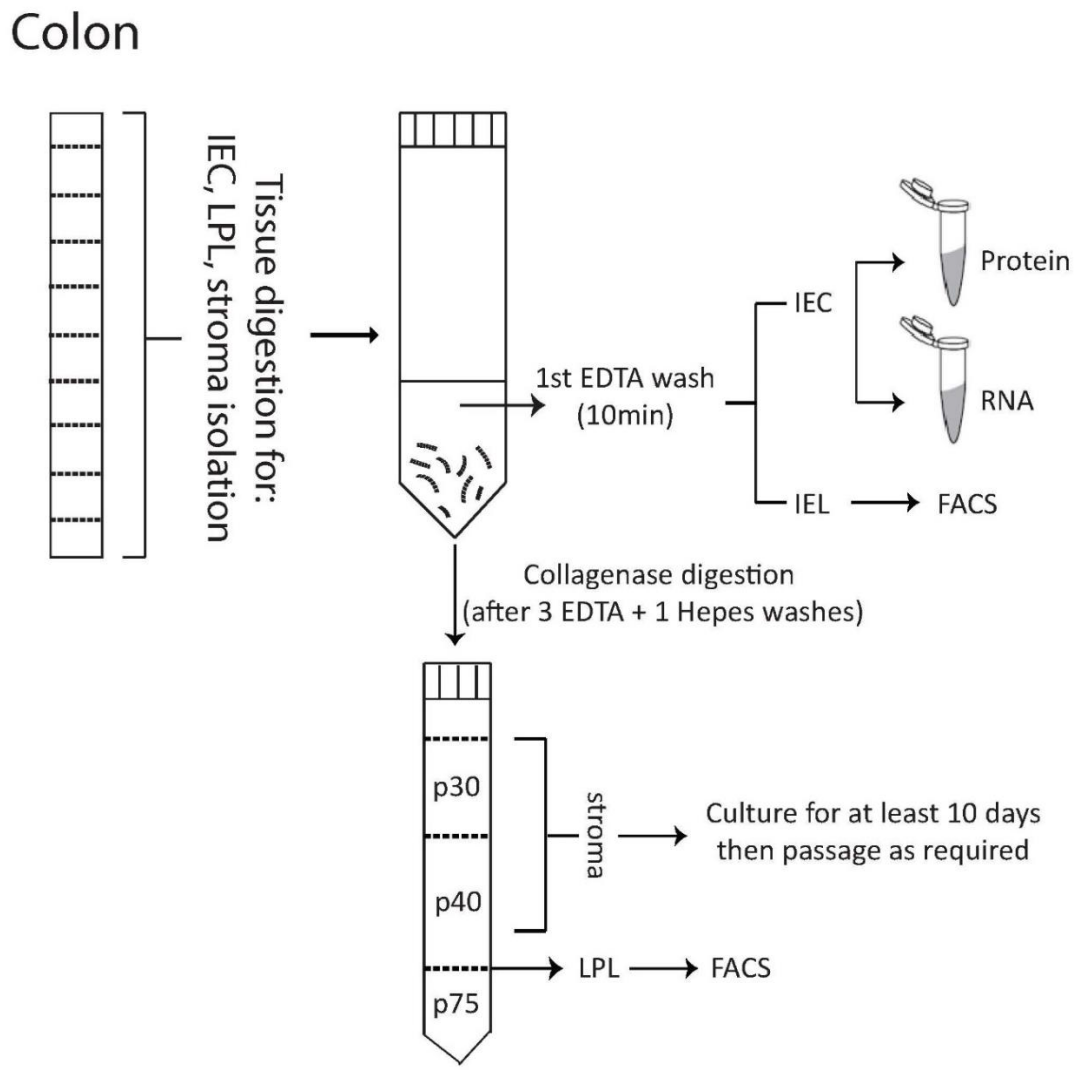


Figure 2.3. Summary of cell isolation from lamina propria leukocytes and stroma cells

2.7.3. Ex vivo culture of primary intestinal epithelial cells into 3D organoids and monolayers

Primary IEC organoids were cultured using methods established by Sato *et al.* (see Figure 2.4 for schematic overview) (505). Briefly, cecal fragments were harvested from WT mice, washed extensively in ice cold PBS and incubated in 2 mM EDTA in PBS for 90 min. The resulting crypt fractions were vigorously resuspended in 10% FCS/PBS, centrifuged and then embedded in 20µl of matrigel/well and seeded in 24-well plates. Matrigel was polymerized for 10 min at 37^0 C, followed by the addition of 400 µl/well of basal conditioned medium [Advanced Dulbecco's Modified Eagle Medium (DMEM)/F12 supplemented with 1%P/S, 10 mM HEPES, 5X GlutaMax, 1×N2, 1×B27

(all from Invitrogen), and 1 mM N-acetylcysteine (NAC) (Sigma)], supplemented with the following growth and differentiation factors: 50 ng/ml EGF (Invitrogen), 10µM coiled-coil containing protein kinase (ROCK) inhibitor Y27632 (Sigma), a 1:5 dilution of Wnt3A and Noggin, and a 1:10 dilution of R-spondin-1.

Fully concentrated Wnt3A and R-spondin-1 were obtained by culturing of recombinant murine L929 Wnt3A and R-spondin-1-expressing cells. Fully concentrated Noggin was obtained by culturing recombinant murine HEK 293 Noggin-expressing cells. Culture supernatants were harvested, filtered and concentrations of recombinant proteins were compared to previously tested batches with optimised protein concentrations via spotblot (Noggin and R-spondin-1) or a β-catenin stabilisation assay (Wnt3A). Organoids were cultured for at least 5 days after which cells were either seeded into monolayers or differentiated ON in conditioned-media supplemented with all growth and differentiating factors but with Wnt3A concentration reduced by 100-fold in order to perform pertinent experimental protocols.

IEC monolayers were generated by collecting the matrigel embedded organoids in PBS and digested in 1x TrypLE animal origin-free cell dissociation enzyme (Invitrogen). Cells were centrifuged and resuspended in the basal conditioned media and growth factors described above. Then cells were seeded at a density of 3-4 3D organoids/monolayer in 800µl of media per well in 24-well plates previously coated with 200µl/well of 51µg/ml Collagen I, Rat Tail (Life Technologies) in 0.02 M acetic acid (Sigma) (Figure 2.4). Monolayers were differentiated ON in growth factors-supplemented conditioned-media with a 1:100 diluted Wnt3A concentration to perform pertinent experimental protocols.

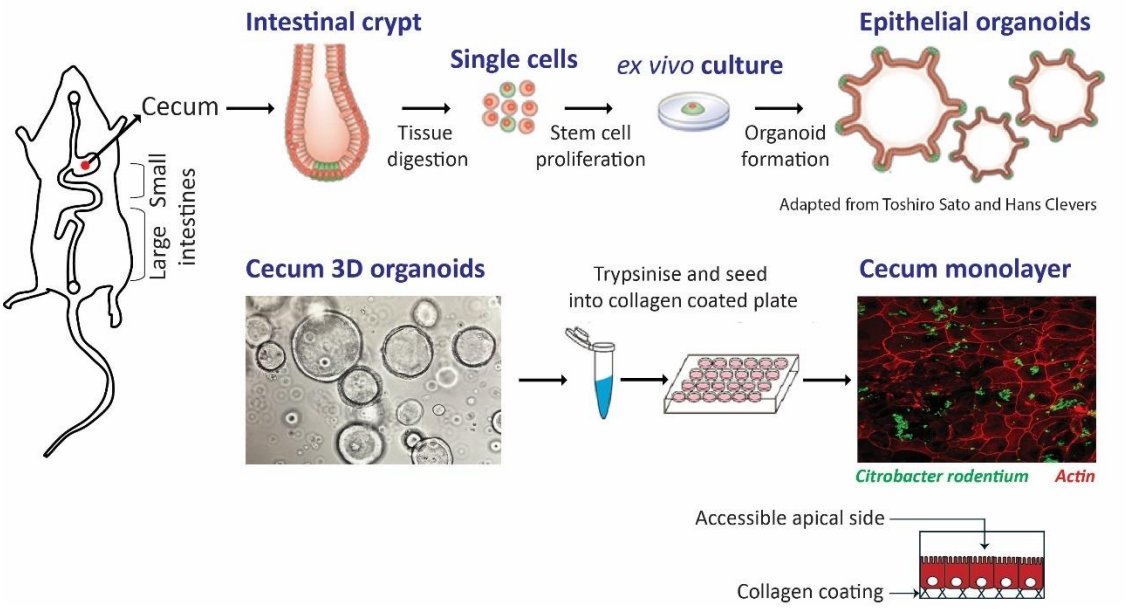


Figure 2.4. *Ex vivo* IEC 3D organoids and monolayers.

3D organoids: intestinal tissue was isolated from the mouse intestine and digested to enrich for intestinal crypts. The digested intestinal crypts were seeded into matrigel in the presence of Wnt3A, R-spondin-1 and Noggin to promote the growth of intestinal stem cells which form 3D organoids with crypt-like branches. Organoids can be repeatedly propagated through digesting and subsequent passaging in the presence of optimal growth factors.

Monolayers: The stem cell enriched 3D organoids were dissociated into single cells and then seeded in excess onto a collagen-coated well and in the presence of the same growth factors as in the 3D organoids. This leads to the formation of intestinal epithelial monolayers. The two IEC culture models are complementary as they facilitate access to the two highly polarised sides of the epithelium. The 3D organoid system allows access to the basolateral surface of the IEC, allowing us to mimic the response to cytokine secretion by lamina propria leukocytes, or to responses to PAMP following breach of the epithelial barrier by pathogens. Conversely, IEC monolayers allow access to the apical surface of the epithelium, permitting analyses of host-pathogen interactions during infection or invasion.

2.7.4. Isolation of bone marrow derived macrophages (BMDM)

Bone marrow was flushed from femur and tibia with PBS and a 26G needle. Cells were washed and resuspended in complete RPMI 1640 medium (10% FCS, 1x Pen/Strep, 1x GlutaMax) supplemented with 15% L929 cell conditioned media. Cells were cultured at 37^0 C in a 5% CO_2 incubator in 15 cm bacterial plastic petri dishes (Falcon, BD Bioscience) for three days before adding fresh media. On day 6, the medium was completely changed before detaching BMDM on day 7 using PBS/10 mM EDTA containing 4 mg/ml lidocaine (Sigma Aldrich) and plating at $1x10^6$cells/well in a 24-well plate. As positive controls for inflammasome activation BMDM pre-treated with 20 ng/ml LPS 4-12h (Alexis biochemical) (LPS priming did not exceed 12h to avoid

excessive dampening of the priming effect as described by Gurung *et al.* (541)). The next day BMDM were washed three times with PBS before treatment with either 5μM Nigericin or 5 mM ATP (both from Sigma Aldrich) for 5 hours and 2 hours, respectively.

2.8.*Ex vivo* culture of organ explants

To measure cytokine levels from colonic, cecal and spleen tissues, ~0.5 cm tissue pieces were cut, washed in PBS-1% BSA and kept in PBS-1% BSA + P/S for at least 30 min to prevent bacterial overgrowth. Next, tissue pieces were weighed and transferred into a single well of a 48-well plate with 400μl of RPMI 1640 supplemented with 10% FBS, 100 units/mL penicillin, 0.1 mg/mL streptomycin and 1:1000 β-mercaptoethanol, and incubated ON at 37^0 C and 5% CO_2. Supernatants were then collected and stored at -20^0 C prior to further analysis.

2.9.Flow cytometry

2.9.1. Surface FACS staining

Cell suspensions of spleen and LPL were prepared as previously described. Cell numbers were determined with a haemocytometer or automatic cell counter. Approximately $2x10^6$ splenocytes and ~$0.2\text{-}0.5X10^6$ LPL were used for FACS staining. Cells were plated in 96-well V- bottom plates, and centrifuged at 1500 rpm for 3 min. Supernatants were discarded and cells were resuspended in 100μl PBS-0.1% BSA containing 1:100 FcR block (eBioscience) and 1:1000 live Dead stain (eBioscience) and incubated for 15 min at 4^0 C. Next, samples were centrifuged for 1500 rpm/3 min, supernatants were discarded and cells resuspended in PBS-0.1%BSA containing surface antibodies at the relevant dilution (Table 2.2) for 30 min at 4^0 C in the dark. Cells were then washed in PBS-0.1%BSA and fixed with 200μl of 2% paraformaldehyde (PFA) prior to FACS analysis.

For intracellular cytokine staining, fresh spleen, MLN or LPL cell suspensions were restimulated in 96-well plates for 3h at 37^0 C 5% CO_2 in 200μl RPMI 1640/10% FCS containing 100 U/ml penicillin/streptomycin, 2 mM L-glutamine and 0.05 mM 2-mercaptoethanol, supplemented with 0.1μg/ml Phorbol 12-myristate 13-acetate (PMA), 1μg/ml ionomycin and 10μg/ml Brefeldin A (Insight Biotechnology, Wembley, UK).

Following surface staining as described above, cells were fixed in Fixation/Permeabilization Buffer (eBioscience) for 30 min at RT. Samples were then centrifuged and cells resuspended in BSA-PBS and stored ON at 4^0 C protected from light. The following day, cells were washed in 1X permeabilization buffer (eBioscience) containing 2% Rat serum to block non-specific antibody binding. Samples were centrifuged at 1500 rpm for 3 min and resuspended in 50µl 1X permeabilization buffer (eBioscience) containing appropriate concentrations of antibodies and incubated for 30 min at 4^oC in the dark. Finally, cells were resuspended in PBS-0.1% BSA for FACS analysis.

2.10.Cytokine secretion and inflammasome activation assays

2.10.1. Quantification of cytokine levels

Cytokine levels from supernatants collected from BMDM, 3D organoids and IEC monolayer and organ explants were measured by ELISA.

- IL-1β was measured using Mouse IL-1β Ready-Set-Go ELISA (eBioscience) according to manufacturer instructions.
- IL-1α was measured using Mouse IL-1α Ready-Set-Go ELISA (Affimetrix) according to manufacturer instructions.
- IL-18 was measured using a sandwich ELISA with matched coating/capture (D047-3; MBL, R&D) and detection (D048-6; MBL, R&D) antibodies. Recombinant IL-18 (B004-2; MBL, R&D) was used to construct a standard curve.
    - **Note:** this IL-18 ELISA is unable to fully discriminate between the pro- and active forms of IL-18 with a documented cross reactivity of 10% (personal communication with R&D Systems). In addition, the pro-form of IL-18 is commonly released into the supernatant upon cell death. Therefore, results should be interpreted with some caution, especially at longer *in vitro* time-points as debri from cell death accumulates.
- IL-22 was measured using Mouse IL-22 DuoSet ELISA (R&D).

3,3',5,5'-Tetramethylbenzidine (TMB) (eBioscience) was used as a substrate and all reactions were stopped with 2 M H_2SO_4.

2.10.2. Caspase-1 activation assays

Caspase-Glo® 1 Inflammasome Assay was used following manufacturer's instructions (Promega). Assay was performed with 50µl of cell supernatant in flat and opaque-bottom 96-well plates that were opaque and white in colour. This is a bioluminescent method to selectively measure the activity of caspase-1. The Caspase-Glo® 1 Inflammasome Assay relies on a luminogenic caspase-1 substrate, Z-WEHD-aminoluciferin, in a lytic reagent. Addition of this reagent leads to cell lysis and active caspase-1 cleavage of the luminogenic substrate leading to generation of light by a recombinant luciferase.

2.11.Gene expression analyses

2.11.1. Tissue processing for RNA isolation

Snap-frozen *in vivo* tissue pieces: were homogenized for 40 s at 6.5 m/s using glass beads in a FASTPREP-24 (MP) in 350µl of RLT buffer with β-mercaptoethanol and proceeded to RNA isolation as below or stored at -80^0 C for future RNA isolation.

IEC monolayers and 3D organoids: were resuspended in RLT buffer with β-mercaptoethanol and stored at -80^0 C for further processing as outlined below.

Bacterial liquid cultures: bacteria were harvested from liquid cultures at ~7 OD_{600} and stored at -80^0 C or resuspended in 350µl RLT buffer with β-mercaptoethanol and homogenized for 5 min at 6.5 m/s using glass beads in a FASTPREP-24 (MP). Once homogenised, samples were immediately processed for RNA isolation and purification as outlined below.

2.11.2. RNA isolation and quantitative PCR (qPCR)

***In vivo* tissue pieces, IEC 3D organoids and monolayers**: total RNA was isolated using the RNeasy Mini Kit (Qiagen, Hilden, Germany), according to the manufacturer's

instructions. Next, 2µg of RNA were reverse transcribed using SuperScript III Reverse Transcriptase Kit (Invitrogen, Carlsbad, CA) and oligo-dT primers (Sigma), according to the manufacturer's instructions. qPCR reactions of mammalian samples were performed in duplicates and 4µL cDNA in duplicates in a final reaction volume of 20µL and was amplified using TaqMan Gene Expression Assay probes from Applied Biosystems (Foster City, CA), Eurogentec qPCR mix (RT-QP2X-03) with the cycling conditions recommended by manufacturer for use in the Applied Biosystems StepOnePlus Real-Time PCR System. Expression levels were normalized to *Hprt* (hypoxanthine phosphoribosyl transferase- housekeeping gene) and calculations were made using the either the $2^{-\Delta Ct}$ or the $2^{-\Delta\Delta Ct}$ method (542).

Bacterial cultures: total RNA was isolated using the RNeasy Mini Kit (Qiagen, Hilden, Germany), according to the manufacturer's instructions. Next, 2µg of RNA were reverse transcribed using SuperScript III Reverse Transcriptase Kit (Invitrogen, Carlsbad, CA) and oligo-dT primers (Sigma), according to the manufacturer's instructions. qPCR reactions of samples were performed in duplicates and cDNA was amplified using primers described in Table 2.4 and SYBR Green reagents mix (Agilent Brilliant III Ultra-fast Master Mix; 600889) with the cycling conditions recommended by manufacturer for use in the Applied Biosystems StepOnePlus Real-Time PCR System. Expression levels were normalized to *rrsA* (housekeeping gene) and calculations were made using the either the $2^{-\Delta Ct}$ or the $2^{-\Delta\Delta Ct}$ method (542). Of note, values obtained when normalising to *rrsA* are likely to be an underestimation of total expression levels in *C. rodentium* since the *rrsA* gene is a commonly used housekeeping gene present in all enterobacteria and therefore will account for bacteria other than *C. rodentium* in the gut (540).

2.12.Western Blot

2.12.1. Preparation of colon and cecum tissue pieces

Cecal and colonic tissues that were snap-frozen at the time of sacrifice were homogenized using glass beads in a FASTPREP-24 (MP) in 200µl of RIPA buffer (1% NP-40, 0.1% Sodium dodecyl sulfate (SDS), 50 mM Tris-HCl pH 7.4, 150 mM NaCl, 0.5% Sodium Deoxycholate, 1 mM EDTA) containing a 1X protease inhibitor cocktail (Roche, Basel, Switzerland) for 40 s at 6.5 m/s. Homogenate was then centrifuged at 13000 rpm at 4^0 C

for 15 min and supernatant was transferred to a new tube. Samples were frozen at -80^0 C for storage or protein quantification and denaturation was carried out prior to immunoblotting as indicated below.

2.12.2. Preparation of 3D organoids and IEC monolayers samples

Total protein extracts were prepared by lysing organoids/monolayers in 50-80µl/well of RIPA buffer containing a 1X protease inhibitor cocktail (Roche, Basel, Switzerland). Lysates were centrifuged at 13000 rpm at 4^0 C for 15 min and supernatant was transferred to a new tube. Samples were frozen at -80^0 C for storage or protein quantification and denaturation was carried out prior to immunoblotting as indicated below.

2.12.3. Protein quantification

Protein levels were normalised using the Bio-Rad DC Protein Assay, according to the manufacturer's instructions. A standard curve was made by 2- fold serial dilution of a 2 mg/ml solution of BSA in PBS. Colour reactions were detected by absorbance measurement at 650-750 nm on a 96-well plate reader, following manufacturer's instructions. Samples were then normalised by resuspending in 1X sample buffer (5X: 60 mM Tris HCl pH 6.8, 2% SDS, 0.02% Bromophenol Blue, 5% β-Mercaptoethanol, all from Sigma Aldrich).

2.12.4. Protein precipitation

Proteins were precipitated from supernatants to measure secreted proteins, including active caspase-1 and active IL-18. Supernatants were thawed and then concentrated with chloroform/methanol precipitation as follows: 1 volume of methanol and 0.25 volumes of chloroform were mixed with samples into a homogenous suspension. This mix was centrifuged for 5 min at 4^0 C and 13000 rpm. In this step, the protein precipitates at the interface between methanol and chloroform. The top layer was gently removed and replaced with another volume of methanol. The tube with the mix was gently inverted

and centrifuged for further 15 min at 4^0 C and 13000 rpm. Supernatants were discarded and samples were air dried for 10 min at 37^0 C prior to resuspension in 1x sample buffer. Protein samples were then boiled at 95^0 C for 5-10 min and placed immediately on ice for 1 min before centrifuging for 5 min at 4^0 C and 13000 rpm. Finally, samples were loaded and resolved on a SDS gel as described below.

2.12.5. Western Blots

Protein normalised between samples of interest (5-20 ug/sample) were resolved by SDS-polyacrylamide gel electrophoresis (PAGE) (Bio-Rad Mini-PROTEAN TGX 4-20% gels) at 100 V. Protein transfer was carried out at 35 V for 1h onto a methanol-activated polyvinylidene difluoride (PVDF) membrane (GE Healthcare) at 4^0 C. Membranes were then blocked with PBS-0.5% Tween-20 (Sigma Aldrich) containing 5% milk powder (Marvel) for 1h at RT. Next, the membrane was incubated with primary antibody at 4^0 C ON (Table 2.2).

The next day, the membrane was washed 4 times for 5 min each with PBS/0.2% Tween-20 before incubating with horseradish peroxidase (HRP)-conjugated secondary antibody (denoted in Table 2.2) for 1h at RT. After 5 washes with PBS/0.2% Tween-20 for 15 min each to remove non-specifically bound secondary antibody, membranes were incubated with SuperSignal West Femto (Thermo Scientific) according to the manufacturers' instructions. Membranes were developed using medical X-ray film (Fuji) and a RP X-OMAT developer (Kodak Limited, UK). Where possible, membranes were incubated in stripping buffer (0.2 M glycine, 1% SDS, 10% Tween-20, β-mercaptoethanol) for 10 min. After repeating this step once, membranes were washed twice in PBS for 10 min and twice in PBS-0.5% Tween-20 for 5 min. Membranes were then blocked and re-probed with primary and secondary antibodies as described above.

2.13.Cell death measurements

2.13.1. LDH release

LDH (lactate dehydrogenase) release into the supernatants of stimulated 3D organoids, BMDM and IEC monolayers was measured using the CytoTox 96® Non-Radioactive

Cytotoxicity kit (Promega), following the manufacturer's protocol. This assay relies in the conversion of a tetrazolium salt into a red formazan product. The absorbance is proportional to the number of lysed cells. Visible wavelength absorbance data are collected using a standard 96-well plate reader.

2.13.2. ApoTox-Glo Triplex Assay

In order to measure cell death and viability at the same time as caspase-3 and -7 activities, the Promega ApoTox-Glo Triplex assay was used according to the manufacturer's instructions. Assay was performed in white opaque-bottom 96-well plates. This assay relies on the use of GF-AFC and bis-AAF-R110 substrates. GF-AFC can enter live cells and is then cleaved by the live-cell protease to release AFC. bis-AAF-R110 cannot enter live cells but instead is cleaved by the dead-cell protease to release R110. AFC and R110 release can be measured by fluorescence at different wavelengths and infer on cell viability and cytotoxicity, respectively.

2.14.Fluorescence microscopy

2.14.1. IEC monolayer staining

Monolayers were grown on a collagen coated coverslip, in a 24-well plate as previously indicated. Following stimulation, monolayers were washed in PBS three times for 5 min and then fixed for 10 min with 3% paraformaldehyde in PBS. Next, monolayers were washed two times in PBS prior to permeabilization and blocking for 30 min (in 10% normal goat serum (NGS) and 0.5% saponin in PBS-5% BSA). Samples were then washed once more in PBS and probed with primary antibodies (Table 2.2) diluted in 5% NGS and 0.5% saponin in PBS- 5% BSA for 60 min at RT. Next, samples were washed 3 times with PBS and stained with secondary antibodies (Table 2.2) diluted in PBS- 5% BSA for 30 min at RT in the dark. Then, slides were washed twice for 5 min in PBS. All the above steps were performed with the coverslip still in the 24-well plate. Finally, coverslips were gently removed from the well with forceps and mounted with DAPI-containing Vectashield (Vector Laboratories, Burlingame, USA) onto a slide. Images

were acquired with an Olympus Fluoview FV1000 confocal microscope and Olympus Fluoview Software (Olympus, Tokyo, Japan).

2.14.2. Immunohistochemistry in in vivo tissue

Formalin-fixed and paraffin-embedded cecal and colonic tissues prepared as previously described (Figure 2.2) then deparaffinized and rehydrated with xylene and ethanol. Subsequently, antigen retrieval was performed by submerging slides in 10 mM (pH6) citrate buffer for 40 min at 96^0 C using a pressure cooker. Slides were then blocked with 5% BSA and 10% NGS in a moist chamber at RT for 1 h. Following this, slides were probed with primary antibodies stated in Table 2.2 in PBS with 5% BSA and 10% NGS at 4^0 C ON (or 60 min at RT). After 2 washes in PBS, slides were stained with secondary antibodies stated in Table 2.2 in PBS with 5% BSA and 10% NGS for 30-60 min at RT. Finally, slides were washed and then mounted with DAPI-containing Vectashield (Vector Laboratories, Burlingame, USA). Images were acquired with an Olympus Fluoview FV1000 confocal microscope and Olympus Fluoview Software (Olympus, Tokyo, Japan).

2.15.Genotyping

Mice were genotyped using ear tissue samples. Samples were digested ON at 55^0 C in lysis buffer (5 mM EDTA, 100 mM Tris-HCl, 0.2% SDS, 200 mM NaCl and 0.2 mg/ml, proteinase K (Bioline)). DNA was isolated from the digested supernatants by precipitation with isopropanol (1:1 volume). Following centrifugation at X for X, DNA pellets were washed with 70% ethanol and dried for 10 min at 37^0 C. DNA was then resuspended in 100 µl of ddH_2O. PCR reactions were carried on in a total volume of 15µl using Taq polymerase (0.7 U/µl, Invitrogen), PCR buffer (1x, Bioline), MgCl2 solution (2 mM, Bioline), dNTP mix (0.2 mM, Sigma), primers (0.5 µM) and 1 ul of DNA samples.

DNA for *Atg16l1*$^{fl/fl}$ and Cre PCR was amplified under following conditions:

1. 94^0 C, 4 min
2. 94^0 C, 30 s
3. 60^0 C, 30 s

4. 72^0 C, 1 min
5. 30 cycles from step 2
6. 72^0 C, 5 min
7. Hold at 4^0 C

DNA for *Asc*$^{fl/fl}$ PCR was amplified under following conditions:

1. 95^0 C, 5 min
2. 95^0 C, 45 s
3. 57^0 C, 30 s
4. 72^0 C, 40 s
5. 40 cycles from step 2
6. 72^0 C, 5 min
7. Hold at 4^0 C

2.16. Cloning of *ler* gene and transformation into *C. rodentium*

2.16.1. C. rodentium chemically competent protocol

A single bacterial colony from an LB plate was inoculated into 2 ml LB broth and grown ON at 37^0 C shaking. From this ON culture, 1 ml was inoculated into 100 ml of LB broth and vigorously shaken at 37^0 C until an OD_{600} of ~ 0.6 was reached. Upon reaching the desired OD_{600}, cells were chilled on ice for 20 min and subsequently centrifuged for 10 min at 4000 rpm and 4^0 C. Supernatant was then discarded and the cell pellet re-suspended in 50 ml of cold 50 mM $CaCl_2$ supplemented with 15% glycerol and kept on ice for 20 min. Cells were centrifuged once more as previously described, supernatant was again removed and the cell pellet resuspended in 5 ml of cold 50 mM $CaCl_2$ supplemented with 15% glycerol. Finally, cells were stored in 300 µl aliquots at -80^0 C.

2.16.2. Gene amplification and cloning

Genomic DNA from *C. rodentium* was isolated utilising the Qiagen DNeasy Blood and Tissue Kit as per the manufacturer's instructions. Genes encoding for the proteins of interest were amplified using PCR from *C. rodentium* genomic DNA utilising the Q5 Hot Start high fidelity polymerase (M0494S, New England Biolabs; NEB) and proofreading KOD Hot Start DNA Polymerase (Novagen), following the manufacturer's protocol and employing the oligonucleotide primers described in Table 2.4. The thermal cycling was done as follows: a 4 min initial denaturation at 94^0 C then 30 cycles of denaturation for

30 s at 94^0 C, primer annealing at 55^0 C for 30 secs, extension at 58^0 C for 1 min/Kb and a final extension for 10 min at 72^0 C. The correct size of the PCR amplification product was confirmed via gel electrophoresis in a 1% agarose gel with 0.5% Tris-acetate-EDTA buffer.

Amplified genes were subsequently PCR purified with Qiagen PCR purification kit following manufacturer's instructions. Pure PCR product (1µg) was then digested with KpnI and PstI enzymes for 1h 30 min at 37^0 C in NEB buffer (restriction sites were added at both ends of the amplified gene of interest though PCR, with the specified primers in Table 2.4). Following digestion, PCR products were PCR purified again as above. The plasmid pBAD33 (4µg) was digested under the same conditions as the PCR products. Next, digested pBAD33 was gel purified using the Gel Extraction Kit from Qiagen following manufacturer's instructions.

Digested and PCR purified PCR products were cloned into digested and gel purified pBAD33 by ligating each fragment to the plasmid with Thermo T4 ligase (in corresponding buffer) for 1h at 22^0 C. Product was then transformed into chemically competent *C. rodentium* and pBAD33 positive colonies were selected through chloramphenicol selection.

Successfully transformed colonies were picked and streaked onto fresh LB agar plates (chloramphenicol; 34 µg/ml) and allowed to grow ON. Cell lysate was prepared from each colony employing one cycle of freezing (-80^0 C for 10 min) and thawing (95^0 C for 15 min). Cell lysates were then used as DNA template for PCR screening with vector primers (Table 2.4). Taq Polymerase was used for the screening PCR and the thermal cycling was done as follows: an initial denaturing step at 94^0 C for 5 minutes followed by 30 cycles of: denaturation for 30 s at 94^0 C, primer annealing at 58^0 C for 30 secs, extension at 72^0 C for 1 min/Kb. Clones with the correct sized insert were selected and grown in LB broth at 37^0 C. Plasmids were then purified (QIAprep® Miniprep, Qiagen) and sent for sequencing (GATC Biotech) to confirm the absence of mutations.

Cloned *ler* (LEE encoded regulator) and *glrA* (Global Regulator of LEE-Activator), genes were amplified from *C. rodentium* genome and cloned into a PBAD plasmid for gene expression induction upon Arabinose supplementation of the media (Figure 2.5). To induce the expression of genes cloned into the pBAD plasmid, a single colony of *C. rodentium* transformed with pBAD plasmid was grown in LB chloramphenicol (34

μg/ml) ON at 37^0 C to stationary phase. The next day the culture was diluted to OD_{600} of 0.05 and grown for 1 h, after which L-arabinose (MPBio;100706) was added into the media. *C. rodentium* was allowed to grow to log phase (OD_{600} 1-1.5), before harvesting by centrifugation and subsequently used for infection.

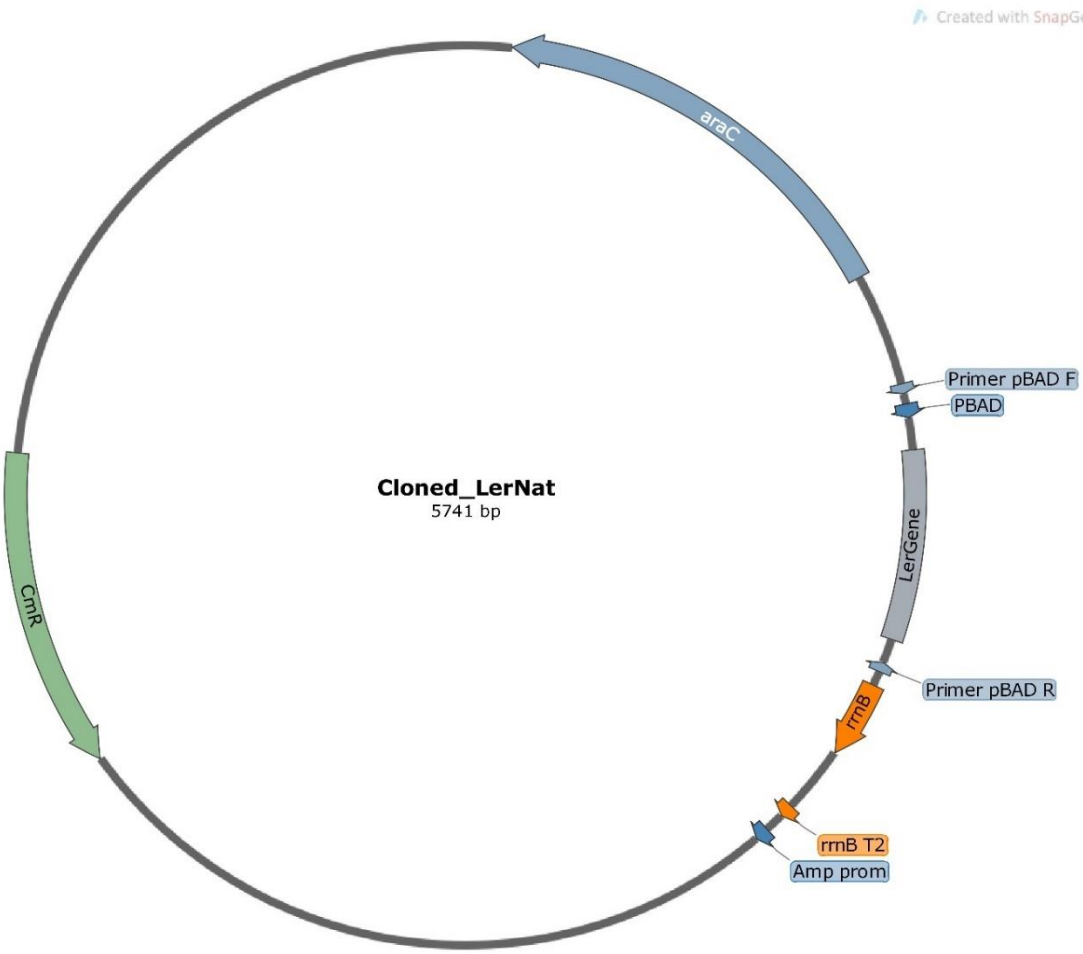


Figure 2.5. Map of pBAD33 vector containing the *ler* gene of *C. rodentium* under an arabinose inducible promoter. *AraC*: gene for *AraC* regulatory protein; *CmR*: chloramphenicol resistance marker; Primer pBAD F: forward primer used for sequencing; Primer pBAD R: reverse primer used for sequencing; PBAD: promoter; LerGene: cloned *ler* gene; *rrnB*: transcription terminator; Amp prom: ampicillin resistance gene promoter.

2.17.Statistics

Statistical significance between two *in vivo* treatment groups in this thesis was calculated using the nonparametric Mann-Whitney test. Except for weight curves and antibody titres, where p-values were determined by two-way ANOVA with Bonferroni post-tests. Statistical significance between two *in vitro* treatment groups in this thesis was calculated using an unpaired t-test. Statistics were calculated using GraphPad Prism 6 software. Differences were considered statistically significant when p: *$p<0.05$; **$p<0.001$; ***$p<0.0001$; ****$p<0.00001$.

Chapter 3: Protective role of epithelial *Asc* expression during intestinal infection with *Citrobacter rodentium*

3.1.Introduction

Diverse PRR are expressed by a range of cell types in the gut, including IEC, phagocytes and lymphocytes, but it is not clear how PRR signals in different cell types are co-ordinated to maintain homeostasis and host defence (543, 544). NLR are a diverse family of PRR that can be expressed by macrophages, monocytes, dendritic cells, neutrophils, and epithelial cells (167). Subsets of NLR play a critical role in driving the activation of the inflammasome, a multi-molecular scaffold that drives the activation of caspase-1, a key component in the inflammatory signalling cascade (190, 207). The major consequence of inflammasome formation is the auto-cleavage and consequent activation of caspase-1, a cytosolic protease that mediates the cleavage and secretion of the inflammatory cytokines IL-1β and IL-18 and also triggers an inflammatory form of cell death termed pyroptosis, targeted at clearing invading pathogens (545). Investigating the activation of this macromolecular complex facilitates a better understanding of its role in protective immunity, as well as in aberrant inflammatory responses associated with hyper-secretion of these cytokines (166, 340).

GWAS have identified many loci that influence susceptibility to intestinal inflammation. Many of these genes play a role in inflammation and innate immunity, and include: *IL-1R* (160), *IL-18R1-IL-18RAP* locus (161, 162), *IL-23*, and PRR such as *NOD2* and *NLRP3*(160). Although genetic and experimental data point to a key role for NLR and inflammasomes in regulating intestinal immunity and inflammation, several key issues remain poorly understood. These include the precise mechanisms of NLR activation and co-ordination of downstream effector responses and the way that NLR sensing contributes to protection and pathology.

In addition, there are contradictory data on the effects of NLR contribution to intestinal pathology. Nlrp3 and Nlrp6 inflammasome activation, for example, has been shown to protect from acute inflammation induced by administration of DSS (242, 256). However, other investigators reported pathogenic roles for Nlrp3 and caspase-1 in DSS colitis (486). These conflicting results could reflect cell-type specific effects of NLR activation that might occur in the context of different intestinal microbiota. Moreover, functional analyses of NLR and inflammasomes have been largely restricted to studies with

haematopoietic cells, and the effects of inflammasome activation in tissue cells, such as IEC, remain to be investigated in detail. Finally, although recent work from our group implied a role for Nlrp3 and Nlrc4 activation in the intestinal epithelium in protection against the mucosal pathogen *C. rodentium* (231, 249), the mechanisms responsible remain to be determined.

C. rodentium infection is a well characterised model of acute intestinal infection and inflammation (453). Previous work by our group and others, demonstrated that the inflammasome, specifically the inflammasome adaptor protein Asc, is important for limiting colonization and pathology in *C. rodentium*-infected mice (249, 345). Bone marrow chimera experiments revealed that when mice were deficient in Asc or Nlrp3 or Nlrc4 within the non-hematopoietic compartment, *C. rodentium* was able to colonise the cecal and colonic tissues of these mice to a greater extent (231, 249). This higher colonisation was accompanied with increased pathology and weight loss. This work suggested a role for inflammasomes in radio-resistant cells (249), which include cells of the intestinal epithelium, stromal cells and radiation resistant tissue resident phagocytes.

Additional evidence suggesting an important role for inflammasomes in the intestinal epithelium comes from observations that inflammasome components are highly expressed in the intestinal epithelium, including Nlrc4 and IL-18 (231, 255). Furthermore, signalling through IL-18, which is activated and released as a downstream consequence of inflammasome activation, has been linked to intestinal pathologies and protection against intestinal pathogens, including *C. rodentium* (251, 345). Indeed, *IL-18R*$^{-/-}$ and *IL-18*$^{-/-}$ mice exhibit increased *C. rodentium*-induced pathology and bacterial loads in intestinal tissues (249, 345).

In order to study the specific role of epithelial inflammasomes in protecting against *C. rodentium* infection, we generated mice that are selectively deficient in the key inflammasome adaptor Asc only within the intestinal epithelium. This was done by crossing a transgenic strain in which Asc is flanked by loxP recombination sites (*Asc*$^{fl/fl}$) (537) with another transgenic strain expressing the Cre recombinase under the control of the epithelial cell-specific promoter Villin (Villin-Cre). IEC-specific inflammasome deficient mice will be referred to as *Asc*$^{\Delta IVC}$, and their inflammasome competent littermate controls will be referred to as *Asc*$^{fl/fl}$. Littermate controls were used throughout these studies in order to avoid any potential confounding effects of microbiota differences

(362). In addition, where possible, *Asc*$^{\Delta IVC}$ and *Asc*$^{fl/fl}$ littermates were studied in parallel with fully deficient Asc KO mice which will be referred to as *Asc*$^{-/-}$. As *Asc*$^{-/-}$ originate from a different colony to the *Asc*$^{\Delta IVC}$ and *Asc*$^{fl/fl}$ mouse colony, mice were cohoused for at least 21 days prior to infection to minimize the potential confounding effects of microbiota drift (362).

Impaired innate immunity is a key factor influencing the susceptibility to infection and, as revealed by GWAS, inflammatory conditions. We aim to assess the mechanisms through which IEC inflammasome activation may influence the course of *C. rodentium* infection. This chapter will describe the observations made during *C. rodentium* infection studies in *Asc*$^{fl/fl}$, *Asc*$^{\Delta IVC}$ and *Asc*$^{-/-}$ mice, starting with the verification of IEC-specific ablation of *Asc* in *Asc*$^{\Delta IVC}$ mice.

3.2.Results

3.2.1. Asc deficiency within the intestinal epithelium of *Asc$^{\Delta VC}$* mice

To study the precise role of inflammasome activation within the intestinal epithelium we used a Cre-lox strategy to generate *Asc$^{\Delta VC}$* mice that lacked the adaptor protein Asc specifically in their IEC. To confirm that *Asc$^{\Delta VC}$* mice were deficient in Asc selectively within the intestinal epithelium, we isolated IEC from the colons of *Asc$^{fl/fl}$* and *Asc$^{\Delta VC}$* mice and subjected IEC lysates were to western blotting with anti-Asc antibody. We observed that IEC lysates from *Asc$^{\Delta VC}$* mice showed a dramatic reduction in Asc expression relative to IEC lysates from *Asc$^{fl/fl}$* littermates (Figure 3.1A). However, some residual Asc protein was still observed in IEC preparations from *Asc$^{\Delta VC}$* mice, which could reflect some contamination of the IEC fractions with LPL and IEL or to inefficient Cre deletion in some crypts (Figure 3.1A, Figure 3.4). Next, we made lysates from snap-frozen whole colonic tissue samples isolated from *Asc$^{\Delta VC}$*, *Asc$^{fl/fl}$* or *Asc$^{-/-}$* mice and again assayed Asc expression by western blotting. We observed that Asc was completely absent from the colon lysates of *Asc$^{-/-}$* mice, whilst it was still present at high levels in *Asc$^{fl/fl}$* colon samples, and was again dramatically reduced in *Asc$^{\Delta VC}$* colonic tissue (Figure 3.1B). As IEC are the principal cellular component of the colon tissue sections analysed, these results are consistent with a loss of Asc in IEC of *Asc$^{\Delta VC}$* mice (Figure 3.1B).

To further assess Asc expression *in vivo*, we performed immunohistochemical staining of Asc in paraffin-embedded intestinal tissue sections isolated from *Asc$^{\Delta VC}$* and *Asc$^{fl/fl}$* littermates. Sections were probed with DAPI, anti-Asc and anti-E-cadherin antibodies, and secondary antibodies for Asc (anti-rabbit-488), and E-cadherin (anti-mouse-555) were used for fluorescence microscopy. We observed that cytosolic Asc staining was ubiquitous in IEC in both the colon and cecum samples isolated from *Asc$^{fl/fl}$* mice, whereas there was very little detectable signal in samples from *Asc$^{\Delta VC}$* littermates (Figure 3.2 and Figure 3.3). However, a more detailed examination suggested that the deletion of Asc in the intestinal epithelium of *Asc$^{\Delta VC}$* mice was not 100% efficient in all mice, as we observed a few Asc-positive crypts in cecal sections in 2 out of 10 individual *Asc$^{\Delta VC}$* mice that we examined. These Asc positive crypts were evident in the cecum of these selected *Asc$^{\Delta VC}$* mice, but were not found in the colon (Figure 3.4). From the *Asc$^{\Delta VC}$* mice that had Asc-positive crypts, approximately 88 out of ~5000 intestinal crypts counted (1.8%) were

positive for Asc, and these were found in patches in the cecal tissues of *Asc*$^{\Delta VC}$ mice (Figure 3.4). Of note, under homeostatic SPF conditions, we did not observe any morphological or behavioural abnormalities in *Asc*$^{\Delta VC}$ mice or in their *Asc*$^{fl/fl}$ littermates (Figure 3.2 and Figure 3.3).

Lastly, to assess whether *Asc*$^{\Delta VC}$ mice retained Asc protein expression in their haematopoietic cell compartment, we performed IHC staining of the intestinal tissues of *C. rodentium* infected mice. At day 14 post infection, we observed dense infiltrates of Asc-positive cells in the lamina propria of *Asc*$^{\Delta VC}$ mice, but no detectable expression of Asc in IEC (Figure 3.5).

Taken together, these results indicate that the Cre-lox strategy used was highly efficient in selectively ablating Asc expression in IEC, while not affecting Asc expression in haematopoietic cell compartments of *Asc*$^{\Delta VC}$ mice.

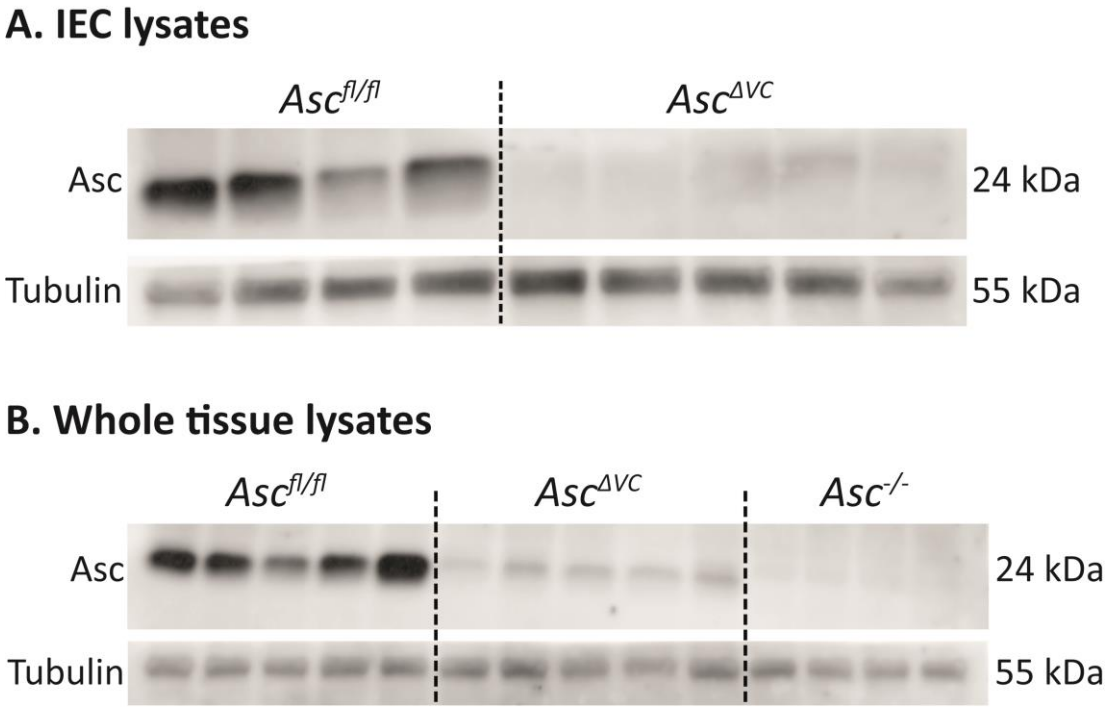


Figure 3.1. Asc deficiency in intestinal epithelial cells from *Asc$^{\Delta VC}$* mice. (A) IEC were collected by washing colonic tissue pieces from *Asc$^{fl/fl}$* and *Asc$^{\Delta VC}$* mice in EDTA. Asc expression by IEC lysates was then determined by western blot. (B) Asc expression was determined by western blotting for Asc in cell lysates from snap-frozen whole colonic tissue isolated from Asc$^{fl/fl}$, *Asc$^{\Delta VC}$* or *Asc$^{-/-}$* mice. Tubulin was used as loading control. Each lane represents an individual mouse (n = 4-5 per group).

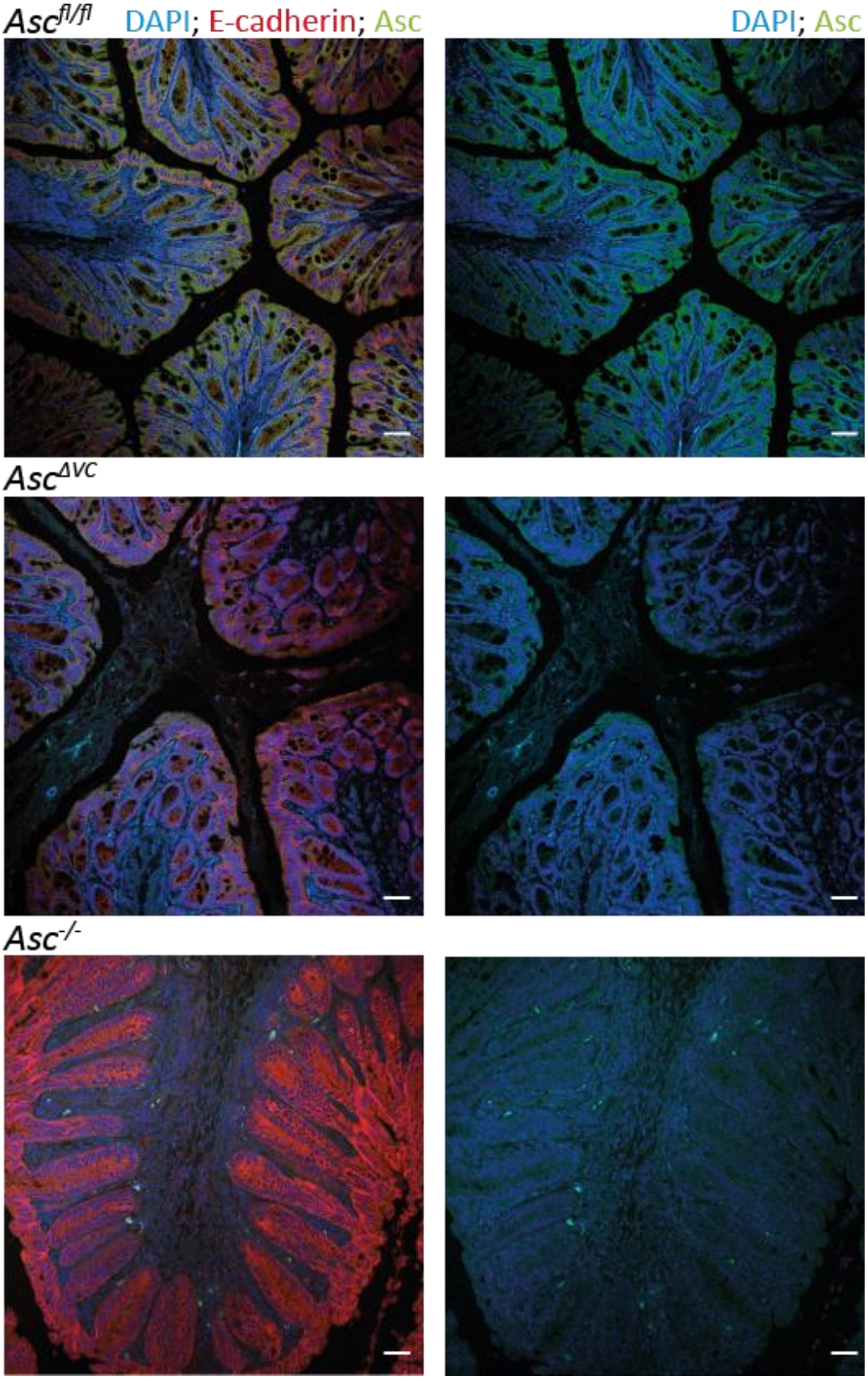


Figure 3.2. Colonic intestinal epithelial cells from *Asc*$^{\Delta VC}$ mice are deficient in Asc. Colon tissue samples were isolated from *Asc*$^{fl/fl}$ and *Asc*$^{\Delta VC}$ littermates at steady state and *Asc*$^{-/-}$ mice at 14 days p.i. with 10^9 *C. rodentium* CFU. Tissue sections were paraffin-embedded and subsequently stained for Asc (green), E-cadherin (red) and DAPI (blue). Bar= 20µm. Data representative of n=5-10 mice per genotype.

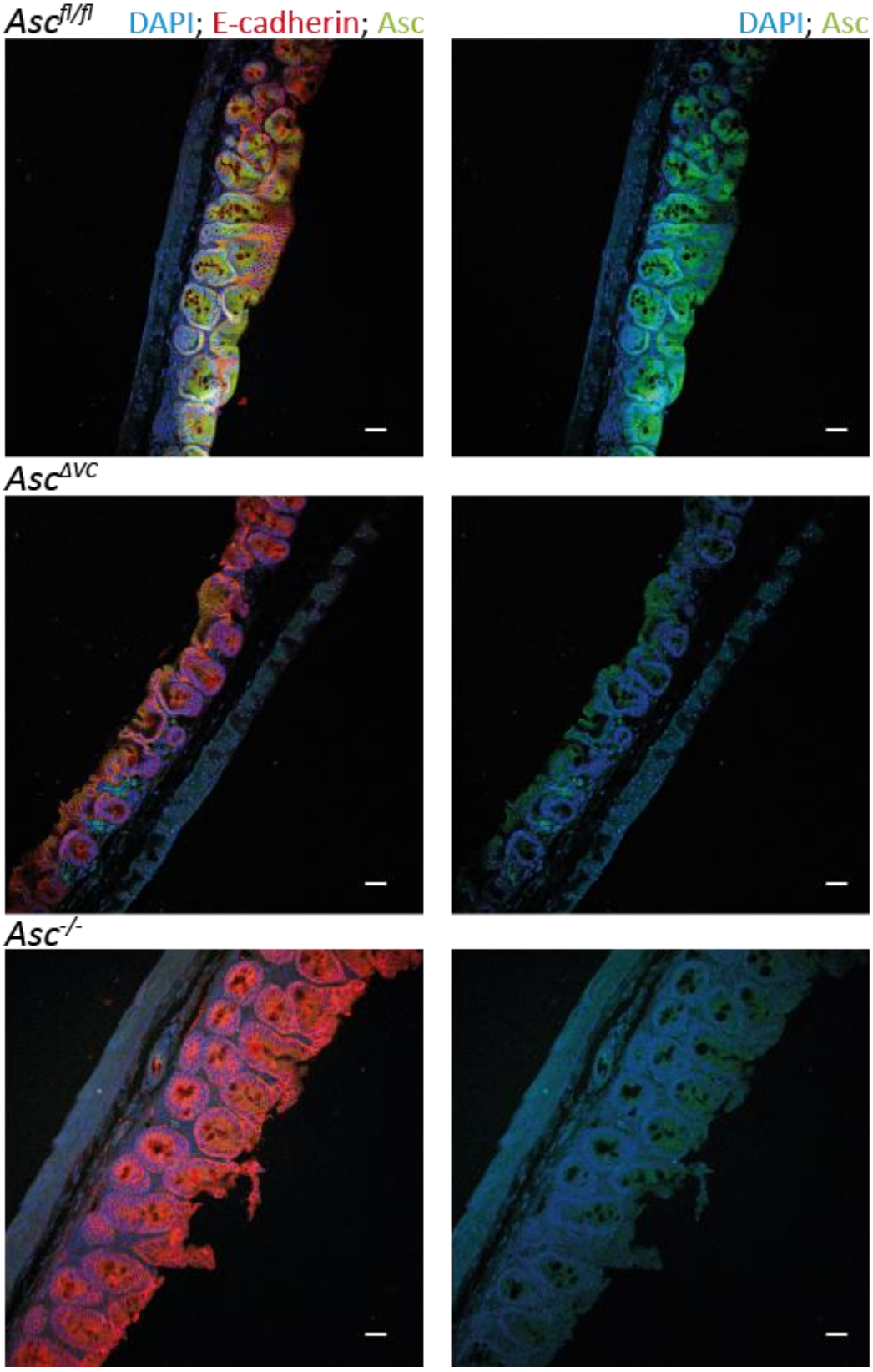


Figure 3.3. Cecal intestinal epithelial cells from *Asc*$^{\Delta VC}$ mice are deficient in Asc. Cecal tissue samples were isolated from *Asc*$^{fl/fl}$ and *Asc*$^{\Delta VC}$ littermates at steady state and *Asc*$^{-/-}$ mice at 14 days p.i. with 10^9 *C. rodentium* CFU. Tissue sections were paraffin-embedded and subsequently stained for Asc (green), E-cadherin (red) and DAPI (blue). Bar= 20μm. Data representative of n=5-10 mice per genotype.

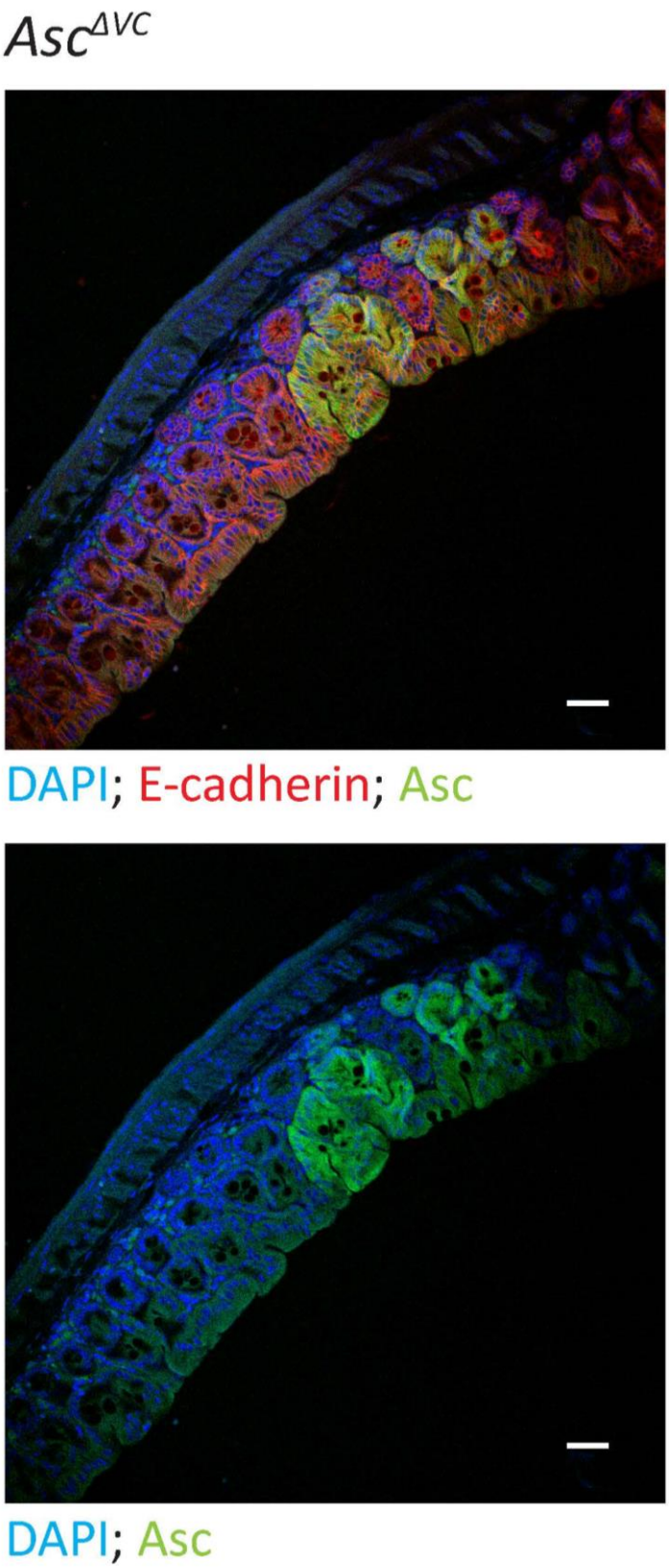


Figure 3.4. Rare Asc-positive cecal crypts were present in a minority of *Asc*$^{\Delta VC}$ mice. Cecal tissue was isolated from *Asc*$^{\Delta VC}$ mice at steady state. Tissue sections were paraffin-embedded and subsequently stained for Asc (green), E-cadherin (red) and DAPI (blue). Bar= 20μm. Staining is representative of one of two *Asc*$^{\Delta VC}$ mice that contained Asc-positive crypts, from a total of 10 mice that were analysed.

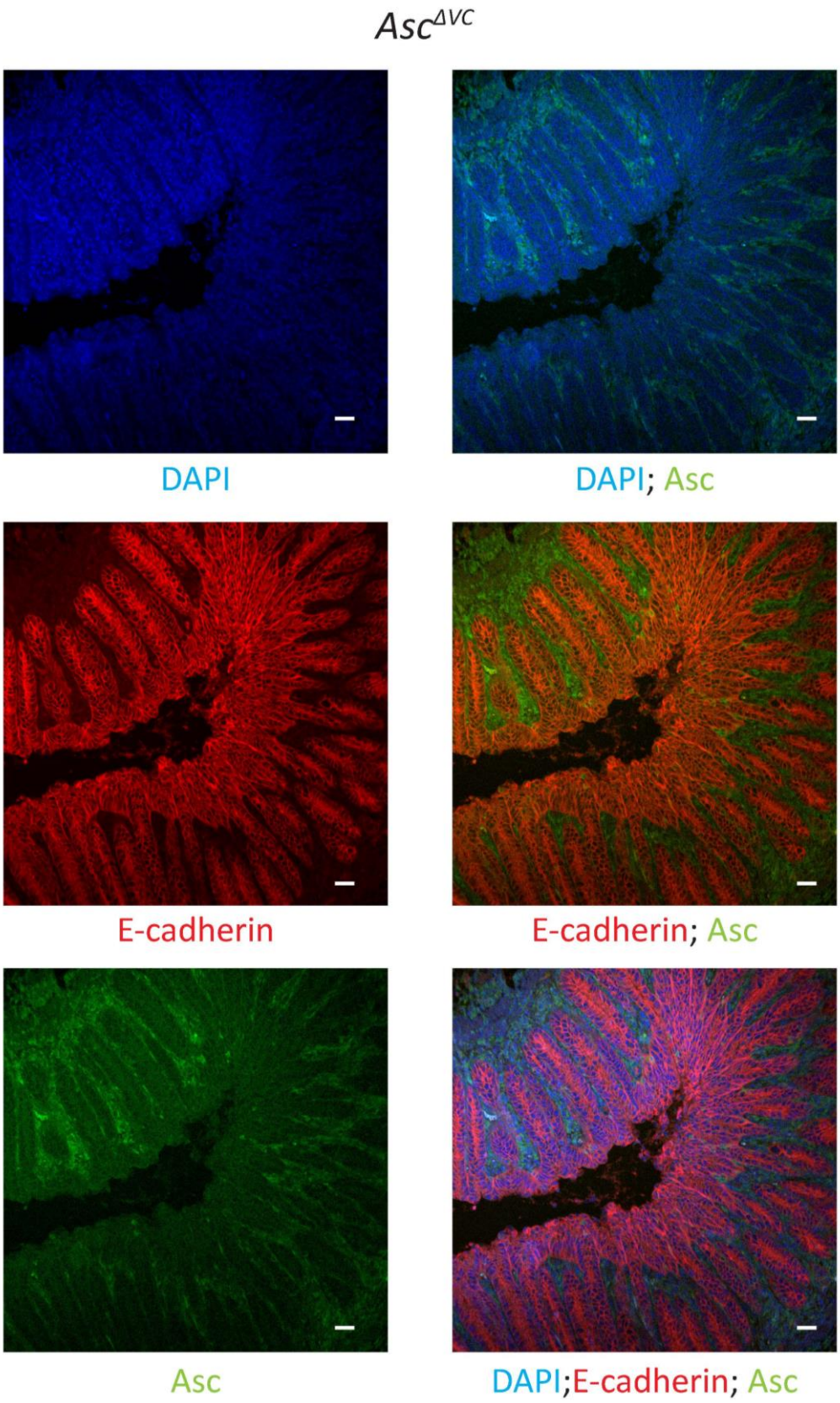


Figure 3.5. *C. rodentium*-infected *Asc*$^{\Delta VC}$ mice harbour Asc-sufficient cells in their lamina propria. Colon tissue was isolated from *Asc*$^{\Delta VC}$ mice at 14 days post oral infection with 10^9 *C. rodentium* CFU. Tissue sections were paraffin-embedded and subsequently stained for Asc (green), E-cadherin (red) and DAPI (blue). Bar= 20µm. Data are representative of n=10 mice.

3.2.2. Asc in the intestinal epithelium is involved in protection against *C. rodentium* infection

Having confirmed the generation of IEC-specific Asc knock-out mice ($Asc^{\Delta VC}$), we then infected cohorts of $Asc^{fl/fl}$, $Asc^{\Delta VC}$ and $Asc^{-/-}$ mice with *C. rodentium* and monitored various disease parameters. Although all infected mice suffered weight loss compared to the uninfected controls, we observed that both $Asc^{\Delta VC}$ mice and $Asc^{-/-}$ mice exhibited a discrete and transient increase in body weight loss compared to $Asc^{fl/fl}$ mice (Figure 3.6). A significantly increased loss of body weight was observed in $Asc^{\Delta VC}$ compared to $Asc^{fl/fl}$ mice at 13 and 14 days p.i. (Figure 3.6), when the infection is at its peak in the colon (460). Notably, a similar significant increase in weight loss was observed in $Asc^{-/-}$ mice compared to $Asc^{\Delta VC}$ mice, between day 12 and 14 post infection (Figure 3.6). These results suggest that signalling via Asc, specifically via epithelial Asc, limits *C. rodentium* infection-driven weight loss.

We next determined the impact of epithelial Asc on *C. rodentium*-induced intestinal inflammation. For this purpose, colonic and cecal tissues were paraffin-embedded, sectioned, then stained with H&E to assess intestinal pathology in a semi-quantitative manner. As expected (460), in all mice, the intestinal inflammation reached its peak at day 8 in the cecum and at day 14 in the distal colon (Figure 3.7). We observed a modest, but significant, increase in histopathology scores at day 14 p.i. and day 21 p.i. in the colons of $Asc^{\Delta VC}$ mice compared with their $Asc^{fl/fl}$ littermates (Figure 3.7). However, in these experiments the complete $Asc^{-/-}$ mice did not exhibit increased intestinal pathology when compared to $Asc^{fl/fl}$ mice, with the exception of day 14 p.i. in the cecum (Figure 3.7). Overall, these observations suggest that despite the exacerbated weight loss present in $Asc^{\Delta VC}$ mice during *C. rodentium* infection, the associated intestinal pathology is only marginally affected by epithelial Asc expression.

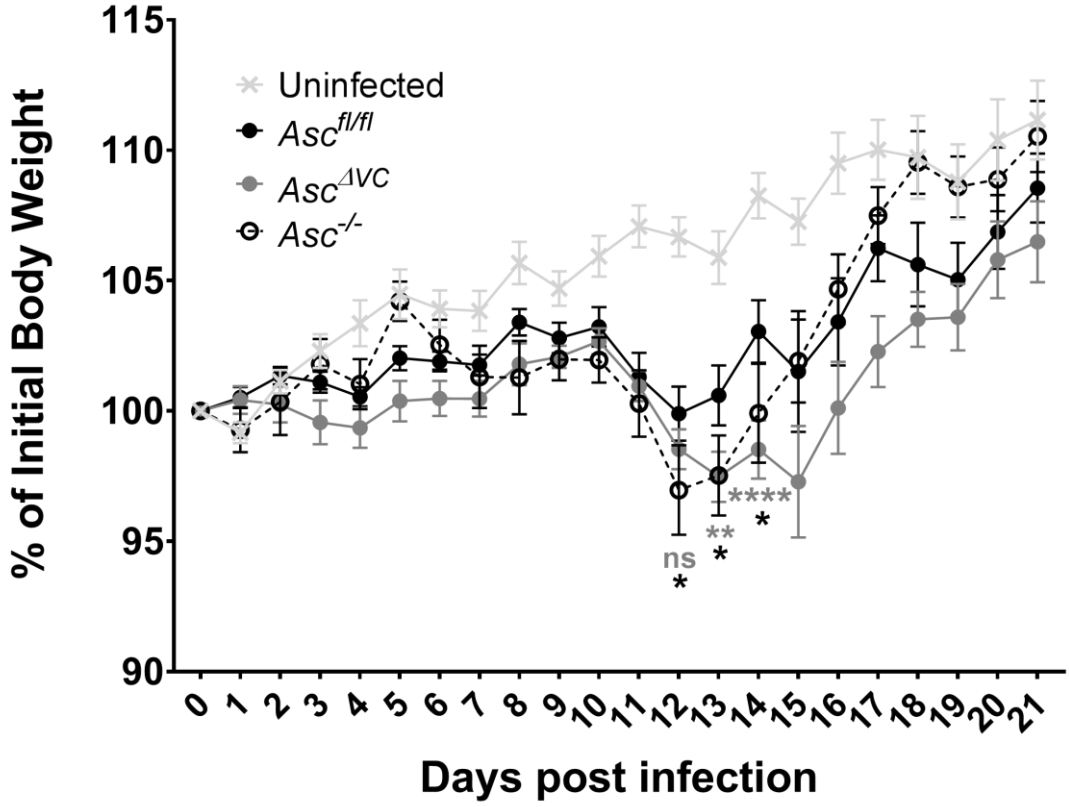


Figure 3.6. *C. rodentium* infected $Asc^{\Delta VC}$ mice exhibit increased weight loss compared to $Asc^{fl/fl}$ littermates. Cohorts of $Asc^{fl/fl}$, $Asc^{\Delta VC}$ and $Asc^{-/-}$ mice were infected orally with *C. rodentium* (~10^9 CFU) and weighed daily until sacrifice. Symbols denote mean body weights (±SEM) as a percentage of the initial body weight. Grey asterisks indicate significance for $Asc^{\Delta VC}$ compared with $Asc^{fl/fl}$. Black asterisks indicates significance for $Asc^{-/-}$ compared with $Asc^{fl/fl}$. Statistical significance between the groups was inferred from an ordinary two-way ANOVA multiple comparisons test with Bonferroni correction. P-value summary: *p<0.05; **p<0.001; ***p<0.0001; ****p<0.00001. Data represent 6 pooled experiments with total mouse numbers per groups as follows; day 8 n=10-16 (no $Asc^{-/-}$ included); day 14 n=19-25; day 21 n=10-11.

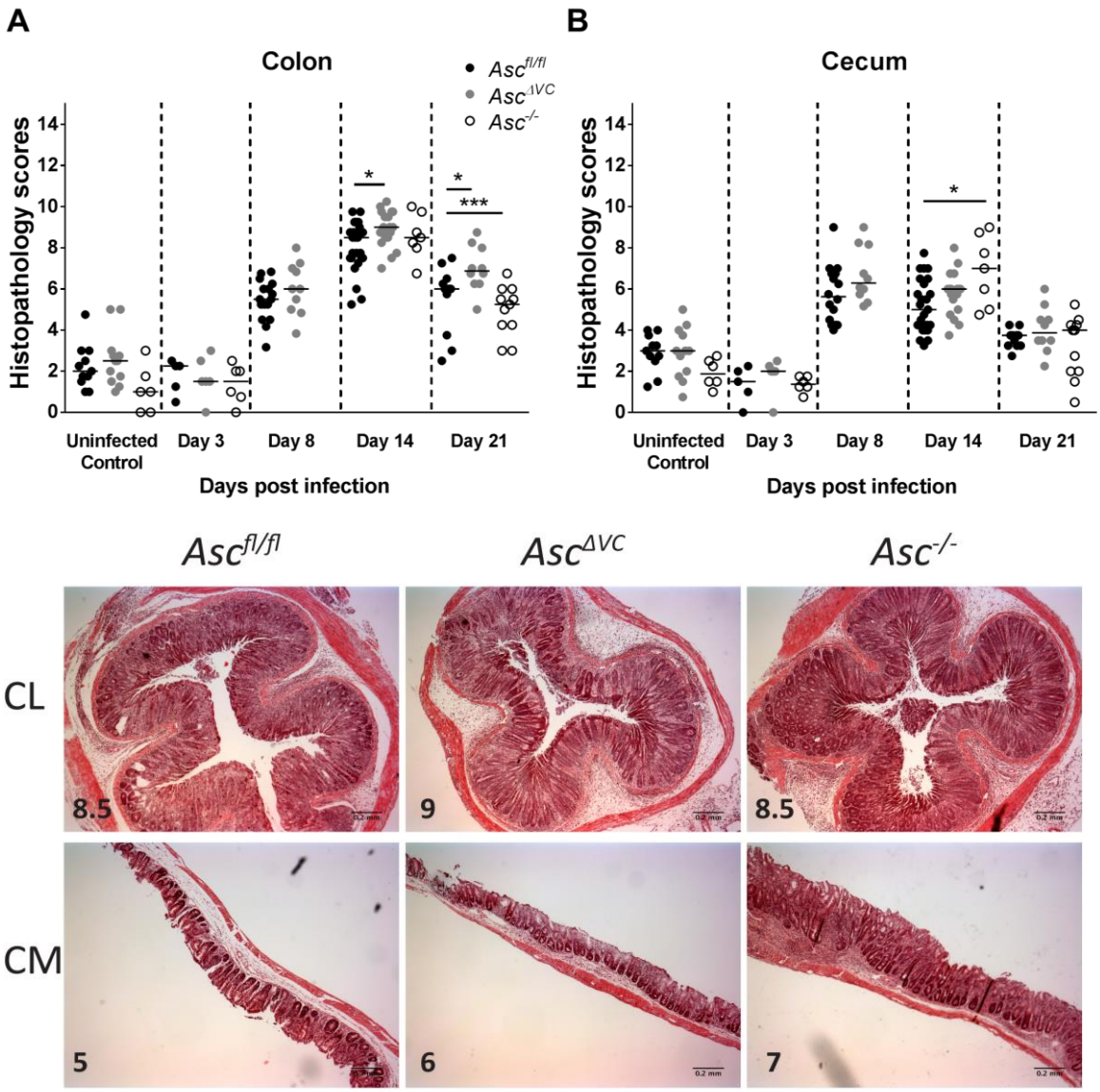


Figure 3.7. *C. rodentium*-infected *Asc*$^{\Delta VC}$ mice exhibit increased pathology compared to *Asc*$^{fl/fl}$ littermates. *Asc*$^{fl/fl}$, *Asc*$^{\Delta VC}$ and *Asc*$^{-/-}$ mice were infected orally with *C. rodentium* (~10^9 CFU) and sacrificed at day 3, 8, 14 and 21 post infection. Inflammation scores in the colon (A) and cecum (B) and representative photomicrographs depicting H&E staining of colon (A) and cecal (B) sections (magnification x50). Symbols denote individual immunohistopathology scores. Horizontal bars indicate group medians. Statistical significance between the groups was determined by the Mann-Whitney test. P-value summary: *p<0.05; **p<0.001; ***p<0.0001; ****p<0.00001. Six to 25 mice per group per time point from at least 2 independent experiments were analysed (day 3 depicts data from 1 experiment).

3.2.3. *Asc*$^{\Delta VC}$ mice have an impaired ability to control tissue-adherent *C. rodentium* colonization

We next assessed the role of epithelial Asc expression in controlling *C. rodentium* burden during *in vivo* infection. For this purpose, we quantified the tissue-adherent *C. rodentium* in the cecum and the colon of all infected mice, as well as the planktonic *C. rodentium* in cecal contents of mice. We observed that early *C. rodentium* colonisation (day 3 p.i.) in the cecum, colon and cecal contents was similar in *Asc*$^{fl/fl}$, *Asc*$^{\Delta VC}$ and *Asc*$^{-/-}$ mice (Figure 3.8 and Figure 3.9). Although similar colonisation levels were found in the cecum and cecal contents in all three genotypes at day 8p.i. (Figure 3.8B and Figure 3.9), there was a modest but significant increase in tissue-adherent *C. rodentium* in the colon of *Asc*$^{\Delta VC}$ mice compared to *Asc*$^{fl/fl}$ littermates (Figure 3.8A).

Moreover, by day 14 p.i. there were significant increases in both planktonic (cecal contents) and tissue-adherent (colon and cecum) *C. rodentium* in *Asc*$^{\Delta VC}$ mice and *Asc*$^{-/-}$ mice when compared to *Asc*$^{fl/fl}$ mice (Figure 3.8 and Figure 3.9). Nevertheless, although *Asc*$^{\Delta VC}$ and *Asc*$^{-/-}$ mice harboured higher bacterial loads on day 14 p.i., all groups of mice were largely able to clear the *C. rodentium* infection by day 21 p.i. Notably, *Asc*$^{-/-}$ mice still had increased CFU in their cecal contents at this time point (Figure 3.8 and Figure 3.9). Importantly, *Asc*$^{\Delta VC}$ and *Asc*$^{-/-}$ mice had similar *C. rodentium* colonisation levels throughout all time points and in all tissues (Figure 3.8 and Figure 3.9).

Importantly, these differences in pathogen colonisation were only evident locally in infected intestinal tissues, as there were no significant differences in the systemic spread of *C. rodentium*, denoted by similar levels of *C. rodentium* in liver and spleen tissues of in *Asc*$^{fl/fl}$, *Asc*$^{\Delta VC}$ and *Asc*$^{-/-}$ mice at all time points (Figure 3.10).

Overall, these data show that epithelial inflammasomes play an important role in controlling colonization levels of *C. rodentium* in intestinal tissues.

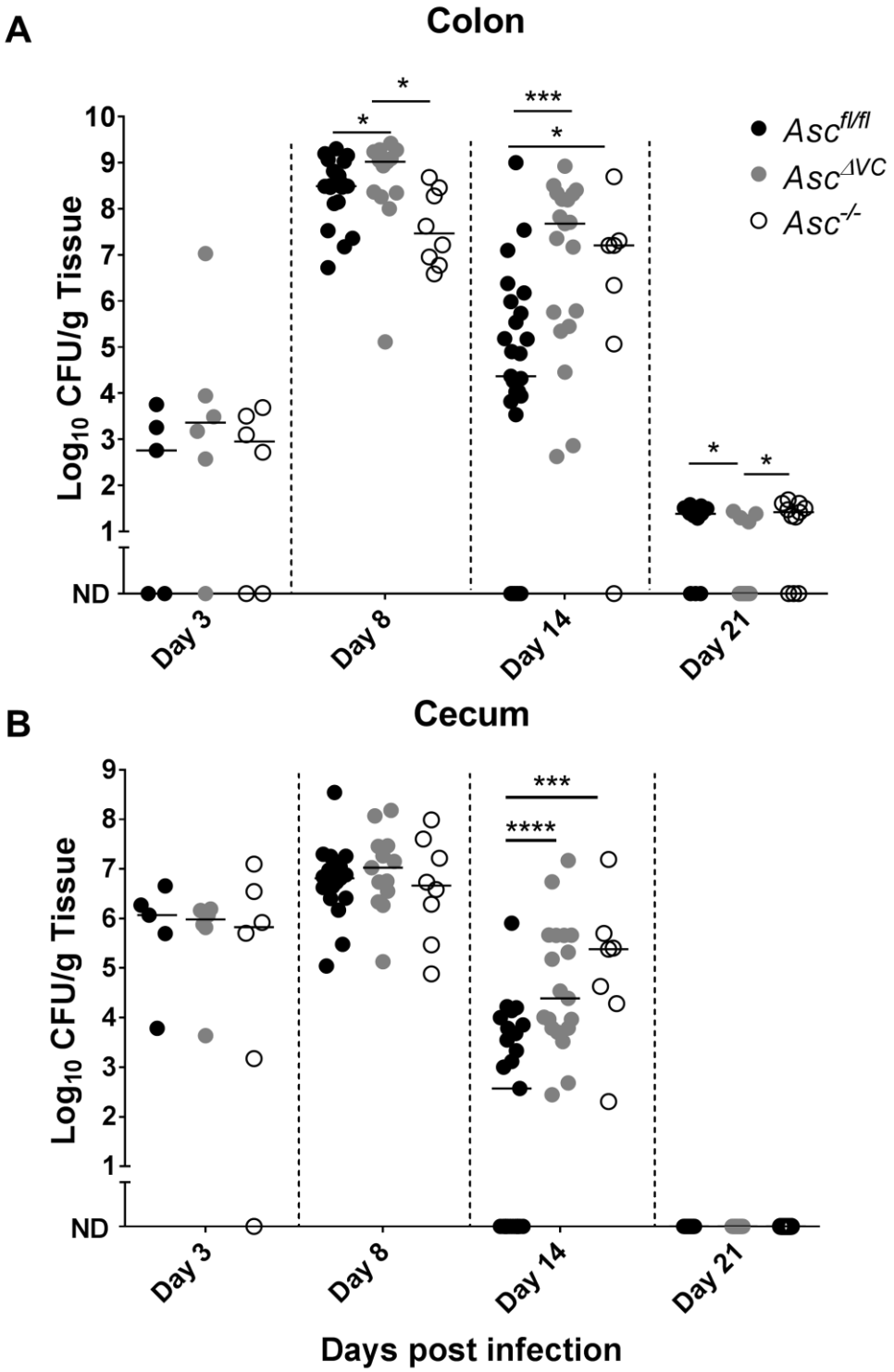


Figure 3.8. *C. rodentium* infected *Asc*$^{\Delta VC}$ mice display increased tissue adherent bacteria in intestinal tissues. Cohorts of *Asc*$^{fl/fl}$, *Asc*$^{\Delta VC}$ and *Asc*$^{-/-}$ mice were infected orally with *C. rodentium* (10^9 CFU) and sacrificed at day 3, 8, 14 or 21 post infection. Symbols denote tissue-adherent *C. rodentium* CFU in the (A) colon and (B) cecum. Horizontal bars indicate group medians. Statistical significance between the groups was determined by the Mann-Whitney test. P-value summary: *p<0.05; **p<0.001; ***p<0.0001; ****p<0.00001. Five to 25 mice per group per time point from at least 2 independent experiments were analysed (day 3 depicts data from 1 experiment).

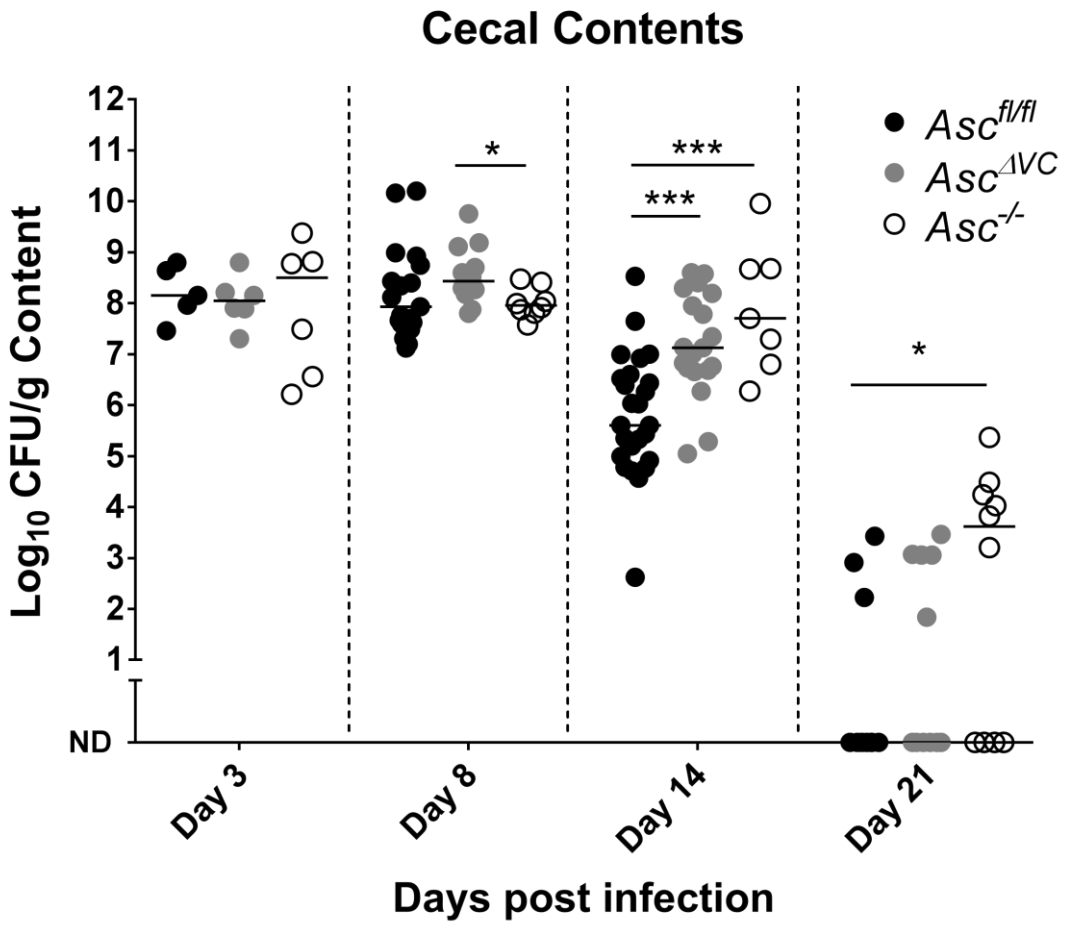


Figure 3.9. *C. rodentium* infected *Asc*$^{\Delta VC}$ mice display increased planktonic bacteria in the cecal contents. Cohorts of *Asc*$^{fl/fl}$, *Asc*$^{\Delta VC}$ and *Asc*$^{-/-}$ mice were infected orally with *C. rodentium* (~10^9 CFU) and sacrificed at day 3, 8, 14 or 21 post infection. Symbols denote planktonic *C. rodentium* CFU in the cecal contents of infected mice. Horizontal bars indicate group medians. Statistical significance between the groups was determined by the Mann-Whitney test. P-value summary: *p<0.05; **p<0.001; ***p<0.0001; ****p<0.00001. Five to 25 mice per group per time point from at least 2 independent experiments were analysed (day 3 depicts data from 1 experiment).

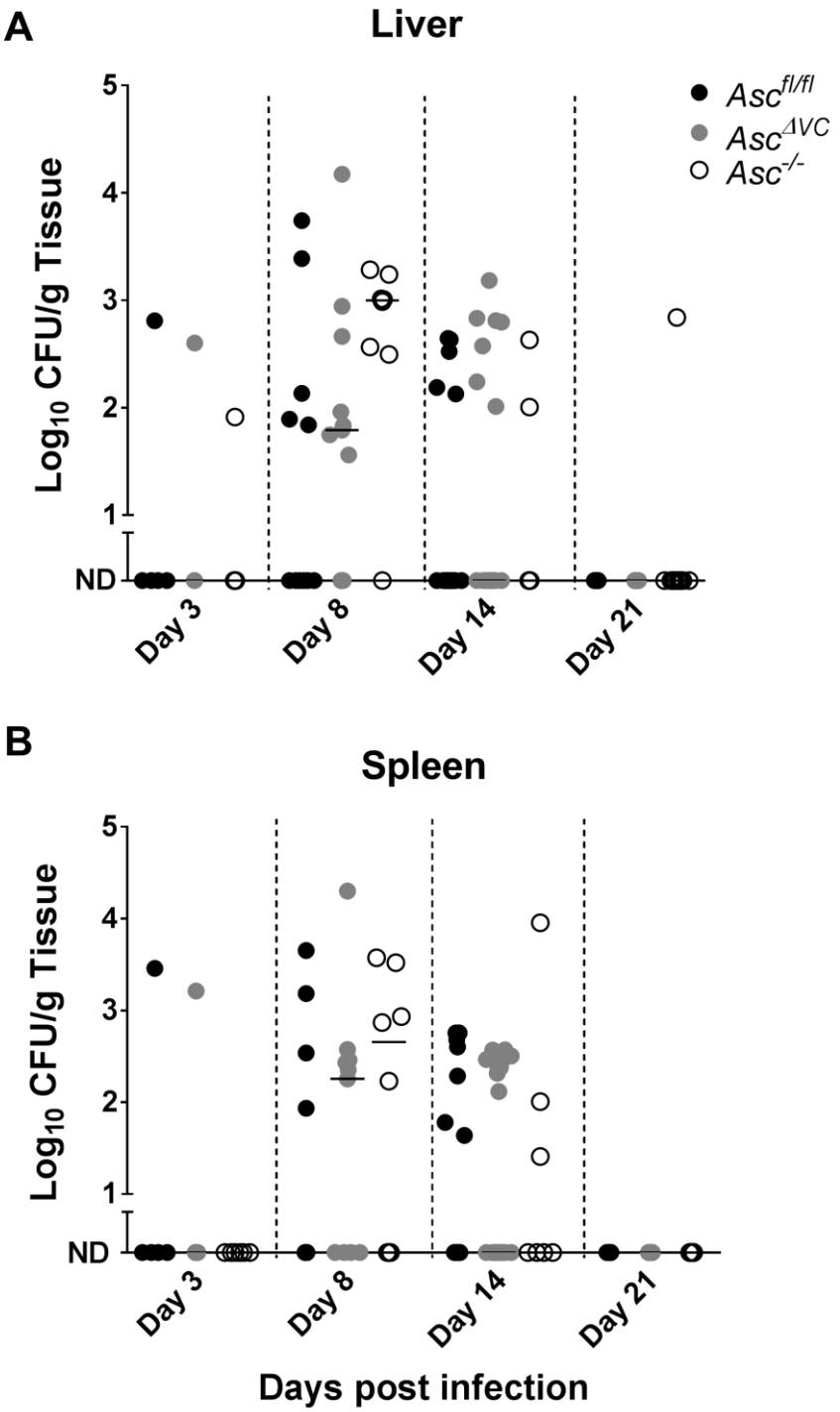


Figure 3.10. *C. rodentium* infected $Asc^{\Delta VC}$ and $Asc^{fl/fl}$ mice have comparable systemic *C. rodentium* spread. Cohorts of $Asc^{fl/fl}$, $Asc^{\Delta VC}$ and $Asc^{-/-}$ mice were infected orally with *C. rodentium* (~10^9 CFU) and sacrificed at day 3, 8, 14 or 21 post infection. Symbols denote tissue adherent *C. rodentium* CFU in the (A) liver and (B) spleen of infected mice. Horizontal bars indicate group medians. Statistical significance between the groups was determined by the Mann-Whitney test. P-value summary: *p<0.05; **p<0.001; ***p<0.0001; ****p<0.00001. Five to 25 mice per group per time point from at least 2 independent experiments were analysed (day 3 depicts data from 1 experiment).

3.2.4. Comparable systemic immune activation and neutrophil tissue infiltration in *Asc$^{\Delta VC}$* and *Asc$^{fl/fl}$* mice following *C. rodentium* infection

Previous studies in our lab indicated that *Asc$^{-/-}$* mice also exhibited increased systemic immune activation compared to WT mice after *C. rodentium* infection (249). Therefore, we also assessed general inflammation and cellular immunity in *Asc$^{\Delta VC}$* and *Asc$^{fl/fl}$* mice following *C. rodentium* infection. We found that *Asc$^{fl/fl}$*, *Asc$^{\Delta VC}$* and *Asc$^{-/-}$* mice all exhibited comparable splenomegaly during the peak phase of *C. rodentium* infection (days 8-14 p.i.) (Figure 3.11).

Previous studies also associated decreased inflammasome activation with higher recruitment of neutrophils into the infected site during *C. rodentium* infection (231, 249). Although we observed a trend towards increased neutrophil infiltration into the lamina propria and spleens of *Asc$^{\Delta VC}$* compared to *Asc$^{fl/fl}$* mice at day 8p.i., these differences were not statistically significant, and neutrophil accumulation at other time points was comparable in both groups (Figure 3.12). In addition, analyses of T cell recruitment to the lamina propria during *C. rodentium* infection did not reveal any significant differences between $CD4^+$ T helper cell populations in *Asc$^{fl/fl}$*, *Asc$^{\Delta VC}$* or *Asc$^{-/-}$* mice (Data not shown; FACS data acquired by Dr. Alison Murphy, Mucosal Immunology Group, Sir William Dunn School of Pathology, University of Oxford).

Overall, these results suggest that epithelial inflammasomes have little impact on neutrophil or T cell accumulation following *C. rodentium* infection.

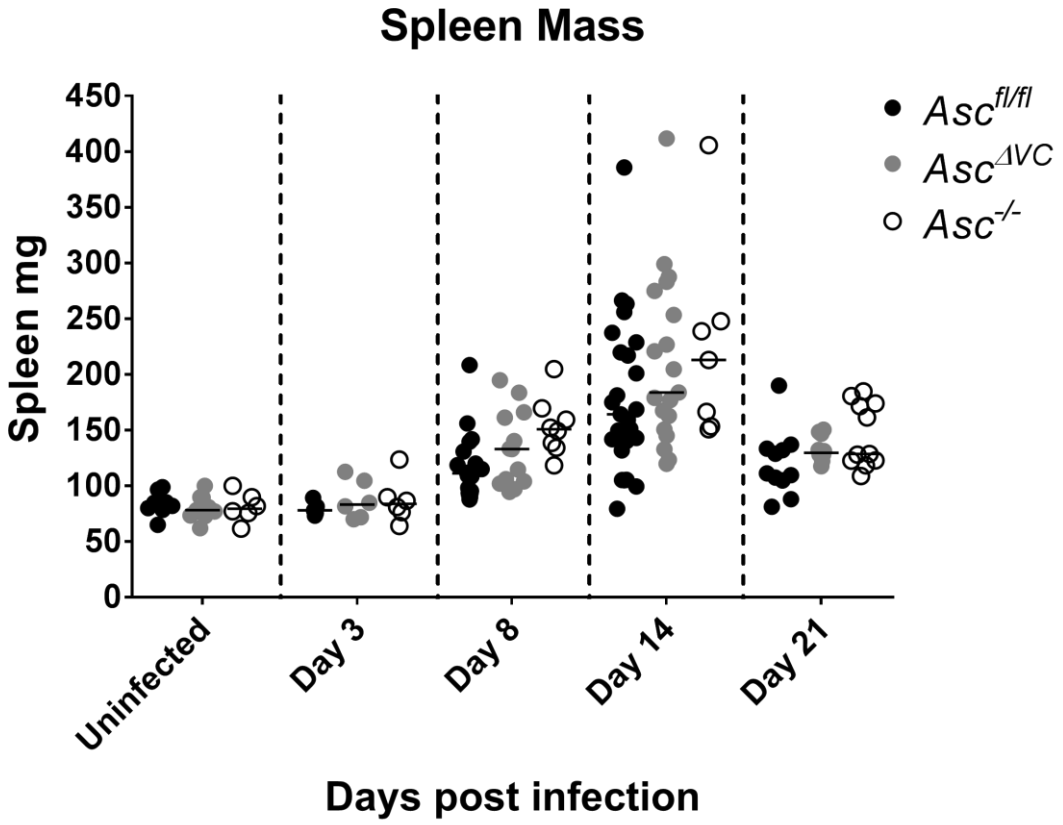


Figure 3.11. *Asc*$^{\Delta VC}$ and *Asc*$^{fl/fl}$ mice have comparable systemic immune activation upon *C. rodentium* infection. Cohorts of *Asc*$^{fl/fl}$, *Asc*$^{\Delta VC}$ and *Asc*$^{-/-}$ mice were infected orally with *C. rodentium* (~10^9 CFU) and sacrificed at day 3, 8, 14 or 21 post infection. Symbols denote individual spleen weights and horizontal bars indicate group medians. Statistical significance between the groups was determined by the Mann-Whitney test. P-value summary: *p<0.05; **p<0.001; ***p<0.0001; ****p<0.00001. Data from 5 to 25 mice per group per time point from at least 2 independent experiments (day 3 depicts data from 1 experiment).

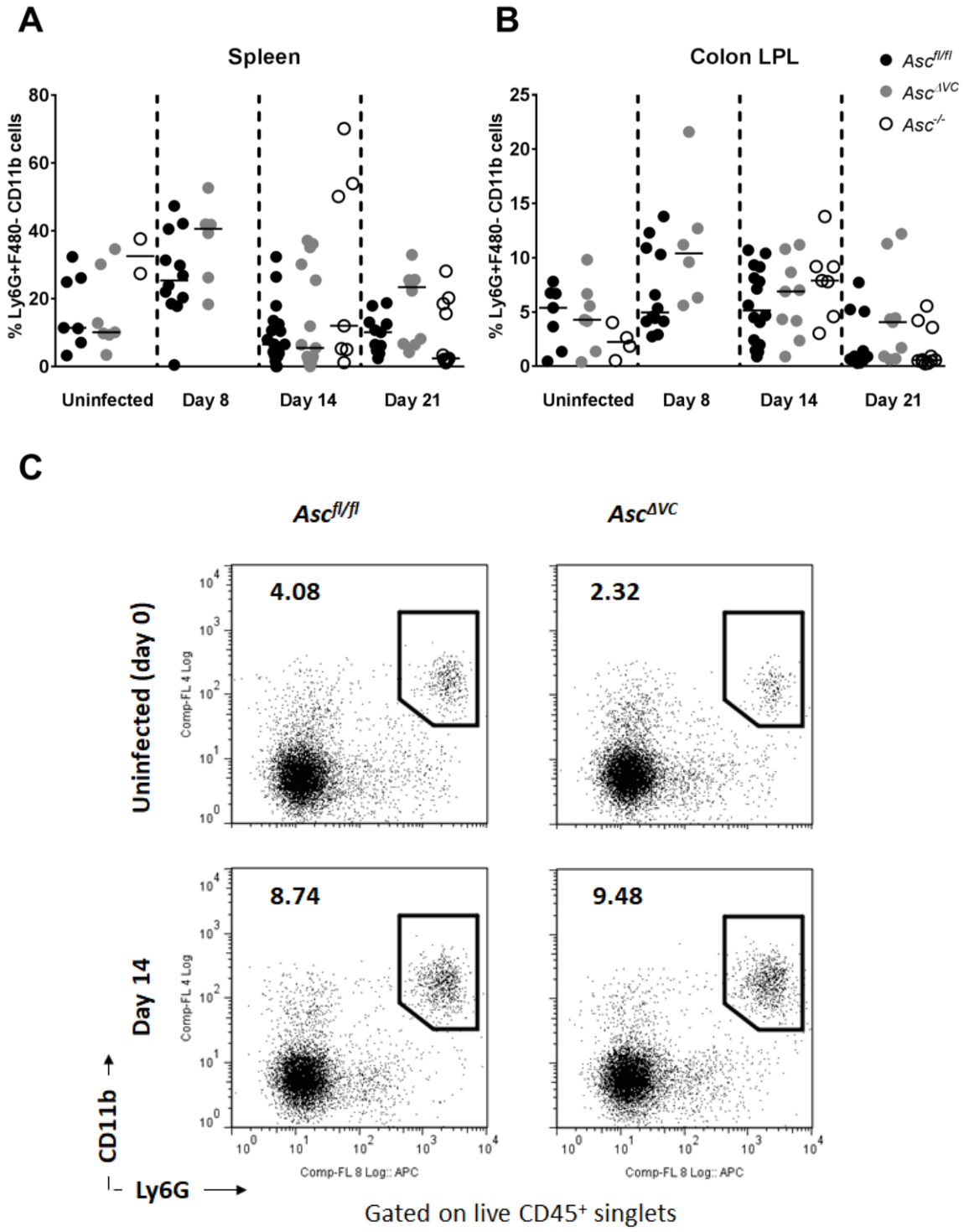


Figure 3.12. Asc deficiency is associated with a trend towards increased neutrophil recruitment during *C. rodentium* infection. Cohorts of *Asc*$^{fl/fl}$, *Asc*$^{\Delta VC}$ and *Asc*$^{-/-}$ mice were infected orally with *C. rodentium* (~10^9 CFU) and sacrificed at day 8, 14 or 21 post infection. Symbols denote total neutrophil frequencies (Live CD45$^+$ CD11b^{hi}Ly6G^{hi}) in spleen (A) and colon (B) of infected mice. Representative FACS plots for spleen day 14p.i. show gating used to define neutrophils (C). Each symbol represents an individual mouse and horizontal bars are group median values. Statistical significance between the groups was determined by the Mann-Whitney test. P-value summary: *p<0.05; **p<0.001; ***p<0.0001; ****p<0.00001. Data from 5 to16 per group per time point, with mice pooled from at least 2 independent experiments. Note: FACS data acquired by Dr. Alison Murphy, Sir William Dunn School of Pathology, University of Oxford).

3.2.5. Reduced levels of inflammasome activation in intestinal tissues of *Asc*$^{\Delta VC}$ mice following *C. rodentium* infection

We next assessed inflammasome activation through immunoblotting for caspase-1 and IL-18. Whole colonic and cecal tissue was snap-frozen at the time of sacrifice, lysed and prepared for immunoblotting as previously detailed. We assessed tissues from *C. rodentium*-infected *Asc*$^{\Delta VC}$ and *Asc*$^{fl/fl}$ littermates at the time points of peak inflammation in the cecum (day 8 p.i.) and colon (day 14 p.i.). We observed that activated (cleaved) caspase-1 was clearly detectable in intestinal tissue lysates isolated from *Asc*$^{fl/fl}$ mice, but was almost undetectable in intestinal tissue lysates isolated from *Asc*$^{\Delta VC}$ mice (Figure 3.13). This was not due to any differential expression of caspase-1, as comparable amounts of inactive pro-caspase-1 were present in intestinal tissue lysates from *Asc*$^{\Delta VC}$ and *Asc*$^{fl/fl}$ mice (Figure 3.13). Moreover, although activated IL-18 levels in both colon and cecum lysates were comparable in *Asc*$^{\Delta VC}$ mice and *Asc*$^{fl/fl}$ mice at day 8 p.i. (Figure 3.13 A and B), IL-18 activation was markedly reduced in the colon and cecum of *Asc*$^{\Delta VC}$ mice at 14 days p.i (Figure 3.13 C and D).

To further assess inflammasome activation during *C. rodentium* infection, secreted IL-18 levels were determined in supernatants collected from cecal, colonic and splenic organ explants that were isolated at various time points post infection. As expected, *Asc*$^{-/-}$ mice had significantly lower IL-18 levels in all tissues at steady state compared to *Asc*$^{fl/fl}$ and *Asc*$^{\Delta VC}$ mice (Figure 3.14). In contrast, *Asc*$^{\Delta VC}$ mice displayed similar IL-18 levels to *Asc*$^{fl/fl}$ littermates at steady state in the colon and spleen (Figure 3.14 A and C), but had significantly reduced IL-18 levels in the cecum (Figure 3.14 B).

Throughout *C. rodentium* infection, *Asc*$^{-/-}$ mice continued to display almost undetectable levels of IL-18, both systemically and in intestinal tissues (Figure 3.14). Early during infection (day 3 p.i.), we observed that *Asc*$^{\Delta VC}$ and *Asc*$^{fl/fl}$ littermates displayed similar IL-18 levels in all tissues. However, at day 8 p.i., a non-significant trend towards decreased IL-18 secretion in *Asc*$^{\Delta VC}$ compared to *Asc*$^{fl/fl}$ mice emerged in intestinal tissues (Figure 3.14 A and B) but not systemically (Figure 3.14 C). By day 14 p.i., intestinal explants from *Asc*$^{\Delta VC}$ mice secreted significantly lower amounts of IL-18 compared to those isolated from *Asc*$^{fl/fl}$ littermates (Figure 3.14 A and B). However, even at this peak time point of disease, spleen explants from *Asc*$^{\Delta VC}$ and *Asc*$^{fl/fl}$ littermates secreted comparable levels of IL-18 (Figure 3.14 C). Similarly, during the resolution phase of the infection

(day 21 p.i.), IL-18 secretion was significantly reduced in intestinal explants from *Asc*$^{\Delta VC}$ mice compared with *Asc*$^{fl/fl}$ littermates, whereas IL-18 secretion was comparable in the spleen of both groups (Figure 3.14 A, B and C).

Taken together, these results show that epithelial inflammasomes make a significant contribution to local IL-18 production in the intestine during *C. rodentium* infection, but do not impact on systemic IL-18 secretion.

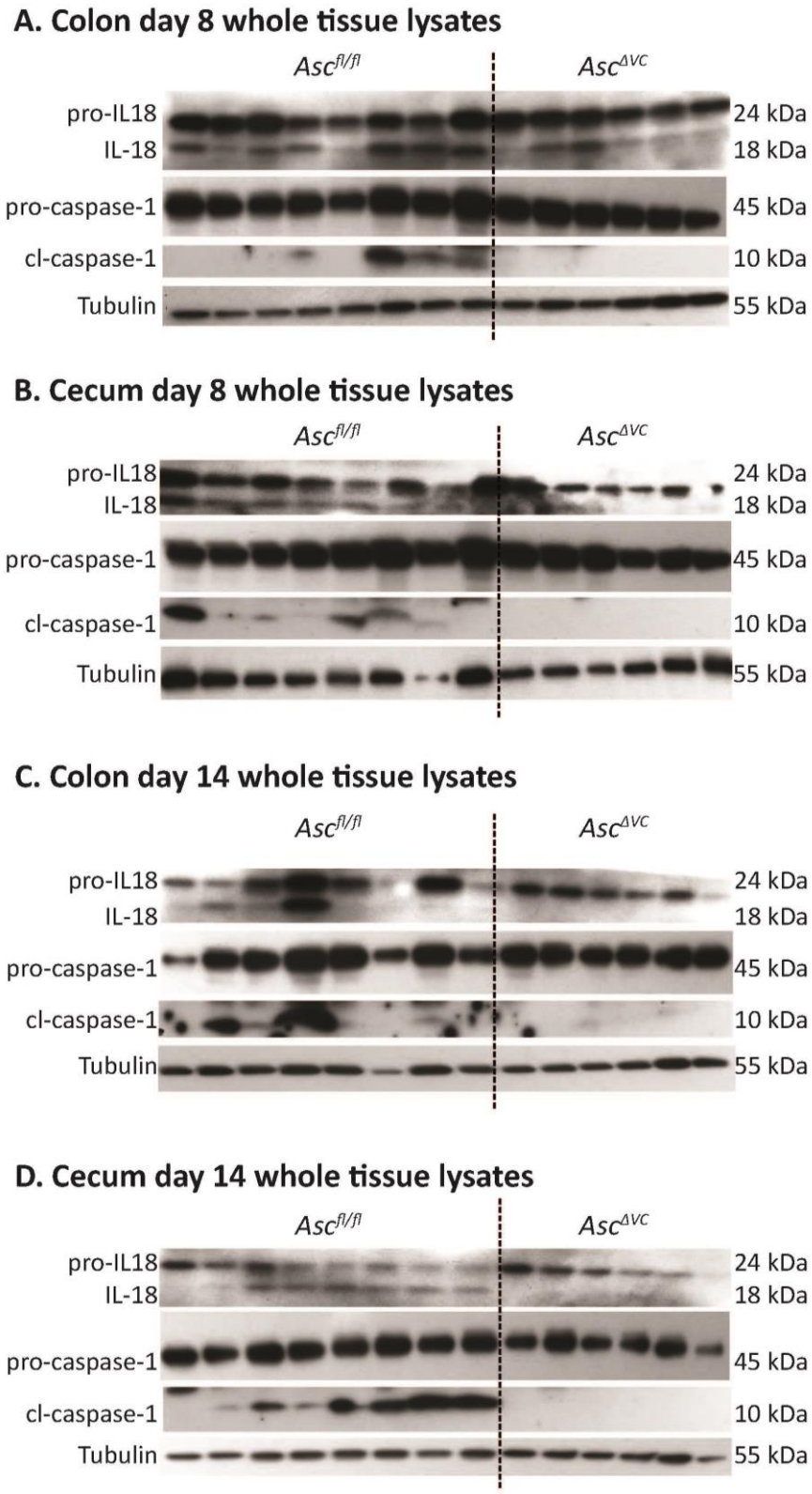


Figure 3.13. Reduced intestinal Caspase-1 and IL-18 activation in *Asc*$^{\Delta VC}$ mice during *C. rodentium* infection. Cohorts of *Asc*$^{fl/fl}$, *Asc*$^{\Delta VC}$ and *Asc*$^{-/-}$ mice were infected orally with *C. rodentium* (~10^9 CFU). and sacrificed at days 8 and 14 p.i. Caspase-1 and IL-18 immunoblots were performed on lysed homogenates of whole colon (A and B) and cecum (C and D) tissue. Tubulin was used as loading control. Each lane represents an individual mouse (n = 6-8 per group). Data representative of 2 independent experiments per time point.

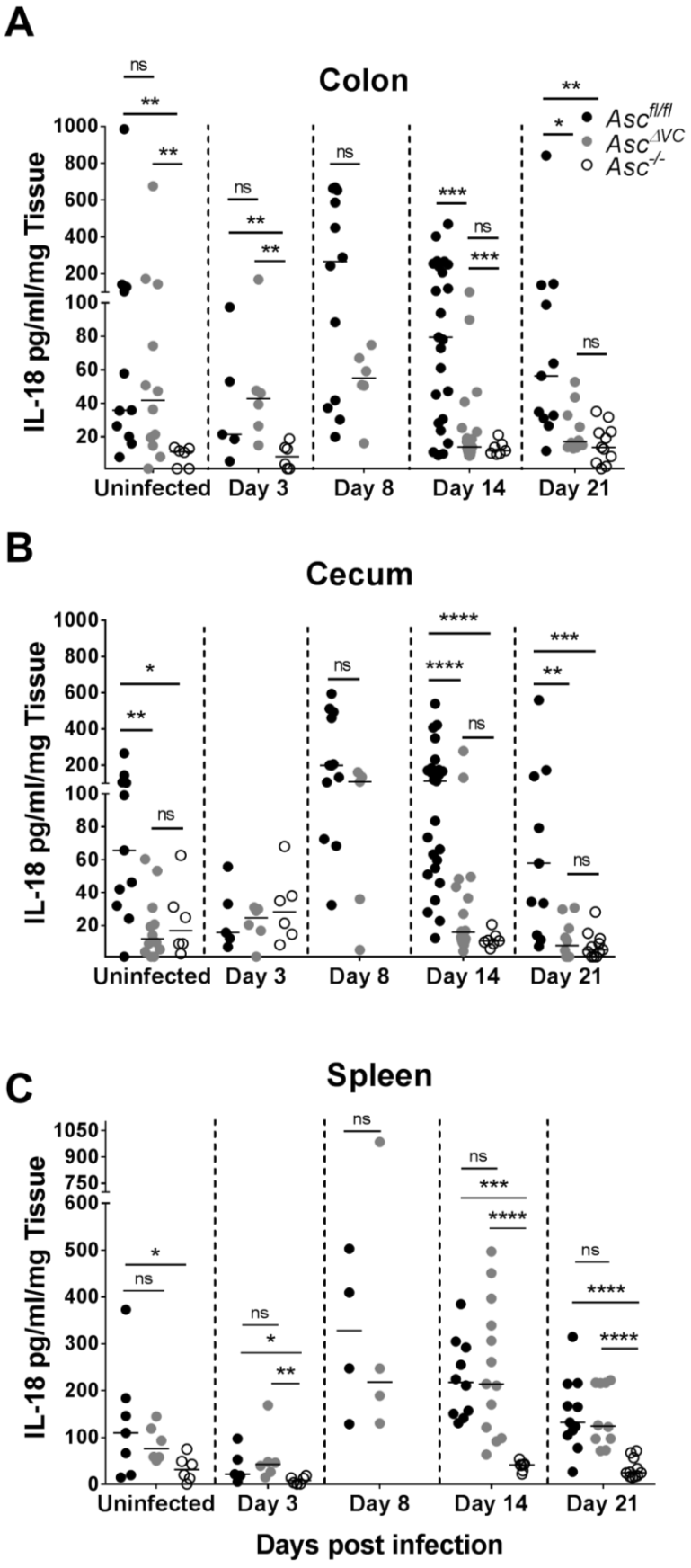


Figure 3.14. Reduced IL-18 secretion in intestinal tissues of *Asc$^{\Delta VC}$* mice upon *C. rodentium* infection. Cohorts of *Asc$^{fl/fl}$*, *Asc$^{\Delta VC}$* and *Asc$^{-/-}$* mice were infected orally with *C. rodentium* (~10^9 CFU) and sacrificed at day 3, 8, 14 or 21 post infection. Symbols denote IL-18 pg/ml per mg of tissue explant from colon (A), cecum (B) and spleen (C). Horizontal bars indicate group medians. Statistical significance between the groups was determined by the Mann-Whitney test. P-value summary: *p<0.05; **p<0.001; ***p<0.0001; ****p<0.00001. Data from 5 to 25 mice per group per time point from at least 2 independent experiments (day 3 depicts data from 1 experiment). Note: ELISA test performed by Dr. Alison Murphy, Sir William Dunn School of Pathology, University of Oxford.

3.2.5.1. Other inflammasome-associated cytokine responses are unaffected in *Asc*$^{\Delta VC}$ mice.

Having established that IL-18 levels are significantly reduced in *Asc*$^{\Delta VC}$ mice at the peak of infection (14 days p.i.), we analysed the status of the other two inflammasome-associated cytokines, IL-1β and IL-1α. IL-1β, like IL-18, is processed by active caspase-1 upon inflammasome formation (267). Conversely, IL-1α does not rely on post-translational processing for activation. Both pro- IL-1α (31kDa) and cleaved-IL-1α (18kDa) are bioactive (374). Nevertheless, some enzymes, like calpain-like proteases, are able to cleave IL-1α intracellularly (546). The release of IL-1α is associated with inflammasome-dependent cell death (547). We performed ELISA analysis of cecal and colonic organ explants for active IL-1β and whole IL-1α.

We observed very low levels of both IL-1β and IL-1α in intestinal tissues isolated from all three genotypes of mice, at all time-points analysed (Figure 3.15). Of note, the levels observed were close to the detection limit of the assay (4pg/ml for IL-1α and 8pg/ml for IL-1β). Therefore, the use of these results to infer differences between genotypes must be done with caution. However, IL-1β and IL-1α levels did not seem to differ between the three genotypes analysed (*Asc*$^{\Delta VC}$, *Asc*$^{-/-}$ and *Asc*$^{fl/fl}$) or at any time point during infection. These results indicate that epithelial inflammasomes do not contribute to local IL-1β or IL-1α production upon *C. rodentium* infection and that these cytokines are not significantly induced during this infection.

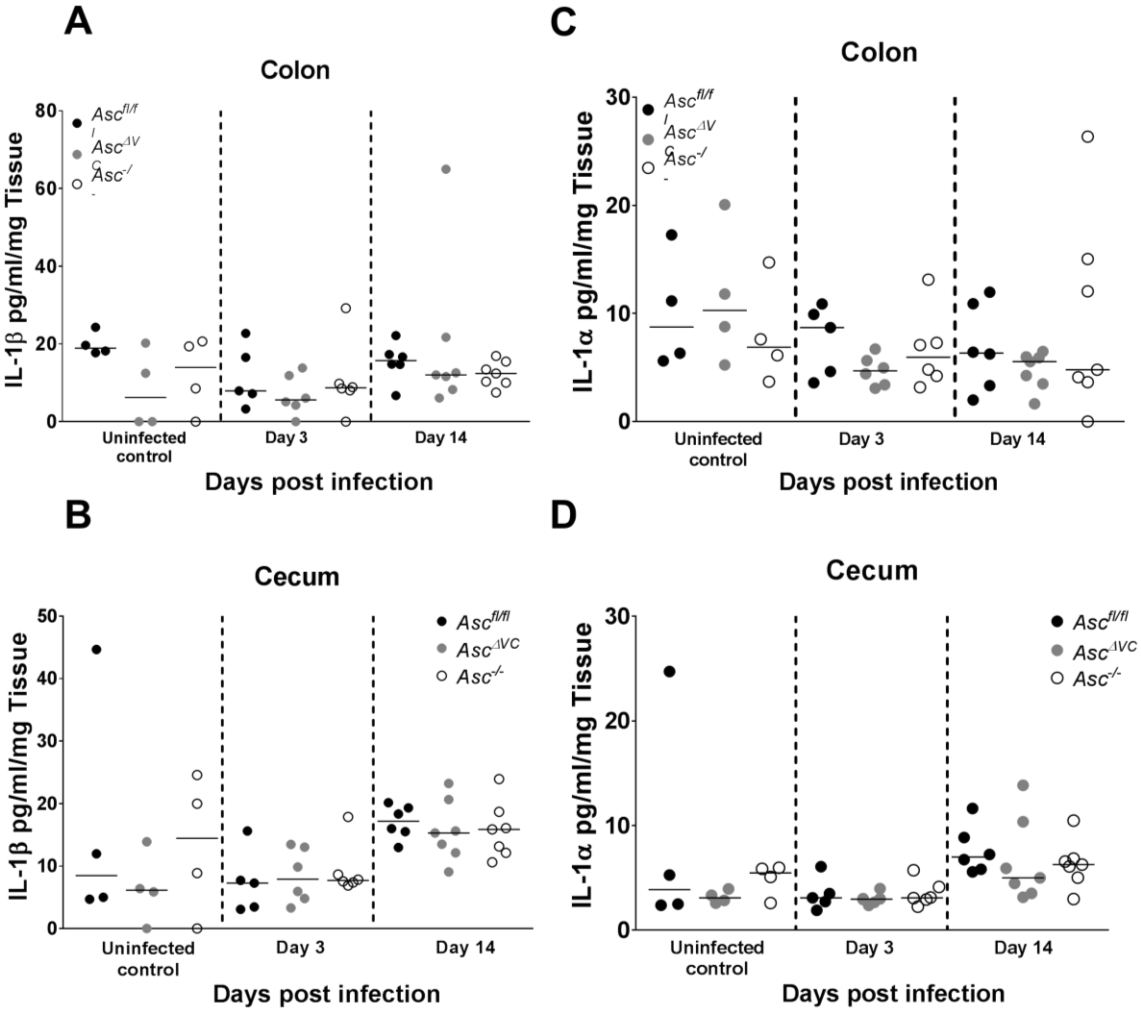


Figure 3.15. IL-1β or IL-1α secretion is not induced in intestinal tissues during *C. rodentium* infection. Cohorts of *Asc*$^{fl/fl}$, *Asc*$^{\Delta VC}$ and *Asc*$^{-/-}$ mice were infected orally with *C. rodentium* (~10^9 CFU) and sacrificed at day 3 or 14 post infection. Symbols denote IL-1β pg/ml per mg of tissue explant from colon (A), cecum (B) and IL-1α pg/ml per mg of tissue explant from colon (C), cecum (D). Horizontal bars indicate group medians. Statistical significance between the groups was determined by the Mann-Whitney test. Data from 4 to 7 mice per group per time point from at least 2 independent experiments (day 3 depicts data from 1 experiment). Note: ELISA test performed by Dr. Alison Murphy, Sir William Dunn School of Pathology, University of Oxford.

3.2.6. Asc deficiency within the epithelium does not affect the IL-22/AMP axis

Recently, IL-18 production was linked to an increase in IL-22 (369), an important cytokine known to regulate AMP production and mucosal barrier integrity (121, 479, 548). Enhanced IL-18 secretion in response to elevated IL-22 has been shown to contribute to host defence during *C. rodentium* infection (369). As reduced intestinal IL-18 production was associated with increased tissue-adherent bacterial burden in the $Asc^{\Delta VC}$ mice during the peak of *C. rodentium* infection, we examined whether this might be explained by impaired induction of the IL-22/AMP response.

To analyse IL-22 responses, organ tissue explants were isolated at various time points throughout the course of *C. rodentium* infection and, after 24h culture, supernatants were collected and IL-22 analysed by ELISA. However, we found that only very low levels of IL-22 were detected in the colonic and cecal explants, both at steady state and during *C. rodentium* infection, in all cohorts of mice studied, with no discernible differences between samples from $Asc^{fl/fl}$ and $Asc^{\Delta VC}$ mice (Figure 3.16).

We investigated AMP responses by carrying out transcriptional analysis of various AMP genes in colonic IEC via qRT-PCR. Although there was a clear induction of *S100A8* expression at day 14 p.i., there were comparable levels of *S100A8* expression in colonic IEC isolated from $Asc^{\Delta VC}$ mice and $Asc^{fl/fl}$ mice at all time points (Figure 3.17 A). Parallel analyses showed that *Ang4* and *Retnla* expression was comparable between $Asc^{fl/fl}$ and $Asc^{\Delta VC}$ mice at all time points and that there was no increase of these AMP during infection (Figure 3.17 B and C). Overall, these results argue against any impaired IL-22 or AMP responses in $Asc^{\Delta VC}$ mice.

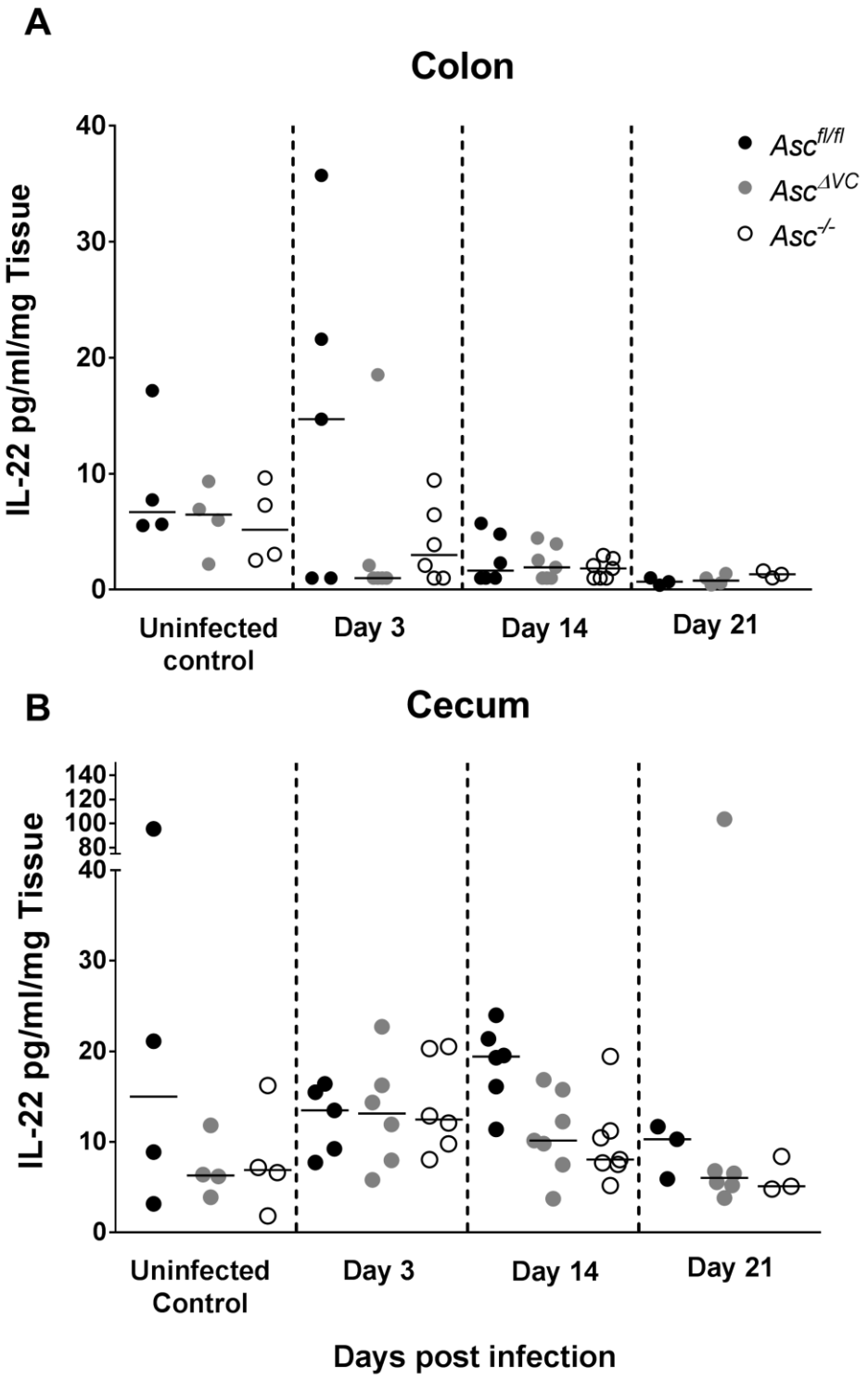


Figure 3.16. Comparable, low levels of IL-22 secretion in intestinal tissues of *Asc*$^{fl/fl}$, *Asc*$^{\Delta VC}$ and *Asc*$^{-/-}$ mice upon *C. rodentium* infection. Cohorts of *Asc*$^{fl/fl}$, *Asc*$^{\Delta VC}$ and *Asc*$^{-/-}$ mice were infected orally with *C. rodentium* (~10^9) and sacrificed at day 3, 14 or 21 post infection. Symbols denote IL-22 pg/ml per mg of tissue explant from colon (A), cecum (B). Horizontal bars indicate group medians. Statistical significance between the groups was determined by the Mann-Whitney test. Data from 4 to 7 mice per group per time point from at least 2 independent experiments (day 3 depicts data from 1 experiment). Note: ELISA test performed by Dr. Alison Murphy, Sir William Dunn School of Pathology, University of Oxford.

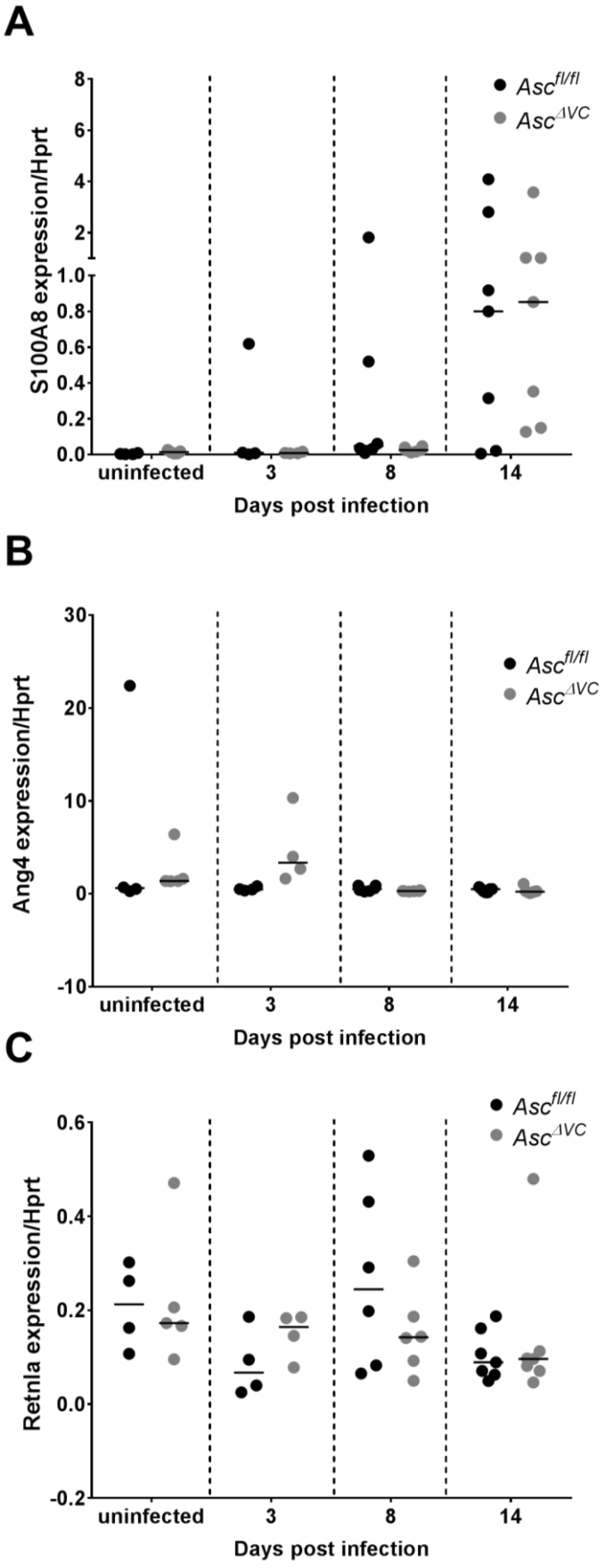


Figure 3.17. Comparable AMP responses in colonic IEC from *Asc*$^{fl/fl}$ and *Asc*$^{\Delta VC}$ mice upon *C. rodentium* infection. Cohorts of *Asc*$^{fl/fl}$ and *Asc*$^{\Delta VC}$ mice were orally infected with *C. rodentium* (~10^9 CFU) and sacrificed at day 3, 8 or 14 post infection. Symbols denote ΔCT values of *S100A8* (A), *Ang4* (B) and *Retnla* (C) obtained by qPCR analysis of cDNA preparations from isolated colonic IEC. Horizontal bars indicate group medians. All values were normalised to the ΔCT values of the *Hprt* house keeping gene. Statistical significance between the groups was determined by the Mann-Whitney test. Data from 4 to 6 mice per group per time point from at least 2 independent experiments (day 3 depicts data from 1 experiment).

3.2.7. Reduced caspase-8 activation in intestinal tissues of *Asc$^{\Delta VC}$* mice.

Despite pyroptosis being the main form of cell death related to the inflammasome, components of the inflammasome platform, including Nlrc4 and Asc, have been previously shown to interact with caspase-8 to drive non-lytic cell death both *in vivo* and *in vitro* (230, 549). We therefore analysed caspase-8 activation in cecal and colonic tissue lysates from *Asc$^{fl/fl}$*, *Asc$^{\Delta VC}$* and *Asc$^{-/-}$* mice infected with *C. rodentium*. In uninfected *Asc$^{fl/fl}$* and *Asc$^{\Delta VC}$* control mice, we observed relatively low levels of caspase-8 and IL-18 cleavage in both the cecum and colon (Figure 3.18 and Figure 3.19).

However, by day 8 p.i., we could detect caspase-8 and IL-18 cleavage in intestinal tissues of *C. rodentium*-infected mice (Figure 3.18). At this time point, we observed similar levels of caspase-8 and IL-18 activation in *Asc$^{fl/fl}$* and *Asc$^{\Delta VC}$* mice in the colon (Figure 3.18 A), but we found that caspase-8 and IL-18 cleavage were noticeably decreased in the cecum of *Asc$^{\Delta VC}$* mice compared to *Asc$^{fl/fl}$* mice (Figure 3.18 B). Furthermore, at day 14 p.i., we observed that activation of IL-18 and caspase-8 in the colon was markedly lower in *Asc$^{\Delta VC}$* mice compared to *Asc$^{fl/fl}$* mice (Figure 3.19 A). However, at this time point, caspase 8 and IL-18 activation in the cecum was very low in both *Asc$^{\Delta VC}$* and *Asc$^{fl/fl}$* mice, similar to that observed in uninfected controls (Figure 3.19 B). Like *Asc$^{\Delta VC}$* mice, fully deficient *Asc$^{-/-}$* mice also displayed decreased caspase 8 and IL-18 activation in the colon at day 8 p.i., as well as abolished caspase-1 activation, when compared to *C. rodentium*-infected WT mice (Figure 3.20).

Overall, consistent with our previous observations (Figure 3.14), we found that caspase-8 and IL-18 activation during *C. rodentium* infection were markedly reduced in *Asc$^{\Delta VC}$* mice. These reductions were most prominent in the cecum at day 8 and in the colon at day 14 p.i. which represent the time points corresponding to the peak of infection in the respective tissues (Figure 3.18 and Figure 3.19). These results indicate that epithelial inflammasomes contribute to caspase-8 activation in the intestine during *C. rodentium* infection.

We further investigated potential differences in cell death and proliferation between *Asc$^{\Delta VC}$* and *Asc$^{fl/fl}$* mice by transcriptional analysis of colonic IEC expression of *caspase-8* and *Ki67*. We observed that at steady state in uninfected mice, *caspase-8* and *Ki67* were expressed at similar levels in colonic IEC isolated from *Asc$^{\Delta VC}$* and *Asc$^{fl/fl}$* mice (Figure

3.21). However, at day 8p.i. *Asc*$^{fl/fl}$ colonic IEC displayed significantly increased expression of *caspase-8* and *Ki67* compared to *Asc*$^{\Delta IVC}$ IEC (Figure 3.21). These results suggest that inflammasome activation in IEC may regulate cell death and proliferation.

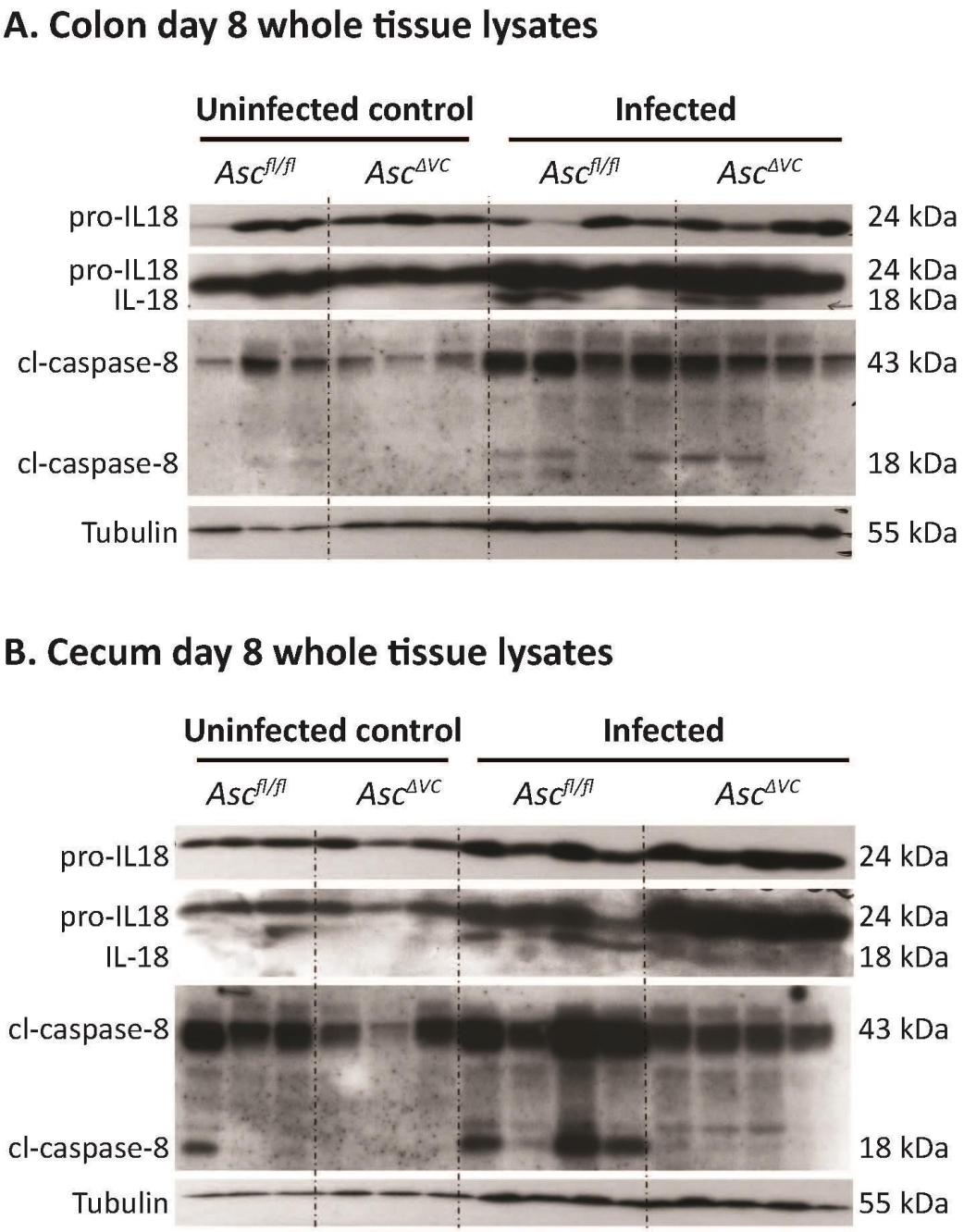


Figure 3.18. Reduced caspase-8 activation in the cecum of Asc$^{\Delta VC}$ mice at day 8 p.i. with *C. rodentium*. Cohorts of *Asc*$^{fl/fl}$, and *Asc*$^{\Delta VC}$ mice were infected orally with *C. rodentium* (~10^9 CFU) and sacrificed on day 8 p.i. Colonic (A) and cecal (B) tissue lysates were subjected to immunoblotting to assess IL-18 and caspase-8 activation. Tubulin was used as loading control. Each lane represents an individual mouse (n = 4 per group). Data representative of 2 independent experiments per time point.

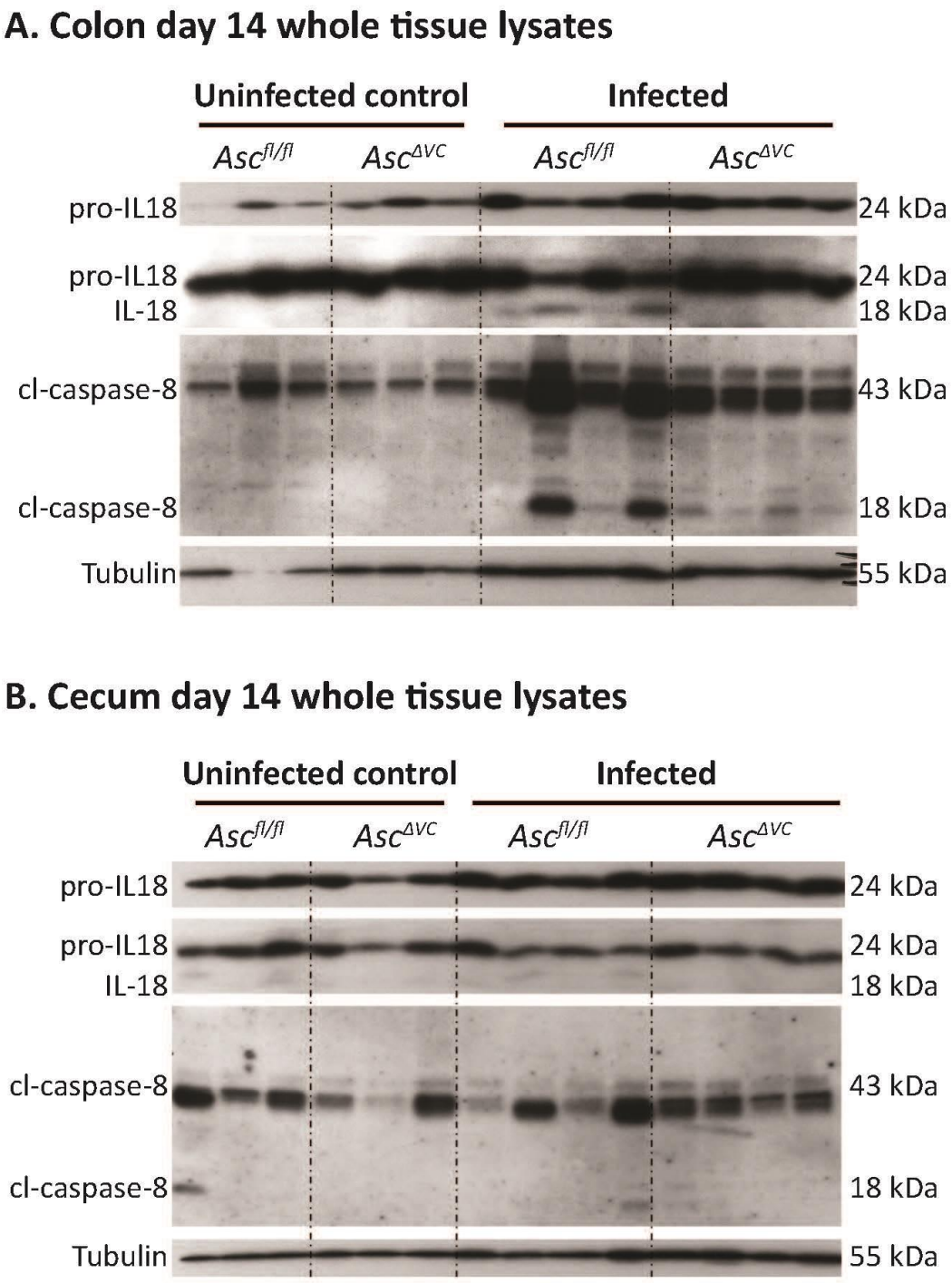


Figure 3.19. Reduced caspase-8 activation in the colon of Asc$^{\Delta VC}$ mice at day 8 p.i. with *C. rodentium*. Cohorts of *Asc$^{fl/fl}$*, and *Asc$^{\Delta VC}$* mice were infected orally with *C. rodentium* (~10^9 CFU) and sacrificed at day 14 p.i. Colonic (A) and cecal (B) tissue lysates were subjected to immunoblotting to assess IL-18 and caspase-8 activation. Tubulin was used as loading control. Each lane represents an individual mouse (n = 4 per group). Data representative of 2 independent experiments per time point.

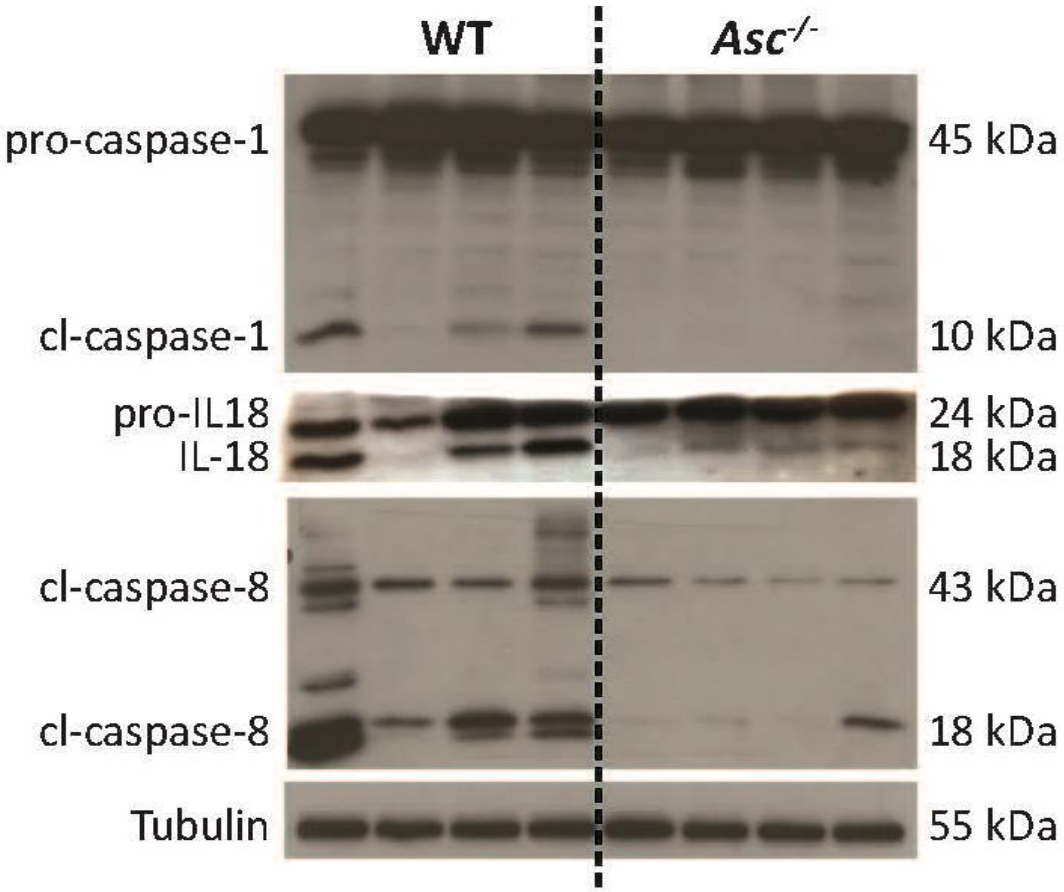


Figure 3.20. Reduced caspase-8, caspase-1 and IL-18 activation in the colons of *Asc*$^{-/-}$ mice during *C. rodentium* infection. Cohorts of *Asc*$^{-/-}$, and WT mice were infected orally with *C. rodentium* (~10^9 CFU) and sacrificed at day 8 p.i. at which colonic tissues were snap-frozen and prepared for immunoblotting to assess IL-18, caspase-1 and caspase-8 activation. Tubulin was used as loading control. Each lane represents an individual mouse (n = 4 per group). Data is of one experiment.

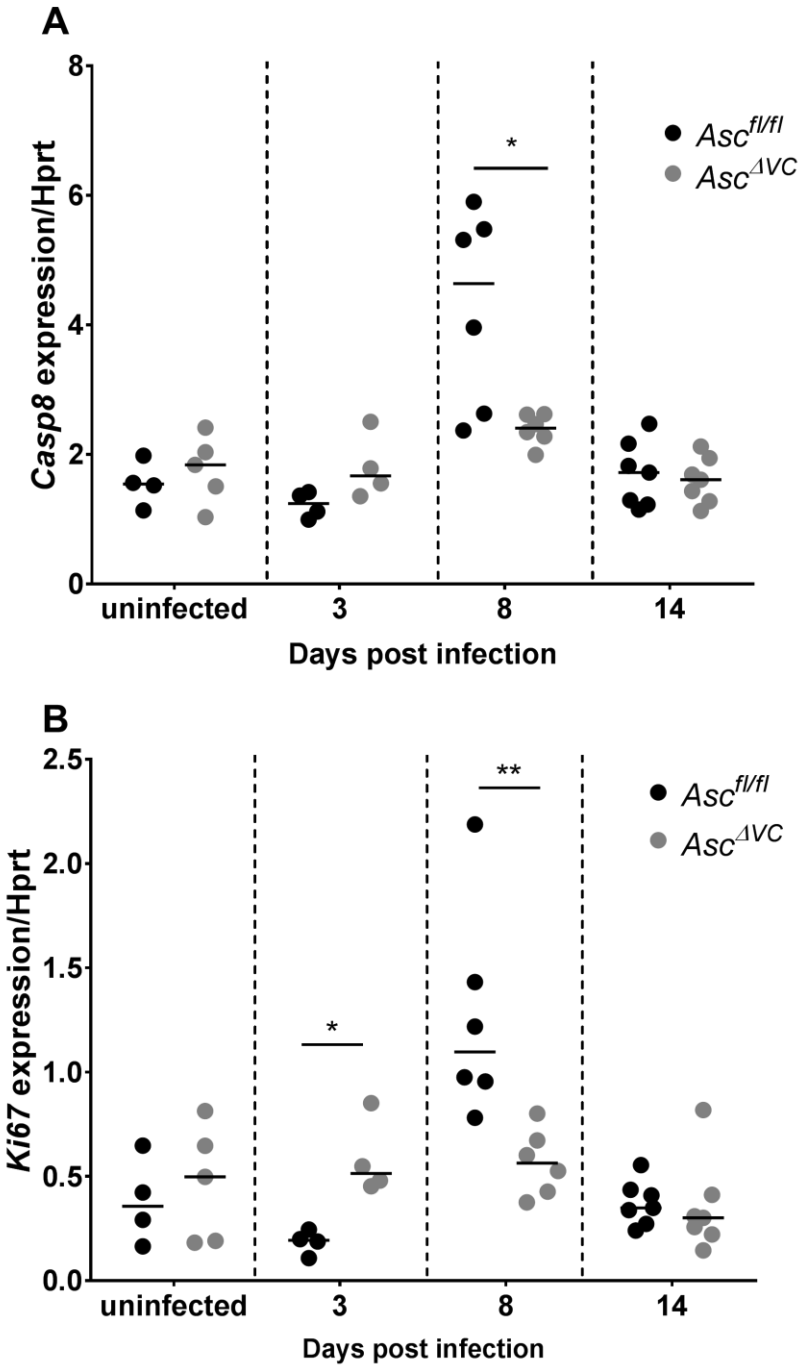


Figure 3.21. Colonic IEC from *Asc*$^{\Delta VC}$ mice show reduced expression of caspase-8 and Ki67 during *C. rodentium* infection. Cohorts of *Asc*$^{fl/fl}$ and *Asc*$^{\Delta VC}$ mice were infected orally with *C. rodentium* (~10^9 CFU) and sacrificed on day 3, 8 or 14 post infection. Symbols denote ΔCT values of *caspase-8* (A), *Ki-67* (B) obtained by qPCR analysis of cDNA preparations from isolated colonic IEC. All values were normalised to the ΔCT values of the *Hprt* house keeping gene. Horizontal bars indicate group medians. Statistical significance between the groups was determined by the Mann-Whitney test. P-value summary: *p<0.05; **p<0.001; ***p<0.0001; ****p<0.00001. Data from 4 to 6 mice per group per time point from at least 2 independent experiments (day 3 depicts data from 1 experiment).

3.2.8. Asc speck formation in IEC during *C. rodentium* infection.

Inflammasome activation in myeloid cells has been reported to result in the formation of very large multi-molecular agglomerations of inflammasome components, termed specks. Specks have been purported to act as inflammasome perpetuating and amplifying signals (326, 327). However, the formation of these inflammasome-associated specks has not yet been reported to occur in IEC. We therefore assessed Asc speck formation in the intestinal epithelium upon *C. rodentium* infection, by performing immunohistochemical staining of Asc in paraffin-embedded intestinal tissue sections.

At steady state in the colon of uninfected $Asc^{fl/fl}$ mice, we observed only very rare formation of Asc agglomerations, resembling specks, and were found in cells at the edge of the tips of intestinal epithelial crypts (Figure 3.22 A).Interestingly, however, we observed formation of Asc specks in the cecum of *C. rodentium*-infected $Asc^{fl/fl}$ mice (Figure 3.22 D and E). Remarkably, these Asc specks were only detected in the dislodging epithelial cells at the surface of the crypts (Figure 3.22 D and E). The difficulty to detect more speck positive cells may be because cells that activate the inflammasome and form specks are dying and dislodging away from the tissue.

As a control for antibody specificity, we observed that Asc staining was absent in the epithelium of the control $Asc^{\Delta IEC}$ mice at steady state (data not shown) and upon *C. rodentium* infection (Figure 3.22 B and C). These findings indicate that Asc specks can form in IEC, that they are increased during *C. rodentium* infection, and that they are restricted to IEC that appear to be extruded from the tips of the crypts.

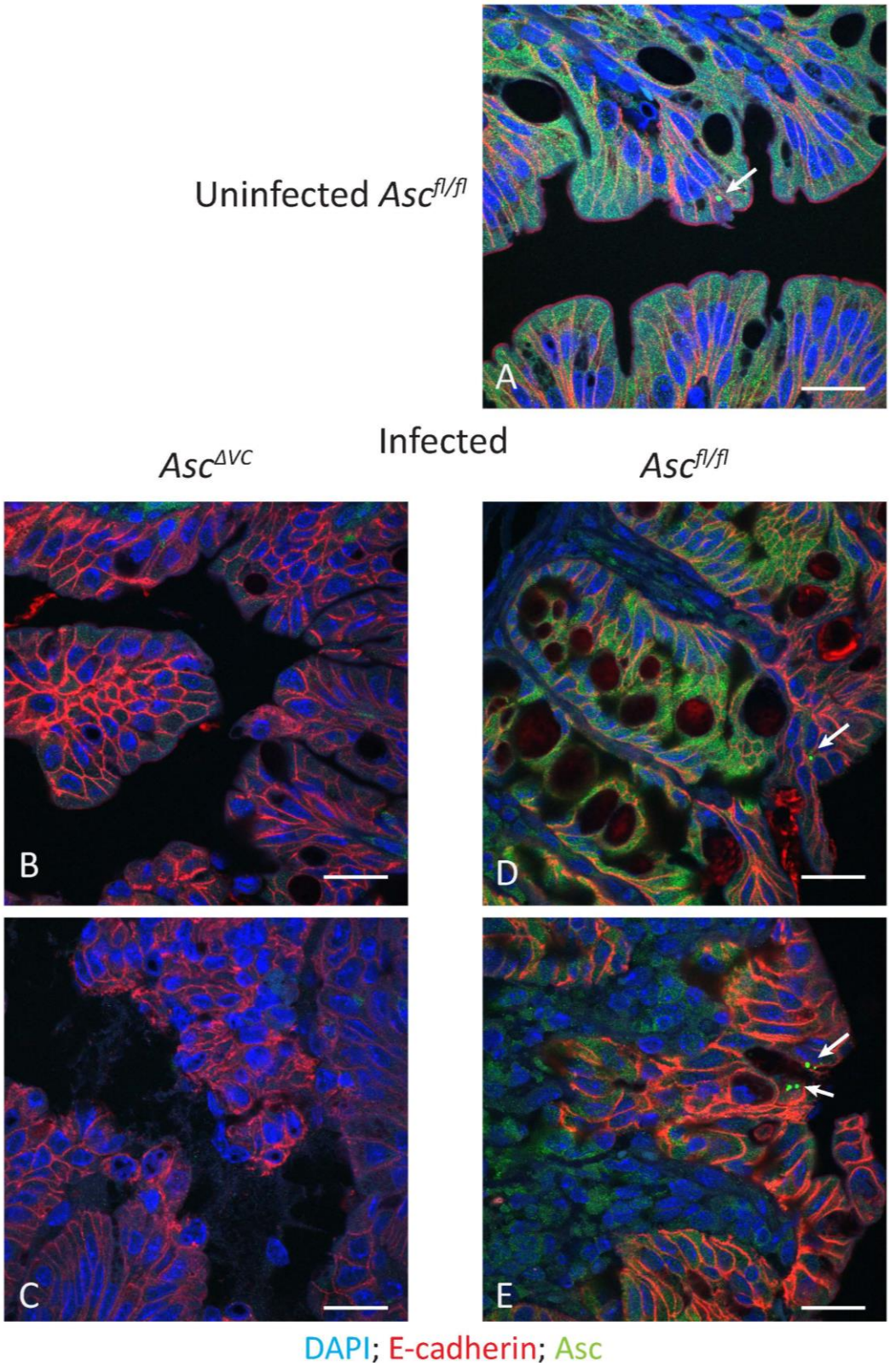


Figure 3.22. Asc speck formation in the epithelium of *Asc*$^{fl/fl}$ mice upon *C. rodentium* infection. Colon (A) and cecum (B, C, D, E) tissue samples were isolated from uninfected *Asc*$^{fl/fl}$ mice (A) and from *Asc*$^{fl/fl}$ and *Asc*$^{\Delta VC}$ mice at 14 days post oral infection with *C. rodentium* (~10^9 CFU) (B, C, D, E). Tissue sections were paraffin- embedded and subsequently stained for Asc (green), E-cadherin (red) and DAPI (blue). Bar= 20µm. Data representative of n=5-10 mice per group from one experiment.

3.3.Discussion

Previous work by our group and others, has demonstrated that the inflammasomes are important for limiting colonization and pathology in *C. rodentium* infected mice (231, 249, 345). Furthermore, bone marrow chimera experiments revealed that when mice were deficient in Asc, Nlrp3 or Nlrc4 within the radio-resistant compartment only, *C. rodentium* could colonise the cecal and colonic tissues of these mice to a greater extent (231, 249). Radio-resistant cells include IEC, stromal cells and radiation-resistant tissue resident phagocytes.

Our focus on IEC inflammasomes was spurred on by observations that several inflammasome components are expressed at high levels in the steady state intestinal epithelium, implicating their importance in immune monitoring of this mucosal barrier site (231, 255). To study epithelial inflammasome responses to *C. rodentium*, we selectively deleted Asc within IEC, using a Cre-lox genetic approach. Here, we report that while both $Asc^{\Delta IVC}$ and $Asc^{fl/fl}$ mice could ultimately clear *C. rodentium* infection, $Asc^{\Delta IVC}$ mice harboured higher levels of *C. rodentium* in their intestinal tissues compared to $Asc^{fl/fl}$ mice. The increased pathogen colonization in $Asc^{\Delta IVC}$ mice phenocopied that observed in $Asc^{-/-}$ mice that were infected in parallel. These data show that epithelial inflammasomes are key players in limiting *C. rodentium* colonisation in intestinal tissues.

Recent studies show that intestinal epithelial inflammasomes contribute to clearance of invading pathogens like *Salmonella*. Indeed, Naip/Nlrc4 and caspase-11 were important in controlling intracellular *S.* Tm loads in infected epithelial tissues (220, 230, 251). Our results demonstrate that IEC inflammasome responses are also important in controlling the burden of infection of attaching and effacing enteric pathogens that do not actively invade the intestinal epithelium. Since we did not observe drastic changes in any of the immune cell populations analysed or in spleen mass between the different mice genotypes during *C. rodentium* infection, we hypothesis that these observations are likely to be due to epithelial specific responses.

Although no changes were reported at the cellular level, we observed that overall inflammasome activation in infected tissues was reduced in $Asc^{\Delta IVC}$ mice, denoted by reduced activation of caspase-1 and IL-18 in the intestine. Interestingly, the reduction in inflammasome signalling was more evident during the peak of infection and bacterial burden in the cecum (day 8 p.i.) and colon (day 14 p.i.). Importantly, IL-18 levels

systemically in the spleen were comparable between *Asc*$^{\Delta VC}$ and *Asc*$^{fl/fl}$ mice. Conversely, *Asc*$^{-/-}$ mice had reduced IL-18 levels both systemically and in intestinal tissues during all stages of *C. rodentium* infection, and at steady state. This data supports a role for epithelial inflammasomes in controlling local but not systemic levels of IL-18.

Reduced IL-18 production has been previously linked to increased susceptibility to *C. rodentium* (345). However, the specific mechanism by which IL-18 signalling may control pathogen burden remains undefined. Inflammasome activation in epithelial cells, specifically the Asc-dependent Nlrp6 inflammasome formation, was previously linked to elevated IL-18 levels in the intestine as well as enhanced AMP production from IEC (241, 242, 249), possibly through influencing IL-22 signalling (369). Indeed, both IL-18 and IL-22 were shown to be involved in a positive feedback loop where IL-18 also drives an increase in IL-22 levels (369). Administration of rIL-18 to IEC decreased their production of IL-22 binding protein allowing for greater amounts of IL-22 signalling (248). Interestingly, co-administration of IL-22 and IL-18 induced re-programming of IEC gene expression, not observed with either cytokine alone, which correlated with protection against rotavirus infection (1). These reports suggest that these cytokines may act in concert in the intestine to promote AMP responses (373). In support of this, IL-18 and caspase-1 activation were found to control the AMP Ang4 at its transcriptional level (241). Furthermore, *Ang4* and *Retnla* AMP were also found to be greatly downregulated in colonic IEC from Asc deficient mice early during *C. rodentium* infection (249).

It is for these reasons that we measured IL-22 production and AMP responses in intestinal tissues and IEC, respectively. We observed very low level of IL-22 secretion by intestinal tissues of all infected mice, and overall did not see any clear difference in the secretion of this cytokine between *Asc*$^{\Delta VC}$ and *Asc*$^{fl/fl}$ mice. Furthermore, we could not detect changes in the expression of the IL-22 linked AMP, *S100A8* (one of the two subunits of calprotectin) (550), or in the expression of *Ang4* and *Retnla* (241, 249). These results, are in stark contrast with previous reports and do not support a role epithelial inflammasomes in controlling *C. rodentium* burden though AMP signalling. Further studies will investigate the production of IL-18BP and IL-22BP in *Asc*$^{\Delta VC}$ and *Asc*$^{fl/fl}$ mice to have a clear picture on the IL-18-IL-22 epithelial inflammasome regulatory axis (267, 551).

Neither the specific mechanism nor the intestinal tissues responsible for IL-18 driven protection against *C. rodentium* were identified (249, 345). We have shown that IEC

production of IL-18 during *C. rodentium* is drastically reduced in $Asc^{\Delta VC}$ mice. However, we were unable to identify a specific role for epithelial IL-18 in the control of *C. rodentium* burden. Since IL-18 receptor is highly expressed in the effector $CD4^+$ T cell compartment of the LP and in NK cells (255, 352), it is possible that epithelial IL-18 may be signalling to these cells to promote *C. rodentium* clearance. Interestingly, during *Salmonella* infection IL-18-elicited NK cell perforin responses were important in controlling inflammation and defence against enteric pathogens (352). However, we could not detect any alterations in immune cell populations in the LP during infection of $Asc^{\Delta VC}$ mice. Therefore, we hypothesise that IL-18 is acting directly on the epithelium leading to control of *C. rodentium* burden via an unidentified mechanism.

Intact IL-1 signalling was also linked to the control of *C. rodentium* infection (345, 346). Similar to previous publications (249), we were unable to detect significant levels of IL-1β in the tissues of infected mice. Thus, it is unlikely that IL-1β plays a strong role in controlling *C. rodentium* burden in $Asc^{\Delta VC}$ mice. Since IL-1β is primarily produced by myeloid cells, it would be desirable to assess IL-1β production from freshly isolated macrophages and DC. Nevertheless, there is growing body of evidence suggesting that IEC are poor expressers of IL-1β (246, 552). Therefore, we speculate that IL-1β production in $Asc^{\Delta VC}$ and $Asc^{fl/fl}$ mice is unaffected and does not explain the higher *C. rodentium* burden observed in $Asc^{\Delta VC}$ mice.

For long, the inflammasome has been considered to modulate microbiota composition. Indeed, the deletion of Nlrp6 and Asc were shown to lead to intestinal dysbiosis, allegedly due to AMP impairment (242). However, recent reports from Mamantopoulos *et al.* dismissed a role for Nlrp6 and Asc in the control of microbiota composition (362). This later study performed phylogenetic analyses on gut microbiota in Asc and Nlrp6 mice with the use of littermate controls, unlike previous studies. They observed no genetic-dependent microbiota drift upon inflammasome deletion. Additionally, they corroborated their observations in different animal facilities. These contrasting studies remark the need for careful experimental design when analysing host genetic effects on the gut microbiota (362).

The literature supports a role for the microbiota composition in modulating host susceptibility to *C. rodentium* (56, 448, 553, 554). We observed that infected $Asc^{\Delta VC}$ and $Asc^{-/-}$ mice experienced only a mild and transiently increased weight loss and only a

modest increase in pathology relative to *Asc*$^{fl/fl}$ mice. These observations are inconsistent with previous studies from our group where *Asc*$^{-/-}$ mice presented greater and more sustained body weight loss, as well as markedly increased intestinal pathology in *Asc*$^{-/-}$ mice infected with *C. rodentium* when compared with WT controls (249). Considering Mamantopoulos *et al.* research, we hypothesise that these different results could partially arise from variations in the intestinal microbiota between the different mice colonies (249). In the studies presented in this thesis, *Asc*$^{-/-}$ mice were co-housed with *Asc*$^{\Delta VC}$ and *Asc*$^{fl/fl}$ mice, therefore it is possible that the reduced disease exacerbation may be indicative of a less inflammatory microbiome present in the *Asc*$^{\Delta VC}$/*Asc*$^{fl/fl}$ mice colony.

The mechanisms of clearance of invading pathogens by epithelial inflammasomes has proven somewhat difficult to determine. However, recent publications shed some light on the mechanisms involved in IEC-intrinsic restriction of *S.* Tm invasion. The innate immune sensor Nlrc4 and its Naip adaptors were shown to be essential for the extrusion of infected IEC into the intestinal lumen following *S.* Tm challenge of streptomycin-treated mice (220). Furthermore, by using an inducible construct to drive the expression of Nlrc4 specifically in the intestinal epithelium, Rauch *et. al.* showed that IEC-specific Nlrc4 activation by FlaTox was sufficient to drive pathology, IEC death and IL-18 release (230). IEC extrusion may represent a cell-intrinsic defence mechanism that serves to limit the rate of pathogen colonization of the intestinal epithelium.

Inflammasome activation upon infection classically results in the death of the infected cell. The inflammasome-dependent cell death is pyroptosis, and despite being the main form of cell death associated with inflammasome responses, other non-lytic forms of cell death have been observed upon inflammasome activation. Interestingly, components of the inflammasome platform, including Nlrc4 and Asc, were shown to interact with caspase-8 to drive non-lytic cell death both *in vivo* and *in vitro* (230, 549). Furthermore, upon abolition of pyroptosis by GsdmD genetic deletion, the caspase-8-dependent cell death downstream of FlaTox-driven Nlrc4 inflammasome activation in IEC became evident. This was observed both *in vivo* and *in vitro* IEC organoids (230). GsdmD and caspase-8 are constitutively expressed in the gastrointestinal epithelium (401). Therefore, both pathways have a 'ready to go' potential to occur *in vivo* upon inflammasome activation.

Interestingly, we observed that the inflammasome activation *in vivo* during *C. rodentium* infection, was accompanied by an increased activation of caspase-8. Remarkably, IL-18 activation correlated with caspase-8 and caspase-1 activation. Furthermore, in $Asc^{\Delta VC}$ and $Asc^{-/-}$ mice, the reduction in inflammasome activation was accompanied by a dramatic reduction in caspase-8 activation. These results suggest that caspase-8 and caspase-1 triggered cell deaths are either co-regulated or inter-regulated.

Further investigation of cell proliferation and death markers, *Ki67* and *caspase-8* respectively, revealed a trend towards reduced transcription of these markers in $Asc^{\Delta VC}$ compared to $Asc^{fl/fl}$ at day 8p.i. These responses agree with our proposed link between inflammasomes and caspase-8 responses. Furthermore, the reduction in *Ki67* in $Asc^{\Delta VC}$ mice is interesting because IEC production of IL-18 has previously been linked to epithelial protective effects such as wound healing (239, 358, 371, 372, 555), and in driving IL-22 (369), a cytokine important for mucosal barrier integrity (121, 548).

Since IL-18 is drastically reduced in inflammasome deficient animals, the epithelial cell repair upon infection could be affected as well as the ability to expel infected cells from the intestinal epithelium. We hypothesise that upon inflammasome activation, caspase-8 epithelial responses may contribute to the clearance of *C. rodentium in vivo*, by facilitating the death of infected cells, and perhaps forcing the epithelium to initiate repair responses.

Cell death and the release of pro-inflammatory cytokines and alarmins are the major contribution of inflammasome towards inflammatory responses (325). Interestingly, pyroptotic cells have been shown to release parts of the inflammasome complex that can activate immune cells if engulfed by other phagocytic cells (326, 328). This ultimately leads to amplification of inflammasome signalling (326). The release of these particles is a consequence of Asc speck formation. These structures have not previously been reported within IEC neither *in vivo* nor *in vitro*. Here, we report Asc speck formation *in vivo* upon *C. rodentium* infection, although further characterisation of these specks is needed to quantify and validate this observation and its potential roles in *C. rodentium* clearance from infected IEC.

Overall, we showed that epithelial inflammasomes are important in the clearance of *C. rodentium* from intestinal tissues. We attribute this role, primarily, to an epithelium intrinsic effect, since we do not observe significant changes in the proportions of immune

cell populations mediating *C. rodentium* clearance. Furthermore, we also showed that inflammasomes are important for maintaining an adequate IL-18 response during the peak of *C. rodentium* infection. Despite the published links between IL-18 and AMP response, we did not find sufficient evidence to support a role for AMP production in controlling *C. rodentium* burden downstream of epithelial inflammasomes. However, we showed that inflammasome activation and IL-18 release is accompanied by activation of caspase-8. Additionally, reduced inflammasome activation in intestinal tissues of $Asc^{\Delta VC}$ and $Asc^{-/-}$ mice correlated with a reduction in caspase-8 activation during *C. rodentium* infection. Although we are uncertain of how these responses are interconnected, we hypothesise that activation of caspase-8 upon inflammasome activation in the intestinal epithelium may contribute to the clearance of *C. rodentium in vivo.*

Chapter 4: Regulation of inflammasome components in the intestinal epithelium - an organoid approach.

4.1.Introduction

The direct contact of the intestinal epithelium with the diverse microbiota makes epithelial cells an interesting site to study in innate immunity. Far from being merely a physical barrier, the intestinal epithelium and IEC, play active roles in bridging immune recognition and signalling with effector responses.

PRR signalling networks are key processes that orchestrate the onset of tolerogenic or inflammatory responses at mucosal sites. To date, the majority of work has focused on the role of the haematopoietic compartment in microbial detection and inflammation. Nevertheless, non-haematopoietic cells, particularly IEC, are now appreciated to be important contributors to PRR signalling circuits in the gut (556). PRR sensing in the intestinal epithelium has been implicated in key processes preserving immune homeostasis, such as maintenance and repair of the epithelial barrier, mucus secretion, and AMP production (557-559). Given that the luminal content occasionally carries pathogenic microorganisms or toxins, effective PRR signalling within IEC also contributes to protection against enteric pathogens by initiating immune responses against the invading threat and inducing tissue repair (343, 560, 561).

Genetic and experimental data highlight a key role for NLR and inflammasomes in regulating intestinal immunity and inflammation (220, 231, 249, 562). Unsurprisingly, due to the proximity of IEC to microbial stimuli, increasing amount of evidence places IEC inflammasomes at the forefront of antimicrobial defence at the host-lumen interface (249, 255, 361, 563, 564). Indeed, recent reports show that inflammasome signalling in IEC is important in mediating extrusion of *S.* Tm infected epithelial cells from the epithelial layer to limit pathogen colonisation (220, 251). Additionally, we have previously reported that NLR activation in a non-hematopoietic compartment was protective during acute intestinal infection triggered by *C. rodentium* (231, 249). Furthermore, we have generated transgenic mice in which the key inflammasome adaptor molecule Asc is selectively ablated in IEC ($Asc^{\Delta IVC}$) and observed that epithelial inflammasomes are important for controlling *C. rodentium* clearance in these mice.

Several key issues, such as the precise mechanisms of NLR activation and co-ordination of downstream effector responses in IEC, remain poorly understood in comparison to cells of the immune compartment, especially DC and macrophages. Our aim in this chapter is to dissect the mechanisms of inflammasome activation and regulation in IEC, with a special interest in mechanisms mediating pathogen clearance from infected IEC. To focus on IEC intrinsic responses, we investigated this question with the use of *ex vivo* cultures of primary IEC organoids.

Until recently, *in vitro* studies of IEC biology largely relied on the use of immortalised cancerous cell lines. However, intestinal epithelial organoids provide an *ex vivo* system for studying functional outputs of primary IEC, in a way that is closer to the *in vivo* intestinal epithelial niche (565). Organoids are composed of different cell types, including stem cells capable of self-renewal and expansion, in addition to differentiated cell types of the intestinal epithelium, such as enterocytes, Paneth cells and goblet cells (505, 566).

In the organoid system, cells that have undergone differentiation have a limited life-span and can no longer self-renew or be propagated, much like mature enterocytes *in vivo* (505). IEC are highly polarised and this can also be observed in the organoids, where the basolateral side faces the outside, in contact with the matrigel matrix, and the apical side faces the inside of the 3D structure (566). Therefore, we also generated primary IEC monolayers that have the apical side accessible for experimental challenge and the basolateral side anchored on a collagen-coated surface. Together, these techniques enabled us to functionally assess IEC responses to intestinal bacteria and other inflammasome modulating and activating stimuli *in vitro*.

4.2.Results

4.2.1. Inflammasome signal 1 in the epithelium: IL-22 upregulates the expression of IL-18

Although inflammasome processed IL-18 is often secreted by IEC, the regulation of pro-IL-18 expression and other inflammasome components within IEC remains poorly understood. Classical inflammasome activation is viewed as a two-signal model. Signal one is a priming signal, provided by TLR ligand binding, that induces the transcription of pro-IL-18 and pro-IL-1β as well as some NLR (281, 567). Signal 2 is the NLR activation signal, typically provided by DAMP, including ATP and microbial components that reach the cellular cytosol (207).

Various PAMP were explored as potential inflammasome priming agents in IEC organoids, including LPS and flagellin, shown to prime the inflammasome in myeloid cells (281). However, none of these stimuli had a positive effect on *pro-Il-18* expression in 3D primary cecal IEC organoids (Figure 4.1A). We further hypothesised that inflammatory stimuli may be important regulators of inflammasomes in IEC. Therefore, an array of inflammatory cytokines was used to stimulate 3D cecal IEC organoids and the expression of *pro-Il-18* was assessed. Although the vast majority of cytokines had no effect on *pro-Il-18* expression, we found that IL-22 stimulation consistently led to an up-regulation of *pro-Il-18* mRNA by 2-2.5-fold (Figure 4.1A). Titration of IL-22 concentration revealed that induction of IL-18 mRNA expression in IEC reached saturation at 100 ng/ml of IL-22 (Figure 4.1B). Analysis of IL-18 protein by western blotting confirmed that pro-IL-18 (24 kDa) was elevated in IL-22 treated IEC organoids, compared to untreated organoids (Figure 4.1 C). Notably, *pro-Il-18* expression and protein were observed at steady state in the absence of stimulation in IEC organoids (Figure 4.1 C).

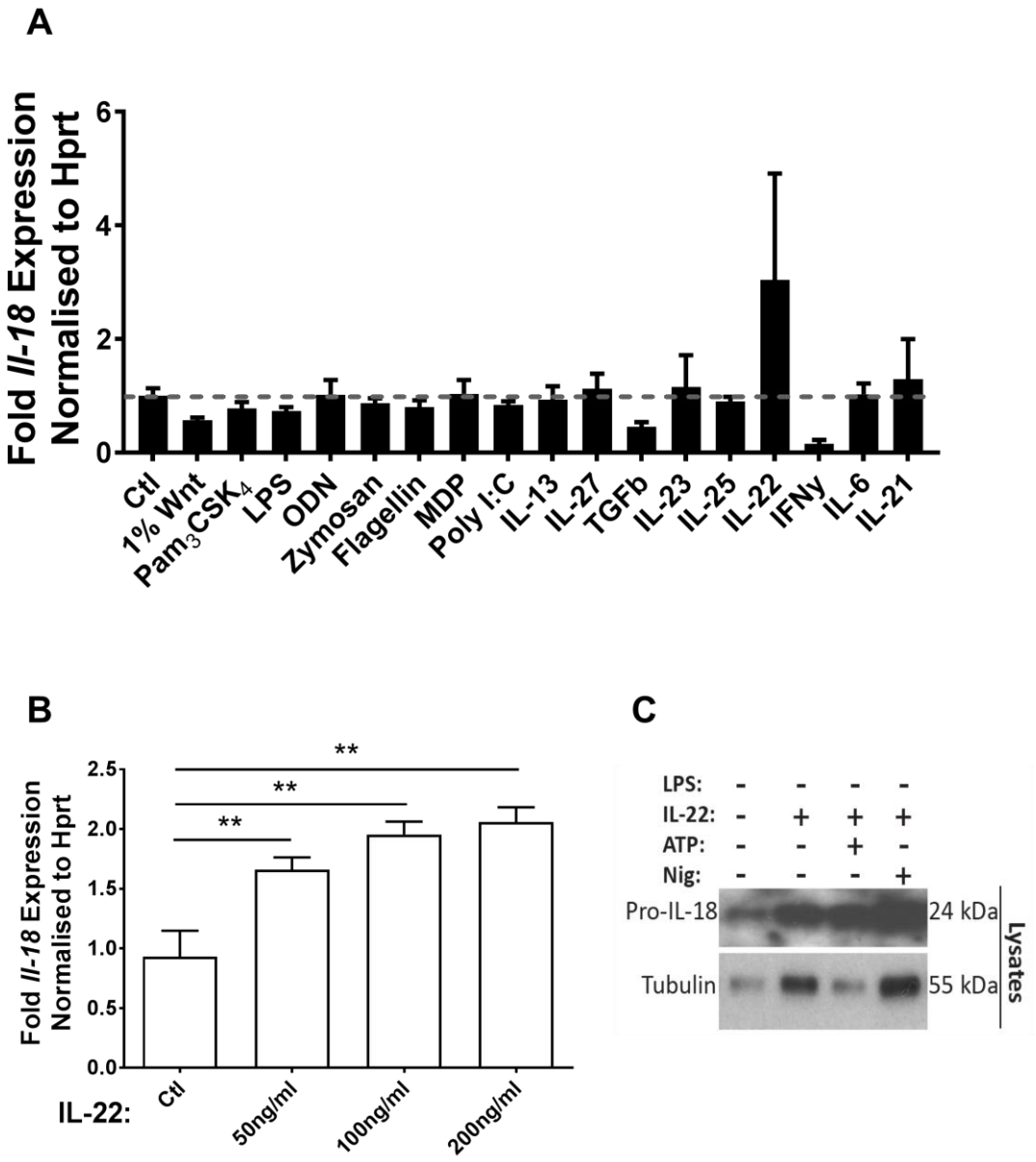


Figure 4.1. IL-22 induces pro-IL-18 expression in primary IEC. (A-C) *Il-18* mRNA expression levels were measured by qPCR in 3D cecal IEC organoids stimulated for 16h with different cytokines and PAMP. *Il-18* mRNA levels were normalised to the housekeeping gene *Hprt* and the fold expression in stimulated samples were compared to untreated controls (Ctl). (A) 3D cecal IEC organoids stimulated for 16h with different cytokines and PAMP (concentrations are indicated in the Materials and Methods section). (B) 3D cecal IEC organoids stimulated with IL-22 for 16h, at concentrations ranging 50-200 ng/ml. (C) Western blot for the pro- form of IL-18 in cell lysates of 3D organoids following culture in the presence or absence of IL-22 (100 ng/ml) for 24h. IL-22 primed organoids were also treated with ATP 5 mM or nigericin 5 µM for 1h. Tubulin used as loading control. (A, B, C) Treatments were performed in triplicate organoid wells. qPCR experiments were performed in technical duplicates. Error bars represent standard deviation from the sample mean. An unpaired t-test was used for statistical analysis; *p<0.05; **p<0.001; ***p<0.0001; ****p<0.00001. Data represented in A and C is from one experiment and data in B is representative of 2 independent experiments.

4.2.2. Nlrp3 activating DAMP fail to activate the inflammasome in IEC

Upon inflammasome activation, caspase-1 is auto-proteolytically cleaved, releasing the active forms of caspase-1, consisting of a 10 kDa (p10) and a 20 kDa (p20) fragment, into the cell supernatant (316). Thus, we assessed inflammasome activation in 3D IEC organoids by evaluating the maturation and secretion of caspase-1 in the supernatants of stimulated cells, by western blot analysis. Of note, upon inflammasome activation cells undergo lytic cell death. Consequently, it is common to observe the release of uncleaved pro-caspase-1 (45 kDa) into the cell supernatants (Figure 4.2).

ATP and nigericin are well characterised Nlrp3 inflammasome activators in LPS-primed myeloid cells, and are commonly used positive controls for Nlrp3 activation (568). Thus, we used ATP and nigericin as Nlrp3 activators to stimulate IEC organoids. Organoids were primed with IL-22 before stimulation to maximise *pro-IL-18* expression. As a positive control for inflammasome activation upon ATP and nigericin treatment we assayed BMDM in parallel. As expected, BMDM treated with ATP or nigericin displayed inflammasome activation with the active caspase-1 fragment (p10) readily detected in cell supernatants (Figure 4.2). Notably, BMDM were only able to activate the inflammasome upon LPS priming before ATP and nigericin treatment, whilst inflammasome activation did not proceed upon IL-22 priming (Figure 4.2).

In contrast, priming with IL-22 followed by stimulation with ATP or nigericin did not drive inflammasome activation in cecal WT IEC organoids, and the active form of caspase-1 could not be detected in the IEC cell supernatants (Figure 4.2). These observations indicate that IEC organoids are unable to activate the Nlrp3 inflammasome in response to ATP or nigericin.

Of note, unlike BMDM that were stimulated in reduced-serum media, IEC organoids were treated in media containing serum in order to maximise IEC survival. As a result, a higher total protein content was precipitated and concentrated from organoid supernatants compared to BMDM, which could explain the increased size of the pro-caspase form detected in these samples.

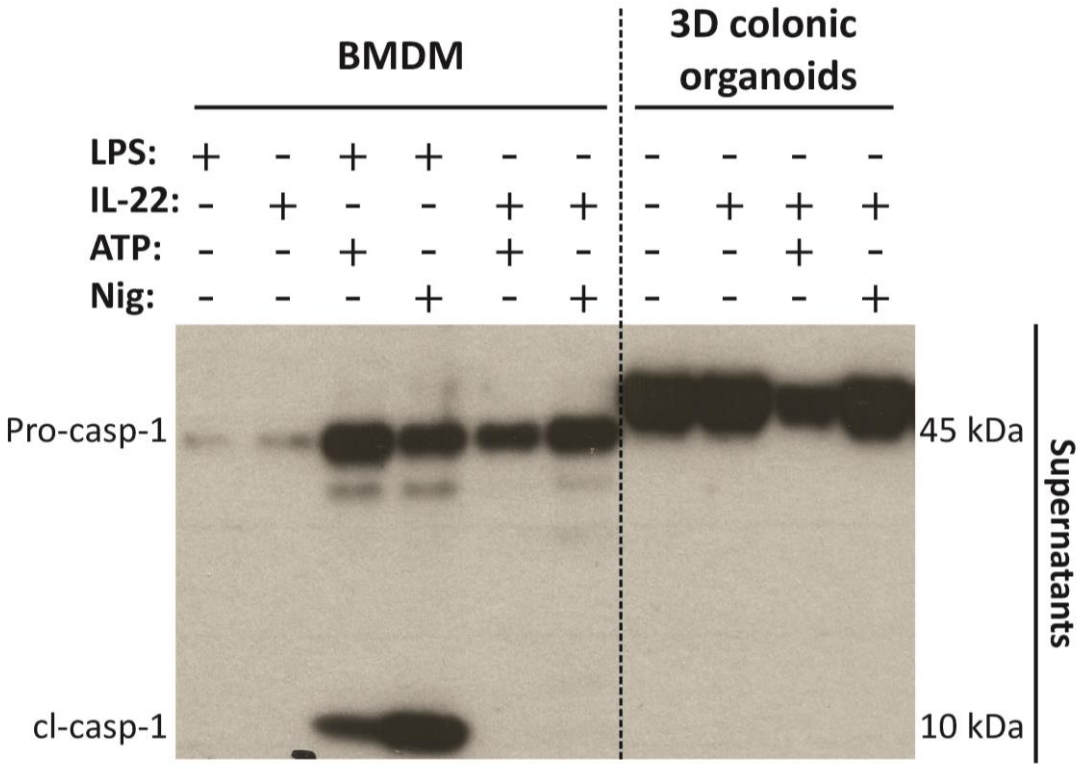


Figure 4.2. Nlrp3 inflammasomes are not classically activated in primary IEC. BMDM or 3D primary cecal IEC organoids were primed with LPS (100 ng/ml) for 12h or 24h, respectively or with IL-22 (50 ng/ml) for 24h. This was followed by stimulation with ATP (5 mM) or nigericin (5 µM) for 1h. Cell supernatants were then collected for analysis of caspase-1 activation by western blot. Stimulations were performed in biological duplicates. Supernatants from duplicate wells were pooled for protein precipitation and western blotting. Data are representative of 7 independent experiments (with ATP concentrations ranging 5-20mM and nigericin concentrations ranging 5-25µM for up to 5h).

4.2.3. Differential expression of Nlrp3 and Nlrc4 in IEC, stromal cells and myeloid cells

A potential explanation for the lack of Nlrp3 inflammasome activation in IEC organoids is that Nlrp3 may not be expressed at sufficiently high levels in primary IEC. Therefore, we compared the expression levels of inflammasome components in the 3D primary cecal organoids with that of BMDM. We found that *pro-Il-18* mRNA expression levels at steady state were 6-fold higher in 3D primary cecal IEC organoids compared to BMDM (Figure 4.3A). In addition, we observed that the *Il-18* mRNA levels in primary cecal IEC remained unchanged in LPS treated organoids but significantly increased following IL-22 treatment (Figure 4.3A). In contrast, IL-22 had no effect on BMDM expression of *Il-18* (Figure 4.3A). Furthermore, although LPS increased the expression of *Il-18* mRNA in BMDM, the levels were still markedly lower than those found in cecal IEC (Figure 4.3A).

We also detected approximately 4-fold higher levels of expression of *Nlrc4* mRNA in primary cecal IEC organoids in comparison to BMDM (Figure 4.3B). Additionally, IL-22 moderately increased *Nlrc4* expression in IEC organoids whilst it had no impact on *Nlrc4* expression by BMDM (Figure 4.3 B). Conversely, LPS stimulation significantly increased expression of *Nlrc4* in BMDM, whilst not affecting *Nlrc4* expression by IEC organoids (Figure 4.3 B).

Nlrp3 was readily detectable at steady state in BMDM and was significantly increased upon stimulation with LPS (~4-fold), but not with IL-22 (Figure 4.3 C). Conversely, we found that *Nlrp3* mRNA expression was undetectable in primary cecal IEC organoids, irrespective of treatment with IL-22 or LPS (Figure 4.3 C). Together, these data demonstrate that IEC and BMDM have differential expression of inflammasome components, with *Il18* and *Nlrc4* being more highly expressed in the IEC and *Nlrp3* in the BMDM.

Previous studies suggested that non-hematopoietic Nlrp3 expression was important for protection against intestinal inflammation or injury (249, 256). We therefore investigated whether *in vitro* cultured cecal stromal cells expressed *Nlrp3* and other inflammasome components. We found that *Asc* expression was significantly lower in LPS primed stroma compared to BMDM (Figure 4.4 A). Similarly, although *Nlrp3* expression was detectable in LPS primed cecal stromal cells, expression levels were significantly lower than found in LPS primed BMDM, but approximately 4-fold higher than in non-primed BMDM

(Figure 4.4 B). Furthermore, *Il-18* expression in LPS primed stroma was approximately 4-fold lower than found in LPS primed BMDM (Figure 4.4 C). These observations demonstrate that *Nlrp3* may be expressed by stromal cells upon LPS priming, but that they express only low levels of *Asc* and *Il-18*.

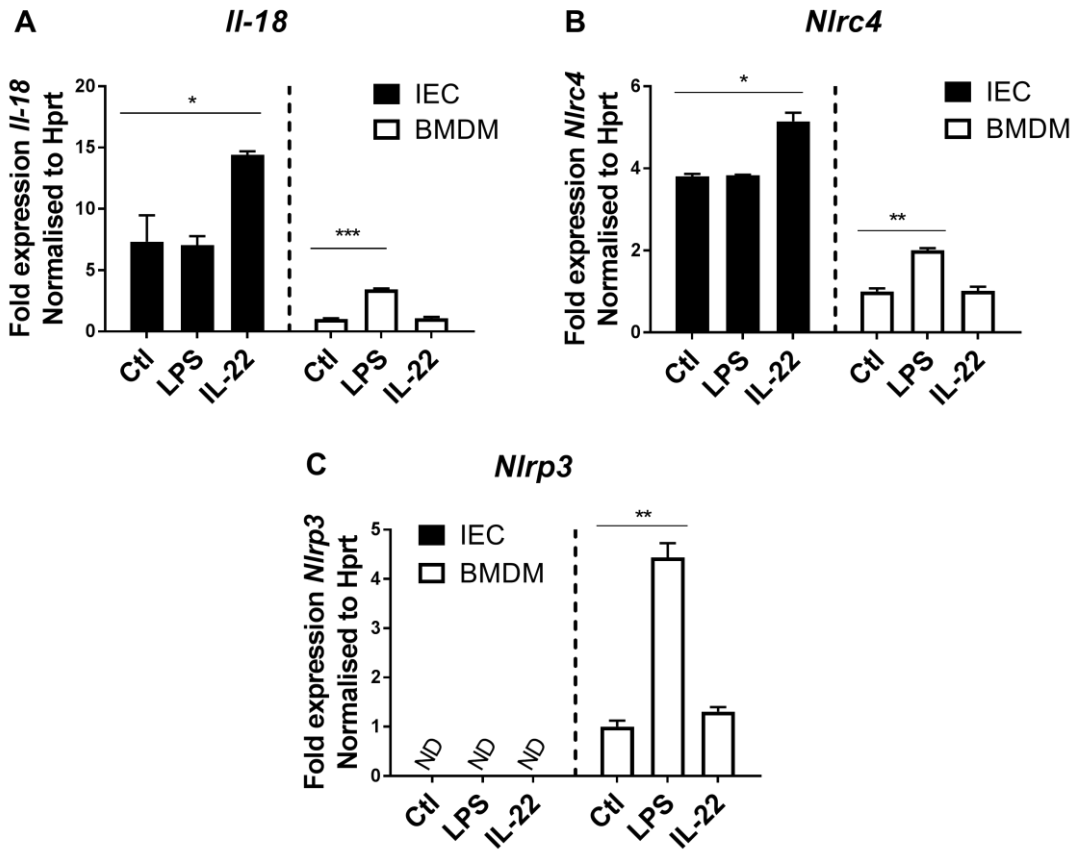


Figure 4.3 Differential expression of inflammasome components by primary IEC and BMDM. BMDM or 3D primary cecal IEC organoids were treated for 12h and 24h, respectively with LPS (100 ng/ml) or for 24h with IL-22 (100 ng/ml). qPCR was used to analysed expression of IL-18 (A), *Nlrc4* (B) and *Nlrp3* (C). Expression levels were normalised to the house-keeping gene *Hprt*. Fold expression in stimulated samples were compared to untreated BMDM controls (BMDM Ctl). Treatments were performed in duplicate organoid wells. qPCR experiments were performed in technical duplicates. Error bars represent standard deviation from the sample mean. An unpaired t-test was used for statistical analysis; *p<0.05; **p<0.001; ***p<0.0001; ****p<0.00001. ND (not detectable). Data are representative of 2 independent experiments.

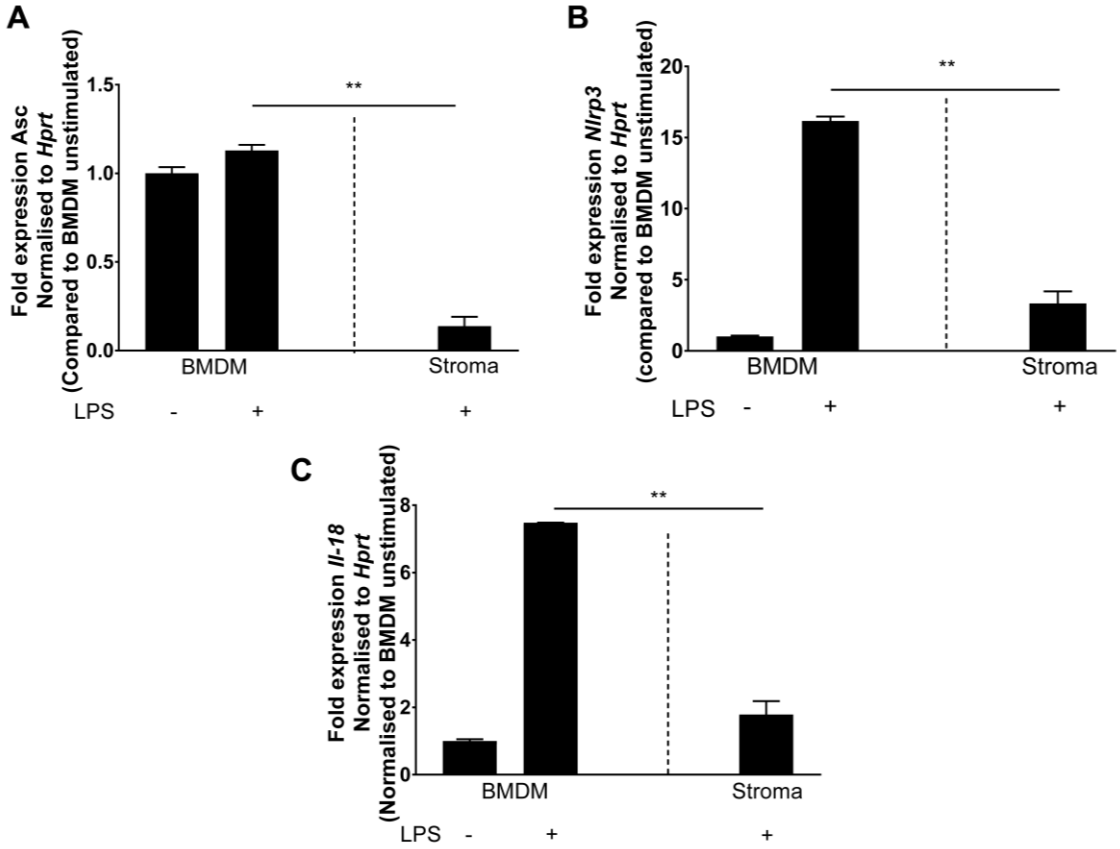


Figure 4.4. Differential expression of inflammasome components by stroma and BMDM. BMDM or stroma were treated for 12h with LPS (100 ng/ml). qPCR was used to analysed expression of *Asc* (A), *Nlrp3* (B) and *Il-18* (C). Expression levels were normalised to the house-keeping gene *Hprt*. Fold expression in all samples were compared to untreated BMDM controls (BMDM Ctl). Treatments were performed in duplicate organoid wells. qPCR experiments were performed in technical duplicates. Error bars represent standard deviation from the sample mean. An unpaired t-test was used for statistical analysis; *p<0.05; **p<0.001; ***p<0.0001; ****p<0.00001. ND (not detectable). Data are representative of 2 independent experiments.

4.2.4. Epithelial responses to challenge with enteric pathogens

To investigate IEC inflammasome responses to enteric pathogens, we challenged primary IEC *ex vivo* with *S.* Typhimurium or *C. rodentium*. As 3D organoids do not allow bacteria to access the apical IEC surface, we generated polarised primary IEC monolayers that could be infected by applying the bacterial challenges to the apical surface.

4.2.4.1. Epithelial inflammasomes are not primed upon challenge with C. rodentium or S. Typhimurium

Differentiated IEC monolayers were stimulated overnight with either *C. rodentium* or *S.* Tm and assessed for expression of the inflammasome components *Nlrc4*, *Nlrp3* and *Il-18* as well as the chemokine *Cxcl2*. Infection with *C. rodentium* led to significantly increased *Cxcl2* transcription in primary IEC monolayers (Figure 4.5 A), confirming that the bacterial challenge had induced an inflammatory response in the IEC. In contrast, we observed that *Il-18* and *Nlrc4* expression were not significantly altered in primary IEC monolayers after challenge with *C. rodentium* (Figure 4.5 B and C). As expected, we could not detect *Nlrp3* expression in IEC monolayers upon *C. rodentium* challenge (Figure 4.5 D).

Similarly, *Il18* and *Nlrc4* expression were not significantly altered in primary IEC monolayers after challenge with *S.*Tm (Figure 4.6 B and C). Again, we could not detect *Nlrp3* expression in IEC monolayers upon *S.*Tm exposure (Figure 4.6 D). However, *S.*Tm led to significantly increased *Cxcl2* transcription in primary IEC monolayers (Figure 4.6 A), confirming that the bacterial challenge had elicited an inflammatory response.

Together, these results indicate that infection with these Gram-negative bacterial pathogens does not prime inflammasome expression in primary IEC.

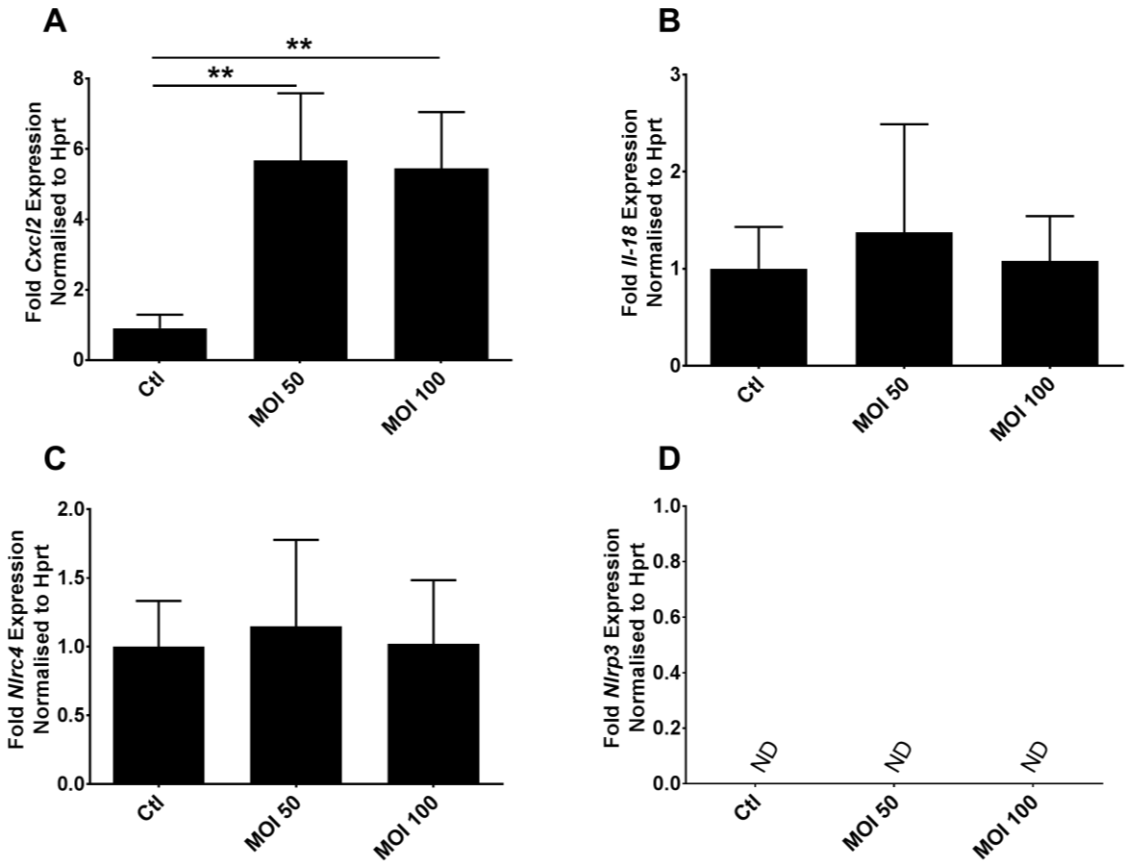


Figure 4.5. *C. rodentium* infection does not alter expression of inflammasome components by primary IEC monolayers. Primary cecal IEC monolayers were stimulated with *C. rodentium* at the indicated MOI for 2h, followed by 1h incubation with Gentamycin (100 µg/ml) and 16h incubation in medium, after which RNA was isolated. (A) *Cxcl2* (B) *Il18*, (C) *Nlrc4* and (D) *Nlrp3* expression levels were measured by qPCR. Gene induction was normalised to the house-keeping gene *Hprt* and the fold expression represents the comparison of each sample to the untreated control (Ctl). Treatments were performed in duplicate organoid wells. qPCR experiments were performed in technical duplicates. Error bars represent standard deviation from the sample mean. An unpaired t-test was used for statistical analysis; *p<0.05; **p<0.001; ***p<0.0001; ****p<0.00001. ND. (not detectable). Data are representative of 2 independent experiments.

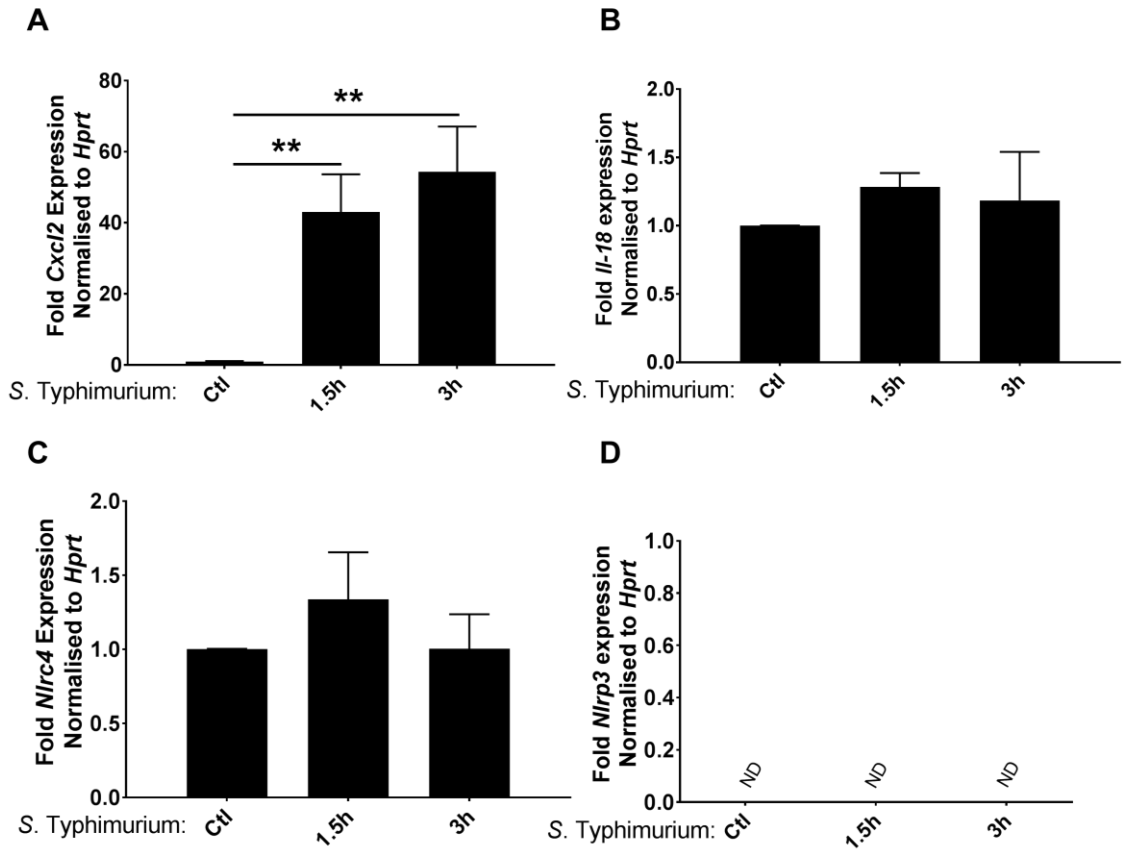


Figure 4.6. *Salmonella* Typhimurium infection does not alter expression of inflammasome components by primary IEC monolayers. Primary cecal IEC monolayers were stimulated with S. Typhimurium at MOI 100 for 1.5h or 3h, after which RNA was isolated. (A) *Cxcl2*, (B) *Il-18*, (C) *Nlrc4* and (D) *Nlrp3* expression levels were measured by qPCR. Gene induction was normalised to the house-keeping gene *Hprt* and the fold expression represents the comparison of each sample to the untreated control (Ctl). Treatments were performed in duplicate organoid wells. qPCR experiments were performed in technical duplicates. Error bars represent standard deviation from the sample mean. An unpaired t-test was used for statistical analysis; *p<0.05; **p<0.001; ***p<0.0001; ****p<0.00001. ND. (not detectable). Data are representative of 2 independent experiments.

4.2.4.2. Salmonella Typhimurium elicits more powerful inflammasome responses in IEC compared to Citrobacter rodentium

As we detected high steady state levels of *Nlrc4* expression in IEC organoids, we hypothesised that the invasive pathogen *S.* Typhimurium could activate the Nlrc4 inflammasome in our IEC monolayer system.

To test this hypothesis, differentiated cecal IEC monolayers were challenged with *S.* Tm and cell supernatants were then collected to assess inflammasome activation by western blot analysis of caspase-1 and IL-18 cleavage. Stimulation of IEC monolayers with *S.* Tm drove caspase-1 cleavage and release into the supernatant (Figure 4.7 A). *S.*Tm has been described to activate both Nlrp3 and Nlrc4 inflammasomes (569). To assess the requirement of the different epithelial inflammasome components *Nlrp3*$^{-/-}$, *Nlrc4*$^{-/-}$ or *Asc*$^{-/-}$ IEC monolayers were stimulated with *S.* Tm. Interestingly, we observed that *S.* Tm treatment of *Nlrp3*$^{-/-}$ monolayers resulted in the cleavage and activation of caspase-1 and IL-18 (Figure 4.7 B). Similarly, *Asc*$^{-/-}$ monolayers treated with *S.* Tm were also able to activate caspase-1 and IL-18, although to a lesser extent than WT or *Nlrp3*$^{-/-}$ monolayers (Figure 4.7 B). Conversely, *Nlrc4*$^{-/-}$ IEC monolayers did not exhibit caspase-1 nor IL-18 cleavage and release in response to *S.*Tm infection (Figure 4.7 B). These results show that *S.* Tm activates Nlrc4 inflammasomes in IEC.

Since *C. rodentium* is an attaching and effacing pathogen, we hypothesised that it would also drive inflammasome activation in IEC. We therefore infected WT, *Nlrp3*$^{-/-}$, *Nlrc4*$^{-/-}$ or *Asc*$^{-/-}$ IEC monolayers with *C. rodentium*, or *S.* Tm as a positive control, and measured secretion of active IL-18. In agreement with our western blot analysis (Figure 4.7), *S.* Tm challenge of IEC monolayers resulted in IL-18 release from WT, *Nlrp3*$^{-/-}$ and, to a lesser extent, *Asc*$^{-/-}$ monolayers but not from *Nlrc4*$^{-/-}$ (Figure 4.8). In contrast, we did not observe IL-18 secretion from any IEC monolayer following stimulation with *C. rodentium* (Figure 4.8). Notably, if IEC monolayers were pre-treated with a pan-caspase inhibitor (ZVAD-FMK), *S.*Tm-induced IL-18 secretion was abolished, confirming that IL-18 secretion by IEC was caspase-dependent (Figure 4.8).

All inflammasomes engage with the adaptor protein Asc for the full activation and cleavage of caspase-1 (316). Upon inflammasome activation, Asc assembles into a large protein complex termed a "speck". Asc specks have mostly been described in myeloid

cells, including DC and macrophages (570). In most cases, only one speck of around 1μm forms in an individual cell upon inflammasome activation (571). In myeloid cells, the formation of Asc "specks" was proposed as a readout of inflammasome activation upstream of caspase-1 and IL-18 cleavage and release (570). Therefore, we investigated whether inflammasome activation in IEC was accompanied by the formation of Asc specks. IEC monolayers were challenged with either *S*.Tm or *C. rodentium* and subjected to immunohistochemistry staining for Asc, as previously explained. Finally, stained monolayers were imaged by confocal microscopy for visualisation of Asc specks. To maximise the chances of observing Asc speck formation, cells can be pre-treated with a pan-caspase inhibitor (ZVAD-FMK) to avoid excessive cell death (572). Therefore, some monolayers were also treated with ZVAD-FMK for 30 min prior to bacterial challenge.

We observed punctate Asc agglomerations, consistent with Asc specks, forming in WT and *Nlrp3*$^{-/-}$ IEC monolayers following infection with *S*. Tm (Figure 4.9 and Figure 4.10). As expected, we did not observe these agglomerations in *Asc*$^{-/-}$ IEC monolayers infected with *S*.Tm (Figure 4.9 and Figure 4.10). Interestingly, *Nlrc4*$^{-/-}$ IEC monolayers infected with *S*.Tm exhibited diffuse cytosolic Asc staining without speck formation (Figure 4.9 and Figure 4.10). Thus, *S.* Tm-driven Nlrc4 inflammasome activation in IEC is associated with the formation of Asc specks.

In contrast, consistent with the lack of inflammasome activation that we observed previously, we could not detect any Asc speck formation upon *C. rodentium* infection of IEC monolayers (Figure 4.9). To maximise the chances of observing Asc speck formation, cells can be pre-treated with a pan-caspase inhibitor (ZVAD-FMK) to avoid excessive cell death (572). Therefore, some monolayers were also treated with ZVAD-FMK for 30min prior to bacterial challenge. This treatment increased the frequency of speck occurrence in IEC infected with *S.* Tm, but still did not reveal any speck formation in IEC monolayers infected with *C. rodentium* (data not shown),

Due to their different interactions with IEC, we considered the possibility that the inflammasome response in IEC monolayers upon *C. rodentium* infection might be delayed compared to the response triggered by *S.* Tm infection. Therefore, we compared IL-18 release by *S.* Tm or *C. rodentium* infected IEC monolayers at various time points post-challenge. We observed that IL-18 release by IEC increased over time when infected

with S. Tm (Figure 4.11). Furthermore, *S.*Tm stimulated *Asc*$^{-/-}$ IEC had significantly decreased IL-18 secretion compared to WT IEC at 12h p.i. (Figure 4.11). In contrast, IEC monolayers infected with *C. rodentium* released barely detectable levels of IL-18 into the supernatant, with only WT IEC monolayers at 12h p.i. having IL-18 levels that exceeded the background levels of the assay. (Figure 4.11).

As a final effort to explore IEC inflammasome activation by *C. rodentium*, IEC monolayers were primed with IL-22 for 24h before infection to maximise *pro-IL-18* production, followed by infection with a high dose (MOI 100) of *C. rodentium* for 4h or 16h. However, even under these conditions, active cleaved caspase-1 was not detected in either the cell supernatants or the lysates of *C. rodentium* infected WT cecal IEC monolayers (Figure 4.12).

In conclusion, although the IEC appear to sense the presence of *C. rodentium,* this pathogen does not seem to lead to inflammasome activation in primary IEC *in vitro*. Conversely, *S.*Tm infection is able to drive a robust inflammasome response in primary IEC monolayers, leading to Asc speck formation, as a well as caspase-1 and IL-18 cleavage and secretion. Interestingly, this response seems to be dependent on Nlrc4 and partially dependent on Asc, but independent of Nlrp3.

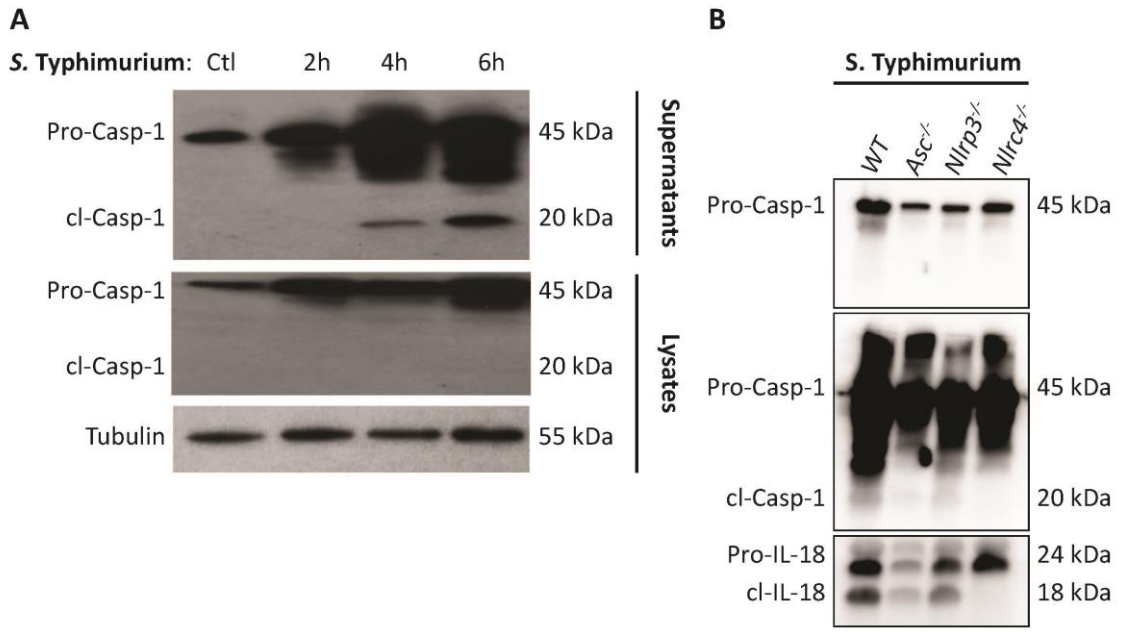


Figure 4.7. *S*. Typhimurium activates the inflammasome in primary IEC monolayers in an Nlrc4-dependent manner. (A) WT cecal IEC monolayers were stimulated with *S*. Typhimurium at MOI 100 for 2h, 4h or 6h. Cell supernatants and lysates were then collected and assessed by western blot analysis of cleaved (cl) caspase-1. Tubulin was used as a loading control for lysates. (B) WT, *Nlrp3*$^{-/-}$, *Nlrc4*$^{-/-}$ and *Asc*$^{-/-}$ cecal IEC monolayers were stimulated with *S*. Typhimurium at MOI 100 for 5h. Cell supernatants were then collected and assessed by western blot analysis of cleaved (cl) caspase-1 and IL-18. (A and B) Stimulations were performed in pooled biological duplicates (wells). Data are representative of 3 (A) or 2 (B) independent experiments.

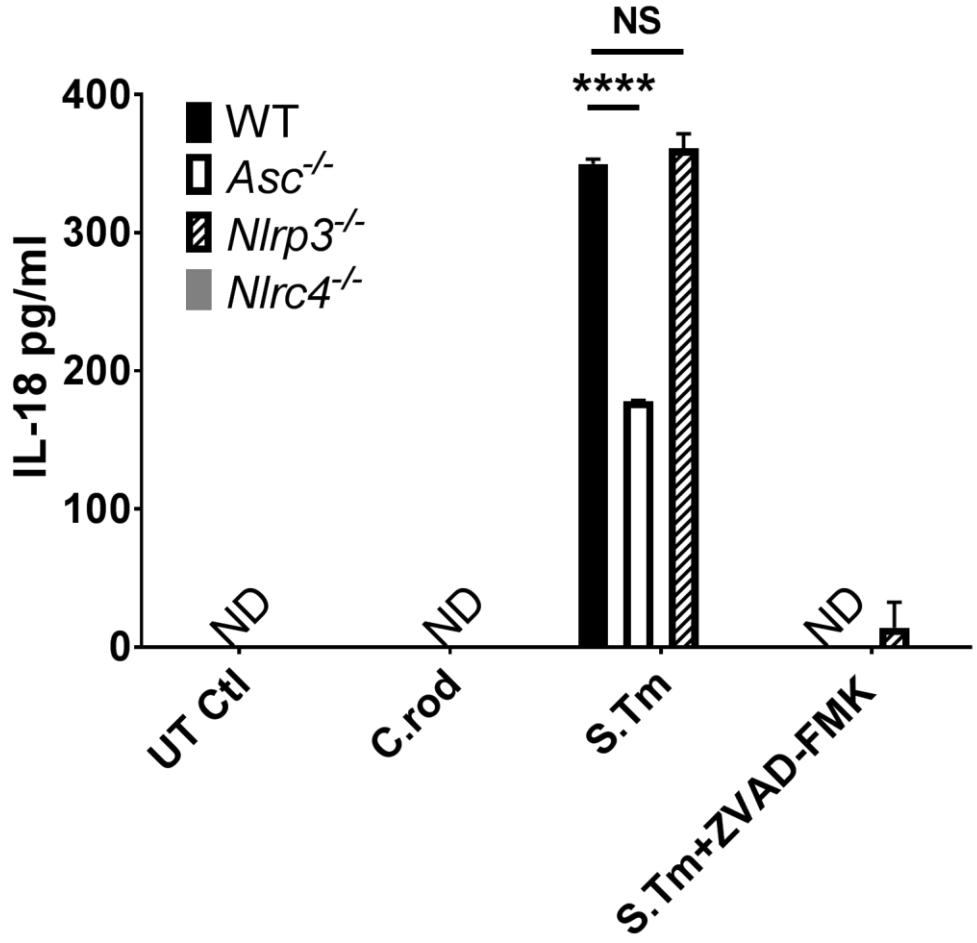


Figure 4.8. Stimulation with *S*. Typhimurium, but not *C. rodentium*, leads to IL-18 release from IEC monolayers. WT, *Nlrp3*$^{-/-}$, *Nlrc4*$^{-/-}$ and *Asc*$^{-/-}$ cecal IEC monolayers were stimulated with *S*. Typhimurium or *C. rodentium* at MOI 1 for 5h. Some IEC were treated with the pan caspase inhibitor ZVAD-FMK (add concentration) for 30min prior to *S*. Tm infection. After stimulation, cell supernatants were collected and IL-18 secretion measured by ELISA. Error bars represent standard deviation from the sample mean. An unpaired t-test was used for statistical analysis; *p<0.05; **p<0.001; ***p<0.0001; ****p<0.00001. ND. (not detectable). ELISA performed in technical duplicates and stimulations were performed in biological duplicates (2-wells). Data are representative of 2 independent experiments.

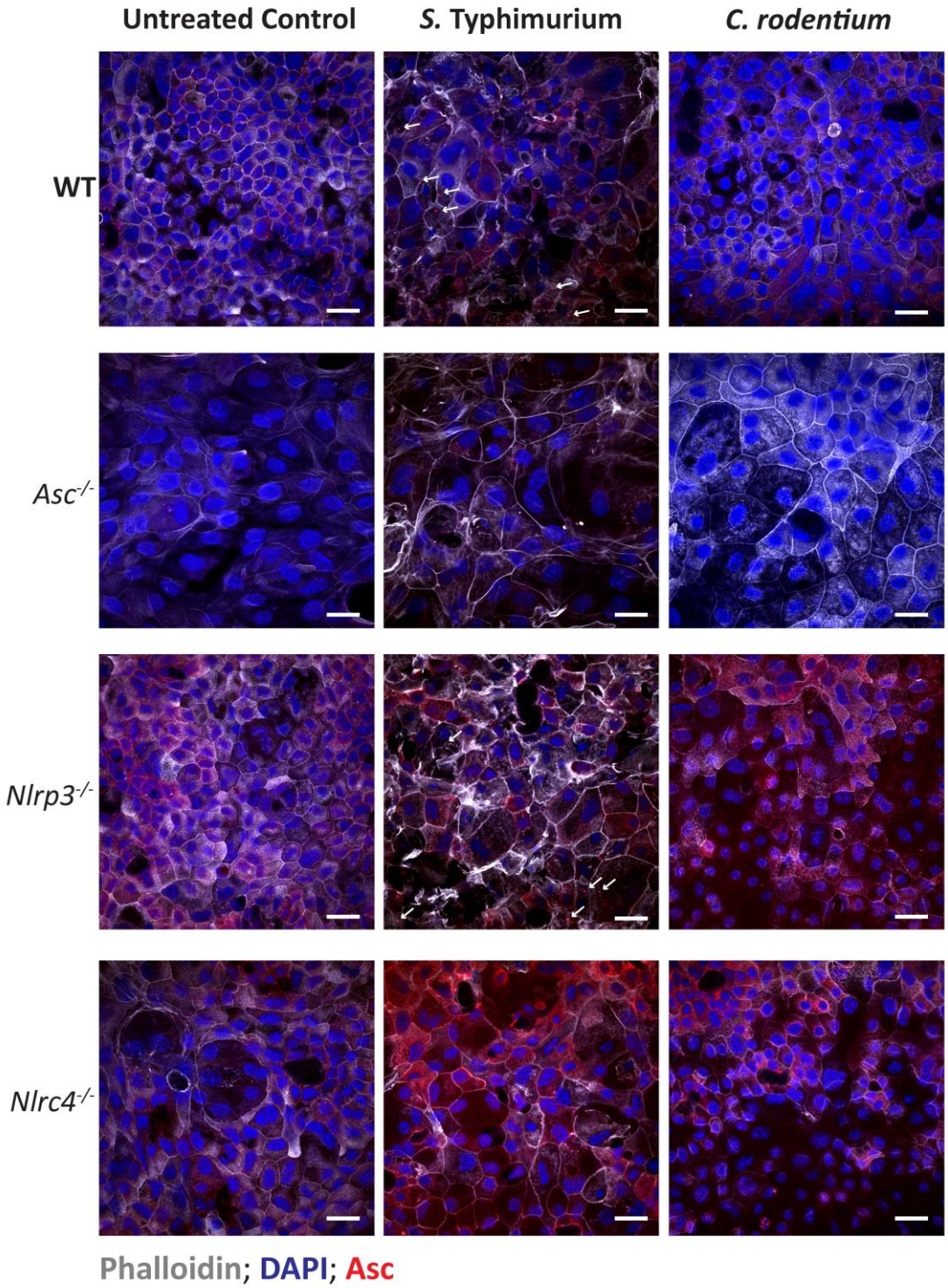


Figure 4.9. Asc speck formation in *S.* Typhimurium treated IEC monolayers. WT, *Nlrp3*$^{-/-}$, *Nlrc4*$^{-/-}$ and *Asc*$^{-/-}$ cecal IEC monolayers were stimulated with *S.* Typhimurium or *C. rodentium* at MOI 1 for 5h. Following infection, monolayers were stained for Asc (red), Phalloidin (grey) and DAPI (blue). Bar= 10µm. Images were acquired under X60 magnification. Asc specks are indicated by white arrows. For higher magnification see Figure 4.10. Results are representative of 2 independent experiments.

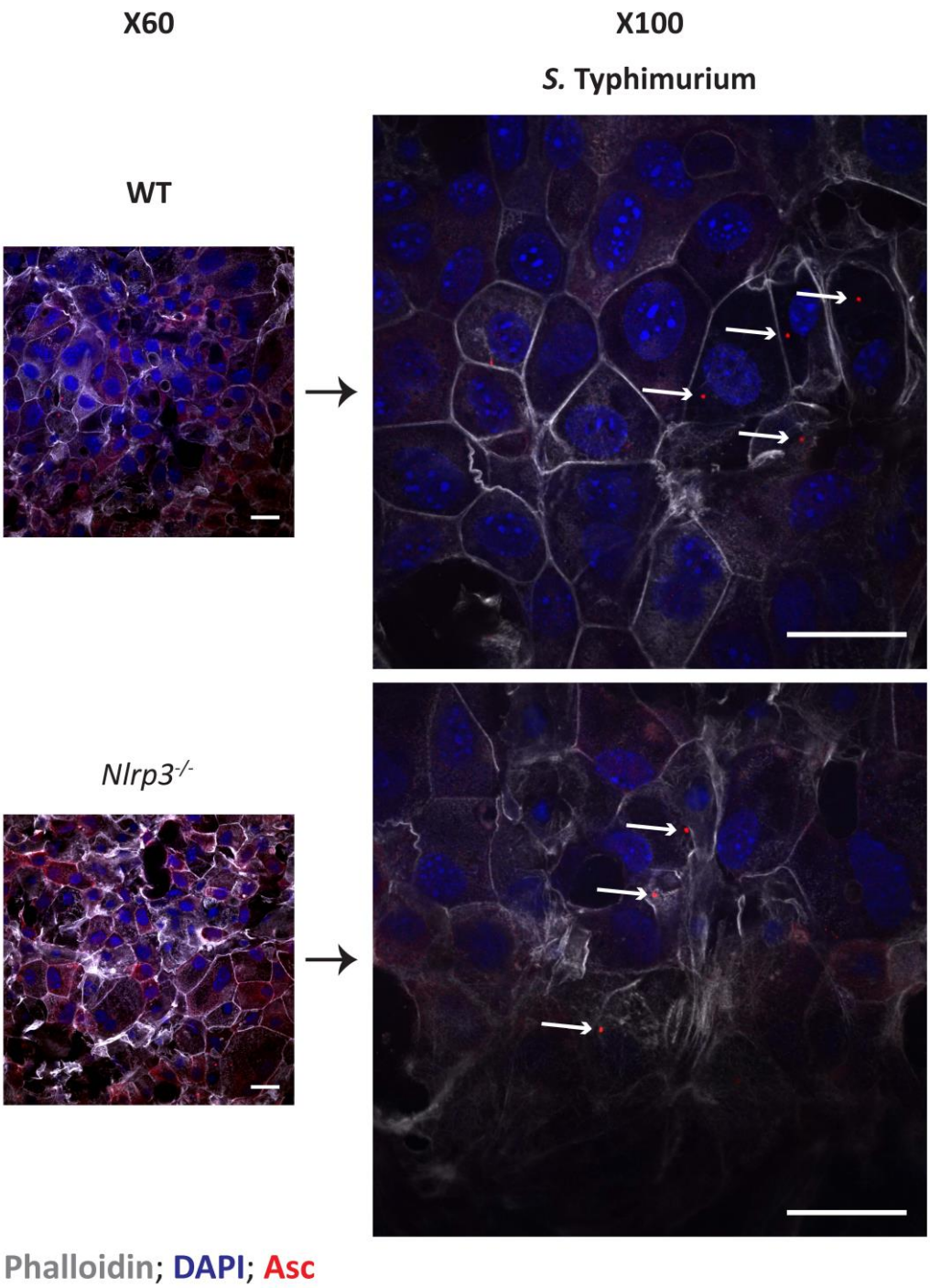


Figure 4.10. Asc speck formation in *S*. Typhimurium treated IEC monolayers. Cecal IEC monolayers were infected with *S*. Typhimurium as described in Figure 4.9. Following infection, monolayers were stained for Asc (red), Phalloidin (grey) and DAPI (blue). Bar= 10µm. Images were acquired under x60 and X100 magnification.

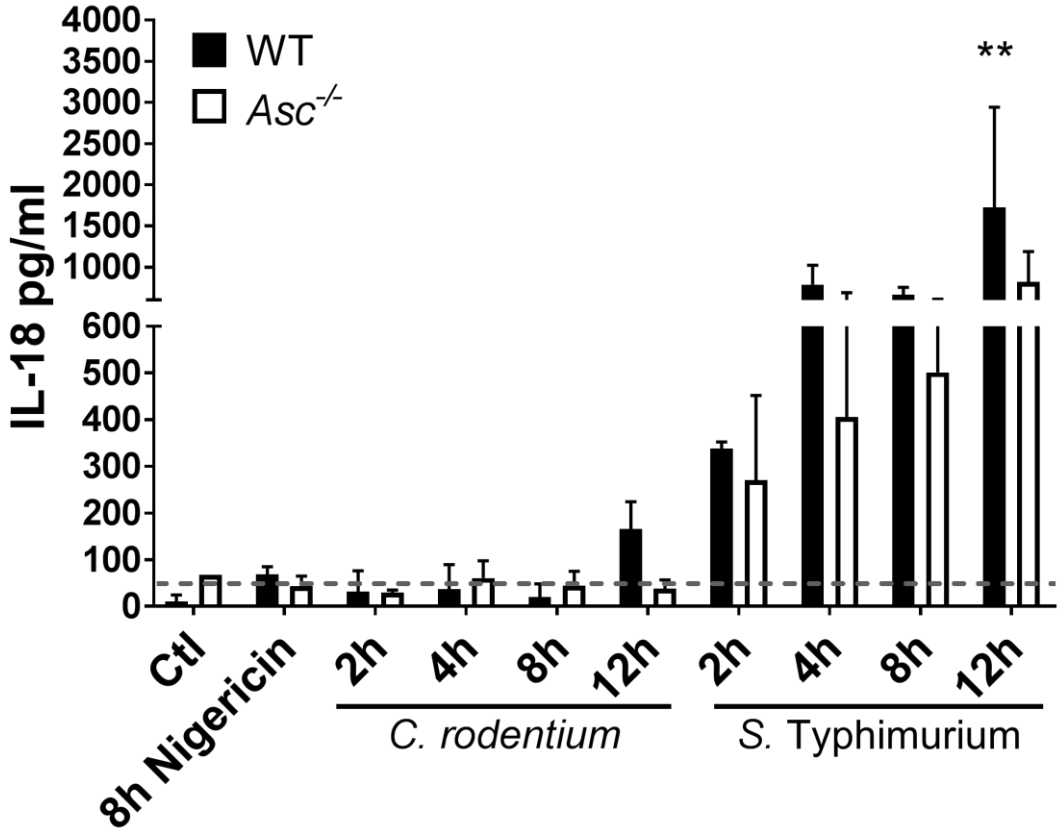


Figure 4.11. Kinetics of IL-18 release from IEC monolayers infected with *S.* Typhimurium or *C. rodentium*. WT, and *Asc*$^{-/-}$ cecal IEC monolayers were stimulated with *S.* typhimurium or *C. rodentium* at MOI 1 for the indicated time points. An 8h treatment with nigericin at 20 µM was included. After stimulation, supernatants were collected for analysis of IL-18 secretion by ELISA. Dotted line denotes the limit of detection of the assay. ELISA performed in technical duplicates and stimulations were performed in biological duplicates (2-wells). Error bars represent standard deviation from the sample mean. A two-way ANOVA was used for statistical analysis; *p<0.05; **p<0.001; ***p<0.0001; ****p<0.00001. Data are from one experiment.

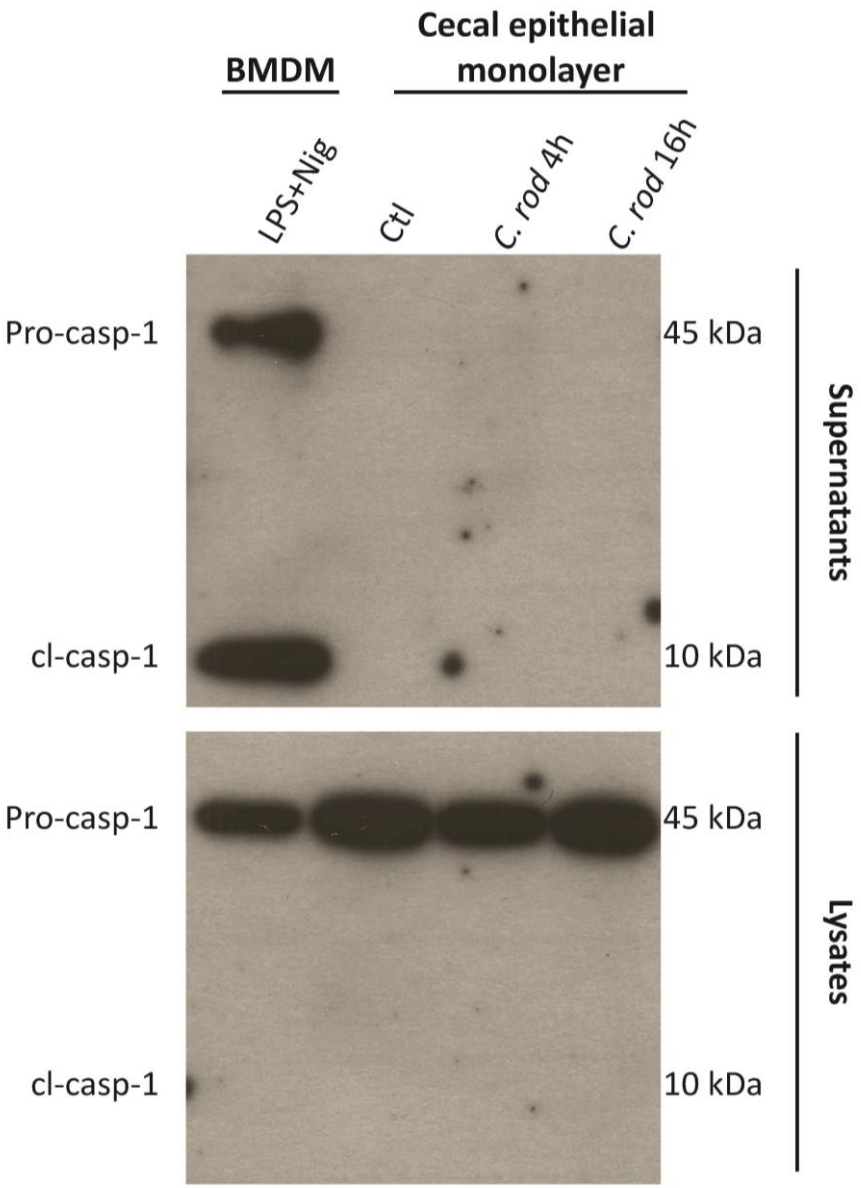


Figure 4.12. *C. rodentium* is unable to drive inflammasome activation in IEC monolayers. Western blot for the active and pro-forms of caspase-1 in cell supernatants and lysates from IL-22 (50 ng/ml for 24h) primed cecal IEC monolayers stimulated with *C. rodentium* at MOI 100 for the indicated time points. LPS (100 ng/ml for 12h) primed BMDM subsequently stimulated with nigericin (5 µM) for 1h were used as control for active caspase-1 detection by western blot. Stimulations were performed in pooled biological duplicates. Data are representative of 5 independent experiments.

4.2.4.3. IEC death upon challenge with enteric pathogens

Another classical hallmark of inflammasome activation is pyroptosis, a lytic form of cell death that can be quantified by measuring the levels of LDH, a stable cytosolic enzyme, released into the supernatant upon cell lysis.

To assess pyroptosis, WT cecal IEC monolayers were stimulated with *C. rodentium* or *S.* Tm, supernatants were then collected and LDH release measured. We observed an increase in cell lysis of IEC upon infection with *C. rodentium*, denoted by a 15-20% increase in LDH release compared to untreated cells at 3h p.i. (Figure 4.13 A). At 19h p.i., LDH release was around 60-70% in *C. rodentium*-infected IEC, but high levels of cell lysis were also observed in untreated IEC (Figure 4.13 A). Monolayers infected with *S.*Tm displayed 15-30% increase in cell lysis at 3h p.i. compared to untreated controls and by 19h p.i. 90-100% of *S.* Tm-infected IEC had undergone cell lysis (Figure 4.13 A).

We next compared cell death between WT, *Nlrp3*$^{-/-}$, *Nlrc4*$^{-/-}$ and *Asc*$^{-/-}$ IEC monolayers following *C. rodentium* or *S.*Tm challenge. In order to compare treatment-induced cell death between monolayers of different genotypes, LDH release in stimulated cells was normalised to the untreated control of the same genotype, denoted as fold LDH release. IEC monolayers were treated with *S.*Tm and *C. rodentium* at MOI 1 for 5h, after which LDH release into the supernatant was measured. We observed that *S.* Tm-infected WT, *Nlrp3*$^{-/-}$ or *Asc*$^{-/-}$ IEC monolayers displayed markedly increased LDH release compared to their respective untreated controls (Figure 4.13 B). However, *Nlrc4*$^{-/-}$ IEC monolayers seemed to be resistant to S.Tm-induced cell death (Figure 4.13 B). Treatment with the pan-caspase inhibitor ZVAD-FMK reduced LDH release by IEC of all genotypes (Figure 4.13 B). In contrast to *S.* Tm infection, *C. rodentium*-infected IEC monolayers did not exhibit any increase in LDH release (Figure 4.13 B).

LDH assays were somewhat variable and measurements were strongly dependent on the culture media, which made it difficult to interpret the results with confidence (data not shown). Therefore, we further assessed cell death with the ApoTox-Glo Triplex assay, which can simultaneously detect both cellular viability and cytotoxicity. Furthermore, this assay relies on fluoresce measurements instead of absorbance, which can help reduce the background and improve sensitivity.

Viability and cytotoxicity within IEC monolayers were recorded at 2h, 4h, 8h and 12h p.i. with *C. rodentium* or *S*.Tm at MOI 1 (Figure 4.14). We observed that cell viability remained unchanged upon *C. rodentium* challenge of IEC monolayers (Figure 4.14 A). However, a significant reduction in cell viability was observed in *S.* Tm-infected IEC, with cell viability decreasing as the infection progressed (Figure 4.14 A). Nevertheless, we observed comparable decreases in cell viability in WT and *Asc*$^{-/-}$ IEC monolayers challenged with *S*. Tm (Figure 4.14 A). As expected, cytotoxicity was inversely associated with the observed trends in cell viability. We observed that *C. rodentium* did not induce significant cytotoxicity in IEC monolayers assayed 2h, 4h and 8h p.i., but increased cytotoxicity was observed at 12h p.i. (Figure 4.14 B). When IEC monolayers were challenged with *S*. Tm, significantly increased cytotoxicity was detected at all time points during the infection (Figure 4.14 B). Consistent with our results in the LDH assays, *S*. Tm infection induced comparable cell cytotoxicity in WT and *Asc*$^{-/-}$ IEC monolayers (Figure 4.14 B).

Overall, *S.*Tm seems to induce a more robust cytotoxic response compared to *C. rodentium*. Furthermore, we found no evidence of increased susceptibility to cytotoxicity in *Asc*$^{-/-}$ IEC monolayers compared to WT monolayers.

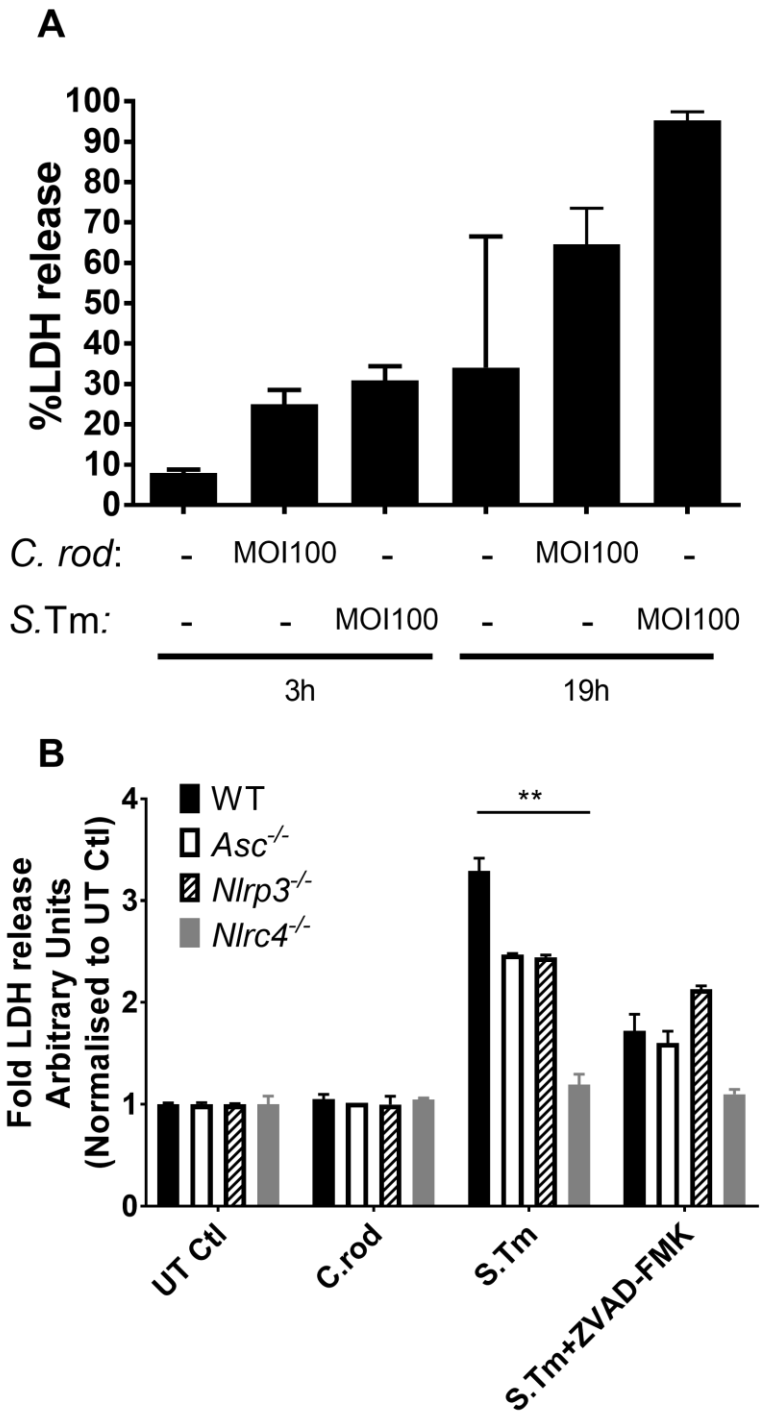


Figure 4.13. LDH release upon *C. rodentium* or *S.* Typhimurium infection of cecal IEC monolayers. (A) Percentage LDH release into the supernatants of cecal IEC monolayers treated with *C. rodentium* or *S. Typhimurium* at MOI 100 for the indicated time points. Percentage release was calculated using a maximum release control (completely lysed IEC monolayers). (B) Fold LDH release into the supernatants of cecal IEC monolayers treated with *C. rodentium* or *S.* Typhimurium at MOI 1 for 5h. Fold release represents the comparison of each sample to the untreated control (UT Ctl) of the same genotype. Stimulations were performed in biological duplicates (2-wells) and LDH measurements were performed in technical duplicates. Error bars represent standard deviation from the sample mean. An unpaired t-test was used for statistical analysis; *p<0.05; **p<0.001; ***p<0.0001; ****p<0.00001.

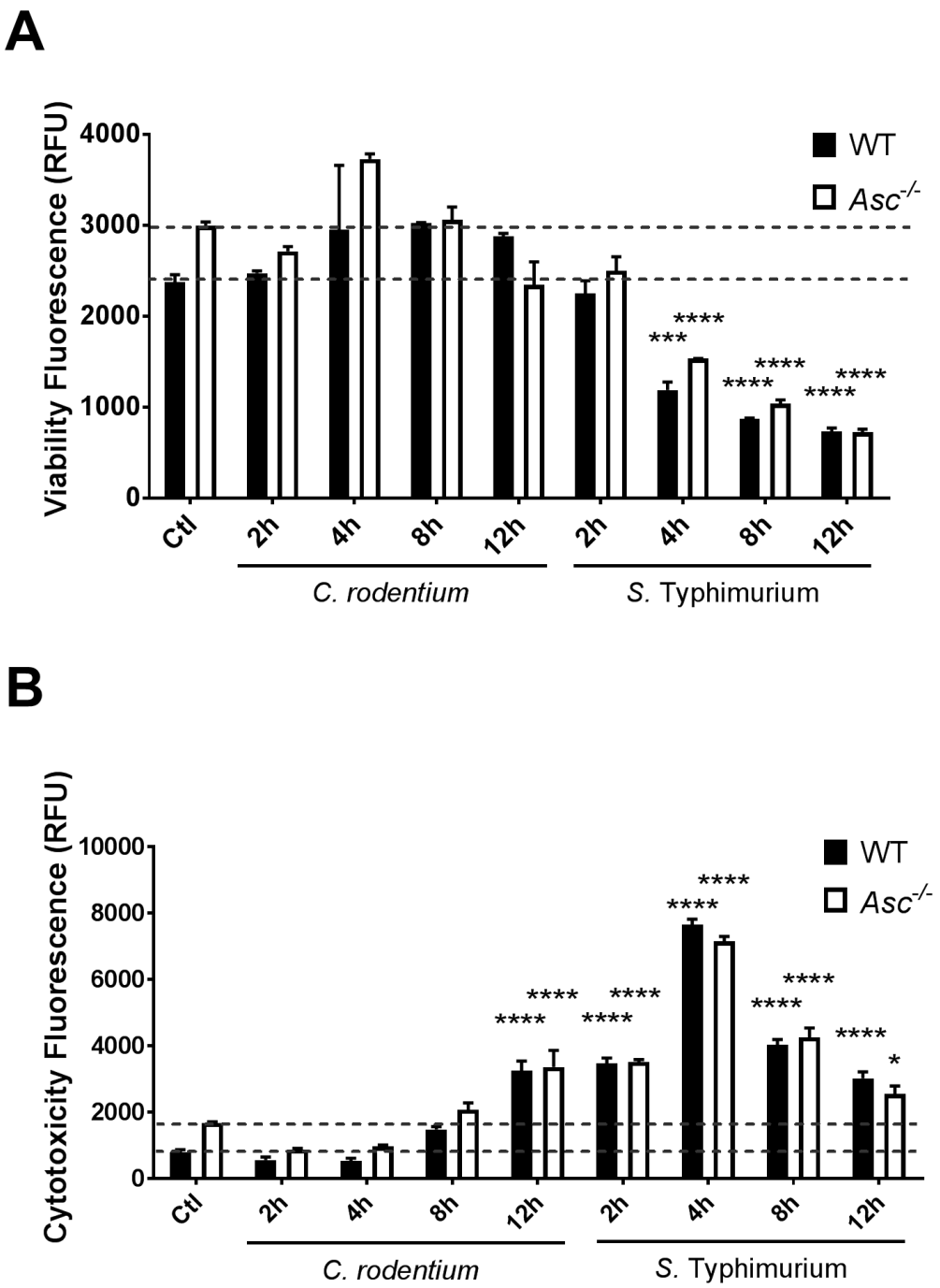


Figure 4.14. Cell viability and cytotoxicity upon *C. rodentium* or *S.* Typhimurium infection of cecal IEC monolayers. (A and B) WT or *Asc*$^{-/-}$ IEC monolayers were infected with *C. rodentium* or *S. Typhimurium* at MOI 1 for the indicated time points. (A) Cell viability measured via the ApoTox-Glo Triplex, represented as relative fluorescence units (RFU). (B) Cell cytotoxicity measured via the ApoTox-Glo Triplex, represented as relative fluorescence units (RFU). Dotted lines mark the background viability or cytotoxicity level of the untreated controls (Ctl). Measurements were performed in technical duplicates of biological/well duplicates. Error bars represent standard deviation from the sample mean. A two-way ANOVA was used for statistical analysis; all treated samples were compared to the untreated control (Ctl); *$p<0.05$; **$p<0.001$; ***$p<0.0001$; ****$p<0.00001$.

4.2.4.4. Circumventing the absence of virulence in LB-grown C. rodentium

Like *E. coli*, *C. rodentium* relies on the expression of virulence factors encoded in the LEE pathogenicity island for successful infection of the host (448).

It is not completely clear how *C. rodentium* regulates the expression of virulence genes *in vivo* (468, 540). However, it is clear that this pathogen becomes hyper-virulent after passage through the mouse intestine (468, 540) and that hyper-virulent *C. rodentium* exhibits higher levels of expression of LEE pathogenicity island genes and T3SS effector genes compared with *in vitro* LB-grown bacteria (467).

We hypothesised that the *in vitro* LB-grown *C. rodentium* we used to challenge IEC monolayers may have down-regulated expression of virulence factors, which could explain the lack of inflammasome activation. To circumvent this, we attempted to optimise LEE and T3SS expression in the bacterium by infecting IEC monolayers with host-adapted *C. rodentium*. We collected feces from *C. rodentium*-infected or uninfected control mice, at the peak of infection (day 7-10 p.i.), and prepared fecal bacteria (467). IEC monolayers were infected with 0.1 mg/ml of homogenised feces in media supplemented with naladixic acid (50 µg/ml) to select for *C. rodentium*. IL-18 ELISA of IEC monolayer supernatants were employed to measure inflammasome activation and *S.* Tm infection was used as a positive control. As expected, no IL-18 release was observed from IEC monolayers treated with feces from uninfected mice (negative controls) (Figure 4.15). Conversely, *S.* Tm infection led to IL-18 release from both WT and *Asc*$^{-/-}$ IEC monolayers, with significantly decreased IL-18 levels detected in *Asc*$^{-/-}$ monolayers (Figure 4.15). However, we observed no IL-18 release from IEC monolayers upon challenge with fecal *C. rodentium* (Figure 4.15).

The lack of inflammasome activation observed with fecal *C. rodentium* stimulation of IEC monolayers prompted us to investigate ways in which we could drive the expression of virulence genes in *C. rodentium in vitro*. Constructs were generated aimed at driving exogenous *ler* expression, the central positive regulator controlling LEE genes (573), or *glrA* expression, a positive *ler* regulator (574). In total, four constructs were made: two contained either *ler* or *glrA* in their native form and the other two contained either *ler* or *glrA* sequences preceded by a ribosome binding site (RBS) sequence to potentially improve their translation. These constructs were used to transform *C. rodentium* and the

expression of *ler* and *tir* (a LEE encoded virulence factor required for attachment and colonisation (575)) was tested by qPCR.

We compared *ler* and *tir* expression in our transformants to that of LB grown *C. rodentium* and to fecal samples from *C. rodentium*-infected mice. We also assayed *ler* and *tir* expression in *C. rodentium* grown under different *in vitro* conditions that have been reported to affect virulence (574). These included growths in either low or high glucose, in DMEM media, and in either microaerophilic or normal aerobic conditions. We used an overnight LB-grown culture of *C. rodentium* as negative control, since these conditions are known to downregulate *C. rodentium* virulence (451, 573, 574). cDNA was isolated from fresh fecal pellets or from liquid bacterial cultures with an OD_{600} ~0.7 (mid-log growth phase). For our *ler* or *glrA* transformed *C. rodentium* strains, overnight cultures were grown for 1h (or to an OD_{600} 0.2) and then arabinose was added to drive exogenous *ler* and *glrA* expression, and cultures were then allowed to grow for another 1h until an OD_{600} 0.7-1 was reached. Notably, *C. rodentium* strains overexpressing *ler* or *glrA*, grew at a slower rate than WT *C. rodentium*, attesting to the costly expression of T3SS (data not shown).

As expected, we did not detect *ler* or *tir* expression in fecal samples from uninfected mice (Figure 4.16). However, samples from *C. rodentium* infected mice exhibited ~100-fold increase in *ler* expression and ~25-fold increase in *tir* expression compared to overnight LB *C. rodentium* cultures (Figure 4.16). Mid-log phase *C. rodentium* grown in LB exhibited ~10-fold and ~5-fold increased expression of *ler* and *tir*, respectively, compared to overnight LB-grown *C. rodentium* (Figure 4.16). Growth of *C. rodentium* in DMEM increased *ler* expression 30-50-fold compared to overnight LB culture, regardless of glucose concentration (Figure 4.16 A). However, culture in DMEM did not increase expression of *tir* to the same extent, raising it by only ~5-10-fold (Figure 4.16 B).

Interestingly, *C. rodentium* expressing the *ler* and *glrA* constructs exhibited *ler* and *tir* expression levels that were similar or greater than fecal *C. rodentium*, with the *ler* native construct having the highest *ler* and *tir* expression (Figure 4.16). As expected the empty plasmid, referred to as vector only, had a *ler* and *tir* expression similar to overnight LB *C. rodentium* cultures (Figure 4.16). In general, non-arabinose induced transformants displayed markedly reduced *ler* and *tir* expression compared to arabinose treated cultures

(Figure 4.16). However, even in the absence of arabinose, *C. rodentium* containing the *ler* native construct had high *ler* and *tir* expression levels (Figure 4.16).

In conclusion, we observed that LB-grown *C. rodentium* displays reduced *ler* and *tir* expression compared to host-adapted fecal *C. rodentium*. We also demonstrated that expression of *ler* and *tir* could be greatly enhanced by transforming the bacteria with plasmids that overexpress *ler* and *glrA*.

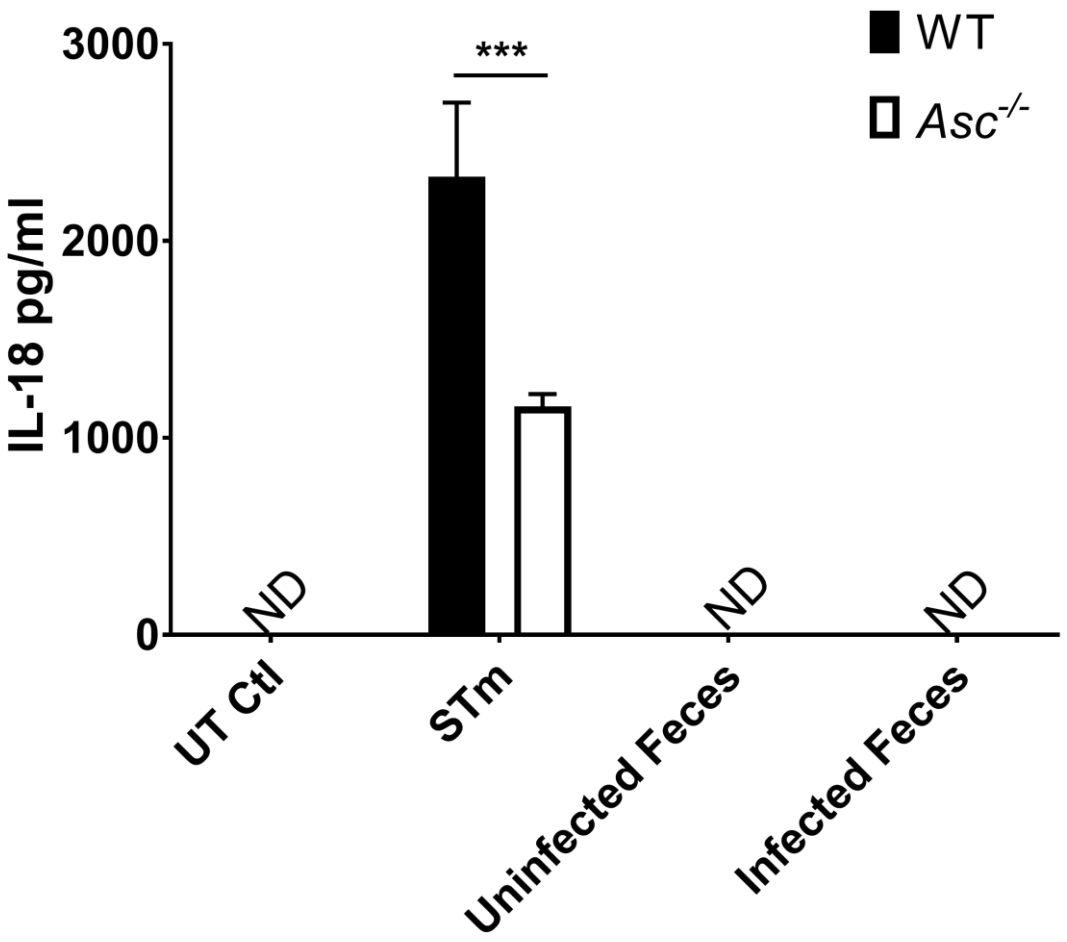


Figure 4.15. Lack of IL-18 release by IEC challenged with fecal host-adapted *C. rodentium*. WT, and *Asc*$^{-/-}$ cecal IEC monolayers were stimulated with *S.* Typhimurium at MOI 100 for 5h or with fecal pellets isolated from *C. rodentium* infected mice for 12h. Cell supernatants were then collected for analysis of IL-18 secretion by ELISA. Stimulations were performed in duplicate wells. ELISA performed in technical duplicates. Error bars represent standard deviation from the sample mean. An unpaired t-test was used for statistical analysis; *p<0.05; **p<0.001; ***p<0.0001; ****p<0.00001, ND (not detectable). Data are representative of 2 independent experiments.

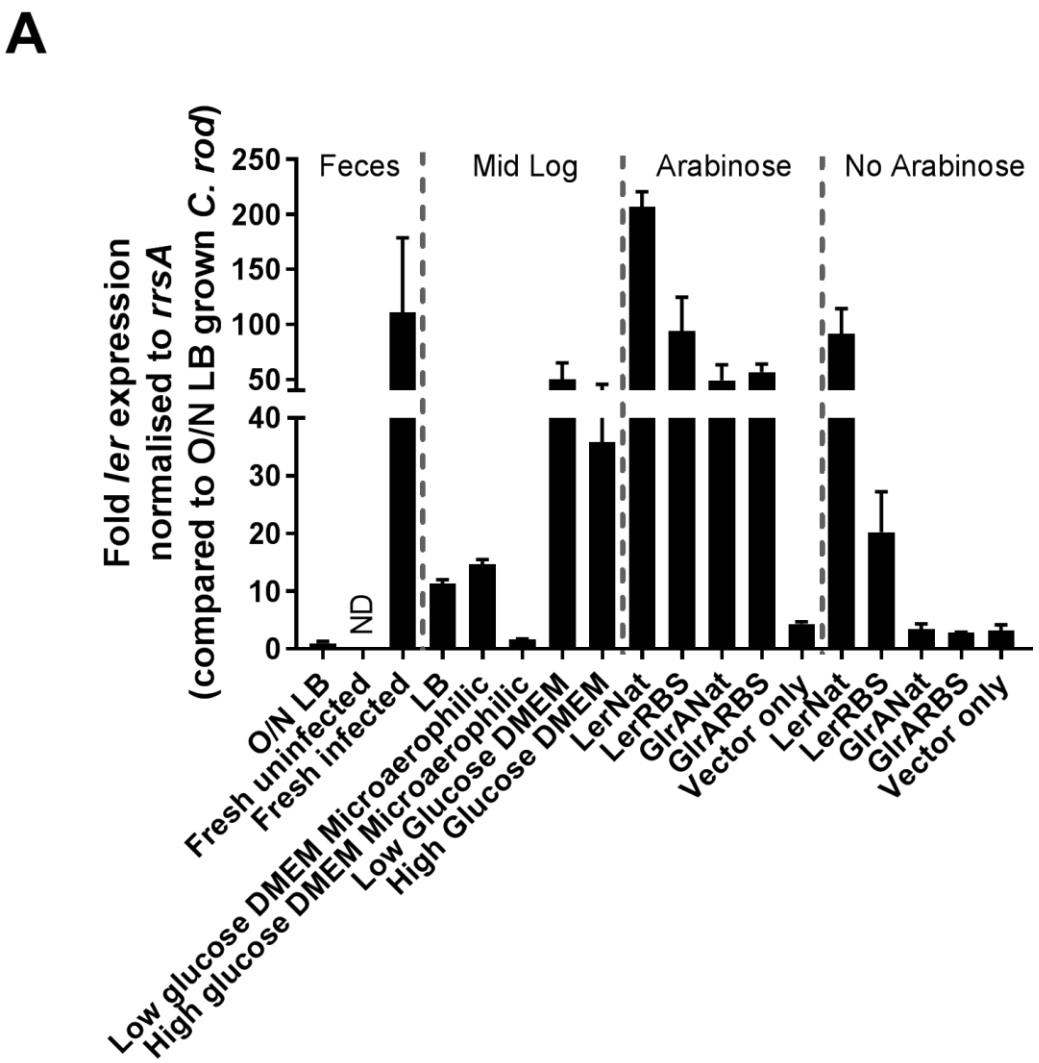


Figure 4.16. Modulation of virulence genes expression in *C. rodentium*. cDNA was isolated from homogenised faeces from mice infected with *C. rodentium* and from *C. rodentium* grown to mid-log growth phase following different culture conditions: LB media, high or low glucose DMEM and at either microaerophilic or normal aerobic conditions. In addition, cDNA was isolated from mid-log LB-grown (with or without arabinose). *C. rodentium* transformants expressing either *ler* or *glrA* in their native form (LerNat and GlrANat) or preceded by a ribosome binding site; RBS (LerRBS and GlrARBS). *C. rodentium* transfected with empty pBAD vector and also grown in LB to mid-log phase were used as negative controls. (A) Fold *ler* expression and (B) fold *tir* expression were measured by qPCR and normalised to the house-keeping gene *rrsA*. Fold expression represents the comparison of each sample to overnight stationary-phase grown *C. rodentium* (O/N LB). qPCR experiments were performed in technical duplicates of biological triplicates. Error bars represent standard deviation from the sample mean. Data is of one experiment. ND (not detectable). Figure continues next page.

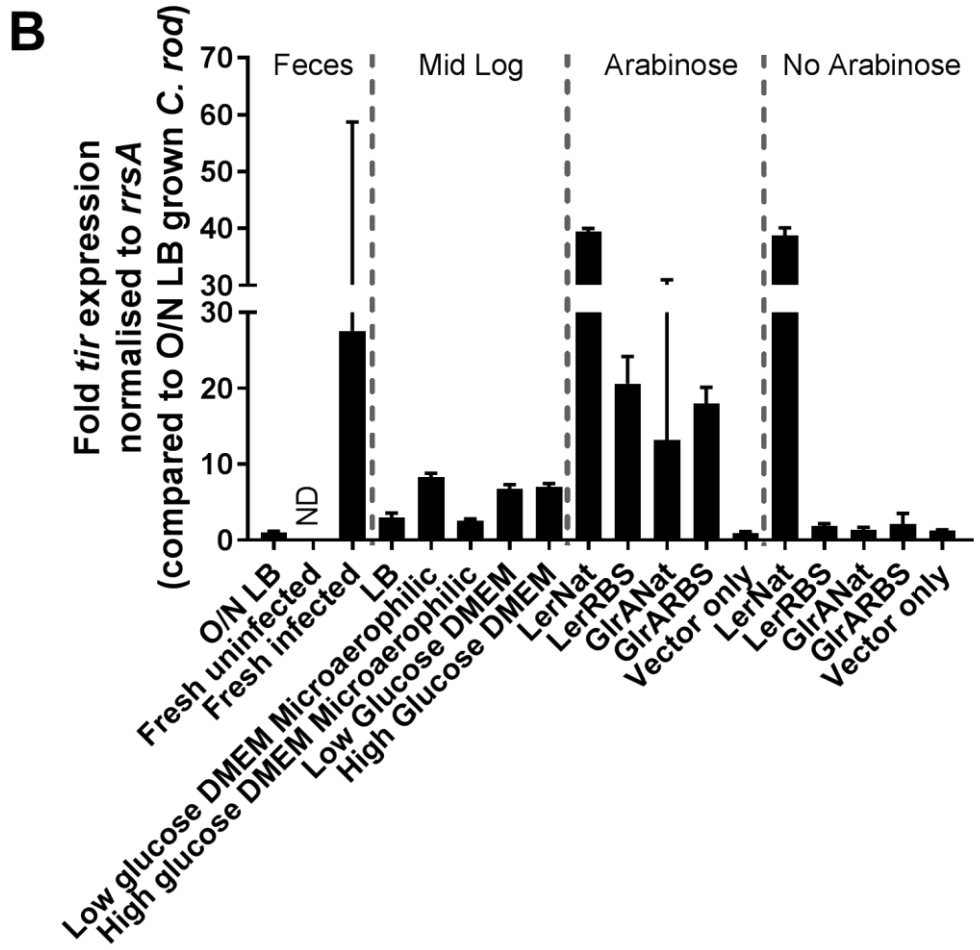


Figure 4.16. Continuation. Modulation of virulence genes expression in *C. rodentium*.

4.2.4.5. Increased attachment of C. rodentium to Asc-deficient IEC

As we were unable to detect inflammasome activation in IEC upon *C. rodentium* challenge, we assessed the ability of *C. rodentium* to interact with primary IEC monolayers *in vitro*. Thus, IEC monolayers were grown on coverslips in 24-well plates and challenged with LB grown *C. rodentium*. As *C. rodentium* may downregulate expression the LEE pathogenicity island when it is grown in LB (467), we also used host-adapted *C. rodentium* isolated from feces of infected mice as a positive control for LEE expressing *C. rodentium* (467). After bacterial challenge, coverslips were washed and subjected to immunofluorescence staining to assess the level of attachment/interaction between *C. rodentium* and IEC.

We observed that host-adapted *C. rodentium* could successfully interact with WT IEC monolayers 5h p.i., as evidenced by discrete foci of bacteria on the IEC surface (Figure 4.17). However, when monolayers were infected with LB-grown *C. rodentium* for 5h, no attached *C. rodentium* were observed (data not shown). Nevertheless, when IEC monolayers were exposed to LB-grown *C. rodentium* for longer time points (12-24h), we observed *C. rodentium* foci on the IEC monolayers (Figure 4.17). Moreover, we observed that both host-adapted and LB-grown *C. rodentium* seemed to colonize the *Asc*$^{-/-}$ IEC monolayers to a greater extent than the WT IEC monolayers, as shown by the increased number of bacterial foci on the *Asc*$^{-/-}$ IEC monolayers (Figure 4.17).

To quantify the *C. rodentium* burden, IEC monolayers were infected as above with either LB-grown *C. rodentium* for 12h, or with host-adapted fecal *C. rodentium* for 5h, followed by thorough washing to remove non-adherent bacteria and treatment with 0.1% Triton X to recover adherent bacteria. The supernatants resulting from the Triton treatment were then serially diluted and subsequently plated on nalidixic acid agar plates before counting CFU the following day. As a negative control, IEC monolayers were infected with a *tir*-deficient *C. rodentium* (*Δtir*) mutant that is unable to attach to IEC and form pedestals (450).

We found comparable CFU burdens in WT and *Asc*$^{-/-}$ IEC monolayers, either with LB grown or fecal *C. rodentium* (Figure 4.18). Moreover, IEC monolayers challenged with the *C. rodentium Δtir* non-attaching strain yielded similar CFU counts as IEC monolayers infected with WT *C. rodentium* (Figure 4.18). This suggests that there is passive

attachment of *C. rodentium* to IEC monolayers independent of *tir* and/or that the washing step was not sufficiently stringent to remove all bacteria present in the supernatants.

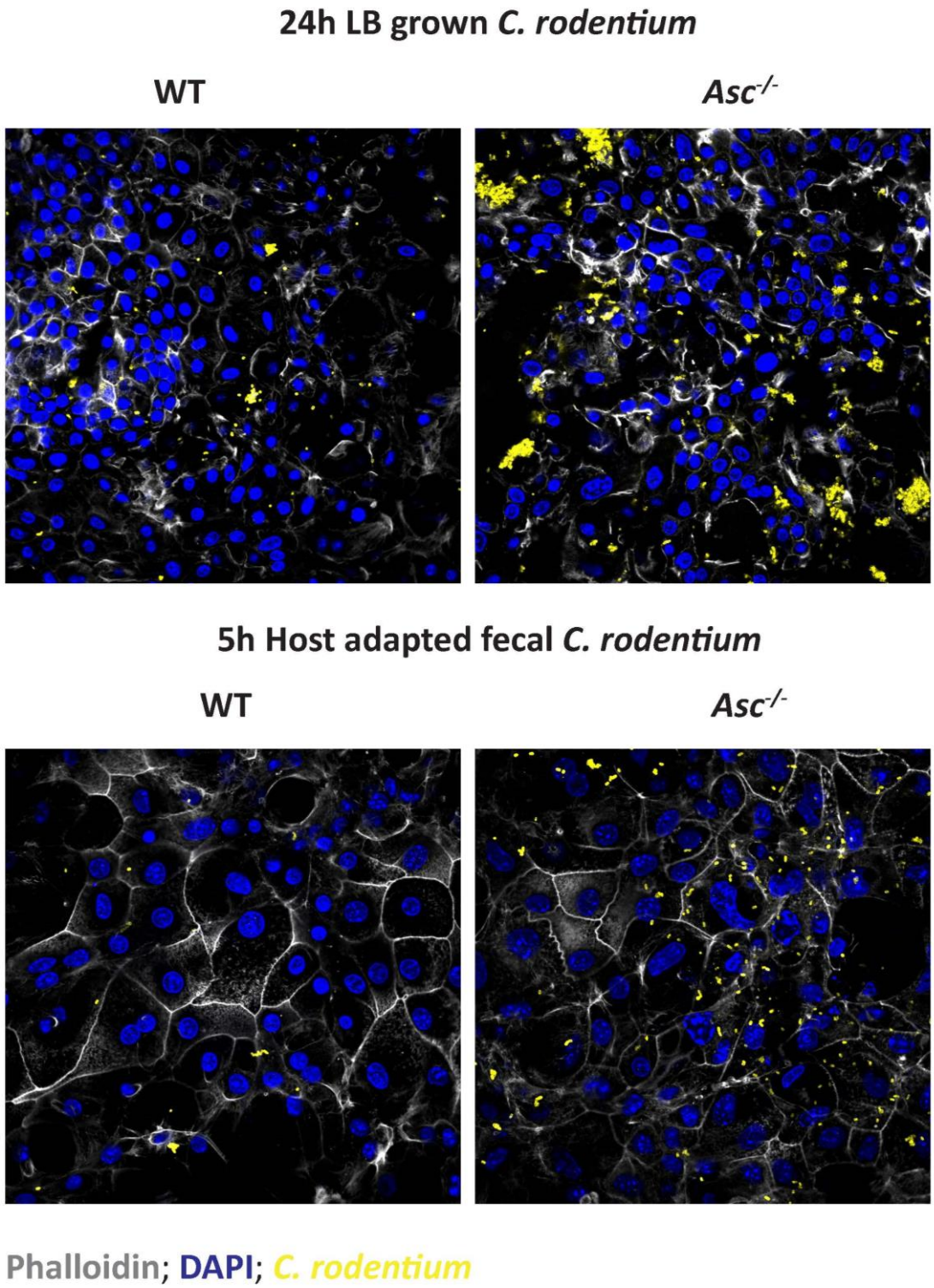


Figure 4.17. Increased attachment of *Citrobacter rodentium* to Asc-deficient IEC monolayers. WT and *Asc*$^{-/-}$ cecal IEC monolayers were challenged with LB-adapted *C. rodentium* at MOI 1 for 24h (upper panel) or for 5h with host-adapted *C. rodentium* from fecal pellets (lower panel). Following infection, monolayers were fixed with paraformaldehyde and stained for *C. rodentium* (yellow), Phalloidin (grey) and DAPI (blue). Images were acquired under x60 magnification. Data are representative of 4 independent experiments.

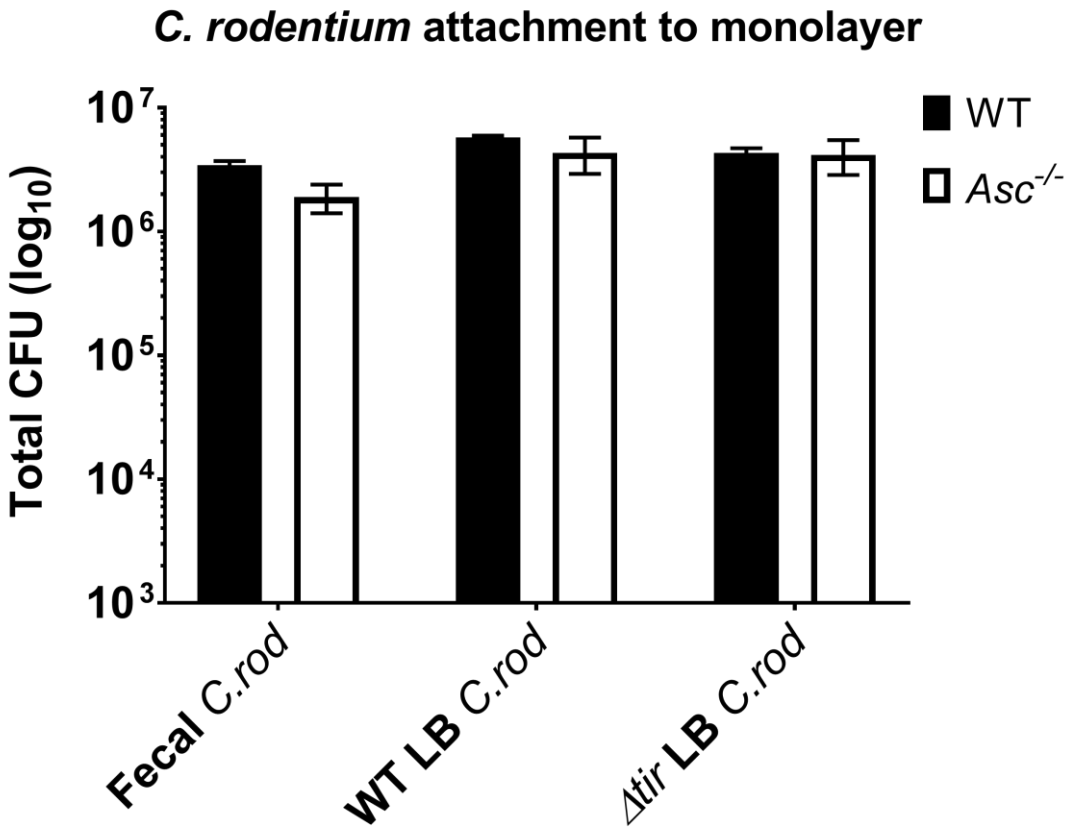


Figure 4.18. Quantification of *C. rodentium* attachment to IEC monolayers. WT and *Asc*$^{-/-}$ cecal IEC monolayers were infected with LB grown *C. rodentium* at MOI 1 for 12h, or with host-adapted *C. rodentium* from fecal pellets of infected mice for 5h. Following infection, monolayers were washed to remove non-adherent bacteria and subsequently treated with Triton X to recover adherent bacteria. Data expressed as Log_{10} CFU per well. Experiments were performed with at least 3 replicate wells. Error bars represent standard deviation from the sample mean. Data are representative of 4 independent experiments.

4.2.4.6. Antimicrobial activity and signalling of Asc vs WT

Inflammasome signalling in the intestinal epithelium has been linked to antimicrobial responses (241, 251). IEC inflammasomes are in close association with the microbiota and the microbial metabolite taurine was shown to induce Nlrp6 inflammasome activation and subsequent IL-18 release. Conversely, histamine and spermine treatment downregulated Nlrp6 inflammasome activation (241). Nlrp6 inflammasomes were reported to be important for the control of the AMP *Ang4* and *Retnlb* at the transcriptional level (241). In support of this observation, *Ang4* and *Retnla* AMP were also found to be greatly down-regulated in cecal tissues from Asc-deficient mice at day 3 post *C. rodentium* infection (249). These observations prompted us to investigate the antimicrobial activity of IEC monolayers against *C. rodentium*.

To assess inflammasome-dependent antimicrobial responses in IEC, we collected supernatants of WT or *Asc*$^{-/-}$ IEC monolayers and incubated them with *C. rodentium*. Monolayers were cultured in the presence or absence of IL-22, a known driver of IEC AMP responses (121). However, we observed no effect on *C. rodentium* growth by either WT or *Asc*$^{-/-}$ IEC supernatants, regardless of IL-22 treatment, compared to the negative control (Figure 4.19 A and B). Thus, under these conditions, we could not detect any antimicrobial activity in primary IEC supernatants.

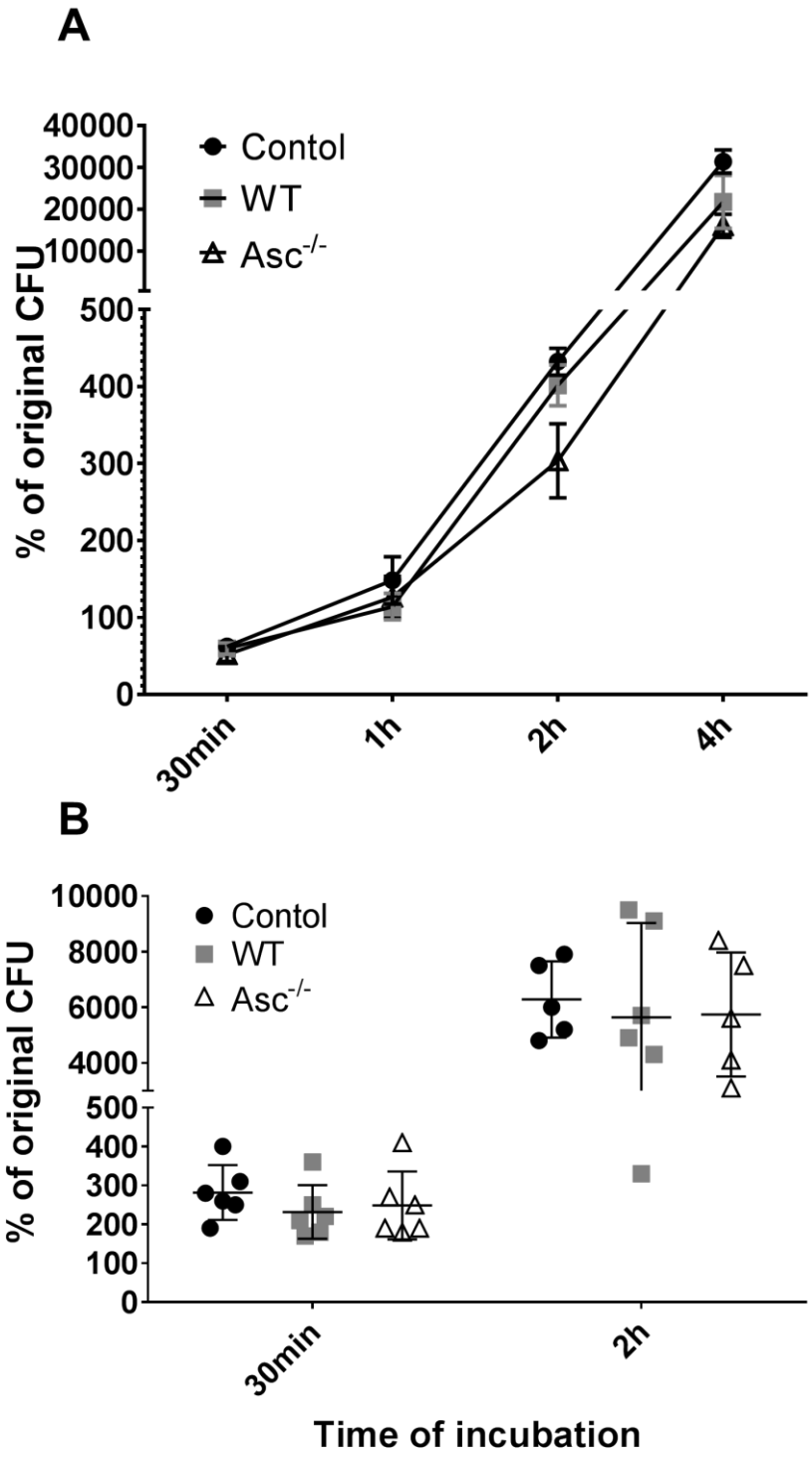


Figure 4.19. Culture supernatants from primary cecal IEC monolayers do not exhibit antibacterial activity against *C. rodentium*. Supernatants were collected from WT or *Asc*$^{-/-}$ IEC monolayers cultured for 24h in the absence (A) or presence of IL-22 (B). Acellular supernatants were used as a negative control. Supernatants were then pooled according to genotype and incubated with *C. rodentium* (10^4 CFU) for the indicated time points. Bacteria from each well were serially diluted and plated for subsequent CFU counting. Recovered CFU at indicated time points are represented as percentage of original CFU (10^4 *C. rodentium* per well). Assay was performed in 4 replicates per condition. Data are representative of 2 independent experiments.

4.3.Discussion

Until recently, *in vitro* studies of IEC biology have largely relied on the use of immortalised cancerous cell lines. However, intestinal epithelial organoids provide an *ex vivo* system for studying functional outputs of primary IEC in a way that is closer to the *in vivo* intestinal epithelial niche (565). We have employed 3D IEC organoids and IEC monolayers to investigate IEC responses to different inflammasome activating and modulatory signals.

We attempted to establish an *in vitro* assay for inflammasome activation in 3D organoids utilising the activation of caspase-1 as a read-out. The conventional protocol used to activate the Nlrp3 inflammasome in myeloid cells only led to detectable active caspase-1 in BMDM. However, this classic Nlrp3 inflammasome stimulation failed to activate caspase-1 in IEC organoids. The failure to activate the Nlrp3 inflammasome in primary IEC prompted us to characterise IEC expression of inflammasome components. In stark contrast to BMDM, we were unable to detect *Nlrp3* expression in primary IEC organoids. Conversely, and in agreement with previous reports, we detected high basal expression of *Nlrc4* and *Il-18* in primary IEC organoids, which was markedly higher than the levels found in resting BMDM (231, 255). These results suggest that IEC and macrophages may utilise different NLR for pathogen sensing and that they have differential capacities for IL-18 secretion.

In the current literature, there is no direct evidence of Nlrp3 expression in IEC (552, 564). Thus, the radio-resistant 'non-hematopoietic' intestinal cell that is responsible for Nlrp3-mediated protection against *C. rodentium* remains to be identified (249). We examined the possibility of stromal cells being the non-hematopoietic cell type expressing *Nlrp3.* Indeed, we could detect *Nlrp3* and *Asc* expression in stroma cells primed with LPS, although at lower levels than LPS primed BMDM. These observations argue for the possibility of functional *Nlrp3* inflammasome in stromal cells, but functional assays are needed to examine this possibility. We further observed that *pro-Il-18* expression levels in stroma and BMDM were strikingly lower than that found in IEC. This supports the idea of IL-18 responses being of key importance in IEC (255). Of note, it is possible that there may be some long-lived tissue macrophages that are radio-resistant. But the gut appears different from most other tissues, as most macrophages appear to be derived from

circulating blood monocytes, rather than self-replenishing tissue-resident macrophages (81-83).

The expression of inflammasome components including IL-18, IL-1β, Nlrp3 and Nlrc4 is controlled by a priming signal in myeloid cells (281). LPS is the best described inflammasome priming signal. However, we observed that in IEC organoids LPS stimulation did not up-regulate the expression of inflammasome components. Since IEC can express the LPS receptor TLR4, the lack of priming of these components in IEC is curious, though not surprising if we consider that the gut epithelium is constantly exposed to high concentrations of LPS derived from the microflora. Indeed, several tolerisation mechanisms towards LPS or other PAMP have been described in different cell types. For instance, IRAK1, an essential mediator of TLR signalling gets degraded upon primary LPS challenge of leukocytes (576). In IEC, reports show that TLR4 and its co-receptor MD-2 have low levels of expression thus rendering IEC poorly responsive to LPS (181, 189, 470, 577).

It remains possible that we have not applied the right priming signal to induce *Nlrp3* expression in primary IEC and the lack of activation observed in our system could point to a different regulatory pathway in the epithelium compared to the myeloid compartment. An array of inflammatory cytokines and TLR ligands other than LPS was explored as possible inflammasome priming signals in IEC. However, none of the tested stimuli led to detectable *Nlrp3* expression. Nevertheless, we observed that IL-22 induced transcriptional up-regulation of *Il-18* and *Nlrc4* in primary IEC. IL-18 priming by IL-22 is consistent with a recent report, where IL-22 produced by T cells and ILC was responsible for maintaining *Il-18* expression in ileal epithelial cells (369). The relatively modest up-regulation of *Il-18* by IL-22 may reflect the high basal *Il-18* expression found in IEC (255, 358, 369). Furthermore, active IL-18 has also been observed in the intestinal epithelium at steady state *in vivo* (255). This suggests a homeostatic role for this cytokine and is consistent with the reported roles for IL-18 in repair of the damaged epithelium and regulation of local $CD4^+$ T cell responses (241, 255, 358).

However, the role of IL-18 in the intestine may be highly context dependent, since it has also been described as a pro-inflammatory cytokine that is elevated in the inflamed intestinal lesions of patients with Crohn's disease (257, 349). Furthermore, studies report IL-18 to be the driver of pathology in a DSS model of colitis (358). Indeed, epithelial

specific deletion of *Il-18* and *Il-18r1* resulted in ameliorated DSS colitis whilst the deletion of the negative regulator of IL-18, IL-18bp, resulted in more severe colitis, possibly due to IL-18 negative regulation of goblet cell maturation (358). Furthermore, recent reports show that epithelial-specific caspase-1 deletion also protects mice from increased susceptibility to DSS allegedly due to absent IL-18 signalling (361). These apparently contradictory roles for IL-18 highlight the requirement for further investigation of the pathways involved in the regulation of IL-18 secretion and the downstream consequences.

Our evidence pointed towards a ready-to-go phenotype for Nlrc4 activation and IL-18 secretion by IEC. Therefore, we examined the activation of Nlrc4 inflammasomes in primary IEC monolayers by challenging them with *S.* Typhimurium, an invasive intestinal pathogen that has been shown to initiate Nlrc4 inflammasome-dependent responses in IEC *in vivo* (220, 230). Our results show that IEC activate Nlrc4 inflammasomes and secrete active IL-18 upon *S.* Tm treatment, even in the absence of Nlrp3 and Asc. These observations are consistent with previous literature suggesting that Nlrc4 can directly interact with and activate caspase-1 through CARD-CARD interactions, despite somewhat relying on Asc for its full activation and efficient IL-1β/18 release in myeloid cells (316). However, currently there is not much evidence in the literature of Asc-independent functional roles for Nlrc4.

Seeding the same number of IEC from different genotypes into monolayers was somewhat challenging, leading to inter-assay variation in terms of magnitude of responses. Therefore, although the release of IL-18 was consistently hampered in *Asc*$^{-/-}$ IEC, we are unable to fully verify if the reduced inflammasome activation of Asc-independent responses was in fact due to the absence of Asc or due to assay technical variations. Furthermore, different batches of IEC organoids of the same genotype were somewhat variable in expression of IL-18. These results indicate the importance of making sure that differences in IEC organoid responses are verified using multiple independently derived primary IEC organoid lines. We are uncertain of the cause behind the variability of IL-18 levels. Each batch of organoids is derived from different mice which were not cohoused and as such the microbiota was not normalised between isolations. Thus, fluctuation in IL-18 levels between experiments with *ex vivo* primary IEC organoid cultures could be explained in part by variations in the microflora, given

that the composition of the microbiota has been reported to modulate inflammasome activation (241).

Besides cytokine release, inflammasome activation upon infection, classically results in the death of the infected cell (383). Nlrc4 and its Naip adaptors were shown to be essential for the extrusion of infected IEC into the intestinal lumen following *S.* Tm challenge of streptomycin-treated mice (220). Moreover, activation of Nlrc4 in IEC also limited *S.* Tm colonization of intestinal tissues and drove IEC death and extrusion (230). In agreement with these data, WT, *Nlrp3*$^{-/-}$ and *Asc*$^{-/-}$ deficient IEC monolayers displayed marked cytotoxicity following infection with *S.* Tm. Conversely, *S.* Tm-triggered only minimal cytotoxicity in *Nlrc4*$^{-/-}$ IEC monolayers. Extrusion of infected IEC through Nlrc4 activation may thus represent an important cell-intrinsic defence mechanism that serves to limit the rate of pathogen colonization of the intestinal epithelium.

Of note, epithelial monolayers undergo normal anoikis and cell turnover when cultured *in vitro* (565). This means that the percentage of LDH release does not only comprise cell lysis upon treatment but also includes cells that lyse upon normal epithelium turnover *in vitro*. This explains the variable and elevated levels of LDH release in untreated cells that are maintained in culture for long time-points. Therefore, results from LDH assays should be complemented with molecular-determinants of cell death mechanisms and/or further techniques that do not solely rely on the quantification of released cytosolic contents.

Another proposed hallmark of inflammasome activation is the formation of Asc agglomerations named "Asc specks". To date, there are no reports of Asc specks being observed in IEC. Here we show that Asc oligomers form in IEC monolayers treated with *S.* Tm. Again, in response to *S.* Tm, Asc specks were detected in WT and *Nlrp3*$^{-/-}$ IEC monolayers whilst they were absent in *Nlrc4*$^{-/-}$ IEC monolayers. Little is known about the consequence of Asc speck formation, but it is established that Asc oligomerisation downstream of the inflammasome is normally accompanied by pyroptosis (318, 326). However, the use of oligomerisation-deficient Asc mutants revealed that speck formation was dispensable for GsdmD cleavage and pyroptosis in macrophages, although Asc oligomerization was required for signal amplification and efficient cytokine processing (571). We have shown that primary IEC monolayers can undergo lytic cell death upon *S.* Tm challenge as well as Asc speck formation. However, this is the first instance where Asc speck formation has been observed in IEC. Therefore, further analysis and

characterization of these speck formations will be required to validate this observation and elucidate their functional relevance both *in vivo* and *in vitro*.

Nlrc4 deficiency in mice has been shown to result in increased susceptibility to *S.* Tm and *C. rodentium* infection (220, 231). Previous results in this thesis indicated that when mice lack Asc selectively in IEC ($Asc^{\Delta IEC}$), they exhibit an impaired ability to clear tissue adherent *C. rodentium*. However, we were unable to detect robust inflammasome activation in *C. rodentium* treated IEC monolayers. Nevertheless, treated cells mounted an inflammatory response, reflected by an up-regulation of *Cxcl2*. Therefore, these results may reflect inefficient infection of IEC under these experimental conditions. We hypothesised that the lack of inflammasome response observed when challenging IEC monolayers with *C. rodentium* may be due to downregulated virulence factor expression in LB-grown *C. rodentium* (467, 468). Therefore, we infected IEC monolayers with a more virulent host-adapted *C. rodentium* collected directly from feces of *C. rodentium* infected mice (467). However, fecal *C. rodentium* also failed to drive inflammasome activation in IEC monolayers.

The precise regulation of the virulence mechanisms that allow *C. rodentium* to infect mice are not fully understood (573). *C. rodentium* virulence seems to be partially controlled through microbiota competition for the same metabolic niche in the intestine (468, 578). Indeed, GM mice do not develop pathology during *C. rodentium* infection due to the downregulated virulence of the pathogen. Consequently, these mice cannot eradicate the infection and *C. rodentium* remains in the intestinal lumen as planktonic bacteria (468). However, recent studies with a *C. rodentium* strain constitutively expressing *ler* (positive regulator of *C. rodentium*'s virulence genes) showed that expression of virulence genes is not sufficient for colonic colonization (578). Instead, it seems that *C. rodentium* relies on commensals for survival at the colonic mucosa and virulence gene expression (578). Furthermore, *C. rodentium* virulence *in vivo* seems to also be dependent on the stage of infection. Virulence gene downregulation is observed during the late infection stages and this leads to the relocation of *C. rodentium* as planktonic bacteria in the intestinal lumen (468).

The landscape of *C. rodentium* virulence control is very intricate and our knowledge of it remains limited. The inability to mimic the intestinal environment in the IEC monolayer *ex vivo* culture may be hampering our ability to study IEC responses to *C. rodentium*. The

central positive regulator controlling LEE genes is *ler*, a 15 kDa protein encoded by the first gene of the LEE1 operon. *ler* induces LEE gene expression by counteracting the silencing mediated by H-NS, which is regarded as a general virulence negative regulator (574). The expression of *ler* is controlled by several global regulators, among them *glrA*, which is also LEE encoded (574, 579). The repression of LEE expression exerted by H-NS has been proposed to act as a sentinel of bacterial pathogenesis preventing possible detrimental effects to bacterial fitness arising from uncontrolled virulence gene expression (579).

We observed that LB-adapted *C. rodentium* had reduced LEE virulence factor expression compared to host-adapted *C. rodentium*. In light of these results, we engineered *C. rodentium* that would exogenously express *ler* or *glrA* under an arabinose-inducible promoter (573, 574). We observed that our engineered constructs greatly improved the expression of both *ler* and *tir*. Future work will aim to test these strains for their ability to drive inflammasome activation in IEC monolayers.

C. rodentium activation of inflammasomes *in vitro* has been extensively documented in the literature (271, 345, 384, 389). However, this work has largely been restricted to macrophages (345, 448). Macrophages can engulf *C. rodentium* leading to intracellular ingress of LPS capable of activating the non-canonical caspase-11 inflammasome (271). This can occur with *C. rodentium* that lacks a functional T3SS and is thus unable to activate the canonical inflammasome directly (345). Conversely, IEC are not phagocytic cells and thus inflammasome activation likely relies on cytosolic delivery of inflammasome ligands including LPS or parts of the T3SS. Therefore, to assess IEC responses to *C. rodentium in vitro*, it is paramount to find the appropriate conditions to activate *C. rodentium* virulence *in vitro*.

Another interesting feature of these host-pathogen interactions is that bacterial evasion strategies have been reported to counteract inflammasome responses. These, include the inhibition of epithelial caspase-11 via NleF, a T3SS effector protein produced by *E. coli* and *C. rodentium* (391). Likewise, *Yersinia* uses Yopk to evade detection of its T3SS and consequent inflammasome activation in macrophages (413). Furthermore, Gram-negative bacteria, like *Francisella novicida* can modify their LPS to avoid detection by caspase-11 (385). Although we have no direct evidence suggesting that bacterial evasion strategies are responsible for the lack of inflammasome activation observed upon *C. rodentium*

challenge of IEC monolayers, this possibility needs to be considered in the design of experiments investigating *C. rodentium* interactions with IEC.

To examine *C. rodentium* interactions with our IEC monolayer system, we investigated the ability of *C. rodentium* to adhere to IEC monolayers. Initially, *C. rodentium,* like EPEC, interacts with the IEC in a non-intimate manner, forming groups of bacteria on the cell surface, termed the localized adherence (451, 453). Subsequently, Tir is translocated into the host-cell membrane and interacts with intimin, a bacterial outer membrane adhesin (450). Following these events *C. rodentium* induces a localised loss of microvilli and profound actin rearrangements, leading to the formation of actin-rich structures, where the adherent bacteria are associated with actin pedestals (448).

We observed that fecal *C. rodentium* exhibited increased attachment to $Asc^{-/-}$ IEC monolayers compared to WT IEC monolayers. This is consistent with our *in vivo* observations that $Asc^{\Delta VC}$ mice have increased *C. rodentium* burden compared to $Asc^{fl/fl}$ mice. However, CFU quantification of adherent bacteria was hampered by the high level of passive attachment of the bacteria to the IEC monolayer, denoted by high CFU counts in the monolayers infected with *Δtir C. rodentium* (non-attaching mutant). Furthermore, attachment of LB-adapted *C. rodentium* to the IEC monolayer was severely delayed compared to fecal *C. rodentium,* possibly due to down-regulated virulence. Further, analysis and optimisation of the assays are needed to validate the observation of increased attachment of fecal *C. rodentium* to $Asc^{-/-}$ IEC monolayers. This includes implementation of more stringent washing of IEC monolayers, whilst avoiding excessive IEC death, to reduce the amount of passive *C. rodentium* attachment to monolayers. Furthermore, an analysis of actin pedestal formation would be valuable to confirm that fecal *C. rodentium* can form intimate attachment with IEC monolayers (467, 580, 581).

Given that inflammasome responses have been associated with modulating antimicrobial responses in the intestinal epithelium (231, 241, 249, 251), we investigated the antimicrobial activity of IEC monolayers against *C. rodentium*. We observed no *C. rodentium* killing or growth inhibition activity by IEC supernatants released by $Asc^{-/-}$ or WT monolayers, even in the presence of IL-22, which is known to stimulate AMP production by IEC. These observations are somewhat surprising since AMP release *in vivo* is a key feature of IEC defence (121, 480). Nevertheless, it remains possible that we have not applied the right priming signal to induce IEC antimicrobial activity. Indeed, *in*

vivo, antimicrobial activity is regulated by microbial metabolites and the presence of microbiota (241, 582). Therefore, further analysis is needed to understand how the IEC monolayer system can be used to study antimicrobial responses.

Overall, our research has revealed profound differences in inflammasome regulation between IEC and other cell types. We have discovered that IEC inflammasome responses to *S*.Tm are independent of Nlrp3 but heavily dependent on Nlrc4, which appears to function largely in an Asc-independent manner in IEC. We have also shown that IEC respond differently to *C. rodentium* compared to *S*.Tm. This is likely because, unlike *S*.Tm, *C. rodentium* does not actively invade epithelial cells (Figure 4.20). However, further study on how to effectively drive *C. rodentium* virulence *in vitro* is needed to fully investigate the IEC responses to the bacterium.

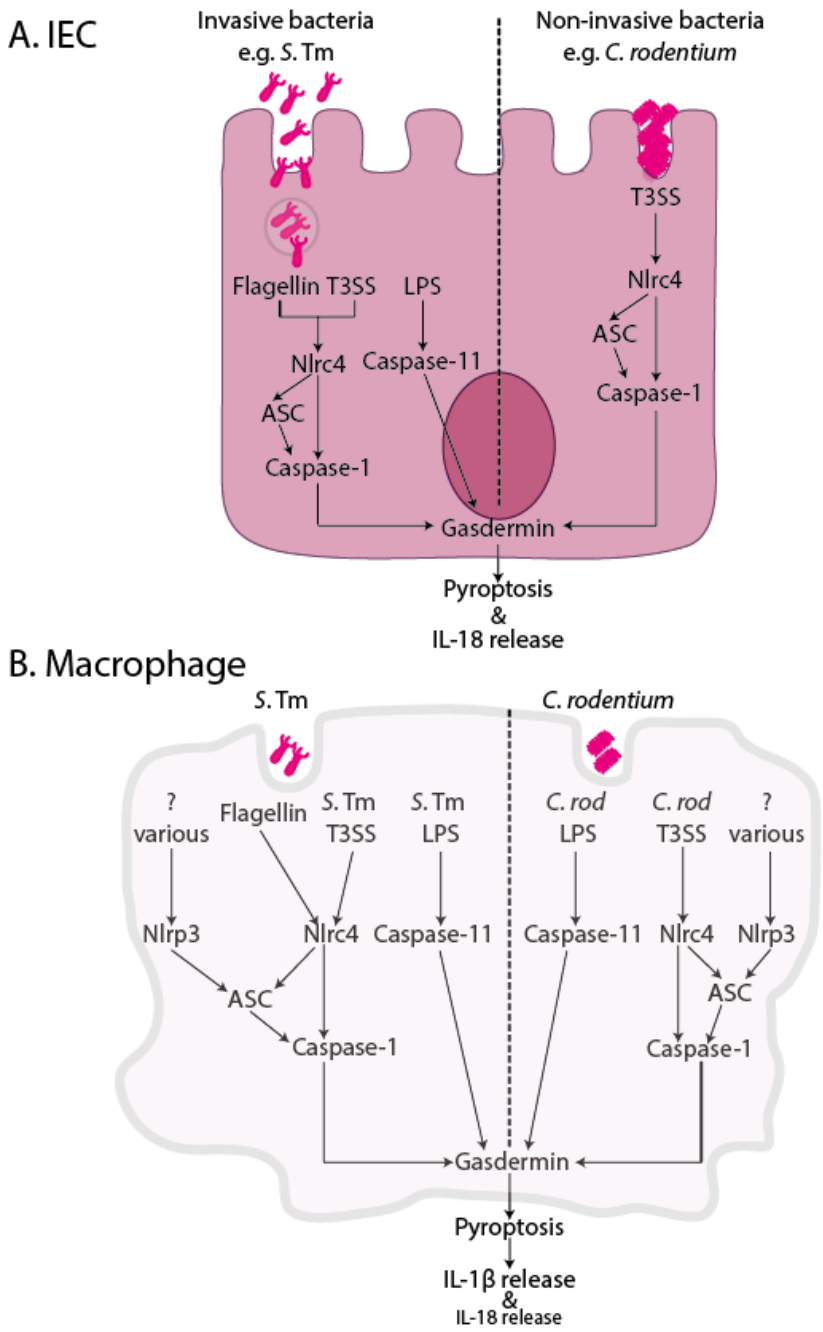


Figure 4.20. Inflammasome activation in *C. rodentium* and *S.* Typhimurium in macrophages (phagocytic) versus IEC (non-phagocytic). *C. rodentium* activation of inflammasomes *in vitro* has been extensively documented in the literature (271, 345, 384, 389). However, this work has largely been restricted to macrophages (345, 448). Macrophages can engulf *C. rodentium* leading to intracellular ingress of LPS capable of activating the non-canonical caspase-11 inflammasome (271). This can occur with *C. rodentium* that lacks a functional T3SS and is thus unable to activate the canonical inflammasome directly (345). Conversely, IEC are not phagocytic cells and thus inflammasome activation likely relies on cytosolic delivery of inflammasome ligands including parts of the T3SS. IEC respond differently to *C. rodentium* compared to *S.*Tm. This is likely because, unlike *S.*Tm, *C. rodentium* does not actively invade epithelial cells. IEC activate Nlrc4 inflammasomes and secrete active IL-18 upon *S.* Tm treatment, even in the absence of Nlrp3 and Asc. However, in the absence of an active T3SS, we observed that *C. rodentium* is unable to activate the inflammasome in IEC. If macrophages or IEC can rely solely on the non-canonical Caspase-11 for the activation of the inflammasome remains to be described.

Chapter 5: General Discussion

5.1. Cell type-specific regulation of PRR is key to understanding the discrimination between commensals and pathogens

The current dogma that self/non-self-discrimination operates through activation of innate immune PRR that recognise conserved PAMP present on microbes provides a solid basis for understanding immune activation following infection of sterile systemic tissues (165). However, this paradigm breaks down in the intestinal tract, which is constitutively colonized with trillions of diverse commensal bacteria that are necessary for maintaining a healthy intestine (163, 583). Intestinal homeostasis and tolerance to the microbiota is not fully understood but its disruption is thought to lead to exacerbated inflammatory responses such as IBD (163). The basis of discrimination between commensals and pathogens may be explained by PRR compartmentalisation, their cell type-specific regulation, post-translational modifications, and their interactions with other immune pathways (163, 584).

Our data revealed a certain level of compartmentalisation of innate immune responses involving PRR sensors of the NLR family. We showed that the expression of Nlrp3 is undetectable in IEC, and that it is dispensable for IEC inflammasome-mediated responses against *S*.Tm challenge of *in vitro* IEC monolayers. Nlrp3 is an inflammasome forming NLR that may be activated by a very wide range of infection or stress-associated stimuli (190). Therefore, it seems logical that such responsive, pro-inflammatory, molecule is absent in IEC that are constantly exposed to the commensal microbiota and diverse cellular stresses. Conversely, Nlrp3 expression is readily induced in the LPL and IEL hematopoietic compartments and contributes to defence against pathogen invasion, at least partially through IL-1β secretion (550, 585).

Cell-type specific adaptations to inflammasome signalling have been reported by other investigators. For instance, Nlrp3 in murine neutrophils was shown to selectively respond to soluble agonists, but not to the particulate, crystalline agonists that can activate Nlrp3 in macrophages (586). However, in the context of bacterial infection neutrophils are an important source of IL-1β and key for the inflammatory signalling cascade leading to pathogen clearance (441, 587, 588). It is possible that IEC, like neutrophils, respond

differently to inflammasome activators that have been primarily described in macrophages. Furthermore, several studies have shown cell-type specific expression patterns of different NLR and inflammasome components. For example, Nlrp6 is enriched at the host-pathogen interface, especially in the IEC compartment, attesting to its proposed regulatory role in barrier maintenance and regulation of mucus secretion (242, 243, 589). Similarly, a recent study reported that Nlrp9b is highly expressed in SI IEC, where it plays an important role in host defence against enteric norovirus infection (246). Conversely, other NLR, such as Nlrp12 and Nlrp3, are enriched in the haematopoietic compartment, where they may respond to a diverse range of threats that might have crossed barrier surfaces (487).

In contrast to Nlrp3, Nlrc4 inflammasome formation is triggered by a reduced number of ligands. It is specifically activated by bacterial components that breach the cellular barriers and actively invade host cells (227-229, 231). We found that Nlrc4 is enriched in the steady state IEC (231), potentially providing the epithelial barrier with a ready-to-go phenotype against invading pathogens. Supporting the importance of Nlrc4 antimicrobial function in the intestinal epithelium, we have shown that caspase-1 and IL-18 activation are Nlrc4-dependent in IEC monolayers responding to *S.* Tm. In keeping with this observation, other investigators have shown that epithelial Nlrc4 and its Naip adaptors are important for the clearance of *S.* Tm from infected IEC (220, 230). In these reports, *S.* Tm clearance downstream of the inflammasome was through Nlrc4-dependent cell death but independent of IL-18. This remarks that pyroptosis and IL-18 secretion may serve different functions during *S.* Tm infection.

We speculate that cell type-specific adaptations are a common feature of NLR signalling networks. However, the environmental and developmental cues that shape differential expression of NLR and inflammasome components in distinct cell types remain poorly understood and require further investigation.

5.2. The response of IEC inflammasomes to pathogenic invasion

Regulation of immune responses are fine-tuned according to cell-lineage and location (77, 163, 168). The intestinal epithelium is a site of special interest in mucosal antimicrobial defence due to its constitutive colonisation with a remarkable array of

microbes. The development of primary IEC organoids has opened a new chapter in IEC research (16). This long-term culture of organoids overcame some of the technical barriers that have hindered *in vitro* research in primary IEC. We and others have shown that IEC organoids and monolayers are a valuable tool to investigate host-pathogen interactions and inflammasome regulation in IEC (230, 246, 504, 522).

Thus far, our data using IEC organoids and monolayers have revealed profound differences in inflammasome responses to pathogenic invasion in BMDM compared to IEC organoids. We showed that caspase-1 and IL-18 can be activated in IEC monolayers upon *S.* Tm stimulation. This inflammasome activation was completely independent of Nlrp3 and completely dependent on Nlrc4, with intermediate inflammasome activation being mediated by Asc. This observation indicates that Nlrc4 can form both an Asc dependent and independent inflammasome. This data is in contrast with observations made in BMDM challenged with *S.* Tm where Nlrc4 and Nlrp3 had redundant roles (590).

In the context of *C. rodentium* infection, inflammasome activation is readily detected in BMDM challenged with this pathogen (345). However, this was not the case in IEC monolayers, where we were unable to detect active caspase-1 nor IL-18 upon *C. rodentium* infection. Unlike *S.* Tm, *C. rodentium* does not actively invade epithelial cells, but forms intimate attachments to the epithelial surface (450). These observations may indicate that inflammasome activation in BMDM relies on the fact that the phagocyte can internalise the bacterium (345). Given that IEC are non-phagocytic cells, *C. rodentium*-triggered inflammasome activation in IEC is likely to require mechanisms that are independent of intracellular localisation of the pathogen.

Nlrp3, Nlrp6 and Nlrc4, as well as the NLR adaptor Asc, have been implicated in the defence against *C. rodentium*. The non-hematopoietic compartment was deemed largely responsible for this protection (231, 243, 249). Here, we have shown that epithelial Asc is indeed important for the rapid clearance of tissue adherent *C. rodentium*. Although both Nlrc4 and Nlrp3 could potentially recognise PAMP derived from *C. rodentium*, the inability to detect Nlrp3 in *in vitro* IEC organoids and their reliance on Nlrc4 for responding against *S.* Tm invasion, strongly suggest that epithelial Nlrc4 mediates *C. rodentium* clearance from infected IEC.

Our data demonstrate the utility of using tissue-specific deletions of inflammasome components to fully establish the cell-type specific roles of inflammasomes in protective

immunity. This will allow the dissection of tissue/cell type-specific circuits without the need of extrapolating conclusions from observations made with the use of bone marrow chimeras. Moreover, complementing *in vivo* research with *in vitro* IEC cultures will also be beneficial for the dissection of cell-type specific mechanisms of inflammasome activation, as well as for identifying the precise ligands and the downstream mechanisms involved.

5.3. Host microbiota sculpts host-pathogen interactions: Challenges of *in vitro* studies.

Host-pathogen interactions are regulated by intricate signalling networks. This intimate relationship is affected by a vast number of factors that we cannot fully reproduce *in vitro.* We hypothesise that *in vitro* LB grown *C. rodentium* has a downregulated virulence response and is therefore unable to intimately interact with IEC monolayers. This may explain why we were unable to observe inflammasome activation upon IEC challenge with *C. rodentium*. It is likely that signals from the host and the microbiota drive bacterial virulence. Indeed, *C. rodentium* infection of GF mice leads to constitutive colonisation of the pathogen in the mouse gut (468). In this microbiota-devoid environment, *C. rodentium* downregulates its virulence genes and does not lead to inflammation or pathology (468).

These observations may imply that IEC do not mount an inflammasome response when virulence remains dormant. This is advantageous to the host as no negative responses are mounted against beneficial microbiota. It is possible that the presence of microbiota in the gut has educated the immune system to remain tolerant to non-virulent microbes. In support of this notion, mice that are deficient in MYD88 display increased susceptibility to DSS induced injury (591). Furthermore, selective ablation of NF-κB signalling in IEC through IEC-specific deletion of the NF-κB essential modulator (NEMO) leads to the development of spontaneous intestinal inflammation (592). These studies suggest that microbiota-host dialogue through PRR sensing in IEC is important for fine-tuning the immune response of the host and for maintaining or restoring intestinal epithelial homeostasis.

Not only is the microbiota able to modulate innate immune responses but it also affects aspects of adaptive immunity. For instance, SFB, part of the murine small intestinal commensal community, drives Th17 cell accumulation in the small intestine (115). Furthermore, SCFA produced by gut microbiota was shown to increase Treg numbers in the gut, which are critical for regulating intestinal inflammation (7). Indeed, this Treg boost was associated with protection against the T-cell transfer model of colitis (7, 593).

The study of host-pathogen interactions is further complicated by the ability of microbes produce virulence factors that allow them to evade immune sensing. For example, *Yersinia* uses Yopk to evade detection of its T3SS and consequent inflammasome activation in macrophages (413). Furthermore, bacteria can modify their LPS to avoid detection by caspase-11 (385). Immune evasion strategies have also been observed in *C. rodentium*. NleB1 and NleF are factors in *E. coli* and *C. rodentium* known to inhibit caspase-8 and -11 signalling, respectively (391, 410). It is possible that *C. rodentium* is actively inhibiting inflammasome activation in the IEC monolayers system, thus providing a possible explanation for the lack of caspase-1 and IL-18 activation observed in this system. However, since we could not observe *C. rodentium*-IEC interactions in *in vitro* monolayers (i.e. pedestal formation), it is more likely that a lack of attachment to *in vitro* IEC is what prevented inflammasome activation.

Understanding how non-invasive pathogens like *C. rodentium* activate the inflammasome in IEC will reveal new insights into the molecular basis of microbial sensing by inflammasomes. Future work in our lab aims to investigate the response of IEC monolayers to *C. rodentium* engineered to express key positive virulence regulators, like *ler* or *glrA* under the control of an inducible promoter. This engineered bacterium should allow us to circumvent the lack of interaction of LB-grown *C. rodentium* with IEC monolayers. Furthermore, to investigate the different effects of *C. rodentium* virulence factors on IEC, we plan to utilise *C. rodentium* mutants lacking specific virulence factors, such as the above-mentioned caspase-signalling inhibitors, NleB1 and NleF, or key components of the T3SS, including EscF, a structural component of the T3SS needle (391, 410, 594). This should identify the precise factors that drive or counteract inflammasome activation in IEC.

Immune responses to pathogen invasion are collaborative with one cell sensing and triggering the responses of others (595). To understand cell-cell interactions in the context

of pathogen stimulation, future work aims to set up co-cultures of IEC organoids/monolayers with cells of the immune system. For example, cultures of IEL with IEC have been reported. This study showed the migration of IEL along the basolateral surface of IEC as well as inwards and outwards from the organoid structures (596). It may also be possible to grow IEC on stromal cells layers, representing an *in vivo* situation.

The possibility to look at the interactions between IEC and immune cells may allow the study of signalling networks that remained previously elusive. For instance, IL-18R is expressed in a variety of different cells, including macrophages, neutrophils, endothelial cells and $CD4^{+}$T cells (255, 597). Furthermore, IL-18R is more highly expressed on T cells of the intestine than other systemic sites rendering the gut highly sensitive to signalling by IL-18 (255). This highlights that the importance of the IL-18 signalling axis in the intestine. The ability to assess the responses of different cell types to IL-18 may be key to identifying the seemingly opposing roles of this cytokine in the immune system. We propose to induce inflammasome activation in response to different stimuli in IEC organoids and measure the responses of cells in co-culture to look for specific and unique effects. Furthermore, by activating inflammasomes in IEC, IL-18 release will be accompanied by pyroptosis, thus we will be able to examine the responses of other cells to this more complicated stimulus that is closer to a physiological scenario.

5.4. Epithelial inflammasomes and cell death

Inflammasome functional studies to date have largely focused on the secretion of downstream soluble mediators. However, there is emerging interest in the role of inflammasome-triggered cell death by pyroptosis (320, 381). GsdmD was identified as a direct downstream target of caspase-1 and caspase-11 and was shown to be required for pyroptosis upon ‘canonical’ and ‘non-canonical’ inflammasome engagement (395, 397-399, 426, 598). Recently, Rauch *et al.* reported that Nlrc4 activation in IEC led to lytic cell death that was dependent on GsdmD. This observation confirms that pyroptosis does occur in IEC and that epithelial pyroptosis may also be reliant on GsdmD (230). Interestingly, in the absence of GsdmD, cell death downstream of Nlrc4 progressed in a non-lytic fashion that appeared to involve caspase-8 (230). Caspase-8 has previously been reported as an effector caspase downstream of inflammasome activation. Caspase-8

interactions with Asc that occur independently of caspase-1 have been reported as 'non-canonical' inflammasome formation (407, 549, 599). Furthermore, AIM2 and Nlrp3 inflammasomes have also been shown to be able to interact with caspase-8 (600).

In a model of *Salmonella* infection of streptomycin-treated mice, Sellin *et al.*, proposed cell extrusion and death downstream of Nlrc4-Naip as a mechanism to clear infected IEC and reduced *S.* Tm burden (220). In this report, IEC extrusion preceded cell death and membrane integrity was maintained. However, the effector caspase involved in this process was not determined. Building upon these reports of cell extrusion and death of infected enterocytes aiding pathogen clearance, we hypothesise that reduced cell death in $Asc^{\Delta VC}$ infected tissues may explain the increased pathogen burden observed in these mice (Figure 5.1). In support of this, we found that $Asc^{\Delta VC}$ as well as $Asc^{-/-}$ intestinal tissues displayed a reduction in activated caspase-8 during *C. rodentium* infection.

The different pathways leading to inflammasome-triggered cell death and their interconnections are not fully understood. It is unknown whether these pathways are simultaneous, mutually exclusive or interdependent. In BMDM, caspase-8 and -3 mediated apoptosis dependent on Asc was reported to occur downstream of AIM2 activating stimuli, in parallel to caspase-1 mediated pyroptosis (549). Interestingly, a lower dose of the stimuli promoted caspase-8 and -3-mediated responses whilst higher doses favoured pyroptosis (549).

These observations raise the possibility of a distinction between a pro-immunogenic cell death signal involving Gsdmd and a pro-silent cell death driven by caspase-8. This distinction may be brought about by a threshold dependent cellular decision between non-lytic and lytic forms of cell death involving caspase-1 (1). Under low stress levels, it would be desirable to deal with the invading threat in an immunologically silent way. However, when the threat is high, an immunogenic cell death could recruit inflammatory cells to help clear the microbial insult. Further investigation needs to be carried out into the role of inflammasome-triggered cell death in IEC and its consequences for infection or inflammatory diseases. For example, does too little IEC death result increased potential for invasive infection due to lack of cell extrusion and does too much IEC death and consequent cytokine secretion perpetuate unnecessary or even chronic inflammation? (1).

With genetic manipulation becoming increasingly more accessible and rapid, the regulation of these pathways could be teased out using novel genetic approaches. To

functionally assess the roles of novel molecules in IEC responses to stimuli *in vitro*, we plan to combine the organoid culture system with the novel CRISPR genome editing technique (601). This will enable deletion of defined genes in IEC, facilitating analyses into the function of specific inflammasome components without the need to generate new stains of transgenic mice. CRISPR-Cas9 has already been applied in the IEC organoid system. For instance, Schwank *et al.* were able to repair a mutation in the cystic fibrosis (CF) transmembrane conductor receptor (CFTR) leading to CF by homologous recombination in cultured IEC organoids derived from CF patients (511).

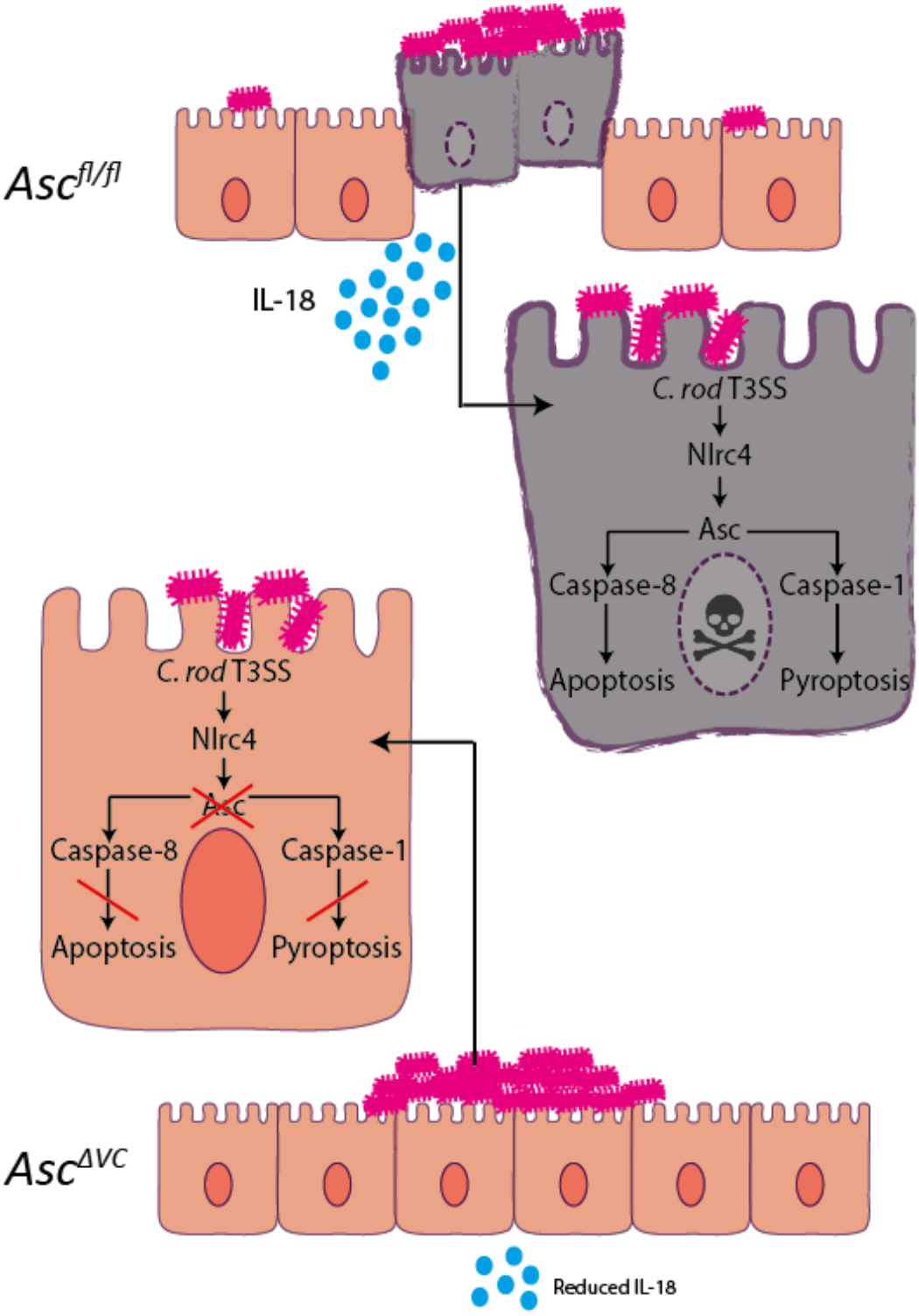


Figure 5.1. Reduced cell death in infected tissues in *Asc*$^{\Delta VC}$ mice may explain the increased pathogen burden compared to *Asc*$^{fl/fl}$. Upon inflammasome activation *in vivo* with *C. rodentium*, IEC activate both caspase-1 and caspase-8, leading to cellular death possibly by pyroptosis and apoptosis, respectively. We have observed that *Asc*$^{\Delta VC}$ intestinal tissues displayed a reduction in activated caspase-8 and caspase-1 during *C. rodentium* infection. We hypothesise that reduced cell death in *Asc*$^{\Delta VC}$ infected tissues may explain the increased pathogen burden observed in these mice compared to *Asc*$^{fl/fl}$ mice. However, how the different inflammasome-triggered cell death pathways are regulated and how they interact with one another remains poorly understood.

5.5. Interconnected circuits of inflammasome effector functions

The immune system responds to sterile injury and to microbial insults, with maintaining homeostasis being one of its most important and challenging functions. Depending on the nature of the threat the outcomes vary from tissue repair to antimicrobial defence. Inflammasome signalling is one of the molecular mechanisms shown to play a role in both defence against pathogens and repair mechanisms (602).

During homeostatic conditions, and thus in the absence of inflammation, the inflammasome-dependent cytokine IL-18 is released from IEC and is believed to have functions in epithelial repair, proliferation and maturation (242, 243, 371, 372). In addition, IL-18 has been implicated in driving IL-22 (369), a cytokine important for AMP production (241) and antimicrobial defence (251, 345) as well as mucosal barrier integrity (369). On the other hand, caspase-1 activation and consequent IL-18 secretion were associated with exacerbated inflammation following DSS administration, which was ameliorated in IEC-specific IL-18 knock outs (*IL-18*$^{\Delta IVC}$) (358) and IEC-specific caspase-1 knock outs (*Casp1*$^{\Delta IVC}$) (361). Supporting an inflammatory role for IL-18, this cytokine was shown to contribute to acute inflammation early during *Salmonella* infection through boosting the accumulation of activated NK cells in the infected mucosa (352). In contrast, reduced levels of IL-18 secretion in Nlrp6 deficient mice were linked to increased DSS susceptibility (242). Furthermore, rIL-18 administration was shown to rescue inflammasome-deficient phenotypes from hyper-susceptibility to DSS colitis (1, 241, 253, 256, 258, 367).

Our data using *C. rodentium* infection of *Asc*$^{\Delta IVC}$ mice revealed that epithelial Asc is important in the clearance of tissue adherent *C. rodentium*. The mechanism by which the inflammasome controls *C. rodentium* tissue burden is thus far unknown. Nevertheless, our data shows that IL-18 secretion is dramatically reduced upon deletion of epithelial Asc. Mice that are deficient in IL-18 signalling (*IL-18*$^{-/-}$ and *IL-18R*$^{-/-}$ mice) have increased *C. rodentium* burden (249, 345). Thus, we hypothesise that IL-18 could be involved in *C. rodentium* clearance. To test this hypothesis, we aim to administer rIL-18 to *C. rodentium* infected mice and assess their ability to clear tissue adherent *C. rodentium.*

The explanation behind these seemingly contrasting roles may lay in the nature of the stimulus and the cellular source of this cytokine. Indeed, stimulus-dependent differential

regulation of inflammasome components has been reported in macrophages. Nlrp3 was shown to respond more potently and with faster kinetics to microbial derived signals compared to sterile ones (602). In the context of enteric infection, the inflammasome may be beneficial for the recruitment of immune cells through IL-18 secretion (251, 345, 352, 391) and the extrusion of infected enterocytes (220, 230). Conversely, in the context of DSS, inflammasome components including IL-18 may be released from ruptured cells leading to abnormally high IL-18 levels and tissue damage (358, 361).

Although the reduction of IL-18 secretion upon epithelial Asc deletion was dramatic, we are uncertain of the full array of consequences of inflammasome activation in the intestinal epithelium. It may be possible to use IEC organoids to identify proteins that are differentially regulated in an inflammasome-dependent manner. For this purpose, one approach would be to subject intestinal epithelial organoids to RNAseq in the presence and absence of inflammasome activating stimuli, including *C. rodentium*. This would allow the identification of new candidate effectors of inflammasome pathways in IEC at steady state and during infection. However, it is worth noting that much of the inflammasome signalling pathway is post-translationally regulated. This means that a transcriptomics approach may not be the most suitable technique to assess changes in inflammasome signalling. Therefore, a proteomics approach could be considered to study the downstream effects of inflammasome activation in IEC.

It is worth re-emphasising that *in vitro* analysis of Nlrp3, Nlrc4 and Asc IEC organoids upon *S.* Tm challenge revealed that inflammasome responses in IEC are highly dependent on Nlrc4 but can proceed in the absence of Asc. It is important to keep this observation in mind when analysing the outcome of *in vivo* experiments relying on Asc deletion. Our data suggests that Asc deletion may not be sufficient to obliterate all inflammasome responses and Nlrc4-dependent functions may still take place independently of Asc. Notably, Broz *et al.* observed that Asc-independent inflammasome responses could lead to cell death, whereas cytokine secretion was compromised in the absence of Asc in *in vitro* macrophages (316). This observation fits with our observation that IL-18 secretion was reduced in the intestinal tissues of $Asc^{\Delta VC}$ mice. Future work aims to fully characterise the pyroptotic profile of $Asc^{\Delta VC}$ intestinal tissues to discover if this may be a protective mechanism in these mice.

The microbiota is a key factor in immune modulation and mucosal homeostasis (1). The improper control and assessment of microbiota has been a significant confounding factor in inflammasome research. Previously, the deletion of some inflammasome components like Nlrp6 and Asc was thought to lead to the development of a dominant dysbiotic microflora that consequently increased susceptibility to DSS treatment (242). However, recent reports demonstrated, with the use of littermate controls and different animal facilities, that Nlrp6 and Asc deletions do not lead to dysbiosis nor to increased susceptibility to injury by DSS (362). This suggests that neither Asc nor Nlrp6 shape the composition of the commensal gut microflora at steady state (362).

Other recent reports demonstrated that inflammasome responses may be influenced by the composition of the microbiota. Indeed, protozoa (603) and microbial metabolites (241) have been shown to modulate inflammasome activation and susceptibility to intestinal inflammation. Therefore, these reports call for proper microbiota normalisation strategies and the use of littermate controls in order to study the inflammasome pathways (1). Furthermore, observations must be interpreted with caution and their validation in different animal facilities will alleviate current inconsistencies in the scientific literature due to differences in microbiota composition.

5.6. Concluding remarks

Our initial interest in the role of inflammasomes in intestinal immunology was sparked by GWAS that revealed that inflammasome-associated genes were linked to IBD susceptibility (160), suggesting that this family of proteins is important for maintenance of intestinal homeostasis. Indeed, inflammasome forming NLR and Asc have been shown to limit the outgrowth and colonisation of colitogenic microbes thus promoting intestinal homeostasis (231, 242, 249). This protection has long been attributed to epithelial inflammasomes. However, this research was mostly conducted with the use of bone marrow chimeras, although IEC-specific deletion of inflammasome components is rapidly emerging. We found that Asc deletion specifically within the intestinal epithelium is important for the clearance of tissue adherent *C. rodentium*. Furthermore, *in vitro* data with IEC organoids suggests that IEC inflammasome responses triggered by enteric pathogens are largely dependent on Nlrc4 and at least partially dependent on Asc. Recent reports show that epithelial Nlrc4 and its Naip adaptors are important for clearance of

enteric pathogens (220, 230). Together, this evidence demonstrates that epithelial inflammasomes are important in antimicrobial defence and that Nlrc4 is likely to be a key mediator of these responses (Figure 5.2).

Basic research into the regulation of inflammasome activation and signalling will lead to greater understanding of enteric infections and IBD. For instance, boosting Nlrc4 and/or Asc activation during pathogenic invasion with enteric pathogens such as *S*.Tm or EPEC/EHEC may be beneficial to aid the rapid clearance of the pathogen. Or perhaps including adjuvants that may trigger these responses in a vaccine may lead to prophylactic protection. These are points of special interest since the use of antibiotic treatment upon invasion with enteric pathogens remains controversial (604). However, inflammasome networks have proven to be very context-specific. Indeed, excessive inflammasome signalling can lead to tissue damage and inflammation. Therefore, in situations where inflammation is deleterious to the host, like in IBD, the identification of small molecules capable of targeting specific inflammasome components (251) could open opportunities for novel clinical interventions (1).

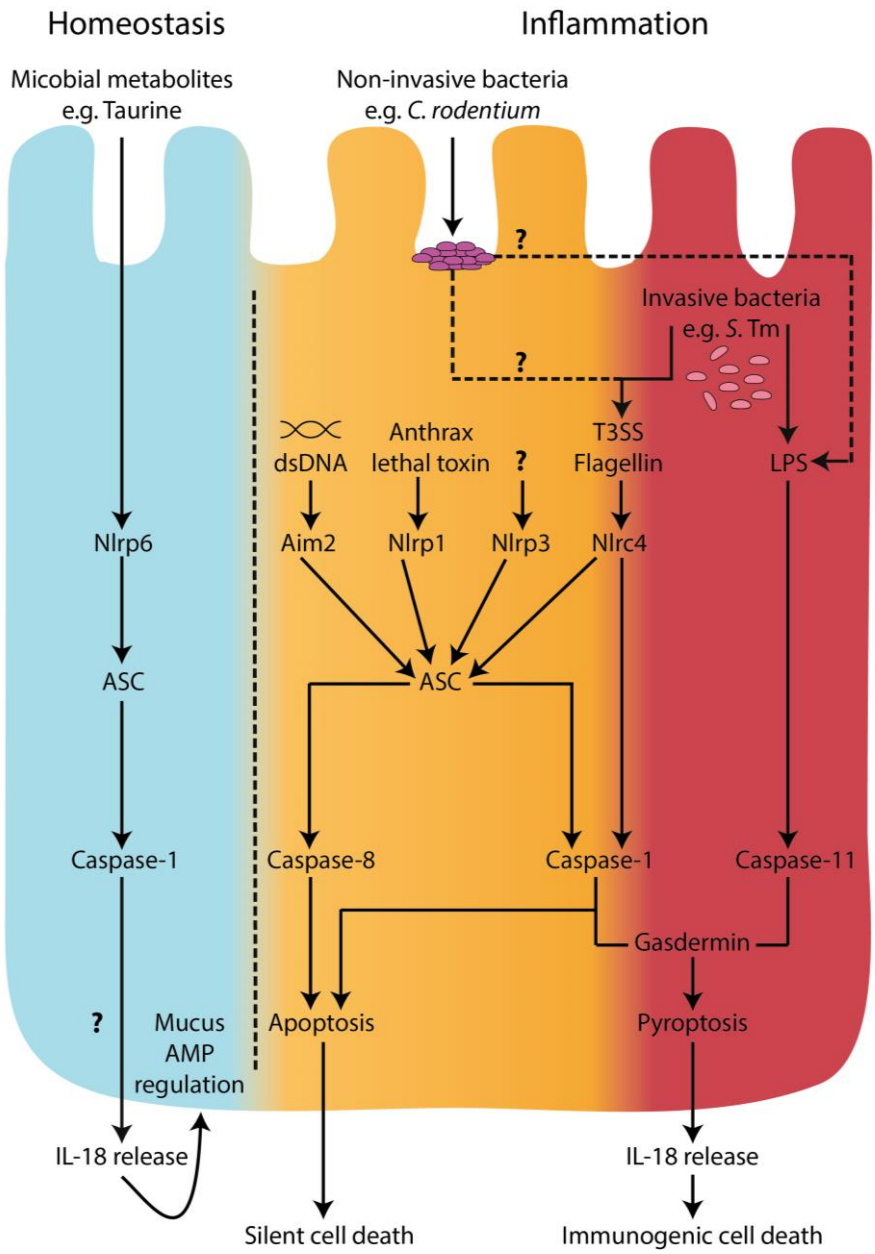


Figure 5.2. Summary figure. During homeostatic conditions, IL-18 secreted by IEC is involved IEC maturation and regulation of mucus secretion (242, 243). These responses are partially regulated by the gut microbiota and its metabolites (241), but the specific mechanisms leading to inflammasome activation are undefined. In the context enteric bacterial infection, IEC engage the Nlrc4 inflammasome and its Naip adaptors to mediate pathogen clearance through inflammasome formation. Nlrc4 and Naip can sense cytosolic flagellin or proteins of the active T3SS. Nlrc4 is capable of mounting both an Asc dependent response and an Asc independent one (230). These responses lead to the activation of different caspases, namely -8, -1 and -11 that mediate various form of cell death resulting in expulsion of infected IEC, thus aiding pathogen clearance. Both caspase-1 and caspase-11 can lead to cell death by pyroptosis through the activation of gasdermin D, which is accompanied by IL-18 secretion (220, 230, 251). Caspase-8 was shown to lead to a non-lytic, silent form of cell death upon Nlrc4 sensing of intracellular flagellin (230). The pathways leading to Nlrc4 activation by *S.* Tm are better characterised due to the ability of S.Tm to actively invade epithelial cells. The specific ligands that lead to *C. rodentium* activation of the Nlrc4 inflammasome in IEC remain undefined. As *C. rodentium* uses a T3SS for IEC infection, it is likely that the T3SS rod or needle proteins, activate the Naip/Nlrc4 inflammasome in IEC.

References

1. Lei-Leston AC, Murphy AG, Maloy KJ. Epithelial Cell Inflammasomes in Intestinal Immunity and Inflammation. *Frontiers in immunology* (2017) **8**:1168. Epub 2017/10/06. doi: 10.3389/fimmu.2017.01168. PubMed PMID: 28979266; PubMed Central PMCID: PMCPMC5611393.

2. Hooper LV, Gordon JI. Commensal host-bacterial relationships in the gut. *Science (New York, NY)* (2001) **292**(5519):1115-8. Epub 2001/05/16. PubMed PMID: 11352068.

3. Artis D. Epithelial-cell recognition of commensal bacteria and maintenance of immune homeostasis in the gut. *Nat Rev Immunol* (2008) **8**(6):411-20. Epub 2008/05/13. doi: 10.1038/nri2316. PubMed PMID: 18469830.

4. Ley RE, Peterson DA, Gordon JI. Ecological and evolutionary forces shaping microbial diversity in the human intestine. *Cell* (2006) **124**(4):837-48. Epub 2006/02/25. doi: 10.1016/j.cell.2006.02.017. PubMed PMID: 16497592.

5. Round JL, Mazmanian SK. The gut microbiome shapes intestinal immune responses during health and disease. *Nature reviews Immunology* (2009) **9**(5):313.

6. Maslowski KM, Mackay CR. Diet, gut microbiota and immune responses. *Nat Immunol* (2011) **12**(1):5-9. Epub 2010/12/21. doi: 10.1038/ni0111-5. PubMed PMID: 21169997.

7. Smith PM, Howitt MR, Panikov N, Michaud M, Gallini CA, Bohlooly YM, et al. The microbial metabolites, short-chain fatty acids, regulate colonic Treg cell homeostasis. *Science (New York, NY)* (2013) **341**(6145):569-73. Epub 2013/07/06. doi: 10.1126/science.1241165. PubMed PMID: 23828891; PubMed Central PMCID: PMCPMC3807819.

8. Buffie CG, Pamer EG. Microbiota-mediated colonization resistance against intestinal pathogens. *Nat Rev Immunol* (2013) **13**(11):790-801. Epub 2013/10/08. doi: 10.1038/nri3535. PubMed PMID: 24096337; PubMed Central PMCID: PMCPMC4194195.

9. Guarner F, Malagelada JR. Gut flora in health and disease. *Lancet* (2003) **361**(9356):512-9. Epub 2003/02/14. doi: 10.1016/S0140-6736(03)12489-0. PubMed PMID: 12583961.

10. van der Waaij D, Berghuis-de Vries JM, Lekkerkerk L-v. Colonization resistance of the digestive tract in conventional and antibiotic-treated mice. *J Hyg (Lond)* (1971) **69**(3):405-11. Epub 1971/09/01. PubMed PMID: 4999450; PubMed Central PMCID: PMCPMC2130899.

11. Nardi RM, Silva ME, Vieira EC, Bambirra EA, Nicoli JR. Intragastric infection of germfree and conventional mice with Salmonella typhimurium. *Brazilian journal of medical and biological research= Revista brasileira de pesquisas medicas e biologicas* (1988) **22**(11):1389-92.

12. Diard M, Sellin ME, Dolowschiak T, Arnoldini M, Ackermann M, Hardt WD. Antibiotic treatment selects for cooperative virulence of Salmonella typhimurium. *Curr Biol* (2014) **24**(17):2000-5. Epub 2014/08/19. doi: 10.1016/j.cub.2014.07.028. PubMed PMID: 25131673.

13. Sekirov I, Tam NM, Jogova M, Robertson ML, Li Y, Lupp C, et al. Antibiotic-induced perturbations of the intestinal microbiota alter host susceptibility to enteric infection. *Infect Immun* (2008) **76**(10):4726-36. Epub 2008/08/06. doi: 10.1128/IAI.00319-08. PubMed PMID: 18678663; PubMed Central PMCID: PMCPMC2546810.

14. Voth DE, Ballard JD. Clostridium difficile toxins: mechanism of action and role in disease. *Clin Microbiol Rev* (2005) **18**(2):247-63. Epub 2005/04/16. doi: 10.1128/CMR.18.2.247-263.2005. PubMed PMID: 15831824; PubMed Central PMCID: PMCPMC1082799.

15. Peterson LW, Artis D. Intestinal epithelial cells: regulators of barrier function and immune homeostasis. *Nat Rev Immunol* (2014) **14**(3):141-53. Epub 2014/02/26. doi: 10.1038/nri3608. PubMed PMID: 24566914.

16. Sato T, Vries RG, Snippert HJ, van de Wetering M, Barker N, Stange DE, et al. Single Lgr5 stem cells build crypt-villus structures in vitro without a mesenchymal niche. *Nature* (2009) **459**(7244):262-5. Epub 2009/03/31. doi: 10.1038/nature07935. PubMed PMID: 19329995.

17. Barker N, van Es JH, Kuipers J, Kujala P, van den Born M, Cozijnsen M, et al. Identification of stem cells in small intestine and colon by marker gene Lgr5. *Nature* (2007) **449**(7165):1003-7. Epub 2007/10/16. doi: 10.1038/nature06196. PubMed PMID: 17934449.

18. Farin HF, Van Es JH, Clevers H. Redundant sources of Wnt regulate intestinal stem cells and promote formation of Paneth cells. *Gastroenterology* (2012) **143**(6):1518-29 e7. Epub 2012/08/28. doi: 10.1053/j.gastro.2012.08.031. PubMed PMID: 22922422.

19. van de Wetering M, Sancho E, Verweij C, de Lau W, Oving I, Hurlstone A, et al. The beta-catenin/TCF-4 complex imposes a crypt progenitor phenotype on colorectal cancer cells. *Cell* (2002) **111**(2):241-50. Epub 2002/11/01. PubMed PMID: 12408868.

20. Moore KA, Lemischka IR. Stem cells and their niches. *Science (New York, NY)* (2006) **311**(5769):1880-5. Epub 2006/04/01. doi: 10.1126/science.1110542. PubMed PMID: 16574858.

21. van der Flier LG, Clevers H. Stem cells, self-renewal, and differentiation in the intestinal epithelium. *Annu Rev Physiol* (2009) **71**:241-60. Epub 2008/09/24. doi: 10.1146/annurev.physiol.010908.163145. PubMed PMID: 18808327.

22. Krausova M, Korinek V. Wnt signaling in adult intestinal stem cells and cancer. *Cell Signal* (2014) **26**(3):570-9. Epub 2013/12/07. doi: 10.1016/j.cellsig.2013.11.032. PubMed PMID: 24308963.

23. Reya T, Clevers H. Wnt signalling in stem cells and cancer. *Nature* (2005) **434**(7035):843-50. Epub 2005/04/15. doi: 10.1038/nature03319. PubMed PMID: 15829953.

24. Eastman Q, Grosschedl R. Regulation of LEF-1/TCF transcription factors by Wnt and other signals. *Curr Opin Cell Biol* (1999) **11**(2):233-40. Epub 1999/04/21. PubMed PMID: 10209158.

25. Olsen AK, Boyd M, Danielsen ET, Troelsen JT. Current and emerging approaches to define intestinal epithelium-specific transcriptional networks. *Am J Physiol Gastrointest Liver Physiol* (2012) **302**(3):G277-86. Epub 2011/11/19. doi: 10.1152/ajpgi.00362.2011. PubMed PMID: 22094602.

26. Binnerts ME, Kim KA, Bright JM, Patel SM, Tran K, Zhou M, et al. R-Spondin1 regulates Wnt signaling by inhibiting internalization of LRP6. *Proceedings of the National Academy of Sciences of the United States of America* (2007) **104**(37):14700-5. Epub 2007/09/07. doi: 10.1073/pnas.0702305104. PubMed PMID: 17804805; PubMed Central PMCID: PMCPMC1965484.

27. Barker N. Adult intestinal stem cells: critical drivers of epithelial homeostasis and regeneration. *Nat Rev Mol Cell Biol* (2014) **15**(1):19-33. Epub 2013/12/12. doi: 10.1038/nrm3721. PubMed PMID: 24326621.

28. Heath JP. Epithelial cell migration in the intestine. *Cell Biol Int* (1996) **20**(2):139-46. Epub 1996/02/01. doi: 10.1006/cbir.1996.0018. PubMed PMID: 8935158.

29. Guan Y, Watson AJ, Marchiando AM, Bradford E, Shen L, Turner JR, et al. Redistribution of the tight junction protein ZO-1 during physiological shedding of mouse intestinal epithelial cells. *Am J Physiol Cell Physiol* (2011) **300**(6):C1404-14. Epub 2011/02/25. doi: 10.1152/ajpcell.00270.2010. PubMed PMID: 21346149; PubMed Central PMCID: PMCPMC3118625.

30. Barker N, van de Wetering M, Clevers H. The intestinal stem cell. *Genes Dev* (2008) **22**(14):1856-64. Epub 2008/07/17. doi: 10.1101/gad.1674008. PubMed PMID: 18628392; PubMed Central PMCID: PMCPMC2735277.

31. Clevers H. The intestinal crypt, a prototype stem cell compartment. *Cell* (2013) **154**(2):274-84. Epub 2013/07/23. doi: 10.1016/j.cell.2013.07.004. PubMed PMID: 23870119.

32. Bevins CL, Salzman NH. Paneth cells, antimicrobial peptides and maintenance of intestinal homeostasis. *Nat Rev Microbiol* (2011) **9**(5):356-68. Epub 2011/03/23. doi: 10.1038/nrmicro2546. PubMed PMID: 21423246.

33. Jones DE, Bevins CL. Paneth cells of the human small intestine express an antimicrobial peptide gene. *J Biol Chem* (1992) **267**(32):23216-25. Epub 1992/11/15. PubMed PMID: 1429669.

34. Johansson ME, Hansson GC. Immunological aspects of intestinal mucus and mucins. *Nat Rev Immunol* (2016) **16**(10):639-49. Epub 2016/08/09. doi: 10.1038/nri.2016.88. PubMed PMID: 27498766.

35. Velcich A, Yang W, Heyer J, Fragale A, Nicholas C, Viani S, et al. Colorectal cancer in mice genetically deficient in the mucin Muc2. *Science (New York, NY)* (2002) **295**(5560):1726-9. Epub 2002/03/02. doi: 10.1126/science.1069094. PubMed PMID: 11872843.

36. Van der Sluis M, De Koning BAE, De Bruijn ACJM, Velcich A, Meijerink JPP, Van Goudoever JB, et al. Muc2-deficient mice spontaneously develop colitis, indicating that MUC2 is critical for colonic protection. *Gastroenterology* (2006) **131**(1):117-29.

37. Karam SM. Lineage commitment and maturation of epithelial cells in the gut. *Front Biosci* (1999) **4**(1):D286-98. Epub 1999/03/17. PubMed PMID: 10077541.

38. Pott J, Hornef M. Innate immune signalling at the intestinal epithelium in homeostasis and disease. *EMBO Rep* (2012) **13**(8):684-98. Epub 2012/07/18. doi: 10.1038/embor.2012.96. PubMed PMID: 22801555; PubMed Central PMCID: PMCPMC3410395.

39. Johansson ME, Larsson JM, Hansson GC. The two mucus layers of colon are organized by the MUC2 mucin, whereas the outer layer is a legislator of host-microbial interactions. *Proceedings of the National Academy of Sciences of the United States of America* (2011) **108 Suppl 1**(Supplement 1):4659-65. Epub 2010/07/10. doi: 10.1073/pnas.1006451107. PubMed PMID: 20615996; PubMed Central PMCID: PMCPMC3063600.

40. Johansson ME, Phillipson M, Petersson J, Velcich A, Holm L, Hansson GC. The inner of the two Muc2 mucin-dependent mucus layers in colon is devoid of bacteria. *Proceedings of the National Academy of Sciences of the United States of America* (2008) **105**(39):15064-9. Epub 2008/09/23. doi: 10.1073/pnas.0803124105. PubMed PMID: 18806221; PubMed Central PMCID: PMCPMC2567493.

41. Mantis NJ, Rol N, Corthesy B. Secretory IgA's complex roles in immunity and mucosal homeostasis in the gut. *Mucosal Immunol* (2011) **4**(6):603-11. Epub 2011/10/07. doi: 10.1038/mi.2011.41. PubMed PMID: 21975936; PubMed Central PMCID: PMCPMC3774538.

42. Boullier S, Tanguy M, Kadaoui KA, Caubet C, Sansonetti P, Corthesy B, et al. Secretory IgA-mediated neutralization of Shigella flexneri prevents intestinal tissue destruction by down-regulating inflammatory circuits. *Journal of immunology (Baltimore, Md : 1950)* (2009) **183**(9):5879-85. Epub 2009/10/16. doi: 10.4049/jimmunol.0901838. PubMed PMID: 19828639.

43. Pabst O. New concepts in the generation and functions of IgA. *Nat Rev Immunol* (2012) **12**(12):821-32. Epub 2012/10/30. doi: 10.1038/nri3322. PubMed PMID: 23103985.

44. Palm NW, de Zoete MR, Cullen TW, Barry NA, Stefanowski J, Hao L, et al. Immunoglobulin A coating identifies colitogenic bacteria in inflammatory bowel disease. *Cell* (2014) **158**(5):1000-10. Epub 2014/08/30. doi: 10.1016/j.cell.2014.08.006. PubMed PMID: 25171403; PubMed Central PMCID: PMCPMC4174347.

45. Mabbott NA, Donaldson DS, Ohno H, Williams IR, Mahajan A. Microfold (M) cells: important immunosurveillance posts in the intestinal epithelium. *Mucosal Immunol* (2013) **6**(4):666-77. Epub 2013/05/23. doi: 10.1038/mi.2013.30. PubMed PMID: 23695511; PubMed Central PMCID: PMCPMC3686595.

46. Miller H, Zhang J, Kuolee R, Patel GB, Chen W. Intestinal M cells: the fallible sentinels? *World J Gastroenterol* (2007) **13**(10):1477-86. Epub 2007/04/28. PubMed PMID: 17461437; PubMed Central PMCID: PMCPMC1876659.

47. Neutra MR, Frey A, Kraehenbuhl JP. Epithelial M cells: gateways for mucosal infection and immunization. *Cell* (1996) **86**(3):345-8. Epub 1996/08/09. PubMed PMID: 8756716.

48. Bjerknes M, Khandanpour C, Moroy T, Fujiyama T, Hoshino M, Klisch TJ, et al. Origin of the brush cell lineage in the mouse intestinal epithelium. *Dev Biol* (2012) **362**(2):194-218. Epub 2011/12/22. doi: 10.1016/j.ydbio.2011.12.009. PubMed PMID: 22185794.

49. Sbarbati A, Osculati F. A new fate for old cells: brush cells and related elements. *J Anat* (2005) **206**(4):349-58. Epub 2005/04/09. doi: 10.1111/j.1469-7580.2005.00403.x. PubMed PMID: 15817103; PubMed Central PMCID: PMCPMC1571484.

50. Gerbe F, Sidot E, Smyth DJ, Ohmoto M, Matsumoto I, Dardalhon V, et al. Intestinal epithelial tuft cells initiate type 2 mucosal immunity to helminth parasites. *Nature* (2016) **529**(7585):226-30. Epub 2016/01/15. doi: 10.1038/nature16527. PubMed PMID: 26762460.

51. Howitt MR, Lavoie S, Michaud M, Blum AM, Tran SV, Weinstock JV, et al. Tuft cells, taste-chemosensory cells, orchestrate parasite type 2 immunity in the gut. *Science (New York, NY)* (2016) **351**(6279):1329-33. Epub 2016/02/06. doi: 10.1126/science.aaf1648. PubMed PMID: 26847546; PubMed Central PMCID: PMCPMC5528851.

52. von Moltke J, Ji M, Liang HE, Locksley RM. Tuft-cell-derived IL-25 regulates an intestinal ILC2-epithelial response circuit. *Nature* (2016) **529**(7585):221-5. Epub 2015/12/18. doi: 10.1038/nature16161. PubMed PMID: 26675736; PubMed Central PMCID: PMCPMC4830391.

53. McDole JR, Wheeler LW, McDonald KG, Wang B, Konjufca V, Knoop KA, et al. Goblet cells deliver luminal antigen to CD103+ dendritic cells in the small intestine. *Nature* (2012) **483**(7389):345-9. Epub 2012/03/17. doi: 10.1038/nature10863. PubMed PMID: 22422267; PubMed Central PMCID: PMCPMC3313460.

54. Shan M, Gentile M, Yeiser JR, Walland AC, Bornstein VU, Chen K, et al. Mucus enhances gut homeostasis and oral tolerance by delivering immunoregulatory signals. *Science (New York, NY)* (2013) **342**(6157):447-53. Epub 2013/09/28. doi: 10.1126/science.1237910. PubMed PMID: 24072822; PubMed Central PMCID: PMCPMC4005805.

55. Sano T, Huang W, Hall JA, Yang Y, Chen A, Gavzy SJ, et al. An IL-23R/IL-22 Circuit Regulates Epithelial Serum Amyloid A to Promote Local Effector Th17 Responses. *Cell* (2015) **163**(2):381-93. Epub 2015/09/29. doi: 10.1016/j.cell.2015.08.061. PubMed PMID: 26411290; PubMed Central PMCID: PMCPMC4621768.

56. Ivanov, II, Atarashi K, Manel N, Brodie EL, Shima T, Karaoz U, et al. Induction of intestinal Th17 cells by segmented filamentous bacteria. *Cell* (2009) **139**(3):485-98. Epub 2009/10/20. doi: 10.1016/j.cell.2009.09.033. PubMed PMID: 19836068; PubMed Central PMCID: PMCPMC2796826.

57. Owens BM, Simmons A. Intestinal stromal cells in mucosal immunity and homeostasis. *Mucosal Immunol* (2013) **6**(2):224-34. Epub 2012/12/14. doi: 10.1038/mi.2012.125. PubMed PMID: 23235744.

58. Powell DW, Pinchuk IV, Saada JI, Chen X, Mifflin RC. Mesenchymal cells of the intestinal lamina propria. *Annu Rev Physiol* (2011) **73**:213-37. Epub 2010/11/09. doi: 10.1146/annurev.physiol.70.113006.100646. PubMed PMID: 21054163; PubMed Central PMCID: PMCPMC3754809.

59. Pinchuk IV, Mifflin RC, Saada JI, Powell DW. Intestinal mesenchymal cells. *Curr Gastroenterol Rep* (2010) **12**(5):310-8. Epub 2010/08/07. doi: 10.1007/s11894-010-0135-y. PubMed PMID: 20690004; PubMed Central PMCID: PMCPMC2975955.

60. Gregorieff A, Pinto D, Begthel H, Destree O, Kielman M, Clevers H. Expression pattern of Wnt signaling components in the adult intestine. *Gastroenterology* (2005) **129**(2):626-38. Epub 2005/08/09. doi: 10.1016/j.gastro.2005.06.007. PubMed PMID: 16083717.

61. Otte JM, Rosenberg IM, Podolsky DK. Intestinal myofibroblasts in innate immune responses of the intestine. *Gastroenterology* (2003) **124**(7):1866-78. Epub 2003/06/14. PubMed PMID: 12806620.

62. Murphy K, Weaver C. *Janeway's immunobiology*: Garland Science (2016).

63. Hoffmann JA, Kafatos FC, Janeway CA, Ezekowitz RA. Phylogenetic perspectives in innate immunity. *Science (New York, NY)* (1999) **284**(5418):1313-8. Epub 1999/05/21. PubMed PMID: 10334979.

64. Medzhitov R. Recognition of microorganisms and activation of the immune response. *Nature* (2007) **449**(7164):819-26. Epub 2007/10/19. doi: 10.1038/nature06246. PubMed PMID: 17943118.

65. Kawamoto H, Minato N. Myeloid cells. *Int J Biochem Cell Biol* (2004) **36**(8):1374-9. Epub 2004/05/19. doi: 10.1016/j.biocel.2004.01.020. PubMed PMID: 15147715.

66. Ganz T, Selsted ME, Szklarek D, Harwig SS, Daher K, Bainton DF, et al. Defensins. Natural peptide antibiotics of human neutrophils. *J Clin Invest* (1985) **76**(4):1427-35. Epub 1985/10/01. doi: 10.1172/JCI112120. PubMed PMID: 2997278; PubMed Central PMCID: PMCPMC424093.

67. Reeves EP, Lu H, Jacobs HL, Messina CG, Bolsover S, Gabella G, et al. Killing activity of neutrophils is mediated through activation of proteases by K+ flux. *Nature* (2002) **416**(6878):291-7. Epub 2002/03/22. doi: 10.1038/416291a. PubMed PMID: 11907569.

68. Hampton MB, Kettle AJ, Winterbourn CC. Inside the neutrophil phagosome: oxidants, myeloperoxidase, and bacterial killing. *Blood* (1998) **92**(9):3007-17. Epub 1998/10/27. PubMed PMID: 9787133.

69. Brinkmann V, Reichard U, Goosmann C, Fauler B, Uhlemann Y, Weiss DS, et al. Neutrophil extracellular traps kill bacteria. *Science (New York, NY)* (2004) **303**(5663):1532-5. Epub 2004/03/06. doi: 10.1126/science.1092385. PubMed PMID: 15001782.

70. Brinkmann V, Zychlinsky A. Beneficial suicide: why neutrophils die to make NETs. *Nat Rev Microbiol* (2007) **5**(8):577-82. Epub 2007/07/17. doi: 10.1038/nrmicro1710. PubMed PMID: 17632569.

71. Nathan C. Neutrophils and immunity: challenges and opportunities. *Nat Rev Immunol* (2006) **6**(3):173-82. Epub 2006/02/25. doi: 10.1038/nri1785. PubMed PMID: 16498448.

72. Gleich GJ, Frigas E, Loegering DA, Wassom DL, Steinmuller D. Cytotoxic properties of the eosinophil major basic protein. *Journal of immunology (Baltimore, Md : 1950)* (1979) **123**(6):2925-7. Epub 1979/12/01. PubMed PMID: 501097.

73. Bochner BS, Schleimer RP. Mast cells, basophils, and eosinophils: distinct but overlapping pathways for recruitment. *Immunological reviews* (2001) **179**(1):5-15. Epub 2001/04/09. PubMed PMID: 11292027.

74. Iwasaki A, Medzhitov R. Regulation of adaptive immunity by the innate immune system. *Science (New York, NY)* (2010) **327**(5963):291-5. Epub 2010/01/16. doi: 10.1126/science.1183021. PubMed PMID: 20075244; PubMed Central PMCID: PMCPMC3645875.

75. Hamilos DL. Antigen presenting cells. *Immunol Res* (1989) **8**(2):98-117. Epub 1989/01/01. PubMed PMID: 2659691.

76. Powrie F, Read S, Mottet C, Uhlig H, Maloy K. Control of immune pathology by regulatory T cells. *Novartis Foundation symposium* (2003) **252**:92-8; discussion 8-105, 6-14. Epub 2003/11/12. PubMed PMID: 14609214.

77. Kabat AM, Srinivasan N, Maloy KJ. Modulation of immune development and function by intestinal microbiota. *Trends Immunol* (2014) **35**(11):507-17. Epub 2014/08/31. doi: 10.1016/j.it.2014.07.010. PubMed PMID: 25172617.

78. Davies LC, Jenkins SJ, Allen JE, Taylor PR. Tissue-resident macrophages. *Nat Immunol* (2013) **14**(10):986-95. Epub 2013/09/21. doi: 10.1038/ni.2705. PubMed PMID: 24048120; PubMed Central PMCID: PMCPMC4045180.

79. Hashimoto D, Chow A, Noizat C, Teo P, Beasley MB, Leboeuf M, et al. Tissue-resident macrophages self-maintain locally throughout adult life with minimal contribution from circulating monocytes. *Immunity* (2013) **38**(4):792-804. Epub 2013/04/23. doi: 10.1016/j.immuni.2013.04.004. PubMed PMID: 23601688; PubMed Central PMCID: PMCPMC3853406.

80. Gordon S, Taylor PR. Monocyte and macrophage heterogeneity. *Nat Rev Immunol* (2005) **5**(12):953-64. Epub 2005/12/03. doi: 10.1038/nri1733. PubMed PMID: 16322748.

81. Bain CC, Bravo-Blas A, Scott CL, Perdiguero EG, Geissmann F, Henri S, et al. Constant replenishment from circulating monocytes maintains the macrophage pool in the intestine of adult mice. *Nat Immunol* (2014) **15**(10):929-37. Epub 2014/08/26. doi: 10.1038/ni.2967. PubMed PMID: 25151491; PubMed Central PMCID: PMCPMC4169290.

82. Bain CC, Mowat AM. Macrophages in intestinal homeostasis and inflammation. *Immunological reviews* (2014) **260**(1):102-17. Epub 2014/06/20. doi: 10.1111/imr.12192. PubMed PMID: 24942685; PubMed Central PMCID: PMCPMC4141699.

83. Guilliams M, Scott CL. Does niche competition determine the origin of tissue-resident macrophages? *Nature Reviews Immunology* (2017).

84. Denning TL, Wang YC, Patel SR, Williams IR, Pulendran B. Lamina propria macrophages and dendritic cells differentially induce regulatory and interleukin 17-producing T cell responses. *Nat Immunol* (2007) **8**(10):1086-94. Epub 2007/09/18. doi: 10.1038/ni1511. PubMed PMID: 17873879.

85. Murai M, Turovskaya O, Kim G, Madan R, Karp CL, Cheroutre H, et al. Interleukin 10 acts on regulatory T cells to maintain expression of the transcription factor Foxp3 and suppressive function in mice with colitis. *Nat Immunol* (2009) **10**(11):1178-84. Epub 2009/09/29. doi: 10.1038/ni.1791. PubMed PMID: 19783988; PubMed Central PMCID: PMCPMC2898179.

86. Medzhitov R. Origin and physiological roles of inflammation. *Nature* (2008) **454**(7203):428-35. Epub 2008/07/25. doi: 10.1038/nature07201. PubMed PMID: 18650913.

87. Karnovsky ML, Lazdins JK. Biochemical criteria for activated macrophages. *Journal of immunology (Baltimore, Md : 1950)* (1978) **121**(3):809-13. Epub 1978/09/01. PubMed PMID: 357654.

88. Rescigno M, Urbano M, Valzasina B, Francolini M, Rotta G, Bonasio R, et al. Dendritic cells express tight junction proteins and penetrate gut epithelial monolayers to sample bacteria. *Nat Immunol* (2001) **2**(4):361-7. Epub 2001/03/29. doi: 10.1038/86373. PubMed PMID: 11276208.

89. Coombes JL, Siddiqui KR, Arancibia-Carcamo CV, Hall J, Sun CM, Belkaid Y, et al. A functionally specialized population of mucosal CD103+ DCs induces Foxp3+ regulatory T cells via a TGF-beta and retinoic acid-dependent mechanism. *J Exp Med* (2007) **204**(8):1757-64. Epub 2007/07/11. doi: 10.1084/jem.20070590. PubMed PMID: 17620361; PubMed Central PMCID: PMCPMC2118683.

90. Sun CM, Hall JA, Blank RB, Bouladoux N, Oukka M, Mora JR, et al. Small intestine lamina propria dendritic cells promote de novo generation of Foxp3 T reg cells via retinoic acid. *J Exp Med* (2007) **204**(8):1775-85. Epub 2007/07/11. doi: 10.1084/jem.20070602. PubMed PMID: 17620362; PubMed Central PMCID: PMCPMC2118682.

91. Laffont S, Siddiqui KR, Powrie F. Intestinal inflammation abrogates the tolerogenic properties of MLN CD103+ dendritic cells. *European journal of immunology* (2010) **40**(7):1877-83. Epub 2010/05/01. doi: 10.1002/eji.200939957. PubMed PMID: 20432234.

92. Meresse B, Cerf-Bensussan N, editors. Innate T cell responses in human gut. 2009: Elsevier.

93. van Wijk F, Cheroutre H, editors. Intestinal T cells: facing the mucosal immune dilemma with synergy and diversity. 2009: Elsevier.

94. Hayday AC. Gammadelta T cells and the lymphoid stress-surveillance response. *Immunity* (2009) **31**(2):184-96. Epub 2009/08/25. doi: 10.1016/j.immuni.2009.08.006. PubMed PMID: 19699170.

95. Bevan MJ. Helping the CD8(+) T-cell response. *Nat Rev Immunol* (2004) **4**(8):595-602. Epub 2004/08/03. doi: 10.1038/nri1413. PubMed PMID: 15286726.

96. Lighvani AA, Frucht DM, Jankovic D, Yamane H, Aliberti J, Hissong BD, et al. T-bet is rapidly induced by interferon-gamma in lymphoid and myeloid cells. *Proceedings of the National Academy of Sciences of the United States of America* (2001) **98**(26):15137-42. Epub 2001/12/26. doi: 10.1073/pnas.261570598. PubMed PMID: 11752460; PubMed Central PMCID: PMCPMC64996.

97. Smeltz RB, Chen J, Ehrhardt R, Shevach EM. Role of IFN-gamma in Th1 differentiation: IFN-gamma regulates IL-18R alpha expression by preventing the negative effects of IL-4 and by inducing/maintaining IL-12 receptor beta 2 expression. *Journal of immunology (Baltimore, Md : 1950)* (2002) **168**(12):6165-72. Epub 2002/06/11. PubMed PMID: 12055229.

98. Neurath MF, Finotto S, Glimcher LH. The role of Th1/Th2 polarization in mucosal immunity. *Nat Med* (2002) **8**(6):567-73. Epub 2002/06/04. doi: 10.1038/nm0602-567. PubMed PMID: 12042806.

99. Zhu J, Yamane H, Paul WE. Differentiation of effector CD4 T cell populations. *Annual review of immunology* (2009) **28**:445-89.

100. Scott P, Pearce E, Cheever AW, Coffman RL, Sher A. Role of cytokines and CD4+ T-cell subsets in the regulation of parasite immunity and disease. *Immunological reviews* (1989) **112**(1):161-82. Epub 1989/12/01. PubMed PMID: 2575073.

101. Suzuki Y, Orellana MA, Schreiber RD, Remington JS. Interferon-gamma: the major mediator of resistance against Toxoplasma gondii. *Science (New York, NY)* (1988) **240**(4851):516-8. Epub 1988/04/22. PubMed PMID: 3128869.

102. Suzuki Y, Remington JS. The effect of anti-IFN-gamma antibody on the protective effect of Lyt-2+ immune T cells against toxoplasmosis in mice. *Journal of immunology (Baltimore, Md : 1950)* (1990) **144**(5):1954-6. Epub 1990/03/01. PubMed PMID: 2106557.

103. Bettelli E, Sullivan B, Szabo SJ, Sobel RA, Glimcher LH, Kuchroo VK. Loss of T-bet, but not STAT1, prevents the development of experimental autoimmune encephalomyelitis. *Journal of Experimental Medicine* (2004) **200**(1):79-87.

104. Trembleau S, Penna G, Bosi E, Mortara A, Gately MK, Adorini L. Interleukin 12 administration induces T helper type 1 cells and accelerates autoimmune diabetes in NOD mice. *J Exp Med* (1995) **181**(2):817-21. Epub 1995/02/01. PubMed PMID: 7836934; PubMed Central PMCID: PMCPMC2191867.

105. Powrie F, Uhlig H. Animal models of intestinal inflammation: clues to the pathogenesis of inflammatory bowel disease. *Novartis Foundation symposium* (2004) **263**:164-74; discussion 74-8, 211-8. Epub 2005/01/27. PubMed PMID: 15669641.

106. Kitajima M, Lee HC, Nakayama T, Ziegler SF. TSLP enhances the function of helper type 2 cells. *European journal of immunology* (2011) **41**(7):1862-71. Epub 2011/04/13. doi: 10.1002/eji.201041195. PubMed PMID: 21484783; PubMed Central PMCID: PMCPMC3124605.

107. Wynn TA. Type 2 cytokines: mechanisms and therapeutic strategies. *Nat Rev Immunol* (2015) **15**(5):271-82. Epub 2015/04/18. doi: 10.1038/nri3831. PubMed PMID: 25882242.

108. Szabo SJ, Kim ST, Costa GL, Zhang X, Fathman CG, Glimcher LH. A novel transcription factor, T-bet, directs Th1 lineage commitment. *Cell* (2000) **100**(6):655-69. Epub 2000/04/13. PubMed PMID: 10761931.

109. Lubberts E, Joosten LA, Chabaud M, van Den Bersselaar L, Oppers B, Coenen-De Roo CJ, et al. IL-4 gene therapy for collagen arthritis suppresses synovial IL-17 and osteoprotegerin ligand and prevents bone erosion. *J Clin Invest* (2000) **105**(12):1697-710. Epub 2000/06/23. doi: 10.1172/JCI7739. PubMed PMID: 10862785; PubMed Central PMCID: PMCPMC378501.

110. Gause WC, Wynn TA, Allen JE. Type 2 immunity and wound healing: evolutionary refinement of adaptive immunity by helminths. *Nat Rev Immunol* (2013) **13**(8):607-14. Epub 2013/07/06. doi: 10.1038/nri3476. PubMed PMID: 23827958; PubMed Central PMCID: PMCPMC3789590.

111. Pulendran B, Artis D. New paradigms in type 2 immunity. *Science (New York, NY)* (2012) **337**(6093):431-5. Epub 2012/07/28. doi: 10.1126/science.1221064. PubMed PMID: 22837519; PubMed Central PMCID: PMCPMC4078898.

112. Mosmann TR, Coffman RL. TH1 and TH2 cells: different patterns of lymphokine secretion lead to different functional properties. *Annual review of immunology* (1989) **7**(1):145-73. Epub 1989/01/01. doi: 10.1146/annurev.iy.07.040189.001045. PubMed PMID: 2523712.

113. Murphy KM, Reiner SL. The lineage decisions of helper T cells. *Nat Rev Immunol* (2002) **2**(12):933-44. Epub 2002/12/04. doi: 10.1038/nri954. PubMed PMID: 12461566.

114. Ivanov II, McKenzie BS, Zhou L, Tadokoro CE, Lepelley A, Lafaille JJ, et al. The orphan nuclear receptor RORγt directs the differentiation program of proinflammatory IL-17+ T helper cells. *Cell* (2006) **126**(6):1121-33.

115. Ivanov, II, Frutos Rde L, Manel N, Yoshinaga K, Rifkin DB, Sartor RB, et al. Specific microbiota direct the differentiation of IL-17-producing T-helper cells in the mucosa of the small intestine. *Cell Host Microbe* (2008) **4**(4):337-49. Epub 2008/10/16. doi: 10.1016/j.chom.2008.09.009. PubMed PMID: 18854238; PubMed Central PMCID: PMCPMC2597589.

116. Korn T, Bettelli E, Oukka M, Kuchroo VK. IL-17 and Th17 Cells. *Annual review of immunology* (2009) **27**:485-517. Epub 2009/01/10. doi: 10.1146/annurev.immunol.021908.132710. PubMed PMID: 19132915.

117. Maloy KJ, Powrie F. Intestinal homeostasis and its breakdown in inflammatory bowel disease. *Nature* (2011) **474**(7351):298-306. Epub 2011/06/17. doi: 10.1038/nature10208. PubMed PMID: 21677746.

118. Littman DR, Rudensky AY. Th17 and regulatory T cells in mediating and restraining inflammation. *Cell* (2010) **140**(6):845-58. Epub 2010/03/23. doi: 10.1016/j.cell.2010.02.021. PubMed PMID: 20303875.

119. Fouser LA, Wright JF, Dunussi-Joannopoulos K, Collins M. Th17 cytokines and their emerging roles in inflammation and autoimmunity. *Immunological reviews* (2008) **226**(1):87-102. Epub 2009/01/24. doi: 10.1111/j.1600-065X.2008.00712.x. PubMed PMID: 19161418.

120. Basu R, O'Quinn DB, Silberger DJ, Schoeb TR, Fouser L, Ouyang W, et al. Th22 cells are an important source of IL-22 for host protection against enteropathogenic bacteria. *Immunity* (2012) **37**(6):1061-75. Epub 2012/12/04. doi: 10.1016/j.immuni.2012.08.024. PubMed PMID: 23200827; PubMed Central PMCID: PMCPMC3678257.

121. Sonnenberg GF, Fouser LA, Artis D. Border patrol: regulation of immunity, inflammation and tissue homeostasis at barrier surfaces by IL-22. *Nat Immunol* (2011) **12**(5):383-90. Epub 2011/04/20. doi: 10.1038/ni.2025. PubMed PMID: 21502992.

122. Sakaguchi S, Yamaguchi T, Nomura T, Ono M. Regulatory T cells and immune tolerance. *Cell* (2008) **133**(5):775-87. Epub 2008/05/31. doi: 10.1016/j.cell.2008.05.009. PubMed PMID: 18510923.

123. Belkaid Y, Tarbell K. Regulatory T cells in the control of host-microorganism interactions (*). *Annual review of immunology* (2009) **27**:551-89. Epub 2009/03/24. doi: 10.1146/annurev.immunol.021908.132723. PubMed PMID: 19302048.

124. Maloy KJ, Powrie F. Regulatory T cells in the control of immune pathology. *Nat Immunol* (2001) **2**(9):816-22. Epub 2001/08/30. doi: 10.1038/ni0901-816. PubMed PMID: 11526392.

125. Ruscher R, Kummer RL, Lee YJ, Jameson SC, Hogquist KA. CD8αα intraepithelial lymphocytes arise from two main thymic precursors. *Nature immunology* (2017) **18**(7):771.

126. Schon MP, Arya A, Murphy EA, Adams CM, Strauch UG, Agace WW, et al. Mucosal T lymphocyte numbers are selectively reduced in integrin alpha E (CD103)-deficient mice. *Journal of immunology (Baltimore, Md : 1950)* (1999) **162**(11):6641-9. Epub 1999/06/03. PubMed PMID: 10352281.

127. Faria AMC, Reis BS, Mucida D. Tissue adaptation: Implications for gut immunity and tolerance. *J Exp Med* (2017) **214**(5):1211-26. Epub 2017/04/23. doi: 10.1084/jem.20162014. PubMed PMID: 28432200; PubMed Central PMCID: PMCPMC5413340.

128. Kwong B, Lazarevic V. T-bet orchestrates CD8αα IEL differentiation. *Immunity* (2014) **41**(2):169-71.

129. Smith TR, Kumar V. Revival of CD8+ Treg-mediated suppression. *Trends Immunol* (2008) **29**(7):337-42. Epub 2008/06/03. doi: 10.1016/j.it.2008.04.002. PubMed PMID: 18514574.

130. Kunisawa J, Takahashi I, Kiyono H. Intraepithelial lymphocytes: their shared and divergent immunological behaviors in the small and large intestine. *Immunological reviews* (2007) **215**:136-53. Epub 2007/02/13. doi: 10.1111/j.1600-065X.2006.00475.x. PubMed PMID: 17291285.

131. Boismenu R, Havran WL. Modulation of epithelial cell growth by intraepithelial gamma delta T cells. *Science (New York, NY)* (1994) **266**(5188):1253-5. Epub 1994/11/18. PubMed PMID: 7973709.

132. Hamada S, Umemura M, Shiono T, Tanaka K, Yahagi A, Begum MD, et al. IL-17A produced by gammadelta T cells plays a critical role in innate immunity against listeria monocytogenes infection in the liver. *Journal of immunology (Baltimore, Md : 1950)* (2008) **181**(5):3456-63. Epub 2008/08/21. PubMed PMID: 18714018; PubMed Central PMCID: PMCPMC2859669.

133. Umemura M, Yahagi A, Hamada S, Begum MD, Watanabe H, Kawakami K, et al. IL-17-mediated regulation of innate and acquired immune response against pulmonary Mycobacterium bovis bacille Calmette-Guerin infection. *Journal of immunology (Baltimore, Md : 1950)* (2007) **178**(6):3786-96. Epub 2007/03/07. PubMed PMID: 17339477.

134. Martin B, Hirota K, Cua DJ, Stockinger B, Veldhoen M. Interleukin-17-producing gammadelta T cells selectively expand in response to pathogen products and environmental signals. *Immunity* (2009) **31**(2):321-30. Epub 2009/08/18. doi: 10.1016/j.immuni.2009.06.020. PubMed PMID: 19682928.

135. Cheroutre H, Lambolez F, Mucida D. The light and dark sides of intestinal intraepithelial lymphocytes. *Nat Rev Immunol* (2011) **11**(7):445-56. Epub 2011/06/18. doi: 10.1038/nri3007. PubMed PMID: 21681197; PubMed Central PMCID: PMCPMC3140792.

136. van Konijnenburg DPH, Mucida D. Intraepithelial lymphocytes. *Current Biology* (2017) **27**(15):R737-R9.

137. Withers DR. Innate lymphoid cell regulation of adaptive immunity. *Immunology* (2016) **149**(2):123-30. Epub 2016/06/25. doi: 10.1111/imm.12639. PubMed PMID: 27341319; PubMed Central PMCID: PMCPMC5011676.

138. Spits H, Cupedo T. Innate lymphoid cells: emerging insights in development, lineage relationships, and function. *Annual review of immunology* (2012) **30**:647-75. Epub 2012/01/10. doi: 10.1146/annurev-immunol-020711-075053. PubMed PMID: 22224763.

139. Tait Wojno ED, Artis D. Innate lymphoid cells: balancing immunity, inflammation, and tissue repair in the intestine. *Cell Host Microbe* (2012) **12**(4):445-57. Epub 2012/10/23. doi: 10.1016/j.chom.2012.10.003. PubMed PMID: 23084914; PubMed Central PMCID: PMCPMC3584448.

140. Spits H, Artis D, Colonna M, Diefenbach A, Di Santo JP, Eberl G, et al. Innate lymphoid cells--a proposal for uniform nomenclature. *Nat Rev Immunol* (2013) **13**(2):145-9. Epub 2013/01/26. doi: 10.1038/nri3365. PubMed PMID: 23348417.

141. Artis D, Spits H. The biology of innate lymphoid cells. *Nature* (2015) **517**(7534):293-301. Epub 2015/01/17. doi: 10.1038/nature14189. PubMed PMID: 25592534.

142. Lanier LL. Up on the tightrope: natural killer cell activation and inhibition. *Nat Immunol* (2008) **9**(5):495-502. Epub 2008/04/22. doi: 10.1038/ni1581. PubMed PMID: 18425106; PubMed Central PMCID: PMCPMC2669298.

143. Moro K, Yamada T, Tanabe M, Takeuchi T, Ikawa T, Kawamoto H, et al. Innate production of T(H)2 cytokines by adipose tissue-associated c-Kit(+)Sca-1(+) lymphoid cells. *Nature* (2010) **463**(7280):540-4. Epub 2009/12/22. doi: 10.1038/nature08636. PubMed PMID: 20023630.

144. Price AE, Liang HE, Sullivan BM, Reinhardt RL, Eisley CJ, Erle DJ, et al. Systemically dispersed innate IL-13-expressing cells in type 2 immunity. *Proceedings of the National Academy of Sciences of the United States of America* (2010) **107**(25):11489-94. Epub 2010/06/11. doi: 10.1073/pnas.1003988107. PubMed PMID: 20534524; PubMed Central PMCID: PMCPMC2895098.

145. Neill DR, Wong SH, Bellosi A, Flynn RJ, Daly M, Langford TK, et al. Nuocytes represent a new innate effector leukocyte that mediates type-2 immunity. *Nature* (2010) **464**(7293):1367-70. Epub 2010/03/05. doi: 10.1038/nature08900. PubMed PMID: 20200518; PubMed Central PMCID: PMCPMC2862165.

146. Mjosberg J, Bernink J, Golebski K, Karrich JJ, Peters CP, Blom B, et al. The transcription factor GATA3 is essential for the function of human type 2 innate lymphoid cells. *Immunity* (2012) **37**(4):649-59. Epub 2012/10/16. doi: 10.1016/j.immuni.2012.08.015. PubMed PMID: 23063330.

147. Lindemans CA, Calafiore M, Mertelsmann AM, O'Connor MH, Dudakov JA, Jenq RR, et al. Interleukin-22 promotes intestinal-stem-cell-mediated epithelial regeneration. *Nature* (2015) **528**(7583):560-4. Epub 2015/12/10. doi: 10.1038/nature16460. PubMed PMID: 26649819; PubMed Central PMCID: PMCPMC4720437.

148. Buonocore S, Ahern PP, Uhlig HH, Ivanov, II, Littman DR, Maloy KJ, et al. Innate lymphoid cells drive interleukin-23-dependent innate intestinal pathology. *Nature* (2010) **464**(7293):1371-5. Epub 2010/04/16. doi: 10.1038/nature08949. PubMed PMID: 20393462; PubMed Central PMCID: PMCPMC3796764.

149. Geremia A, Arancibia-Carcamo CV, Fleming MP, Rust N, Singh B, Mortensen NJ, et al. IL-23-responsive innate lymphoid cells are increased in inflammatory bowel disease. *J Exp Med* (2011) **208**(6):1127-33. Epub 2011/05/18. doi: 10.1084/jem.20101712. PubMed PMID: 21576383; PubMed Central PMCID: PMCPMC3173242.

150. Coccia M, Harrison OJ, Schiering C, Asquith MJ, Becher B, Powrie F, et al. IL-1beta mediates chronic intestinal inflammation by promoting the accumulation of IL-17A secreting innate lymphoid cells and CD4(+) Th17 cells. *J Exp Med* (2012) **209**(9):1595-609. Epub 2012/08/15. doi: 10.1084/jem.20111453. PubMed PMID: 22891275; PubMed Central PMCID: PMCPMC3428945.

151. Suzuki K, Fagarasan S. Diverse regulatory pathways for IgA synthesis in the gut. *Mucosal Immunol* (2009) **2**(6):468-71. Epub 2009/09/11. doi: 10.1038/mi.2009.107. PubMed PMID: 19741602.

152. Fagarasan S, Kawamoto S, Kanagawa O, Suzuki K. Adaptive immune regulation in the gut: T cell-dependent and T cell-independent IgA synthesis. *Annual review of immunology* (2010) **28**:243-73. Epub 2010/03/03. doi: 10.1146/annurev-immunol-030409-101314. PubMed PMID: 20192805.

153. Slack E, Hapfelmeier S, Stecher B, Velykoredko Y, Stoel M, Lawson MA, et al. Innate and adaptive immunity cooperate flexibly to maintain host-microbiota mutualism. *Science (New York, NY)* (2009) **325**(5940):617-20. Epub 2009/08/01. doi: 10.1126/science.1172747. PubMed PMID: 19644121; PubMed Central PMCID: PMCPMC3730530.

154. Kurashima Y, Kiyono H. Mucosal Ecological Network of Epithelium and Immune Cells for Gut Homeostasis and Tissue Healing. *Annual review of immunology* (2017) **35**:119-47. Epub 2017/01/27. doi: 10.1146/annurev-immunol-051116-052424. PubMed PMID: 28125357.

155. Chen GY, Stappenbeck TS. Mucus, it is not just a static barrier. *Sci Signal* (2014) **7**(323):pe11. Epub 2014/05/02. doi: 10.1126/scisignal.2005357. PubMed PMID: 24782564.

156. Coombes JL, Robinson NJ, Maloy KJ, Uhlig HH, Powrie F. Regulatory T cells and intestinal homeostasis. *Immunological reviews* (2005) **204**:184-94. Epub 2005/03/26. doi: 10.1111/j.0105-2896.2005.00250.x. PubMed PMID: 15790359.

157. Kapsenberg ML. Dendritic-cell control of pathogen-driven T-cell polarization. *Nat Rev Immunol* (2003) **3**(12):984-93. Epub 2003/12/04. doi: 10.1038/nri1246. PubMed PMID: 14647480.

158. van de Veerdonk FL, Netea MG, Dinarello CA, Joosten LA. Inflammasome activation and IL-1beta and IL-18 processing during infection. *Trends Immunol* (2011) **32**(3):110-6. Epub 2011/02/22. doi: 10.1016/j.it.2011.01.003. PubMed PMID: 21333600.

159. Shale M, Schiering C, Powrie F. CD4(+) T-cell subsets in intestinal inflammation. *Immunological reviews* (2013) **252**(1):164-82. Epub 2013/02/15. doi: 10.1111/imr.12039. PubMed PMID: 23405904; PubMed Central PMCID: PMCPMC3736165.

160. Khor B, Gardet A, Xavier RJ. Genetics and pathogenesis of inflammatory bowel disease. *Nature* (2011) **474**(7351):307-17. Epub 2011/06/17. doi: 10.1038/nature10209. PubMed PMID: 21677747; PubMed Central PMCID: PMCPMC3204665.

161. Barrett JC, Hansoul S, Nicolae DL, Cho JH, Duerr RH, Rioux JD, et al. Genome-wide association defines more than 30 distinct susceptibility loci for Crohn's disease. *Nat Genet* (2008) **40**(8):955-62. Epub 2008/07/01. doi: 10.1038/ng.175. PubMed PMID: 18587394; PubMed Central PMCID: PMCPMC2574810.

162. Imielinski M, Baldassano RN, Griffiths A, Russell RK, Annese V, Dubinsky M, et al. Common variants at five new loci associated with early-onset inflammatory bowel disease. *Nat Genet* (2009) **41**(12):1335-40. Epub 2009/11/17. doi: 10.1038/ng.489. PubMed PMID: 19915574; PubMed Central PMCID: PMCPMC3267927.

163. Srinivasan N. Telling apart friend from foe: discriminating between commensals and pathogens at mucosal sites. *Innate immunity* (2010) **16**(6):391-404. Epub 2010/01/20. doi: 10.1177/1753425909357577. PubMed PMID: 20083498.

164. Gagliani N, Palm NW, de Zoete MR, Flavell RA. Inflammasomes and intestinal homeostasis: regulating and connecting infection, inflammation and the microbiota. *Int Immunol* (2014) **26**(9):495-9. Epub 2014/06/21. doi: 10.1093/intimm/dxu066. PubMed PMID: 24948595; PubMed Central PMCID: PMCPMC4200027.

165. Janeway CA, Jr. Approaching the asymptote? Evolution and revolution in immunology. *Cold Spring Harb Symp Quant Biol* (1989) **54 Pt 1**:1-13. Epub 1989/01/01. PubMed PMID: 2700931.

166. Davis BK, Wen H, Ting JP. The inflammasome NLRs in immunity, inflammation, and associated diseases. *Annual review of immunology* (2011) **29**:707-35. Epub 2011/01/12. doi: 10.1146/annurev-immunol-031210-101405. PubMed PMID: 21219188; PubMed Central PMCID: PMCPMC4067317.

167. Kumar H, Kawai T, Akira S. Pathogen recognition by the innate immune system. *Int Rev Immunol* (2011) **30**(1):16-34. Epub 2011/01/18. doi: 10.3109/08830185.2010.529976. PubMed PMID: 21235323.

168. Kawai T, Akira S. The role of pattern-recognition receptors in innate immunity: update on Toll-like receptors. *Nat Immunol* (2010) **11**(5):373-84. Epub 2010/04/21. doi: 10.1038/ni.1863. PubMed PMID: 20404851.

169. von Moltke J, Ayres JS, Kofoed EM, Chavarria-Smith J, Vance RE. Recognition of bacteria by inflammasomes. *Annual review of immunology* (2013) **31**:73-106. Epub 2012/12/12. doi: 10.1146/annurev-immunol-032712-095944. PubMed PMID: 23215645.

170. Ayres JS. Inflammasome-microbiota interplay in host physiologies. *Cell Host Microbe* (2013) **14**(5):491-7. Epub 2013/11/19. doi: 10.1016/j.chom.2013.10.013. PubMed PMID: 24237695.

171. Satoh T, Akira S. Toll-Like Receptor Signaling and Its Inducible Proteins. *Microbiol Spectr* (2016) **4**(6). Epub 2017/01/14. doi: 10.1128/microbiolspec.MCHD-0040-2016. PubMed PMID: 28084212.

172. Kawai T, Akira S. Toll-like receptors and their crosstalk with other innate receptors in infection and immunity. *Immunity* (2011) **34**(5):637-50. Epub 2011/05/28. doi: 10.1016/j.immuni.2011.05.006. PubMed PMID: 21616434.

173. Kawasaki T, Kawai T. Toll-like receptor signaling pathways. *Frontiers in immunology* (2014) **5**:461. Epub 2014/10/14. doi: 10.3389/fimmu.2014.00461. PubMed PMID: 25309543; PubMed Central PMCID: PMCPMC4174766.

174. Moresco EM, LaVine D, Beutler B. Toll-like receptors. *Curr Biol* (2011) **21**(13):R488-93. Epub 2011/07/12. doi: 10.1016/j.cub.2011.05.039. PubMed PMID: 21741580.

175. Pahl HL. Activators and target genes of Rel/NF-κB transcription factors. *Oncogene* (1999) **18**(49).

176. Pasare C, Medzhitov R. Toll-like receptors: linking innate and adaptive immunity. *Adv Exp Med Biol* (2005) **560**:11-8. Epub 2005/06/04. doi: 10.1007/0-387-24180-9_2. PubMed PMID: 15932016.

177. Brandl K, Sun L, Neppl C, Siggs OM, Le Gall SM, Tomisato W, et al. MyD88 signaling in nonhematopoietic cells protects mice against induced colitis by regulating specific EGF receptor ligands. *Proceedings of the National Academy of Sciences of the United States of America* (2010) **107**(46):19967-72. Epub 2010/11/03. doi: 10.1073/pnas.1014669107. PubMed PMID: 21041656; PubMed Central PMCID: PMCPMC2993336.

178. Rakoff-Nahoum S, Paglino J, Eslami-Varzaneh F, Edberg S, Medzhitov R. Recognition of commensal microflora by toll-like receptors is required for intestinal homeostasis. *Cell* (2004) **118**(2):229-41. Epub 2004/07/21. doi: 10.1016/j.cell.2004.07.002. PubMed PMID: 15260992.

179. Johansen FE, Kaetzel CS. Regulation of the polymeric immunoglobulin receptor and IgA transport: new advances in environmental factors that stimulate pIgR expression and its role in mucosal immunity. *Mucosal Immunol* (2011) **4**(6):598-602. Epub 2011/10/01. doi: 10.1038/mi.2011.37. PubMed PMID: 21956244; PubMed Central PMCID: PMCPMC3196803.

180. Bruno ME, Frantz AL, Rogier EW, Johansen FE, Kaetzel CS. Regulation of the polymeric immunoglobulin receptor by the classical and alternative NF-kappaB pathways in intestinal epithelial cells. *Mucosal Immunol* (2011) **4**(4):468-78. Epub 2011/04/01. doi: 10.1038/mi.2011.8. PubMed PMID: 21451502; PubMed Central PMCID: PMCPMC3125104.

181. Lotz M, Gutle D, Walther S, Menard S, Bogdan C, Hornef MW. Postnatal acquisition of endotoxin tolerance in intestinal epithelial cells. *J Exp Med* (2006) **203**(4):973-84. Epub 2006/04/12. doi: 10.1084/jem.20050625. PubMed PMID: 16606665; PubMed Central PMCID: PMCPMC2118301.

182. Otte JM, Cario E, Podolsky DK. Mechanisms of cross hyporesponsiveness to Toll-like receptor bacterial ligands in intestinal epithelial cells. *Gastroenterology* (2004) **126**(4):1054-70. Epub 2004/04/02. PubMed PMID: 15057745.

183. Neish AS, Gewirtz AT, Zeng H, Young AN, Hobert ME, Karmali V, et al. Prokaryotic regulation of epithelial responses by inhibition of IkappaB-alpha ubiquitination. *Science (New York, NY)* (2000) **289**(5484):1560-3. Epub 2000/09/01. PubMed PMID: 10968793.

184. Barton GM, Kagan JC. A cell biological view of Toll-like receptor function: regulation through compartmentalization. *Nat Rev Immunol* (2009) **9**(8):535-42. Epub 2009/06/27. doi: 10.1038/nri2587. PubMed PMID: 19556980; PubMed Central PMCID: PMCPMC3934928.

185. Wang J, Hu Y, Deng WW, Sun B. Negative regulation of Toll-like receptor signaling pathway. *Microbes Infect* (2009) **11**(3):321-7. Epub 2009/01/17. doi: 10.1016/j.micinf.2008.12.011. PubMed PMID: 19146978.

186. Gewirtz AT, Navas TA, Lyons S, Godowski PJ, Madara JL. Cutting edge: bacterial flagellin activates basolaterally expressed TLR5 to induce epithelial proinflammatory gene expression. *Journal of immunology (Baltimore, Md : 1950)* (2001) **167**(4):1882-5. Epub 2001/08/08. PubMed PMID: 11489966.

187. Cario E, Rosenberg IM, Brandwein SL, Beck PL, Reinecker HC, Podolsky DK. Lipopolysaccharide activates distinct signaling pathways in intestinal epithelial cell lines expressing Toll-like receptors. *Journal of immunology (Baltimore, Md : 1950)* (2000) **164**(2):966-72. Epub 2000/01/07. PubMed PMID: 10623846.

188. Lee J, Mo JH, Katakura K, Alkalay I, Rucker AN, Liu YT, et al. Maintenance of colonic homeostasis by distinctive apical TLR9 signalling in intestinal epithelial cells. *Nat Cell Biol* (2006) **8**(12):1327-36. Epub 2006/11/28. doi: 10.1038/ncb1500. PubMed PMID: 17128265.

189. Abreu MT. Toll-like receptor signalling in the intestinal epithelium: how bacterial recognition shapes intestinal function. *Nat Rev Immunol* (2010) **10**(2):131-44. Epub 2010/01/26. doi: 10.1038/nri2707. PubMed PMID: 20098461.

190. Latz E. The inflammasomes: mechanisms of activation and function. *Curr Opin Immunol* (2010) **22**(1):28-33. Epub 2010/01/12. doi: 10.1016/j.coi.2009.12.004. PubMed PMID: 20060699; PubMed Central PMCID: PMCPMC2844336.

191. Pandey S, Kawai T, Akira S. Microbial sensing by Toll-like receptors and intracellular nucleic acid sensors. *Cold Spring Harb Perspect Biol* (2014) **7**(1):a016246. Epub 2014/10/11. doi: 10.1101/cshperspect.a016246. PubMed PMID: 25301932; PubMed Central PMCID: PMCPMC4292165.

192. Jin MS, Kim SE, Heo JY, Lee ME, Kim HM, Paik SG, et al. Crystal structure of the TLR1-TLR2 heterodimer induced by binding of a tri-acylated lipopeptide. *Cell* (2007) **130**(6):1071-82. Epub 2007/09/25. doi: 10.1016/j.cell.2007.09.008. PubMed PMID: 17889651.

193. Takeuchi O, Sato S, Horiuchi T, Hoshino K, Takeda K, Dong Z, et al. Cutting edge: role of Toll-like receptor 1 in mediating immune response to microbial lipoproteins. *Journal of immunology (Baltimore, Md : 1950)* (2002) **169**(1):10-4. Epub 2002/06/22. PubMed PMID: 12077222.

194. Bernard JJ, Cowing-Zitron C, Nakatsuji T, Muehleisen B, Muto J, Borkowski AW, et al. Ultraviolet radiation damages self noncoding RNA and is detected by TLR3. *Nat Med* (2012) **18**(8):1286-90. Epub 2012/07/10. doi: 10.1038/nm.2861. PubMed PMID: 22772463; PubMed Central PMCID: PMCPMC3812946.

195. Takemura N, Kawasaki T, Kunisawa J, Sato S, Lamichhane A, Kobiyama K, et al. Blockade of TLR3 protects mice from lethal radiation-induced gastrointestinal syndrome. *Nat Commun* (2014) **5**:3492. Epub 2014/03/19. doi: 10.1038/ncomms4492. PubMed PMID: 24637670; PubMed Central PMCID: PMCPMC3959210.

196. Zhang SY, Jouanguy E, Ugolini S, Smahi A, Elain G, Romero P, et al. TLR3 deficiency in patients with herpes simplex encephalitis. *Science (New York, NY)* (2007) **317**(5844):1522-7. Epub 2007/09/18. doi: 10.1126/science.1139522. PubMed PMID: 17872438.

197. Akira S, Uematsu S, Takeuchi O. Pathogen recognition and innate immunity. *Cell* (2006) **124**(4):783-801. Epub 2006/02/25. doi: 10.1016/j.cell.2006.02.015. PubMed PMID: 16497588.

198. Kang JY, Nan X, Jin MS, Youn SJ, Ryu YH, Mah S, et al. Recognition of lipopeptide patterns by Toll-like receptor 2-Toll-like receptor 6 heterodimer. *Immunity* (2009) **31**(6):873-84. Epub 2009/11/26. doi: 10.1016/j.immuni.2009.09.018. PubMed PMID: 19931471.

199. Mancuso G, Gambuzza M, Midiri A, Biondo C, Papasergi S, Akira S, et al. Bacterial recognition by TLR7 in the lysosomes of conventional dendritic cells. *Nat Immunol* (2009) **10**(6):587-94. Epub 2009/05/12. doi: 10.1038/ni.1733. PubMed PMID: 19430477.

200. Coban C, Igari Y, Yagi M, Reimer T, Koyama S, Aoshi T, et al. Immunogenicity of whole-parasite vaccines against Plasmodium falciparum involves malarial hemozoin and host TLR9. *Cell Host Microbe* (2010) **7**(1):50-61. Epub 2010/02/02. doi: 10.1016/j.chom.2009.12.003. PubMed PMID: 20114028.

201. Yarovinsky F, Zhang D, Andersen JF, Bannenberg GL, Serhan CN, Hayden MS, et al. TLR11 activation of dendritic cells by a protozoan profilin-like protein. *Science (New York, NY)* (2005) **308**(5728):1626-9. Epub 2005/04/30. doi: 10.1126/science.1109893. PubMed PMID: 15860593.

202. Andrade WA, Souza Mdo C, Ramos-Martinez E, Nagpal K, Dutra MS, Melo MB, et al. Combined action of nucleic acid-sensing Toll-like receptors and TLR11/TLR12 heterodimers imparts resistance to Toxoplasma gondii in mice. *Cell Host Microbe* (2013) **13**(1):42-53. Epub 2013/01/08. doi: 10.1016/j.chom.2012.12.003. PubMed PMID: 23290966; PubMed Central PMCID: PMCPMC3552114.

203. Hidmark A, von Saint Paul A, Dalpke AH. Cutting edge: TLR13 is a receptor for bacterial RNA. *Journal of immunology (Baltimore, Md : 1950)* (2012) **189**(6):2717-21. Epub 2012/08/17. doi: 10.4049/jimmunol.1200898. PubMed PMID: 22896636.

204. Li XD, Chen ZJ. Sequence specific detection of bacterial 23S ribosomal RNA by TLR13. *Elife* (2012) **1**:e00102. Epub 2012/10/31. doi: 10.7554/eLife.00102. PubMed PMID: 23110254; PubMed Central PMCID: PMCPMC3482692.

205. Oldenburg M, Kruger A, Ferstl R, Kaufmann A, Nees G, Sigmund A, et al. TLR13 recognizes bacterial 23S rRNA devoid of erythromycin resistance-forming modification. *Science (New York, NY)* (2012) **337**(6098):1111-5. Epub 2012/07/24. doi: 10.1126/science.1220363. PubMed PMID: 22821982.

206. Ausubel FM. Are innate immune signaling pathways in plants and animals conserved? *Nat Immunol* (2005) **6**(10):973-9. Epub 2005/09/24. doi: 10.1038/ni1253. PubMed PMID: 16177805.

207. Latz E, Xiao TS, Stutz A. Activation and regulation of the inflammasomes. *Nat Rev Immunol* (2013) **13**(6):397-411. Epub 2013/05/25. doi: 10.1038/nri3452. PubMed PMID: 23702978; PubMed Central PMCID: PMCPMC3807999.

208. Leipe DD, Koonin EV, Aravind L. STAND, a class of P-loop NTPases including animal and plant regulators of programmed cell death: multiple, complex domain architectures, unusual phyletic patterns, and evolution by horizontal gene transfer. *J Mol Biol* (2004) **343**(1):1-28. Epub 2004/09/24. doi: 10.1016/j.jmb.2004.08.023. PubMed PMID: 15381417.

209. Kofoed EM, Vance RE. Innate immune recognition of bacterial ligands by NAIPs determines inflammasome specificity. *Nature* (2011) **477**(7366):592-5. Epub 2011/08/30. doi: 10.1038/nature10394. PubMed PMID: 21874021; PubMed Central PMCID: PMCPMC3184209.

210. Hu Z, Yan C, Liu P, Huang Z, Ma R, Zhang C, et al. Crystal structure of NLRC4 reveals its autoinhibition mechanism. *Science (New York, NY)* (2013) **341**(6142):172-5. Epub 2013/06/15. doi: 10.1126/science.1236381. PubMed PMID: 23765277.

211. Meunier E, Broz P. Evolutionary Convergence and Divergence in NLR Function and Structure. *Trends Immunol* (2017) **38**(10):744-57. Epub 2017/06/06. doi: 10.1016/j.it.2017.04.005. PubMed PMID: 28579324.

212. Song DH, Lee JO. Sensing of microbial molecular patterns by Toll-like receptors. *Immunological reviews* (2012) **250**(1):216-29. Epub 2012/10/11. doi: 10.1111/j.1600-065X.2012.01167.x. PubMed PMID: 23046132.

213. Tenthorey JL, Kofoed EM, Daugherty MD, Malik HS, Vance RE. Molecular basis for specific recognition of bacterial ligands by NAIP/NLRC4 inflammasomes. *Mol Cell* (2014) **54**(1):17-29. Epub 2014/03/25. doi: 10.1016/j.molcel.2014.02.018. PubMed PMID: 24657167; PubMed Central PMCID: PMCPMC3988258.

214. Ting JP, Lovering RC, Alnemri ES, Bertin J, Boss JM, Davis BK, et al. The NLR gene family: a standard nomenclature. *Immunity* (2008) **28**(3):285-7. Epub 2008/03/18. doi: 10.1016/j.immuni.2008.02.005. PubMed PMID: 18341998; PubMed Central PMCID: PMCPMC2630772.

215. Sanderson IR, Bustin SA, Dziennis S, Paraszczuk J, Stamm DS. Age and diet act through distinct isoforms of the class II transactivator gene in mouse intestinal epithelium. *Gastroenterology* (2004) **127**(1):203-12. Epub 2004/07/06. PubMed PMID: 15236186.

216. Hershberg RM, Cho DH, Youakim A, Bradley MB, Lee JS, Framson PE, et al. Highly polarized HLA class II antigen processing and presentation by human intestinal epithelial cells. *J Clin Invest* (1998) **102**(4):792-803. Epub 1998/08/26. doi: 10.1172/JCI3201. PubMed PMID: 9710448; PubMed Central PMCID: PMCPMC508942.

217. Vance RE. The NAIP/NLRC4 inflammasomes. *Curr Opin Immunol* (2015) **32**:84-9. Epub 2015/01/27. doi: 10.1016/j.coi.2015.01.010. PubMed PMID: 25621709; PubMed Central PMCID: PMCPMC4336817.

218. Maier JK, Balabanian S, Coffill CR, Stewart A, Pelletier L, Franks DJ, et al. Distribution of neuronal apoptosis inhibitory protein in human tissues. *J Histochem Cytochem* (2007) **55**(9):911-23. Epub 2007/05/19. doi: 10.1369/jhc.6A7144.2007. PubMed PMID: 17510375.

219. Allam R, Maillard MH, Tardivel A, Chennupati V, Bega H, Yu CW, et al. Epithelial NAIPs protect against colonic tumorigenesis. *J Exp Med* (2015) **212**(3):369-83. Epub 2015/03/04. doi: 10.1084/jem.20140474. PubMed PMID: 25732303; PubMed Central PMCID: PMCPMC4354369.

220. Sellin ME, Muller AA, Felmy B, Dolowschiak T, Diard M, Tardivel A, et al. Epithelium-intrinsic NAIP/NLRC4 inflammasome drives infected enterocyte expulsion to restrict Salmonella replication in the intestinal mucosa. *Cell Host Microbe* (2014) **16**(2):237-48. Epub 2014/08/15. doi: 10.1016/j.chom.2014.07.001. PubMed PMID: 25121751.

221. Chamaillard M, Hashimoto M, Horie Y, Masumoto J, Qiu S, Saab L, et al. An essential role for NOD1 in host recognition of bacterial peptidoglycan containing diaminopimelic acid. *Nat Immunol* (2003) **4**(7):702-7. Epub 2003/06/11. doi: 10.1038/ni945. PubMed PMID: 12796777.

222. Natividad JM, Petit V, Huang X, de Palma G, Jury J, Sanz Y, et al. Commensal and probiotic bacteria influence intestinal barrier function and susceptibility to colitis in Nod1-/-; Nod2-/- mice. *Inflamm Bowel Dis* (2012) **18**(8):1434-46. Epub 2011/12/14. doi: 10.1002/ibd.22848. PubMed PMID: 22162005.

223. Girardin SE, Boneca IG, Viala J, Chamaillard M, Labigne A, Thomas G, et al. Nod2 is a general sensor of peptidoglycan through muramyl dipeptide (MDP) detection. *J Biol Chem* (2003) **278**(11):8869-72. Epub 2003/01/16. doi: 10.1074/jbc.C200651200. PubMed PMID: 12527755.

224. Girardin SE, Travassos LH, Herve M, Blanot D, Boneca IG, Philpott DJ, et al. Peptidoglycan molecular requirements allowing detection by Nod1 and Nod2. *J Biol Chem* (2003) **278**(43):41702-8. Epub 2003/07/23. doi: 10.1074/jbc.M307198200. PubMed PMID: 12871942.

225. Rosenstiel P, Fantini M, Brautigam K, Kuhbacher T, Waetzig GH, Seegert D, et al. TNF-alpha and IFN-gamma regulate the expression of the NOD2 (CARD15) gene in human intestinal epithelial cells. *Gastroenterology* (2003) **124**(4):1001-9. Epub 2003/04/03. doi: 10.1053/gast.2003.50157. PubMed PMID: 12671897.

226. Petnicki-Ocwieja T, Hrncir T, Liu YJ, Biswas A, Hudcovic T, Tlaskalova-Hogenova H, et al. Nod2 is required for the regulation of commensal microbiota in the intestine. *Proceedings of the National Academy of Sciences of the United States of America* (2009) **106**(37):15813-8. Epub 2009/10/07. doi: 10.1073/pnas.0907722106. PubMed PMID: 19805227; PubMed Central PMCID: PMCPMC2747201.

227. Miao EA, Alpuche-Aranda CM, Dors M, Clark AE, Bader MW, Miller SI, et al. Cytoplasmic flagellin activates caspase-1 and secretion of interleukin 1beta via Ipaf. *Nat Immunol* (2006) **7**(6):569-75. Epub 2006/05/02. doi: 10.1038/ni1344. PubMed PMID: 16648853.

228. Franchi L, Amer A, Body-Malapel M, Kanneganti TD, Ozoren N, Jagirdar R, et al. Cytosolic flagellin requires Ipaf for activation of caspase-1 and interleukin 1beta in salmonella-infected macrophages. *Nat Immunol* (2006) **7**(6):576-82. Epub 2006/05/02. doi: 10.1038/ni1346. PubMed PMID: 16648852.

229. Miao EA, Mao DP, Yudkovsky N, Bonneau R, Lorang CG, Warren SE, et al. Innate immune detection of the type III secretion apparatus through the NLRC4 inflammasome. *Proceedings of the National Academy of Sciences of the United States of America* (2010) **107**(7):3076-80. Epub 2010/02/06. doi: 10.1073/pnas.0913087107. PubMed PMID: 20133635; PubMed Central PMCID: PMCPMC2840275.

230. Rauch I, Deets KA, Ji DX, von Moltke J, Tenthorey JL, Lee AY, et al. NAIP-NLRC4 Inflammasomes Coordinate Intestinal Epithelial Cell Expulsion with Eicosanoid and IL-18 Release via Activation of Caspase-1 and -8. *Immunity* (2017) **46**(4):649-59. Epub 2017/04/16. doi: 10.1016/j.immuni.2017.03.016. PubMed PMID: 28410991; PubMed Central PMCID: PMCPMC5476318.

231. Nordlander S, Pott J, Maloy KJ. NLRC4 expression in intestinal epithelial cells mediates protection against an enteric pathogen. *Mucosal Immunol* (2014) **7**(4):775-85. Epub 2013/11/28. doi: 10.1038/mi.2013.95. PubMed PMID: 24280936; PubMed Central PMCID: PMCPMC4020766.

232. Hu B, Elinav E, Huber S, Booth CJ, Strowig T, Jin C, et al. Inflammation-induced tumorigenesis in the colon is regulated by caspase-1 and NLRC4. *Proceedings of the National Academy of Sciences of the United States of America* (2010) **107**(50):21635-40. Epub 2010/12/02. doi: 10.1073/pnas.1016814108. PubMed PMID: 21118981; PubMed Central PMCID: PMCPMC3003083.

233. Hong M, Yoon SI, Wilson IA. Structure and functional characterization of the RNA-binding element of the NLRX1 innate immune modulator. *Immunity* (2012) **36**(3):337-47. Epub 2012/03/06. doi: 10.1016/j.immuni.2011.12.018. PubMed PMID: 22386589; PubMed Central PMCID: PMCPMC3368889.

234. Tattoli I, Killackey SA, Foerster EG, Molinaro R, Maisonneuve C, Rahman MA, et al. NLRX1 Acts as an Epithelial-Intrinsic Tumor Suppressor through the Modulation of TNF-Mediated Proliferation. *Cell Rep* (2016) **14**(11):2576-86. Epub 2016/03/15. doi: 10.1016/j.celrep.2016.02.065. PubMed PMID: 26971996.

235. Boyden ED, Dietrich WF. Nalp1b controls mouse macrophage susceptibility to anthrax lethal toxin. *Nat Genet* (2006) **38**(2):240-4. Epub 2006/01/24. doi: 10.1038/ng1724. PubMed PMID: 16429160.

236. Faustin B, Lartigue L, Bruey JM, Luciano F, Sergienko E, Bailly-Maitre B, et al. Reconstituted NALP1 inflammasome reveals two-step mechanism of caspase-1 activation. *Mol Cell* (2007) **25**(5):713-24. Epub 2007/03/14. doi: 10.1016/j.molcel.2007.01.032. PubMed PMID: 17349957.

237. Chen C, Wang B, Sun J, Na H, Chen Z, Zhu Z, et al. DAC can restore expression of NALP1 to suppress tumor growth in colon cancer. *Cell Death Dis* (2015) **6**:e1602. Epub 2015/01/23. doi: 10.1038/cddis.2014.532. PubMed PMID: 25611377; PubMed Central PMCID: PMCPMC4669739.

238. Schroder K, Tschopp J. The inflammasomes. *Cell* (2010) **140**(6):821-32. Epub 2010/03/23. doi: 10.1016/j.cell.2010.01.040. PubMed PMID: 20303873.

239. Macia L, Tan J, Vieira AT, Leach K, Stanley D, Luong S, et al. Metabolite-sensing receptors GPR43 and GPR109A facilitate dietary fibre-induced gut homeostasis through regulation of the inflammasome. *Nat Commun* (2015) **6**:6734. Epub 2015/04/02. doi: 10.1038/ncomms7734. PubMed PMID: 25828455.

240. Ruiz PA, Moron B, Becker HM, Lang S, Atrott K, Spalinger MR, et al. Titanium dioxide nanoparticles exacerbate DSS-induced colitis: role of the NLRP3 inflammasome. *Gut* (2017) **66**(7):1216-24. Epub 2016/02/06. doi: 10.1136/gutjnl-2015-310297. PubMed PMID: 26848183; PubMed Central PMCID: PMCPMC5530483.

241. Levy M, Thaiss CA, Zeevi D, Dohnalova L, Zilberman-Schapira G, Mahdi JA, et al. Microbiota-Modulated Metabolites Shape the Intestinal Microenvironment by Regulating NLRP6 Inflammasome Signaling. *Cell* (2015) **163**(6):1428-43. Epub 2015/12/08. doi: 10.1016/j.cell.2015.10.048. PubMed PMID: 26638072; PubMed Central PMCID: PMCPMC5665753.

242. Elinav E, Strowig T, Kau AL, Henao-Mejia J, Thaiss CA, Booth CJ, et al. NLRP6 inflammasome regulates colonic microbial ecology and risk for colitis. *Cell* (2011) **145**(5):745-57. Epub 2011/05/14. doi: 10.1016/j.cell.2011.04.022. PubMed PMID: 21565393; PubMed Central PMCID: PMCPMC3140910.

243. Wlodarska M, Thaiss CA, Nowarski R, Henao-Mejia J, Zhang JP, Brown EM, et al. NLRP6 inflammasome orchestrates the colonic host-microbial interface by regulating goblet cell mucus secretion. *Cell* (2014) **156**(5):1045-59. Epub 2014/03/04. doi: 10.1016/j.cell.2014.01.026. PubMed PMID: 24581500; PubMed Central PMCID: PMCPMC4017640.

244. Normand S, Delanoye-Crespin A, Bressenot A, Huot L, Grandjean T, Peyrin-Biroulet L, et al. Nod-like receptor pyrin domain-containing protein 6 (NLRP6) controls epithelial self-renewal and colorectal carcinogenesis upon injury. *Proceedings of the National Academy of Sciences of the United States of America* (2011) **108**(23):9601-6. Epub 2011/05/20. doi: 10.1073/pnas.1100981108. PubMed PMID: 21593405; PubMed Central PMCID: PMCPMC3111299.

245. Khare S, Dorfleutner A, Bryan NB, Yun C, Radian AD, de Almeida L, et al. An NLRP7-containing inflammasome mediates recognition of microbial lipopeptides in human macrophages. *Immunity* (2012) **36**(3):464-76. Epub 2012/03/01. doi: 10.1016/j.immuni.2012.02.001. PubMed PMID: 22361007; PubMed Central PMCID: PMCPMC3315380.

246. Zhu S, Ding S, Wang P, Wei Z, Pan W, Palm NW, et al. Nlrp9b inflammasome restricts rotavirus infection in intestinal epithelial cells. *Nature* (2017) **546**(7660):667-70. Epub 2017/06/22. doi: 10.1038/nature22967. PubMed PMID: 28636595; PubMed Central PMCID: PMCPMC5787375.

247. Vladimer GI, Weng D, Paquette SW, Vanaja SK, Rathinam VA, Aune MH, et al. The NLRP12 inflammasome recognizes Yersinia pestis. *Immunity* (2012) **37**(1):96-107. Epub 2012/07/31. doi: 10.1016/j.immuni.2012.07.006. PubMed PMID: 22840842; PubMed Central PMCID: PMCPMC3753114.

248. Ratsimandresey RA, Indramohan M, Dorfleutner A, Stehlik C. The AIM2 inflammasome is a central regulator of intestinal homeostasis through the IL-18/IL-22/STAT3 pathway. *Cell Mol Immunol* (2017) **14**(1):127-42. Epub 2016/08/16. doi: 10.1038/cmi.2016.35. PubMed PMID: 27524110; PubMed Central PMCID: PMCPMC5214942.

249. Song-Zhao GX, Srinivasan N, Pott J, Baban D, Frankel G, Maloy KJ. Nlrp3 activation in the intestinal epithelium protects against a mucosal pathogen. *Mucosal Immunol* (2014) **7**(4):763-74. Epub 2013/11/28. doi: 10.1038/mi.2013.94. PubMed PMID: 24280937; PubMed Central PMCID: PMCPMC4048180.

250. Hanby-Flarida MD, Trask OJ, Yang TJ, Baldwin CL. Modulation of WC1, a lineage-specific cell surface molecule of gamma/delta T cells augments cellular proliferation. *Immunology* (1996) **88**(1):116-23. Epub 1996/05/01. PubMed PMID: 8707336; PubMed Central PMCID: PMCPMC1456450.

251. Knodler LA, Crowley SM, Sham HP, Yang H, Wrande M, Ma C, et al. Noncanonical inflammasome activation of caspase-4/caspase-11 mediates epithelial defenses against enteric bacterial pathogens. *Cell Host Microbe* (2014) **16**(2):249-56. Epub 2014/08/15. doi: 10.1016/j.chom.2014.07.002. PubMed PMID: 25121752; PubMed Central PMCID: PMCPMC4157630.

252. Shi J, Zhao Y, Wang Y, Gao W, Ding J, Li P, et al. Inflammatory caspases are innate immune receptors for intracellular LPS. *Nature* (2014) **514**(7521):187-92. Epub 2014/08/15. doi: 10.1038/nature13683. PubMed PMID: 25119034.

253. Oficjalska K, Raverdeau M, Aviello G, Wade SC, Hickey A, Sheehan KM, et al. Protective role for caspase-11 during acute experimental murine colitis. *Journal of immunology (Baltimore, Md : 1950)* (2015) **194**(3):1252-60. Epub 2014/12/31. doi: 10.4049/jimmunol.1400501. PubMed PMID: 25548224; PubMed Central PMCID: PMCPMC4298125.

254. Demon D, Kuchmiy A, Fossoul A, Zhu Q, Kanneganti TD, Lamkanfi M. Caspase-11 is expressed in the colonic mucosa and protects against dextran sodium sulfate-induced colitis. *Mucosal Immunol* (2014) **7**(6):1480-91. Epub 2014/05/23. doi: 10.1038/mi.2014.36. PubMed PMID: 24850431; PubMed Central PMCID: PMCPMC4205216.

255. Harrison OJ, Srinivasan N, Pott J, Schiering C, Krausgruber T, Ilott NE, et al. Epithelial-derived IL-18 regulates Th17 cell differentiation and Foxp3(+) Treg cell function in the intestine. *Mucosal Immunol* (2015) **8**(6):1226-36. Epub 2015/03/05. doi: 10.1038/mi.2015.13. PubMed PMID: 25736457; PubMed Central PMCID: PMCPMC4368110.

256. Zaki MH, Boyd KL, Vogel P, Kastan MB, Lamkanfi M, Kanneganti TD. The NLRP3 inflammasome protects against loss of epithelial integrity and mortality during experimental colitis. *Immunity* (2010) **32**(3):379-91. Epub 2010/03/23. doi: 10.1016/j.immuni.2010.03.003. PubMed PMID: 20303296; PubMed Central PMCID: PMCPMC2982187.

257. Pizarro TT, Michie MH, Bentz M, Woraratanadharm J, Smith MF, Foley E, et al. IL-18, a novel immunoregulatory cytokine, is up-regulated in Crohn's disease: Expression and localization in intestinal mucosal cells. *Journal of Immunology* (1999) **162**(11):6829-35. PubMed PMID: WOS:000080444100066.

258. Dupaul-Chicoine J, Yeretssian G, Doiron K, Bergstrom KS, McIntire CR, LeBlanc PM, et al. Control of intestinal homeostasis, colitis, and colitis-associated colorectal cancer by the inflammatory caspases. *Immunity* (2010) **32**(3):367-78. Epub 2010/03/17. doi: 10.1016/j.immuni.2010.02.012. PubMed PMID: 20226691.

259. Fujii T, Tamura M, Tanaka S, Kato Y, Yamamoto H, Mizushina Y, et al. Gasdermin D (Gsdmd) is dispensable for mouse intestinal epithelium development. *Genesis* (2008) **46**(8):418-23. Epub 2008/08/12. doi: 10.1002/dvg.20412. PubMed PMID: 18693275.

260. Saxena M, Yeretssian G. NOD-Like Receptors: Master Regulators of Inflammation and Cancer. *Frontiers in immunology* (2014) **5**:327. Epub 2014/07/30. doi: 10.3389/fimmu.2014.00327. PubMed PMID: 25071785; PubMed Central PMCID: PMCPMC4095565.

261. Ratsimandresey RA, Dorfleutner A, Stehlik C. An Update on PYRIN Domain-Containing Pattern Recognition Receptors: From Immunity to Pathology. *Frontiers in immunology* (2013) **4**:440. Epub 2013/12/25. doi: 10.3389/fimmu.2013.00440. PubMed PMID: 24367371; PubMed Central PMCID: PMCPMC3856626.

262. Fernandes-Alnemri T, Yu JW, Datta P, Wu J, Alnemri ES. AIM2 activates the inflammasome and cell death in response to cytoplasmic DNA. *Nature* (2009) **458**(7237):509-13. Epub 2009/01/23. doi: 10.1038/nature07710. PubMed PMID: 19158676; PubMed Central PMCID: PMCPMC2862225.

263. Martinon F, Burns K, Tschopp J. The inflammasome: a molecular platform triggering activation of inflammatory caspases and processing of proIL-beta. *Mol Cell* (2002) **10**(2):417-26. Epub 2002/08/23. PubMed PMID: 12191486.

264. Drexler SK, Bonsignore L, Masin M, Tardivel A, Jackstadt R, Hermeking H, et al. Tissue-specific opposing functions of the inflammasome adaptor ASC in the regulation of epithelial skin carcinogenesis. *Proceedings of the National Academy of Sciences of the United States of America* (2012) **109**(45):18384-9. Epub 2012/10/24. doi: 10.1073/pnas.1209171109. PubMed PMID: 23090995; PubMed Central PMCID: PMCPMC3494892.

265. Zmora N, Levy M, Pevsner-Fishcer M, Elinav E. Inflammasomes and intestinal inflammation. *Mucosal Immunol* (2017) **10**(4):865-83. Epub 2017/04/13. doi: 10.1038/mi.2017.19. PubMed PMID: 28401932.

266. Puren AJ, Fantuzzi G, Dinarello CA, editors. Gene expression, synthesis and secretion of IL-18 and IL-18 are differentially regulated in human blood mononuclear cells and mouse spleen cells. 1998: JOHN LIBBEY EUROTEXT LTD 127 AVE DE LA REPUBLIQUE, 92120 MONTROUGE, FRANCE.

267. Dinarello CA, Novick D, Kim S, Kaplanski G. Interleukin-18 and IL-18 binding protein. *Frontiers in immunology* (2013) **4**:289. Epub 2013/10/12. doi: 10.3389/fimmu.2013.00289. PubMed PMID: 24115947; PubMed Central PMCID: PMCPMC3792554.

268. Rathinam VA, Vanaja SK, Fitzgerald KA. Regulation of inflammasome signaling. *Nat Immunol* (2012) **13**(4):333-42. Epub 2012/03/21. doi: 10.1038/ni.2237. PubMed PMID: 22430786; PubMed Central PMCID: PMCPMC3523703.

269. de Zoete MR, Flavell RA. Interactions between Nod-Like Receptors and Intestinal Bacteria. *Frontiers in immunology* (2013) **4**:462. Epub 2014/01/02. doi: 10.3389/fimmu.2013.00462. PubMed PMID: 24381573; PubMed Central PMCID: PMCPMC3865441.

270. de Zoete MR, Palm NW, Zhu S, Flavell RA. Inflammasomes. *Cold Spring Harb Perspect Biol* (2014) **6**(12):a016287. Epub 2014/10/18. doi: 10.1101/cshperspect.a016287. PubMed PMID: 25324215; PubMed Central PMCID: PMCPMC4292152.

271. Kayagaki N, Warming S, Lamkanfi M, Vande Walle L, Louie S, Dong J, et al. Non-canonical inflammasome activation targets caspase-11. *Nature* (2011) **479**(7371):117-21. Epub 2011/10/18. doi: 10.1038/nature10558. PubMed PMID: 22002608.

272. Mortimer L, Moreau F, MacDonald JA, Chadee K. NLRP3 inflammasome inhibition is disrupted in a group of auto-inflammatory disease CAPS mutations. *Nat Immunol* (2016) **17**(10):1176-86. Epub 2016/08/23. doi: 10.1038/ni.3538. PubMed PMID: 27548431.

273. Hoffman HM, Mueller JL, Broide DH, Wanderer AA, Kolodner RD. Mutation of a new gene encoding a putative pyrin-like protein causes familial cold autoinflammatory syndrome and Muckle-Wells syndrome. *Nat Genet* (2001) **29**(3):301-5. Epub 2001/11/01. doi: 10.1038/ng756. PubMed PMID: 11687797; PubMed Central PMCID: PMCPMC4322000.

274. Agostini L, Martinon F, Burns K, McDermott MF, Hawkins PN, Tschopp J. NALP3 forms an IL-1beta-processing inflammasome with increased activity in Muckle-Wells autoinflammatory disorder. *Immunity* (2004) **20**(3):319-25. Epub 2004/03/20. PubMed PMID: 15030775.

275. Conforti-Andreoni C, Ricciardi-Castagnoli P, Mortellaro A. The inflammasomes in health and disease: from genetics to molecular mechanisms of autoinflammation and beyond. *Cell Mol Immunol* (2011) **8**(2):135-45. Epub 2011/01/25. doi: 10.1038/cmi.2010.81. PubMed PMID: 21258359; PubMed Central PMCID: PMCPMC4003142.

276. Kanneganti TD, Lamkanfi M, Nunez G. Intracellular NOD-like receptors in host defense and disease. *Immunity* (2007) **27**(4):549-59. Epub 2007/10/31. doi: 10.1016/j.immuni.2007.10.002. PubMed PMID: 17967410.

277. Man SM, Kanneganti TD. Regulation of inflammasome activation. *Immunological reviews* (2015) **265**(1):6-21. Epub 2015/04/17. doi: 10.1111/imr.12296. PubMed PMID: 25879280; PubMed Central PMCID: PMCPMC4400844.

278. Elinav E, Henao-Mejia J, Flavell RA. Integrative inflammasome activity in the regulation of intestinal mucosal immune responses. *Mucosal Immunol* (2013) **6**(1):4-13. Epub 2012/12/06. doi: 10.1038/mi.2012.115. PubMed PMID: 23212196.

279. Guo H, Callaway JB, Ting JP. Inflammasomes: mechanism of action, role in disease, and therapeutics. *Nat Med* (2015) **21**(7):677-87. Epub 2015/06/30. doi: 10.1038/nm.3893. PubMed PMID: 26121197; PubMed Central PMCID: PMCPMC4519035.

280. Kanneganti TD, Lamkanfi M, Kim YG, Chen G, Park JH, Franchi L, et al. Pannexin-1-mediated recognition of bacterial molecules activates the cryopyrin inflammasome independent of Toll-like receptor signaling. *Immunity* (2007) **26**(4):433-43. Epub 2007/04/17. doi: 10.1016/j.immuni.2007.03.008. PubMed PMID: 17433728.

281. Bauernfeind FG, Horvath G, Stutz A, Alnemri ES, MacDonald K, Speert D, et al. Cutting edge: NF-κB activating pattern recognition and cytokine receptors license NLRP3 inflammasome activation by regulating NLRP3 expression. *The Journal of Immunology* (2009) **183**(2):787-91.

282. Song H, Liu B, Huai W, Yu Z, Wang W, Zhao J, et al. The E3 ubiquitin ligase TRIM31 attenuates NLRP3 inflammasome activation by promoting proteasomal degradation of NLRP3. *Nat Commun* (2016) **7**:13727. Epub 2016/12/09. doi: 10.1038/ncomms13727. PubMed PMID: 27929086; PubMed Central PMCID: PMCPMC5155141.

283. Roy N, Deveraux QL, Takahashi R, Salvesen GS, Reed JC. The c-IAP-1 and c-IAP-2 proteins are direct inhibitors of specific caspases. *EMBO J* (1997) **16**(23):6914-25. Epub 1998/01/31. doi: 10.1093/emboj/16.23.6914. PubMed PMID: 9384571; PubMed Central PMCID: PMCPMC1170295.

284. Rodgers MA, Bowman JW, Fujita H, Orazio N, Shi M, Liang Q, et al. The linear ubiquitin assembly complex (LUBAC) is essential for NLRP3 inflammasome activation. *J Exp Med* (2014) **211**(7):1333-47. Epub 2014/06/25. doi: 10.1084/jem.20132486. PubMed PMID: 24958845; PubMed Central PMCID: PMCPMC4076580.

285. Lopez-Castejon G, Luheshi NM, Compan V, High S, Whitehead RC, Flitsch S, et al. Deubiquitinases regulate the activity of caspase-1 and interleukin-1beta secretion via assembly of the inflammasome. *J Biol Chem* (2013) **288**(4):2721-33. Epub 2012/12/05. doi: 10.1074/jbc.M112.422238. PubMed PMID: 23209292; PubMed Central PMCID: PMCPMC3554938.

286. Py BF, Kim MS, Vakifahmetoglu-Norberg H, Yuan J. Deubiquitination of NLRP3 by BRCC3 critically regulates inflammasome activity. *Mol Cell* (2013) **49**(2):331-8. Epub 2012/12/19. doi: 10.1016/j.molcel.2012.11.009. PubMed PMID: 23246432.

287. Zhou Q, Aksentijevich I, Wood GM, Walts AD, Hoffmann P, Remmers EF, et al. Brief Report: Cryopyrin-Associated Periodic Syndrome Caused by a Myeloid-Restricted Somatic NLRP3 Mutation. *Arthritis Rheumatol* (2015) **67**(9):2482-6. Epub 2015/05/20. doi: 10.1002/art.39190. PubMed PMID: 25988971; PubMed Central PMCID: PMCPMC4551575.

288. Shao BZ, Xu ZQ, Han BZ, Su DF, Liu C. NLRP3 inflammasome and its inhibitors: a review. *Front Pharmacol* (2015) **6**:262. Epub 2015/11/26. doi: 10.3389/fphar.2015.00262. PubMed PMID: 26594174; PubMed Central PMCID: PMCPMC4633676.

289. Verma D, Särndahl E, Andersson H, Eriksson P, Fredrikson M, Jönsson J-I, et al. The Q705K polymorphism in NLRP3 is a gain-of-function alteration leading to excessive interleukin-1β and IL-18 production. *PloS one* (2012) **7**(4):e34977.

290. Ferrari D, Pizzirani C, Adinolfi E, Lemoli RM, Curti A, Idzko M, et al. The P2X7 receptor: a key player in IL-1 processing and release. *Journal of immunology (Baltimore, Md : 1950)* (2006) **176**(7):3877-83. Epub 2006/03/21. PubMed PMID: 16547218.

291. Pelegrin P, Barroso-Gutierrez C, Surprenant A. P2X7 receptor differentially couples to distinct release pathways for IL-1β in mouse macrophage. *Journal of Immunology* (2008) **180**(11):7147-57.

292. Pelegrin P, Surprenant A. Pannexin- 1 mediates large pore formation and interleukin- 1β release by the ATP- gated P2X 7 receptor. *The EMBO journal* (2006) **25**(21):5071-82.

293. Munoz-Planillo R, Kuffa P, Martinez-Colon G, Smith BL, Rajendiran TM, Nunez G. K(+) efflux is the common trigger of NLRP3 inflammasome activation by bacterial toxins and particulate matter. *Immunity* (2013) **38**(6):1142-53. Epub 2013/07/03. doi: 10.1016/j.immuni.2013.05.016. PubMed PMID: 23809161; PubMed Central PMCID: PMCPMC3730833.

294. Tschopp J, Schroder K. NLRP3 inflammasome activation: The convergence of multiple signalling pathways on ROS production? *Nat Rev Immunol* (2010) **10**(3):210-5. Epub 2010/02/20. doi: 10.1038/nri2725. PubMed PMID: 20168318.

295. He Y, Zeng MY, Yang D, Motro B, Nunez G. NEK7 is an essential mediator of NLRP3 activation downstream of potassium efflux. *Nature* (2016) **530**(7590):354-7. Epub 2016/01/28. doi: 10.1038/nature16959. PubMed PMID: 26814970; PubMed Central PMCID: PMCPMC4810788.

296. Petrilli V, Dostert C, Muruve DA, Tschopp J. The inflammasome: a danger sensing complex triggering innate immunity. *Curr Opin Immunol* (2007) **19**(6):615-22. Epub 2007/11/06. doi: 10.1016/j.coi.2007.09.002. PubMed PMID: 17977705.

297. Hentze H, Lin XY, Choi MS, Porter AG. Critical role for cathepsin B in mediating caspase-1-dependent interleukin-18 maturation and caspase-1-independent necrosis triggered by the microbial toxin nigericin. *Cell Death Differ* (2003) **10**(9):956-68. Epub 2003/08/23. doi: 10.1038/sj.cdd.4401264. PubMed PMID: 12934070.

298. Zhou R, Tardivel A, Thorens B, Choi I, Tschopp J. Thioredoxin-interacting protein links oxidative stress to inflammasome activation. *Nat Immunol* (2010) **11**(2):136-40. Epub 2009/12/22. doi: 10.1038/ni.1831. PubMed PMID: 20023662.

299. Oslowski CM, Hara T, O'Sullivan-Murphy B, Kanekura K, Lu S, Hara M, et al. Thioredoxin-interacting protein mediates ER stress-induced beta cell death through initiation of the inflammasome. *Cell Metab* (2012) **16**(2):265-73. Epub 2012/08/14. doi: 10.1016/j.cmet.2012.07.005. PubMed PMID: 22883234; PubMed Central PMCID: PMCPMC3418541.

300. Lerner AG, Upton J-P, Praveen PVK, Ghosh R, Nakagawa Y, Igbaria A, et al. IRE1α induces thioredoxin-interacting protein to activate the NLRP3 inflammasome and promote programmed cell death under irremediable ER stress. *Cell metabolism* (2012) **16**(2):250-64.

301. Subramanian N, Natarajan K, Clatworthy MR, Wang Z, Germain RN. The adaptor MAVS promotes NLRP3 mitochondrial localization and inflammasome activation. *Cell* (2013) **153**(2):348-61. Epub 2013/04/16. doi: 10.1016/j.cell.2013.02.054. PubMed PMID: 23582325; PubMed Central PMCID: PMCPMC3632354.

302. Nakahira K, Haspel JA, Rathinam VA, Lee SJ, Dolinay T, Lam HC, et al. Autophagy proteins regulate innate immune responses by inhibiting the release of mitochondrial DNA mediated by the NALP3 inflammasome. *Nat Immunol* (2011) **12**(3):222-30. Epub 2010/12/15. doi: 10.1038/ni.1980. PubMed PMID: 21151103; PubMed Central PMCID: PMCPMC3079381.

303. Shimada K, Crother TR, Karlin J, Dagvadorj J, Chiba N, Chen S, et al. Oxidized mitochondrial DNA activates the NLRP3 inflammasome during apoptosis. *Immunity* (2012) **36**(3):401-14. Epub 2012/02/22. doi: 10.1016/j.immuni.2012.01.009. PubMed PMID: 22342844; PubMed Central PMCID: PMCPMC3312986.

304. Iyer SS, He Q, Janczy JR, Elliott EI, Zhong Z, Olivier AK, et al. Mitochondrial cardiolipin is required for Nlrp3 inflammasome activation. *Immunity* (2013) **39**(2):311-23. Epub 2013/08/21. doi: 10.1016/j.immuni.2013.08.001. PubMed PMID: 23954133; PubMed Central PMCID: PMCPMC3779285.

305. Lee GS, Subramanian N, Kim AI, Aksentijevich I, Goldbach-Mansky R, Sacks DB, et al. The calcium-sensing receptor regulates the NLRP3 inflammasome through Ca2+ and cAMP. *Nature* (2012) **492**(7427):123-7. Epub 2012/11/13. doi: 10.1038/nature11588. PubMed PMID: 23143333; PubMed Central PMCID: PMCPMC4175565.

306. Murakami T, Ockinger J, Yu J, Byles V, McColl A, Hofer AM, et al. Critical role for calcium mobilization in activation of the NLRP3 inflammasome. *Proceedings of the National Academy of Sciences of the United States of America* (2012) **109**(28):11282-7. Epub 2012/06/27. doi: 10.1073/pnas.1117765109. PubMed PMID: 22733741; PubMed Central PMCID: PMCPMC3396518.

307. Rossol M, Pierer M, Raulien N, Quandt D, Meusch U, Rothe K, et al. Extracellular Ca2+ is a danger signal activating the NLRP3 inflammasome through G protein-coupled calcium sensing receptors. *Nat Commun* (2012) **3**:1329. Epub 2012/12/29. doi: 10.1038/ncomms2339. PubMed PMID: 23271661; PubMed Central PMCID: PMCPMC3535422.

308. Miao EA, Warren SE. Innate immune detection of bacterial virulence factors via the NLRC4 inflammasome. *J Clin Immunol* (2010) **30**(4):502-6. Epub 2010/03/30. doi: 10.1007/s10875-010-9386-5. PubMed PMID: 20349122; PubMed Central PMCID: PMCPMC2993241.

309. Rauch I, Tenthorey JL, Nichols RD, Al Moussawi K, Kang JJ, Kang C, et al. NAIP proteins are required for cytosolic detection of specific bacterial ligands in vivo. *J Exp Med* (2016) **213**(5):657-65. Epub 2016/04/06. doi: 10.1084/jem.20151809. PubMed PMID: 27045008; PubMed Central PMCID: PMCPMC4854734.

310. Wen H, Miao EA, Ting JP. Mechanisms of NOD-like receptor-associated inflammasome activation. *Immunity* (2013) **39**(3):432-41. Epub 2013/09/24. doi: 10.1016/j.immuni.2013.08.037. PubMed PMID: 24054327; PubMed Central PMCID: PMCPMC3835203.

311. Yang J, Zhao Y, Shi J, Shao F. Human NAIP and mouse NAIP1 recognize bacterial type III secretion needle protein for inflammasome activation. *Proceedings of the National Academy of Sciences of the United States of America* (2013) **110**(35):14408-13. Epub 2013/08/14. doi: 10.1073/pnas.1306376110. PubMed PMID: 23940371; PubMed Central PMCID: PMCPMC3761597.

312. Rayamajhi M, Zak DE, Chavarria-Smith J, Vance RE, Miao EA. Cutting edge: Mouse NAIP1 detects the type III secretion system needle protein. *Journal of immunology (Baltimore, Md : 1950)* (2013) **191**(8):3986-9. Epub

2013/09/18. doi: 10.4049/jimmunol.1301549. PubMed PMID: 24043898; PubMed Central PMCID: PMCPMC3819181.

313. Zhao Y, Yang J, Shi J, Gong YN, Lu Q, Xu H, et al. The NLRC4 inflammasome receptors for bacterial flagellin and type III secretion apparatus. *Nature* (2011) **477**(7366):596-600. Epub 2011/09/16. doi: 10.1038/nature10510. PubMed PMID: 21918512.

314. Broz P, Ruby T, Belhocine K, Bouley DM, Kayagaki N, Dixit VM, et al. Caspase-11 increases susceptibility to Salmonella infection in the absence of caspase-1. *Nature* (2012) **490**(7419):288-91. Epub 2012/08/17. doi: 10.1038/nature11419. PubMed PMID: 22895188; PubMed Central PMCID: PMCPMC3470772.

315. Crowley SM, Vallance BA, Knodler LA. Noncanonical inflammasomes: Antimicrobial defense that does not play by the rules. *Cell Microbiol* (2017) **19**(4). Epub 2017/01/25. doi: 10.1111/cmi.12730. PubMed PMID: 28117938.

316. Broz P, von Moltke J, Jones JW, Vance RE, Monack DM. Differential requirement for Caspase-1 autoproteolysis in pathogen-induced cell death and cytokine processing. *Cell Host Microbe* (2010) **8**(6):471-83. Epub 2010/12/15. doi: 10.1016/j.chom.2010.11.007. PubMed PMID: 21147462; PubMed Central PMCID: PMCPMC3016200.

317. Broz P. Inflammasomes: Intracellular detection of extracellular bacteria. *Cell Res* (2016) **26**(8):859-60. Epub 2016/06/11. doi: 10.1038/cr.2016.67. PubMed PMID: 27283800; PubMed Central PMCID: PMCPMC4973328.

318. Abdelaziz DH, Gavrilin MA, Akhter A, Caution K, Kotrange S, Khweek AA, et al. Asc-dependent and independent mechanisms contribute to restriction of legionella pneumophila infection in murine macrophages. *Front Microbiol* (2011) **2**:18. Epub 2011/06/30. doi: 10.3389/fmicb.2011.00018. PubMed PMID: 21713115; PubMed Central PMCID: PMCPMC3112328.

319. Crowley SM, Knodler LA, Vallance BA. Salmonella and the Inflammasome: Battle for Intracellular Dominance. *Curr Top Microbiol Immunol* (2016) **397**:43-67. Epub 2016/07/28. doi: 10.1007/978-3-319-41171-2_3. PubMed PMID: 27460804.

320. Bergsbaken T, Fink SL, Cookson BT. Pyroptosis: host cell death and inflammation. *Nat Rev Microbiol* (2009) **7**(2):99-109. Epub 2009/01/17. doi: 10.1038/nrmicro2070. PubMed PMID: 19148178; PubMed Central PMCID: PMCPMC2910423.

321. Jorgensen I, Miao EA. Pyroptotic cell death defends against intracellular pathogens. *Immunological reviews* (2015) **265**(1):130-42. Epub 2015/04/17. doi: 10.1111/imr.12287. PubMed PMID: 25879289; PubMed Central PMCID: PMCPMC4400865.

322. Kitamura A, Sasaki Y, Abe T, Kano H, Yasutomo K. An inherited mutation in NLRC4 causes autoinflammation in human and mice. *J Exp Med* (2014) **211**(12):2385-96. Epub 2014/11/12. doi: 10.1084/jem.20141091. PubMed PMID: 25385754; PubMed Central PMCID: PMCPMC4235634.

323. Romberg N, Al Moussawi K, Nelson-Williams C, Stiegler AL, Loring E, Choi M, et al. Mutation of NLRC4 causes a syndrome of enterocolitis and autoinflammation. *Nat Genet* (2014) **46**(10):1135-9. Epub 2014/09/15. doi: 10.1038/ng.3066. PubMed PMID: 25217960; PubMed Central PMCID: PMCPMC4177367.

324. Canna SW, de Jesus AA, Gouni S, Brooks SR, Marrero B, Liu Y, et al. An activating NLRC4 inflammasome mutation causes autoinflammation with recurrent macrophage activation syndrome. *Nat Genet* (2014) **46**(10):1140-6. Epub 2014/09/15. doi: 10.1038/ng.3089. PubMed PMID: 25217959; PubMed Central PMCID: PMCPMC4177369.

325. Alvarez-Errico D, Vento-Tormo R, Ballestar E. Genetic and Epigenetic Determinants in Autoinflammatory Diseases. *Frontiers in immunology* (2017) **8**:318. Epub 2017/04/07. doi: 10.3389/fimmu.2017.00318. PubMed PMID: 28382039; PubMed Central PMCID: PMCPMC5360705.

326. Franklin BS, Bossaller L, De Nardo D, Ratter JM, Stutz A, Engels G, et al. The adaptor ASC has extracellular and 'prionoid' activities that propagate inflammation. *Nat Immunol* (2014) **15**(8):727-37. Epub 2014/06/24. doi: 10.1038/ni.2913. PubMed PMID: 24952505; PubMed Central PMCID: PMCPMC4116676.

327. Alberto B-M. The NLRP3 inflammasome is released as a particulate danger signal that amplifies the inflammatory response. *Adobe InDesign CS2 (40)*.

328. Baroja-Mazo A, Martin-Sanchez F, Gomez AI, Martinez CM, Amores-Iniesta J, Compan V, et al. The NLRP3 inflammasome is released as a particulate danger signal that amplifies the inflammatory response. *Nat Immunol* (2014) **15**(8):738-48. Epub 2014/06/24. doi: 10.1038/ni.2919. PubMed PMID: 24952504.

329. Tzeng TC, Schattgen S, Monks B, Wang D, Cerny A, Latz E, et al. A Fluorescent Reporter Mouse for Inflammasome Assembly Demonstrates an Important Role for Cell-Bound and Free ASC Specks during In Vivo

Infection. *Cell Rep* (2016) **16**(2):571-82. Epub 2016/06/28. doi: 10.1016/j.celrep.2016.06.011. PubMed PMID: 27346360; PubMed Central PMCID: PMCPMC5384574.

330. Mariathasan S, Newton K, Monack DM, Vucic D, French DM, Lee WP, et al. Differential activation of the inflammasome by caspase-1 adaptors ASC and Ipaf. *Nature* (2004) **430**(6996):213-8. Epub 2004/06/11. doi: 10.1038/nature02664. PubMed PMID: 15190255.

331. Miao EA, Rajan JV, Aderem A. Caspase-1-induced pyroptotic cell death. *Immunological reviews* (2011) **243**(1):206-14. Epub 2011/09/03. doi: 10.1111/j.1600-065X.2011.01044.x. PubMed PMID: 21884178; PubMed Central PMCID: PMCPMC3609431.

332. Dinarello CA. Interleukin-1. *Digestive diseases and sciences* (1988) **33**(3 Suppl).

333. Ikeda S, Saijo S, Murayama MA, Shimizu K, Akitsu A, Iwakura Y. Excess IL-1 signaling enhances the development of Th17 cells by downregulating TGF-beta-induced Foxp3 expression. *Journal of immunology (Baltimore, Md : 1950)* (2014) **192**(4):1449-58. Epub 2014/01/17. doi: 10.4049/jimmunol.1300387. PubMed PMID: 24431229.

334. Collins T, Read MA, Neish AS, Whitley MZ, Thanos D, Maniatis T. Transcriptional regulation of endothelial cell adhesion molecules: NF-kappa B and cytokine-inducible enhancers. *FASEB J* (1995) **9**(10):899-909. Epub 1995/07/01. PubMed PMID: 7542214.

335. Chou RC, Kim ND, Sadik CD, Seung E, Lan Y, Byrne MH, et al. Lipid-cytokine-chemokine cascade drives neutrophil recruitment in a murine model of inflammatory arthritis. *Immunity* (2010) **33**(2):266-78. Epub 2010/08/24. doi: 10.1016/j.immuni.2010.07.018. PubMed PMID: 20727790; PubMed Central PMCID: PMCPMC3155777.

336. Dinarello CA. Biologic basis for interleukin-1 in disease. *Blood* (1996) **87**(6):2095-147. Epub 1996/03/15. PubMed PMID: 8630372.

337. Satsangi J, Wolstencroft RA, Cason J, Ainley CC, Dumonde DC, Thompson RP. Interleukin 1 in Crohn's disease. *Clin Exp Immunol* (1987) **67**(3):594-605. Epub 1987/03/01. PubMed PMID: 3496997; PubMed Central PMCID: PMCPMC1542614.

338. McAlindon ME, Hawkey CJ, Mahida YR. Expression of interleukin 1 beta and interleukin 1 beta converting enzyme by intestinal macrophages in health and inflammatory bowel disease. *Gut* (1998) **42**(2):214-9. Epub 1998/04/16. PubMed PMID: 9536946; PubMed Central PMCID: PMCPMC1726995.

339. Mahida YR, Wu K, Jewell DP. Enhanced production of interleukin 1-beta by mononuclear cells isolated from mucosa with active ulcerative colitis of Crohn's disease. *Gut* (1989) **30**(6):835-8. Epub 1989/06/01. doi: 10.1136/gut.30.6.835. PubMed PMID: 2787769; PubMed Central PMCID: PMCPMC1434123.

340. Zhang J, Fu S, Sun S, Li Z, Guo B. Inflammasome activation has an important role in the development of spontaneous colitis. *Mucosal Immunol* (2014) **7**(5):1139-50. Epub 2014/01/30. doi: 10.1038/mi.2014.1. PubMed PMID: 24472848; PubMed Central PMCID: PMCPMC4115056.

341. Fiocco U, Vezzu M, Cozzi L, Todesco S. [IL-1Ra (recombinant human IL-1 receptor antagonist) in the treatment of rheumatoid arthritis: the efficacy]. *Reumatismo* (2004) **56**(1 Suppl 1):62-73. Epub 2004/06/18. PubMed PMID: 15201942.

342. de Luca A, Smeekens SP, Casagrande A, Iannitti R, Conway KL, Gresnigt MS, et al. IL-1 receptor blockade restores autophagy and reduces inflammation in chronic granulomatous disease in mice and in humans. *Proceedings of the National Academy of Sciences of the United States of America* (2014) **111**(9):3526-31. Epub 2014/02/20. doi: 10.1073/pnas.1322831111. PubMed PMID: 24550444; PubMed Central PMCID: PMCPMC3948220.

343. Muller AJ, Hoffmann C, Galle M, Van Den Broeke A, Heikenwalder M, Falter L, et al. The S. Typhimurium effector SopE induces caspase-1 activation in stromal cells to initiate gut inflammation. *Cell Host Microbe* (2009) **6**(2):125-36. Epub 2009/08/18. doi: 10.1016/j.chom.2009.07.007. PubMed PMID: 19683679.

344. Ng J, Hirota SA, Gross O, Li Y, Ulke-Lemee A, Potentier MS, et al. Clostridium difficile toxin-induced inflammation and intestinal injury are mediated by the inflammasome. *Gastroenterology* (2010) **139**(2):542-52, 52 e1-3. Epub 2010/04/20. doi: 10.1053/j.gastro.2010.04.005. PubMed PMID: 20398664.

345. Liu Z, Zaki MH, Vogel P, Gurung P, Finlay BB, Deng W, et al. Role of inflammasomes in host defense against Citrobacter rodentium infection. *J Biol Chem* (2012) **287**(20):16955-64. Epub 2012/03/31. doi: 10.1074/jbc.M112.358705. PubMed PMID: 22461621; PubMed Central PMCID: PMCPMC3351318.

346. Lebeis SL, Powell KR, Merlin D, Sherman MA, Kalman D. Interleukin-1 receptor signaling protects mice from lethal intestinal damage caused by the attaching and effacing pathogen Citrobacter rodentium. *Infect Immun*

(2009) **77**(2):604-14. Epub 2008/12/17. doi: 10.1128/IAI.00907-08. PubMed PMID: 19075023; PubMed Central PMCID: PMCPMC2632048.

347. Franchi L, Kamada N, Nakamura Y, Burberry A, Kuffa P, Suzuki S, et al. NLRC4-driven production of IL-1beta discriminates between pathogenic and commensal bacteria and promotes host intestinal defense. *Nat Immunol* (2012) **13**(5):449-56. Epub 2012/04/10. doi: 10.1038/ni.2263. PubMed PMID: 22484733; PubMed Central PMCID: PMCPMC3361590.

348. Thinwa J, Segovia JA, Bose S, Dube PH. Integrin-mediated first signal for inflammasome activation in intestinal epithelial cells. *Journal of immunology (Baltimore, Md : 1950)* (2014) **193**(3):1373-82. Epub 2014/06/27. doi: 10.4049/jimmunol.1400145. PubMed PMID: 24965773; PubMed Central PMCID: PMCPMC4174679.

349. Monteleone G, Trapasso F, Parrello T, Biancone L, Stella A, Iuliano R, et al. Bioactive IL-18 expression is up-regulated in Crohn's disease. *Journal of immunology (Baltimore, Md : 1950)* (1999) **163**(1):143-7. Epub 1999/06/29. PubMed PMID: 10384110.

350. Dinarello CA. The biological properties of interleukin-1. *Eur Cytokine Netw* (1994) **5**(6):517-31. Epub 1994/11/01. PubMed PMID: 7727685.

351. Okamura H, Tsutsi H, Komatsu T, Yutsudo M, Hakura A, Tanimoto T, et al. Cloning of a new cytokine that induces IFN-gamma production by T cells. *Nature* (1995) **378**(6552):88-91. Epub 1995/11/02. doi: 10.1038/378088a0. PubMed PMID: 7477296.

352. Muller AA, Dolowschiak T, Sellin ME, Felmy B, Verbree C, Gadient S, et al. An NK Cell Perforin Response Elicited via IL-18 Controls Mucosal Inflammation Kinetics during Salmonella Gut Infection. *PLoS pathogens* (2016) **12**(6):e1005723. Epub 2016/06/25. doi: 10.1371/journal.ppat.1005723. PubMed PMID: 27341123; PubMed Central PMCID: PMCPMC4920399.

353. Greenfeder SA, Nunes P, Kwee L, Labow M, Chizzonite RA, Ju G. Molecular cloning and characterization of a second subunit of the interleukin 1 receptor complex. *J Biol Chem* (1995) **270**(23):13757-65. Epub 1995/06/09. PubMed PMID: 7775431.

354. Lalor SJ, Dungan LS, Sutton CE, Basdeo SA, Fletcher JM, Mills KH. Caspase-1-processed cytokines IL-1beta and IL-18 promote IL-17 production by gammadelta and CD4 T cells that mediate autoimmunity. *Journal of immunology (Baltimore, Md : 1950)* (2011) **186**(10):5738-48. Epub 2011/04/08. doi: 10.4049/jimmunol.1003597. PubMed PMID: 21471445.

355. Hedl M, Zheng S, Abraham C. The IL18RAP region disease polymorphism decreases IL-18RAP/IL-18R1/IL-1R1 expression and signaling through innate receptor-initiated pathways. *Journal of immunology (Baltimore, Md : 1950)* (2014) **192**(12):5924-32. Epub 2014/05/21. doi: 10.4049/jimmunol.1302727. PubMed PMID: 24842757; PubMed Central PMCID: PMCPMC4146459.

356. Corbaz A, ten Hove T, Herren S, Graber P, Schwartsburd B, Belzer I, et al. IL-18-binding protein expression by endothelial cells and macrophages is up-regulated during active Crohn's disease. *Journal of immunology (Baltimore, Md : 1950)* (2002) **168**(7):3608-16. Epub 2002/03/22. PubMed PMID: 11907126.

357. Naftali T, Novick D, Gabay G, Rubinstein M, Novis B. Interleukin-18 and its binding protein in patients with inflammatory bowel disease during remission and exacerbation. *Isr Med Assoc J* (2007) **9**(7):504-8. Epub 2007/08/23. PubMed PMID: 17710779.

358. Nowarski R, Jackson R, Gagliani N, de Zoete MR, Palm NW, Bailis W, et al. Epithelial IL-18 Equilibrium Controls Barrier Function in Colitis. *Cell* (2015) **163**(6):1444-56. Epub 2015/12/08. doi: 10.1016/j.cell.2015.10.072. PubMed PMID: 26638073; PubMed Central PMCID: PMCPMC4943028.

359. Ishikura T, Kanai T, Uraushihara K, Iiyama R, Makita S, Totsuka T, et al. Interleukin-18 overproduction exacerbates the development of colitis with markedly infiltrated macrophages in interleukin-18 transgenic mice. *J Gastroenterol Hepatol* (2003) **18**(8):960-9. Epub 2003/07/16. PubMed PMID: 12859727.

360. Salcedo R, Worschech A, Cardone M, Jones Y, Gyulai Z, Dai RM, et al. MyD88-mediated signaling prevents development of adenocarcinomas of the colon: role of interleukin 18. *J Exp Med* (2010) **207**(8):1625-36. Epub 2010/07/14. doi: 10.1084/jem.20100199. PubMed PMID: 20624890; PubMed Central PMCID: PMCPMC2916129.

361. Błażejewski AJ, Thiemann S, Schenk A, Pils MC, Gálvez EJ, Roy U, et al. Microbiota Normalization Reveals that Canonical Caspase-1 Activation Exacerbates Chemically Induced Intestinal Inflammation. *Cell Reports* (2017) **19**(11):2319-30.

362. Mamantopoulos M, Ronchi F, Van Hauwermeiren F, Vieira-Silva S, Yilmaz B, Martens L, et al. Nlrp6- and ASC-Dependent Inflammasomes Do Not Shape the Commensal Gut Microbiota Composition. *Immunity* (2017) **47**(2):339-48 e4. Epub 2017/08/13. doi: 10.1016/j.immuni.2017.07.011. PubMed PMID: 28801232.

363. Thaiss CA, Zmora N, Levy M, Elinav E. The microbiome and innate immunity. *Nature* (2016) **535**(7610):65-74. Epub 2016/07/08. doi: 10.1038/nature18847. PubMed PMID: 27383981.

364. Maslowski KM, Vieira AT, Ng A, Kranich J, Sierro F, Yu D, et al. Regulation of inflammatory responses by gut microbiota and chemoattractant receptor GPR43. *Nature* (2009) **461**(7268):1282-6. Epub 2009/10/30. doi: 10.1038/nature08530. PubMed PMID: 19865172; PubMed Central PMCID: PMCPMC3256734.

365. Seo SU, Kamada N, Munoz-Planillo R, Kim YG, Kim D, Koizumi Y, et al. Distinct Commensals Induce Interleukin-1beta via NLRP3 Inflammasome in Inflammatory Monocytes to Promote Intestinal Inflammation in Response to Injury. *Immunity* (2015) **42**(4):744-55. Epub 2015/04/12. doi: 10.1016/j.immuni.2015.03.004. PubMed PMID: 25862092; PubMed Central PMCID: PMCPMC4408263.

366. Kitajima S, Morimoto M, Sagara E, Shimizu C, Ikeda Y. Dextran sodium sulfate-induced colitis in germ-free IQI/Jic mice. *Exp Anim* (2001) **50**(5):387-95. Epub 2002/01/05. PubMed PMID: 11769541.

367. Williams TM, Leeth RA, Rothschild DE, Coutermarsh-Ott SL, McDaniel DK, Simmons AE, et al. The NLRP1 inflammasome attenuates colitis and colitis-associated tumorigenesis. *Journal of immunology (Baltimore, Md : 1950)* (2015) **194**(7):3369-80. Epub 2015/03/01. doi: 10.4049/jimmunol.1402098. PubMed PMID: 25725098; PubMed Central PMCID: PMCPMC4369420.

368. Hu S, Peng L, Kwak YT, Tekippe EM, Pasare C, Malter JS, et al. The DNA Sensor AIM2 Maintains Intestinal Homeostasis via Regulation of Epithelial Antimicrobial Host Defense. *Cell Rep* (2015) **13**(9):1922-36. Epub 2015/12/15. doi: 10.1016/j.celrep.2015.10.040. PubMed PMID: 26655906; PubMed Central PMCID: PMCPMC5477202.

369. Munoz M, Eidenschenk C, Ota N, Wong K, Lohmann U, Kuhl AA, et al. Interleukin-22 induces interleukin-18 expression from epithelial cells during intestinal infection. *Immunity* (2015) **42**(2):321-31. Epub 2015/02/15. doi: 10.1016/j.immuni.2015.01.011. PubMed PMID: 25680273.

370. Reuter BK, Pizarro TT. Commentary: the role of the IL-18 system and other members of the IL-1R/TLR superfamily in innate mucosal immunity and the pathogenesis of inflammatory bowel disease: friend or foe? *European journal of immunology* (2004) **34**(9):2347-55. Epub 2004/08/13. doi: 10.1002/eji.200425351. PubMed PMID: 15307167.

371. Kampfer H, Kalina U, Muhl H, Pfeilschifter J, Frank S. Counterregulation of interleukin-18 mRNA and protein expression during cutaneous wound repair in mice. *J Invest Dermatol* (1999) **113**(3):369-74. Epub 1999/09/01. doi: 10.1046/j.1523-1747.1999.00704.x. PubMed PMID: 10469336.

372. Takagi H, Kanai T, Okazawa A, Kishi Y, Sato T, Takaishi H, et al. Contrasting action of IL-12 and IL-18 in the development of dextran sodium sulphate colitis in mice. *Scand J Gastroenterol* (2003) **38**(8):837-44. Epub 2003/08/28. PubMed PMID: 12940437.

373. Zhang B, Chassaing B, Shi Z, Uchiyama R, Zhang Z, Denning TL, et al. Viral infection. Prevention and cure of rotavirus infection via TLR5/NLRC4-mediated production of IL-22 and IL-18. *Science (New York, NY)* (2014) **346**(6211):861-5. Epub 2014/11/15. doi: 10.1126/science.1256999. PubMed PMID: 25395539; PubMed Central PMCID: PMCPMC4788408.

374. Kim B, Lee Y, Kim E, Kwak A, Ryoo S, Bae SH, et al. The interleukin-1α precursor is biologically active and is likely a key alarmin in the IL-1 family of cytokines. *Frontiers in immunology* (2013) **4**.

375. van de Veerdonk FL, Netea MG. New Insights in the Immunobiology of IL-1 Family Members. *Frontiers in immunology* (2013) **4**:167. Epub 2013/07/13. doi: 10.3389/fimmu.2013.00167. PubMed PMID: 23847614; PubMed Central PMCID: PMCPMC3703542.

376. Lamkanfi M, Sarkar A, Vande Walle L, Vitari AC, Amer AO, Wewers MD, et al. Inflammasome-dependent release of the alarmin HMGB1 in endotoxemia. *Journal of immunology (Baltimore, Md : 1950)* (2010) **185**(7):4385-92. Epub 2010/08/31. doi: 10.4049/jimmunol.1000803. PubMed PMID: 20802146; PubMed Central PMCID: PMCPMC3428148.

377. Vande Walle L, Kanneganti TD, Lamkanfi M. HMGB1 release by inflammasomes. *Virulence* (2011) **2**(2):162-5. Epub 2011/03/23. PubMed PMID: 21422809; PubMed Central PMCID: PMCPMC3265758.

378. von Moltke J, Trinidad NJ, Moayeri M, Kintzer AF, Wang SB, van Rooijen N, et al. Rapid induction of inflammatory lipid mediators by the inflammasome in vivo. *Nature* (2012) **490**(7418):107-11. Epub 2012/08/21. doi: 10.1038/nature11351. PubMed PMID: 22902502; PubMed Central PMCID: PMCPMC3465483.

379. Jorgensen I, Lopez JP, Laufer SA, Miao EA. IL-1beta, IL-18, and eicosanoids promote neutrophil recruitment to pore-induced intracellular traps following pyroptosis. *European journal of immunology* (2016) **46**(12):2761-6. Epub 2016/10/21. doi: 10.1002/eji.201646647. PubMed PMID: 27682622; PubMed Central PMCID: PMCPMC5138142.

380. Lamkanfi M. Emerging inflammasome effector mechanisms. *Nat Rev Immunol* (2011) **11**(3):213-20. Epub 2011/02/26. doi: 10.1038/nri2936. PubMed PMID: 21350580.

381. Shi J, Zhao Y, Wang K, Shi X, Wang Y, Huang H, et al. Cleavage of GSDMD by inflammatory caspases determines pyroptotic cell death. *Nature* (2015) **526**(7575):660-5. Epub 2015/09/17. doi: 10.1038/nature15514. PubMed PMID: 26375003.

382. Aachoui Y, Leaf IA, Hagar JA, Fontana MF, Campos CG, Zak DE, et al. Caspase-11 protects against bacteria that escape the vacuole. *Science (New York, NY)* (2013) **339**(6122):975-8. Epub 2013/01/26. doi: 10.1126/science.1230751. PubMed PMID: 23348507; PubMed Central PMCID: PMCPMC3697099.

383. Aachoui Y, Sagulenko V, Miao EA, Stacey KJ. Inflammasome-mediated pyroptotic and apoptotic cell death, and defense against infection. *Curr Opin Microbiol* (2013) **16**(3):319-26. Epub 2013/05/28. doi: 10.1016/j.mib.2013.04.004. PubMed PMID: 23707339; PubMed Central PMCID: PMCPMC3742712.

384. Kayagaki N, Wong MT, Stowe IB, Ramani SR, Gonzalez LC, Akashi-Takamura S, et al. Noncanonical inflammasome activation by intracellular LPS independent of TLR4. *Science (New York, NY)* (2013) **341**(6151):1246-9. Epub 2013/07/28. doi: 10.1126/science.1240248. PubMed PMID: 23887873.

385. Hagar JA, Powell DA, Aachoui Y, Ernst RK, Miao EA. Cytoplasmic LPS activates caspase-11: implications in TLR4-independent endotoxic shock. *Science (New York, NY)* (2013) **341**(6151):1250-3. Epub 2013/09/14. doi: 10.1126/science.1240988. PubMed PMID: 24031018; PubMed Central PMCID: PMCPMC3931427.

386. Yang J, Zhao Y, Shao F. Non-canonical activation of inflammatory caspases by cytosolic LPS in innate immunity. *Curr Opin Immunol* (2015) **32**:78-83. Epub 2015/01/27. doi: 10.1016/j.coi.2015.01.007. PubMed PMID: 25621708.

387. Meunier E, Dick MS, Dreier RF, Schurmann N, Kenzelmann Broz D, Warming S, et al. Caspase-11 activation requires lysis of pathogen-containing vacuoles by IFN-induced GTPases. *Nature* (2014) **509**(7500):366-70. Epub 2014/04/18. doi: 10.1038/nature13157. PubMed PMID: 24739961.

388. Miao EA, Leaf IA, Treuting PM, Mao DP, Dors M, Sarkar A, et al. Caspase-1-induced pyroptosis is an innate immune effector mechanism against intracellular bacteria. *Nat Immunol* (2010) **11**(12):1136-42. Epub 2010/11/09. doi: 10.1038/ni.1960. PubMed PMID: 21057511; PubMed Central PMCID: PMCPMC3058225.

389. Rathinam VA, Vanaja SK, Waggoner L, Sokolovska A, Becker C, Stuart LM, et al. TRIF licenses caspase-11-dependent NLRP3 inflammasome activation by gram-negative bacteria. *Cell* (2012) **150**(3):606-19. Epub 2012/07/24. doi: 10.1016/j.cell.2012.07.007. PubMed PMID: 22819539; PubMed Central PMCID: PMCPMC3660860.

390. Wang S, Miura M, Jung Y-k, Zhu H, Li E, Yuan J. Murine Caspase-11, an ICE-Interacting Protease, Is Essential for the Activation of ICE. *Cell* (1998) **92**(4):501-9. doi: 10.1016/s0092-8674(00)80943-5. PubMed PMID: WOS:000072251500010.

391. Pallett MA, Crepin VF, Serafini N, Habibzay M, Kotik O, Sanchez-Garrido J, et al. Bacterial virulence factor inhibits caspase-4/11 activation in intestinal epithelial cells. *Mucosal Immunol* (2017) **10**(3):602-12. Epub 2016/09/15. doi: 10.1038/mi.2016.77. PubMed PMID: 27624779; PubMed Central PMCID: PMCPMC5159625.

392. Man SM, Karki R, Briard B, Burton A, Gingras S, Pelletier S, et al. Differential roles of caspase-1 and caspase-11 in infection and inflammation. *Sci Rep* (2017) **7**:45126. Epub 2017/03/28. doi: 10.1038/srep45126. PubMed PMID: 28345580; PubMed Central PMCID: PMCPMC5366862.

393. Kang S-J, Popat R, Bragdon C, Odonnell K, Phelan S, Yuan J, et al. Caspase-11 is not necessary for chemotherapy-induced intestinal mucositis. *DNA and cell biology* (2004) **23**(8):490-5.

394. Kobayashi T, Ogawa M, Sanada T, Mimuro H, Kim M, Ashida H, et al. The Shigella OspC3 effector inhibits caspase-4, antagonizes inflammatory cell death, and promotes epithelial infection. *Cell Host Microbe* (2013) **13**(5):570-83. Epub 2013/05/21. doi: 10.1016/j.chom.2013.04.012. PubMed PMID: 23684308.

395. Aglietti RA, Estevez A, Gupta A, Ramirez MG, Liu PS, Kayagaki N, et al. GsdmD p30 elicited by caspase-11 during pyroptosis forms pores in membranes. *Proceedings of the National Academy of Sciences of the United States of America* (2016) **113**(28):7858-63. Epub 2016/06/25. doi: 10.1073/pnas.1607769113. PubMed PMID: 27339137; PubMed Central PMCID: PMCPMC4948338.

396. Sborgi L, Ruhl S, Mulvihill E, Pipercevic J, Heilig R, Stahlberg H, et al. GSDMD membrane pore formation constitutes the mechanism of pyroptotic cell death. *EMBO J* (2016) **35**(16):1766-78. Epub 2016/07/16. doi: 10.15252/embj.201694696. PubMed PMID: 27418190; PubMed Central PMCID: PMCPMC5010048.

397. Liu X, Zhang Z, Ruan J, Pan Y, Magupalli VG, Wu H, et al. Inflammasome-activated gasdermin D causes pyroptosis by forming membrane pores. *Nature* (2016) **535**(7610):153-8. Epub 2016/07/08. doi: 10.1038/nature18629. PubMed PMID: 27383986; PubMed Central PMCID: PMCPMC5539988.

398. Kayagaki N, Stowe IB, Lee BL, O'Rourke K, Anderson K, Warming S, et al. Caspase-11 cleaves gasdermin D for non-canonical inflammasome signalling. *Nature* (2015) **526**(7575):666-71. Epub 2015/09/17. doi: 10.1038/nature15541. PubMed PMID: 26375259.

399. He WT, Wan H, Hu L, Chen P, Wang X, Huang Z, et al. Gasdermin D is an executor of pyroptosis and required for interleukin-1beta secretion. *Cell Res* (2015) **25**(12):1285-98. Epub 2015/11/28. doi: 10.1038/cr.2015.139. PubMed PMID: 26611636; PubMed Central PMCID: PMCPMC4670995.

400. Ding J, Wang K, Liu W, She Y, Sun Q, Shi J, et al. Pore-forming activity and structural autoinhibition of the gasdermin family. *Nature* (2016) **535**(7610):111-6. Epub 2016/06/10. doi: 10.1038/nature18590. PubMed PMID: 27281216.

401. Saeki N, Sasaki H. Gasdermin superfamily: a novel gene family functioning in epithelial cells. *Endothelium and Epithelium: composition, functions and pathology New York: Nova Science Publishers, Inc* (2012):193-211.

402. Brennan MA, Cookson BT. Salmonella induces macrophage death by caspase-1-dependent necrosis. *Mol Microbiol* (2000) **38**(1):31-40. Epub 2000/10/13. PubMed PMID: 11029688.

403. Labbe K, Saleh M. Cell death in the host response to infection. *Cell Death Differ* (2008) **15**(9):1339-49. Epub 2008/06/21. doi: 10.1038/cdd.2008.91. PubMed PMID: 18566602.

404. Fink SL, Cookson BT. Caspase-1-dependent pore formation during pyroptosis leads to osmotic lysis of infected host macrophages. *Cell Microbiol* (2006) **8**(11):1812-25. Epub 2006/07/11. doi: 10.1111/j.1462-5822.2006.00751.x. PubMed PMID: 16824040.

405. Monack DM, Raupach B, Hromockyj AE, Falkow S. Salmonella typhimurium invasion induces apoptosis in infected macrophages. *Proceedings of the National Academy of Sciences of the United States of America* (1996) **93**(18):9833-8. Epub 1996/09/03. PubMed PMID: 8790417; PubMed Central PMCID: PMCPMC38515.

406. Cookson BT, Brennan MA. Pro-inflammatory programmed cell death. *Trends Microbiol* (2001) **9**(3):113-4. Epub 2001/04/17. doi: http://dx.doi.org/10.1016/S0966-842X(00)01936-3. PubMed PMID: 11303500.

407. Pierini R, Perret M, Djebali S, Juruj C, Michallet MC, Forster I, et al. ASC controls IFN-gamma levels in an IL-18-dependent manner in caspase-1-deficient mice infected with Francisella novicida. *Journal of immunology (Baltimore, Md : 1950)* (2013) **191**(7):3847-57. Epub 2013/08/27. doi: 10.4049/jimmunol.1203326. PubMed PMID: 23975862.

408. Sagulenko V, Thygesen SJ, Sester DP, Idris A, Cridland JA, Vajjhala PR, et al. AIM2 and NLRP3 inflammasomes activate both apoptotic and pyroptotic death pathways via ASC. *Cell Death and Differentiation* (2013) **20**(9):1149-60. doi: 10.1038/cdd.2013.37. PubMed PMID: WOS:000322983900006.

409. Taabazuing CY, Okondo MC, Bachovchin DA. Pyroptosis and Apoptosis Pathways Engage in Bidirectional Crosstalk in Monocytes and Macrophages. *Cell Chem Biol* (2017) **24**(4):507-14 e4. Epub 2017/04/11. doi: 10.1016/j.chembiol.2017.03.009. PubMed PMID: 28392147; PubMed Central PMCID: PMCPMC5467448.

410. Pearson JS, Giogha C, Ong SY, Kennedy CL, Kelly M, Robinson KS, et al. A type III effector antagonizes death receptor signalling during bacterial gut infection. *Nature* (2013) **501**(7466):247-51. Epub 2013/09/13. doi: 10.1038/nature12524. PubMed PMID: 24025841; PubMed Central PMCID: PMCPMC3836246.

411. Yen H, Karino M, Tobe T. Modulation of the Inflammasome Signaling Pathway by Enteropathogenic and Enterohemorrhagic Escherichia coli. *Front Cell Infect Microbiol* (2016) **6**:89. Epub 2016/09/13. doi: 10.3389/fcimb.2016.00089. PubMed PMID: 27617233; PubMed Central PMCID: PMCPMC4999430.

412. Pinaud L, Sansonetti PJ, Phalipon A. Host Cell Targeting by Enteropathogenic Bacteria T3SS Effectors. *Trends Microbiol* (2018). Epub 2018/02/27. doi: 10.1016/j.tim.2018.01.010. PubMed PMID: 29477730.

413. Brodsky IE, Palm NW, Sadanand S, Ryndak MB, Sutterwala FS, Flavell RA, et al. A Yersinia effector protein promotes virulence by preventing inflammasome recognition of the type III secretion system. *Cell Host Microbe* (2010) **7**(5):376-87. Epub 2010/05/19. doi: 10.1016/j.chom.2010.04.009. PubMed PMID: 20478539; PubMed Central PMCID: PMCPMC2883865.

414. Man SM, Kanneganti TD. Converging roles of caspases in inflammasome activation, cell death and innate immunity. *Nat Rev Immunol* (2016) **16**(1):7-21. Epub 2015/12/15. doi: 10.1038/nri.2015.7. PubMed PMID: 26655628; PubMed Central PMCID: PMCPMC4915362.

415. Gurung P, Malireddi RK, Anand PK, Demon D, Vande Walle L, Liu Z, et al. Toll or interleukin-1 receptor (TIR) domain-containing adaptor inducing interferon-beta (TRIF)-mediated caspase-11 protease production integrates Toll-like receptor 4 (TLR4) protein- and Nlrp3 inflammasome-mediated host defense against enteropathogens. *J Biol Chem* (2012) **287**(41):34474-83. Epub 2012/08/18. doi: 10.1074/jbc.M112.401406. PubMed PMID: 22898816; PubMed Central PMCID: PMCPMC3464552.

416. Yi YS. Caspase- 11 non- canonical inflammasome: a critical sensor of intracellular LPS in macrophage-mediated inflammatory responses. *Immunology* (2017).

417. Broz P, Dixit VM. Inflammasomes: mechanism of assembly, regulation and signalling. *Nat Rev Immunol* (2016) **16**(7):407-20. Epub 2016/06/14. doi: 10.1038/nri.2016.58. PubMed PMID: 27291964.

418. Galluzzi L, Vitale I, Abrams JM, Alnemri ES, Baehrecke EH, Blagosklonny MV, et al. Molecular definitions of cell death subroutines: recommendations of the Nomenclature Committee on Cell Death 2012. *Cell Death Differ* (2012) **19**(1):107-20. Epub 2011/07/16. doi: 10.1038/cdd.2011.96. PubMed PMID: 21760595; PubMed Central PMCID: PMCPMC3252826.

419. Kroemer G, Galluzzi L, Vandenabeele P, Abrams J, Alnemri ES, Baehrecke EH, et al. Classification of cell death: recommendations of the Nomenclature Committee on Cell Death 2009. *Cell Death Differ* (2009) **16**(1):3-11. Epub 2008/10/11. doi: 10.1038/cdd.2008.150. PubMed PMID: 18846107; PubMed Central PMCID: PMCPMC2744427.

420. Kerr JF, Wyllie AH, Currie AR. Apoptosis: a basic biological phenomenon with wide-ranging implications in tissue kinetics. *Br J Cancer* (1972) **26**(4):239-57. Epub 1972/08/01. PubMed PMID: 4561027; PubMed Central PMCID: PMCPMC2008650.

421. Galluzzi L, Aaronson SA, Abrams J, Alnemri ES, Andrews DW, Baehrecke EH, et al. Guidelines for the use and interpretation of assays for monitoring cell death in higher eukaryotes. *Cell Death Differ* (2009) **16**(8):1093-107. Epub 2009/04/18. doi: 10.1038/cdd.2009.44. PubMed PMID: 19373242; PubMed Central PMCID: PMCPMC2757140.

422. Galluzzi L, Bravo-San Pedro JM, Vitale I, Aaronson SA, Abrams JM, Adam D, et al. Essential versus accessory aspects of cell death: recommendations of the NCCD 2015. *Cell Death Differ* (2015) **22**(1):58-73. Epub 2014/09/23. doi: 10.1038/cdd.2014.137. PubMed PMID: 25236395; PubMed Central PMCID: PMCPMC4262782.

423. Vandenabeele P, Galluzzi L, Vanden Berghe T, Kroemer G. Molecular mechanisms of necroptosis: an ordered cellular explosion. *Nat Rev Mol Cell Biol* (2010) **11**(10):700-14. Epub 2010/09/09. doi: 10.1038/nrm2970. PubMed PMID: 20823910.

424. Aglietti RA, Dueber EC. Recent Insights into the Molecular Mechanisms Underlying Pyroptosis and Gasdermin Family Functions. *Trends Immunol* (2017) **38**(4):261-71. Epub 2017/02/16. doi: 10.1016/j.it.2017.01.003. PubMed PMID: 28196749.

425. Fernandes-Alnemri T, Wu J, Yu JW, Datta P, Miller B, Jankowski W, et al. The pyroptosome: a supramolecular assembly of ASC dimers mediating inflammatory cell death via caspase-1 activation. *Cell Death Differ* (2007) **14**(9):1590-604. Epub 2007/06/30. doi: 10.1038/sj.cdd.4402194. PubMed PMID: 17599095; PubMed Central PMCID: PMCPMC3345951.

426. Chen X, He WT, Hu L, Li J, Fang Y, Wang X, et al. Pyroptosis is driven by non-selective gasdermin-D pore and its morphology is different from MLKL channel-mediated necroptosis. *Cell Res* (2016) **26**(9):1007-20. Epub 2016/08/31. doi: 10.1038/cr.2016.100. PubMed PMID: 27573174; PubMed Central PMCID: PMCPMC5034106.

427. Cai Z, Jitkaew S, Zhao J, Chiang H-C, Choksi S, Liu J, et al. Plasma membrane translocation of trimerized MLKL protein is required for TNF-induced necroptosis. *Nature cell biology* (2014) **16**(1):55-65.

428. Festjens N, Vanden Berghe T, Vandenabeele P. Necrosis, a well-orchestrated form of cell demise: signalling cascades, important mediators and concomitant immune response. *Biochim Biophys Acta* (2006) **1757**(9-10):1371-87. Epub 2006/09/05. doi: 10.1016/j.bbabio.2006.06.014. PubMed PMID: 16950166.

429. Hitomi J, Christofferson DE, Ng A, Yao J, Degterev A, Xavier RJ, et al. Identification of a molecular signaling network that regulates a cellular necrotic cell death pathway. *Cell* (2008) **135**(7):1311-23. Epub 2008/12/27. doi: 10.1016/j.cell.2008.10.044. PubMed PMID: 19109899; PubMed Central PMCID: PMCPMC2621059.

430. Rothman JE. Mechanisms of intracellular protein transport. *Nature* (1994) **372**(6501):55-63. Epub 1994/11/03. doi: 10.1038/372055a0. PubMed PMID: 7969419.

431. Auron PE, Webb AC, Rosenwasser LJ, Mucci SF, Rich A, Wolff SM, et al. Nucleotide sequence of human monocyte interleukin 1 precursor cDNA. *Proceedings of the National Academy of Sciences of the United States of America* (1984) **81**(24):7907-11. Epub 1984/12/01. PubMed PMID: 6083565; PubMed Central PMCID: PMCPMC392262.

432. Rubartelli A, Cozzolino F, Talio M, Sitia R. A novel secretory pathway for interleukin-1 beta, a protein lacking a signal sequence. *EMBO J* (1990) **9**(5):1503-10. Epub 1990/05/01. PubMed PMID: 2328723; PubMed Central PMCID: PMCPMC551842.

433. Martin-Sanchez F, Diamond C, Zeitler M, Gomez AI, Baroja-Mazo A, Bagnall J, et al. Inflammasome-dependent IL-1beta release depends upon membrane permeabilisation. *Cell Death Differ* (2016) **23**(7):1219-31. Epub 2016/02/13. doi: 10.1038/cdd.2015.176. PubMed PMID: 26868913; PubMed Central PMCID: PMCPMC4946890.

434. Nickel W, Rabouille C. Mechanisms of regulated unconventional protein secretion. *Nat Rev Mol Cell Biol* (2009) **10**(2):148-55. Epub 2009/01/06. doi: 10.1038/nrm2617. PubMed PMID: 19122676.

435. Andrei C, Dazzi C, Lotti L, Torrisi MR, Chimini G, Rubartelli A. The secretory route of the leaderless protein interleukin 1β involves exocytosis of endolysosome-related vesicles. *Molecular biology of the cell* (1999) **10**(5):1463-75.

436. MacKenzie A, Wilson HL, Kiss-Toth E, Dower SK, North RA, Surprenant A. Rapid secretion of interleukin-1β by microvesicle shedding. *Immunity* (2001) **15**(5):825-35.

437. Qu Y, Franchi L, Nunez G, Dubyak GR. Nonclassical IL-1β secretion stimulated by P2X7 receptors is dependent on inflammasome activation and correlated with exosome release in murine macrophages. *The Journal of Immunology* (2007) **179**(3):1913-25.

438. Lopez-Castejon G, Brough D. Understanding the mechanism of IL-1β secretion. *Cytokine & growth factor reviews* (2011) **22**(4):189-95.

439. Monteleone M, Stow JL, Schroder K. Mechanisms of unconventional secretion of IL-1 family cytokines. *Cytokine* (2015) **74**(2):213-8. Epub 2015/04/30. doi: 10.1016/j.cyto.2015.03.022. PubMed PMID: 25922276.

440. Gaidt MM, Ebert TS, Chauhan D, Schmidt T, Schmid-Burgk JL, Rapino F, et al. Human Monocytes Engage an Alternative Inflammasome Pathway. *Immunity* (2016) **44**(4):833-46. Epub 2016/04/03. doi: 10.1016/j.immuni.2016.01.012. PubMed PMID: 27037191.

441. Chen KW, Gross CJ, Sotomayor FV, Stacey KJ, Tschopp J, Sweet MJ, et al. The neutrophil NLRC4 inflammasome selectively promotes IL-1beta maturation without pyroptosis during acute Salmonella challenge. *Cell Rep* (2014) **8**(2):570-82. Epub 2014/07/22. doi: 10.1016/j.celrep.2014.06.028. PubMed PMID: 25043180.

442. Zanoni I, Tan Y, Di Gioia M, Broggi A, Ruan J, Shi J, et al. An endogenous caspase-11 ligand elicits interleukin-1 release from living dendritic cells. *Science (New York, NY)* (2016) **352**(6290):1232-6. Epub 2016/04/23. doi: 10.1126/science.aaf3036. PubMed PMID: 27103670; PubMed Central PMCID: PMCPMC5111085.

443. Evavold CL, Ruan J, Tan Y, Xia S, Wu H, Kagan JC. The Pore-Forming Protein Gasdermin D Regulates Interleukin-1 Secretion from Living Macrophages. *Immunity* (2018) **48**(1):35-44 e6. Epub 2017/12/03. doi: 10.1016/j.immuni.2017.11.013. PubMed PMID: 29195811; PubMed Central PMCID: PMCPMC5773350.

444. Wang S, Miura M, Jung Y-k, Zhu H, Gagliardini V, Shi L, et al. Identification and characterization of Ich-3, a member of the interleukin-1β converting enzyme (ICE)/Ced-3 family and an upstream regulator of ICE. *Journal of Biological Chemistry* (1996) **271**(34):20580-7.

445. Abreu MT, Arnold ET, Thomas LS, Gonsky R, Zhou YH, Hu B, et al. TLR4 and MD-2 expression is regulated by immune-mediated signals in human intestinal epithelial cells. *Journal of Biological Chemistry* (2002) **277**(23):20431-7. doi: 10.1074/jbc.M110333200. PubMed PMID: WOS:000176204500043.

446. Nagata S, Tanaka M. Programmed cell death and the immune system. *Nat Rev Immunol* (2017) **17**(5):333-40. Epub 2017/02/07. doi: 10.1038/nri.2016.153. PubMed PMID: 28163302.

447. Schauer DB, Falkow S. The eae gene of Citrobacter freundii biotype 4280 is necessary for colonization in transmissible murine colonic hyperplasia. *Infect Immun* (1993) **61**(11):4654-61. Epub 1993/11/01. PubMed PMID: 8406863; PubMed Central PMCID: PMCPMC281217.

448. Collins JW, Keeney KM, Crepin VF, Rathinam VA, Fitzgerald KA, Finlay BB, et al. Citrobacter rodentium: infection, inflammation and the microbiota. *Nat Rev Microbiol* (2014) **12**(9):612-23. Epub 2014/08/05. doi: 10.1038/nrmicro3315. PubMed PMID: 25088150.

449. Schauer DB, Falkow S. Attaching and effacing locus of a Citrobacter freundii biotype that causes transmissible murine colonic hyperplasia. *Infect Immun* (1993) **61**(6):2486-92. Epub 1993/06/01. PubMed PMID: 8500884; PubMed Central PMCID: PMCPMC280873.

450. Deng W, Vallance BA, Li Y, Puente JL, Finlay BB. Citrobacter rodentium translocated intimin receptor (Tir) is an essential virulence factor needed for actin condensation, intestinal colonization and colonic hyperplasia in mice. *Molecular Microbiology* (2003) **48**(1):95-115. doi: 10.1046/j.1365-2958.2003.03429.x. PubMed PMID: WOS:000181802600009.

451. Deng W, Puente JL, Gruenheid S, Li Y, Vallance BA, Vazquez A, et al. Dissecting virulence: systematic and functional analyses of a pathogenicity island. *Proceedings of the National Academy of Sciences of the United States of America* (2004) **101**(10):3597-602. Epub 2004/02/28. doi: 10.1073/pnas.0400326101. PubMed PMID: 14988506; PubMed Central PMCID: PMCPMC373508.

452. Garmendia J, Frankel G, Crepin VF. Enteropathogenic and enterohemorrhagic Escherichia coli infections: translocation, translocation, translocation. *Infect Immun* (2005) **73**(5):2573-85. Epub 2005/04/23. doi: 10.1128/IAI.73.5.2573-2585.2005. PubMed PMID: 15845459; PubMed Central PMCID: PMCPMC1087358.

453. Bhinder G, Sham HP, Chan JM, Morampudi V, Jacobson K, Vallance BA. The Citrobacter rodentium mouse model: studying pathogen and host contributions to infectious colitis. *J Vis Exp* (2013) (72):e50222. Epub 2013/03/07. doi: 10.3791/50222. PubMed PMID: 23462619; PubMed Central PMCID: PMCPMC3605715.

454. Chandrakesan P, Roy B, Jakkula LU, Ahmed I, Ramamoorthy P, Tawfik O, et al. Utility of a bacterial infection model to study epithelial-mesenchymal transition, mesenchymal-epithelial transition or tumorigenesis. *Oncogene* (2014) **33**(20):2639-54. Epub 2013/06/12. doi: 10.1038/onc.2013.210. PubMed PMID: 23752178; PubMed Central PMCID: PMCPMC3883801.

455. Higgins LM, Frankel G, Douce G, Dougan G, MacDonald TT. Citrobacter rodentium infection in mice elicits a mucosal Th1 cytokine response and lesions similar to those in murine inflammatory bowel disease. *Infect Immun* (1999) **67**(6):3031-9. Epub 1999/05/25. PubMed PMID: 10338516; PubMed Central PMCID: PMCPMC96617.

456. Lupp C, Robertson ML, Wickham ME, Sekirov I, Champion OL, Gaynor EC, et al. Host-mediated inflammation disrupts the intestinal microbiota and promotes the overgrowth of Enterobacteriaceae. *Cell Host Microbe* (2007) **2**(3):204. Epub 2007/11/23. PubMed PMID: 18030708.

457. Hoffmann C, Hill DA, Minkah N, Kirn T, Troy A, Artis D, et al. Community-wide response of the gut microbiota to enteropathogenic Citrobacter rodentium infection revealed by deep sequencing. *Infect Immun* (2009) **77**(10):4668-78. Epub 2009/07/29. doi: 10.1128/IAI.00493-09. PubMed PMID: 19635824; PubMed Central PMCID: PMCPMC2747949.

458. Luperchio SA, Schauer DB. Molecular pathogenesis of Citrobacter rodentium and transmissible murine colonic hyperplasia. *Microbes Infect* (2001) **3**(4):333-40. Epub 2001/05/04. PubMed PMID: 11334751.

459. Crepin VF, Collins JW, Habibzay M, Frankel G. Citrobacter rodentium mouse model of bacterial infection. *Nat Protoc* (2016) **11**(10):1851-76. Epub 2016/09/09. doi: 10.1038/nprot.2016.100. PubMed PMID: 27606775.

460. Mundy R, MacDonald TT, Dougan G, Frankel G, Wiles S. Citrobacter rodentium of mice and man. *Cell Microbiol* (2005) **7**(12):1697-706. Epub 2005/11/29. doi: 10.1111/j.1462-5822.2005.00625.x. PubMed PMID: 16309456.

461. Borenshtein D, McBee ME, Schauer DB. Utility of the Citrobacter rodentium infection model in laboratory mice. *Curr Opin Gastroenterol* (2008) **24**(1):32-7. Epub 2007/11/29. doi: 10.1097/MOG.0b013e3282f2b0fb. PubMed PMID: 18043230.

462. Collins JW, Meganck JA, Kuo C, Francis KP, Frankel G. 4D multimodality imaging of Citrobacter rodentium infections in mice. *J Vis Exp* (2013) (78). Epub 2013/08/28. doi: 10.3791/50450. PubMed PMID: 23979310; PubMed Central PMCID: PMCPMC3855914.

463. Wiles S, Clare S, Harker J, Huett A, Young D, Dougan G, et al. Organ specificity, colonization and clearance dynamics in vivo following oral challenges with the murine pathogen Citrobacter rodentium. *Cell Microbiol* (2004) **6**(10):963-72. Epub 2004/09/02. doi: 10.1111/j.1462-5822.2004.00414.x. PubMed PMID: 15339271.

464. Wiles S, Pickard KM, Peng K, MacDonald TT, Frankel G. In vivo bioluminescence imaging of the murine pathogen Citrobacter rodentium. *Infect Immun* (2006) **74**(9):5391-6. Epub 2006/08/24. doi: 10.1128/IAI.00848-06. PubMed PMID: 16926434; PubMed Central PMCID: PMCPMC1594854.

465. Ale A, Crepin VF, Collins JW, Constantinou N, Habibzay M, Babtie AC, et al. Model of Host-Pathogen Interaction Dynamics Links In Vivo Optical Imaging and Immune Responses. *Infect Immun* (2017) **85**(1). Epub 2016/11/09. doi: 10.1128/IAI.00606-16. PubMed PMID: 27821583; PubMed Central PMCID: PMCPMC5203651.

466. Wiles S, Dougan G, Frankel G. Emergence of a 'hyperinfectious' bacterial state after passage of Citrobacter rodentium through the host gastrointestinal tract. *Cell Microbiol* (2005) **7**(8):1163-72. Epub 2005/07/13. doi: 10.1111/j.1462-5822.2005.00544.x. PubMed PMID: 16008583.

467. Bishop AL, Wiles S, Dougan G, Frankel G. Cell attachment properties and infectivity of host-adapted and environmentally adapted Citrobacter rodentium. *Microbes Infect* (2007) **9**(11):1316-24. Epub 2007/09/25. doi: 10.1016/j.micinf.2007.06.006. PubMed PMID: 17890132.

468. Kamada N, Kim YG, Sham HP, Vallance BA, Puente JL, Martens EC, et al. Regulated virulence controls the ability of a pathogen to compete with the gut microbiota. *Science (New York, NY)* (2012) **336**(6086):1325-9. Epub 2012/05/15. doi: 10.1126/science.1222195. PubMed PMID: 22582016; PubMed Central PMCID: PMCPMC3439148.

469. Silberger DJ, Zindl CL, Weaver CT. Citrobacter rodentium: a model enteropathogen for understanding the interplay of innate and adaptive components of type 3 immunity. *Mucosal Immunol* (2017) **10**(5):1108-17. Epub 2017/06/15. doi: 10.1038/mi.2017.47. PubMed PMID: 28612839.

470. Lebeis SL, Bommarius B, Parkos CA, Sherman MA, Kalman D. TLR Signaling Mediated by MyD88 Is Required for a Protective Innate Immune Response by Neutrophils to Citrobacter rodentium. *The Journal of Immunology* (2007) **179**(1):566-77. doi: 10.4049/jimmunol.179.1.566. PubMed PMID: WOS:000247497600067.

471. Gibson DL, Ma C, Bergstrom KS, Huang JT, Man C, Vallance BA. MyD88 signalling plays a critical role in host defence by controlling pathogen burden and promoting epithelial cell homeostasis during Citrobacter rodentium-induced colitis. *Cell Microbiol* (2008) **10**(3):618-31. Epub 2007/11/06. doi: 10.1111/j.1462-5822.2007.01071.x. PubMed PMID: 17979981.

472. Bergstrom KS, Sham HP, Zarepour M, Vallance BA. Innate host responses to enteric bacterial pathogens: a balancing act between resistance and tolerance. *Cell Microbiol* (2012) **14**(4):475-84. Epub 2012/01/12. doi: 10.1111/j.1462-5822.2012.01750.x. PubMed PMID: 22233392.

473. Gibson DL, Ma C, Rosenberger CM, Bergstrom KS, Valdez Y, Huang JT, et al. Toll-like receptor 2 plays a critical role in maintaining mucosal integrity during Citrobacter rodentium-induced colitis. *Cell Microbiol* (2008) **10**(2):388-403. Epub 2007/10/04. doi: 10.1111/j.1462-5822.2007.01052.x. PubMed PMID: 17910742.

474. Gibson DL, Montero M, Ropeleski MJ, Bergstrom KS, Ma C, Ghosh S, et al. Interleukin-11 reduces TLR4-induced colitis in TLR2-deficient mice and restores intestinal STAT3 signaling. *Gastroenterology* (2010) **139**(4):1277-88. Epub 2010/07/06. doi: 10.1053/j.gastro.2010.06.057. PubMed PMID: 20600022.

475. Khan MA, Ma C, Knodler LA, Valdez Y, Rosenberger CM, Deng W, et al. Toll-Like Receptor 4 Contributes to Colitis Development but Not to Host Defense during Citrobacter rodentium Infection in Mice. *Infection and Immunity* (2006) **74**(5):2522-36.

476. Mangan PR, Harrington LE, O'Quinn DB, Helms WS, Bullard DC, Elson CO, et al. Transforming growth factor-beta induces development of the T(H)17 lineage. *Nature* (2006) **441**(7090):231-4. Epub 2006/05/02. doi: 10.1038/nature04754. PubMed PMID: 16648837.

477. O'Quinn DB, Palmer MT, Lee YK, Weaver CT. Emergence of the Th17 pathway and its role in host defense. *Advances in immunology* (2008) **99**:115-63. Epub 2009/01/02. doi: 10.1016/S0065-2776(08)00605-6. PubMed PMID: 19117534.

478. Geddes K, Rubino SJ, Magalhaes JG, Streutker C, Le Bourhis L, Cho JH, et al. Identification of an innate T helper type 17 response to intestinal bacterial pathogens. *Nat Med* (2011) **17**(7):837-44. Epub 2011/06/15. doi: 10.1038/nm.2391. PubMed PMID: 21666695.

479. Liang SC, Tan XY, Luxenberg DP, Karim R, Dunussi-Joannopoulos K, Collins M, et al. Interleukin (IL)-22 and IL-17 are coexpressed by Th17 cells and cooperatively enhance expression of antimicrobial peptides. *J Exp Med*

(2006) **203**(10):2271-9. Epub 2006/09/20. doi: 10.1084/jem.20061308. PubMed PMID: 16982811; PubMed Central PMCID: PMCPMC2118116.

480. Zheng Y, Valdez PA, Danilenko DM, Hu Y, Sa SM, Gong Q, et al. Interleukin-22 mediates early host defense against attaching and effacing bacterial pathogens. *Nat Med* (2008) **14**(3):282-9. Epub 2008/02/12. doi: 10.1038/nm1720. PubMed PMID: 18264109.

481. Simmons CP, Clare S, Ghaem-Maghami M, Uren TK, Rankin J, Huett A, et al. Central role for B lymphocytes and CD4+ T cells in immunity to infection by the attaching and effacing pathogen Citrobacter rodentium. *Infect Immun* (2003) **71**(9):5077-86. Epub 2003/08/23. PubMed PMID: 12933850; PubMed Central PMCID: PMCPMC187366.

482. Vallance BA, Deng W, Knodler LA, Finlay BB. Mice lacking T and B lymphocytes develop transient colitis and crypt hyperplasia yet suffer impaired bacterial clearance during Citrobacter rodentium infection. *Infect Immun* (2002) **70**(4):2070-81. Epub 2002/03/16. PubMed PMID: 11895973; PubMed Central PMCID: PMCPMC127821.

483. Maaser C, Housley MP, Iimura M, Smith JR, Vallance BA, Finlay BB, et al. Clearance of Citrobacter rodentium requires B cells but not secretory immunoglobulin A (IgA) or IgM antibodies. *Infect Immun* (2004) **72**(6):3315-24. Epub 2004/05/25. doi: 10.1128/IAI.72.6.3315-3324.2004. PubMed PMID: 15155635; PubMed Central PMCID: PMCPMC415672.

484. Clare S, John V, Walker AW, Hill JL, Abreu-Goodger C, Hale C, et al. Enhanced susceptibility to Citrobacter rodentium infection in microRNA-155-deficient mice. *Infect Immun* (2013) **81**(3):723-32. Epub 2012/12/25. doi: 10.1128/IAI.00969-12. PubMed PMID: 23264052; PubMed Central PMCID: PMCPMC3584869.

485. Allen IC, TeKippe EM, Woodford RM, Uronis JM, Holl EK, Rogers AB, et al. The NLRP3 inflammasome functions as a negative regulator of tumorigenesis during colitis-associated cancer. *J Exp Med* (2010) **207**(5):1045-56. Epub 2010/04/14. doi: 10.1084/jem.20100050. PubMed PMID: 20385749; PubMed Central PMCID: PMCPMC2867287.

486. Bauer C, Duewell P, Mayer C, Lehr HA, Fitzgerald KA, Dauer M, et al. Colitis induced in mice with dextran sulfate sodium (DSS) is mediated by the NLRP3 inflammasome. *Gut* (2010) **59**(9):1192-9. Epub 2010/05/06. doi: 10.1136/gut.2009.197822. PubMed PMID: 20442201.

487. Chen L, Wilson JE, Koenigsknecht MJ, Chou WC, Montgomery SA, Truax AD, et al. NLRP12 attenuates colon inflammation by maintaining colonic microbial diversity and promoting protective commensal bacterial growth. *Nat Immunol* (2017) **18**(5):541-51. Epub 2017/03/14. doi: 10.1038/ni.3690. PubMed PMID: 28288099; PubMed Central PMCID: PMCPMC5395345.

488. Zaki MH, Vogel P, Malireddi RK, Body-Malapel M, Anand PK, Bertin J, et al. The NOD-like receptor NLRP12 attenuates colon inflammation and tumorigenesis. *Cancer Cell* (2011) **20**(5):649-60. Epub 2011/11/19. doi: 10.1016/j.ccr.2011.10.022. PubMed PMID: 22094258; PubMed Central PMCID: PMCPMC3761879.

489. Allen IC, Wilson JE, Schneider M, Lich JD, Roberts RA, Arthur JC, et al. NLRP12 suppresses colon inflammation and tumorigenesis through the negative regulation of noncanonical NF-kappaB signaling. *Immunity* (2012) **36**(5):742-54. Epub 2012/04/17. doi: 10.1016/j.immuni.2012.03.012. PubMed PMID: 22503542; PubMed Central PMCID: PMCPMC3658309.

490. Hurley D, McCusker MP, Fanning S, Martins M. Salmonella-host interactions - modulation of the host innate immune system. *Frontiers in immunology* (2014) **5**:481. Epub 2014/10/24. doi: 10.3389/fimmu.2014.00481. PubMed PMID: 25339955; PubMed Central PMCID: PMCPMC4188169.

491. Boyle EC, Bishop JL, Grassl GA, Finlay BB. Salmonella: from pathogenesis to therapeutics. *J Bacteriol* (2007) **189**(5):1489-95. Epub 2006/12/26. doi: 10.1128/JB.01730-06. PubMed PMID: 17189373; PubMed Central PMCID: PMCPMC1855715.

492. Frost AJ, Bland AP, Wallis TS. The early dynamic response of the calf ileal epithelium to Salmonella typhimurium. *Vet Pathol* (1997) **34**(5):369-86. Epub 1997/11/05. doi: 10.1177/030098589703400501. PubMed PMID: 9381648.

493. Watson KG, Holden DW. Dynamics of growth and dissemination of Salmonella in vivo. *Cell Microbiol* (2010) **12**(10):1389-97. Epub 2010/08/25. doi: 10.1111/j.1462-5822.2010.01511.x. PubMed PMID: 20731667.

494. Niess JH, Brand S, Gu X, Landsman L, Jung S, McCormick BA, et al. CX3CR1-mediated dendritic cell access to the intestinal lumen and bacterial clearance. *Science (New York, NY)* (2005) **307**(5707):254-8. Epub 2005/01/18. doi: 10.1126/science.1102901. PubMed PMID: 15653504.

495. Saini S, Slauch JM, Aldridge PD, Rao CV. Role of cross talk in regulating the dynamic expression of the flagellar Salmonella pathogenicity island 1 and type 1 fimbrial genes. *J Bacteriol* (2010) **192**(21):5767-77. Epub 2010/09/14. doi: 10.1128/JB.00624-10. PubMed PMID: 20833811; PubMed Central PMCID: PMCPMC2953706.

496. Wagner C, Barlag B, Gerlach RG, Deiwick J, Hensel M. The Salmonella enterica giant adhesin SiiE binds to polarized epithelial cells in a lectin-like manner. *Cell Microbiol* (2014) **16**(6):962-75. Epub 2013/12/19. doi: 10.1111/cmi.12253. PubMed PMID: 24345213.

497. dos Reis RS, Horn F. Enteropathogenic Escherichia coli, Samonella, Shigella and Yersinia: cellular aspects of host-bacteria interactions in enteric diseases. *Gut pathogens* (2010) **2**(1):8.

498. Zhou D, Galán J. Salmonella entry into host cells: the work in concert of type III secreted effector proteins. *Microbes and Infection* (2001) **3**(14-15):1293-8. doi: 10.1016/s1286-4579(01)01489-7. PubMed PMID: WOS:000173168500013.

499. Kaiser P, Hardt WD. Salmonella typhimurium diarrhea: switching the mucosal epithelium from homeostasis to defense. *Curr Opin Immunol* (2011) **23**(4):456-63. Epub 2011/07/06. doi: 10.1016/j.coi.2011.06.004. PubMed PMID: 21726991.

500. Ly KT, Casanova JE. Mechanisms of Salmonella entry into host cells. *Cell Microbiol* (2007) **9**(9):2103-11. Epub 2007/06/27. doi: 10.1111/j.1462-5822.2007.00992.x. PubMed PMID: 17593246.

501. Figueira R, Holden DW. Functions of the Salmonella pathogenicity island 2 (SPI-2) type III secretion system effectors. *Microbiology* (2012) **158**(Pt 5):1147-61. Epub 2012/03/17. doi: 10.1099/mic.0.058115-0. PubMed PMID: 22422755.

502. Friedrich N, Hagedorn M, Soldati-Favre D, Soldati T. Prison break: pathogens' strategies to egress from host cells. *Microbiol Mol Biol Rev* (2012) **76**(4):707-20. Epub 2012/12/04. doi: 10.1128/MMBR.00024-12. PubMed PMID: 23204363; PubMed Central PMCID: PMCPMC3510522.

503. Guiney DG, Fierer J. The Role of the spv Genes in Salmonella Pathogenesis. *Front Microbiol* (2011) **2**:129. Epub 2011/07/01. doi: 10.3389/fmicb.2011.00129. PubMed PMID: 21716657; PubMed Central PMCID: PMCPMC3117207.

504. Forbester JL, Goulding D, Vallier L, Hannan N, Hale C, Pickard D, et al. Interaction of Salmonella enterica Serovar Typhimurium with Intestinal Organoids Derived from Human Induced Pluripotent Stem Cells. *Infect Immun* (2015) **83**(7):2926-34. Epub 2015/05/13. doi: 10.1128/IAI.00161-15. PubMed PMID: 25964470; PubMed Central PMCID: PMCPMC4468523.

505. Sato T, Stange DE, Ferrante M, Vries RG, Van Es JH, Van den Brink S, et al. Long-term expansion of epithelial organoids from human colon, adenoma, adenocarcinoma, and Barrett's epithelium. *Gastroenterology* (2011) **141**(5):1762-72. Epub 2011/09/06. doi: 10.1053/j.gastro.2011.07.050. PubMed PMID: 21889923.

506. Yui S, Nakamura T, Sato T, Nemoto Y, Mizutani T, Zheng X, et al. Functional engraftment of colon epithelium expanded in vitro from a single adult Lgr5(+) stem cell. *Nat Med* (2012) **18**(4):618-23. Epub 2012/03/13. doi: 10.1038/nm.2695. PubMed PMID: 22406745.

507. Spence JR, Mayhew CN, Rankin SA, Kuhar MF, Vallance JE, Tolle K, et al. Directed differentiation of human pluripotent stem cells into intestinal tissue in vitro. *Nature* (2011) **470**(7332):105-9. Epub 2010/12/15. doi: 10.1038/nature09691. PubMed PMID: 21151107; PubMed Central PMCID: PMCPMC3033971.

508. Sato T, Clevers H. SnapShot: Growing Organoids from Stem Cells. *Cell* (2015) **161**(7):1700- e1. Epub 2015/06/20. doi: 10.1016/j.cell.2015.06.028. PubMed PMID: 26091044.

509. Barker N, Huch M, Kujala P, van de Wetering M, Snippert HJ, van Es JH, et al. Lgr5(+ve) stem cells drive self-renewal in the stomach and build long-lived gastric units in vitro. *Cell Stem Cell* (2010) **6**(1):25-36. Epub 2010/01/21. doi: 10.1016/j.stem.2009.11.013. PubMed PMID: 20085740.

510. McCracken KW, Cata EM, Crawford CM, Sinagoga KL, Schumacher M, Rockich BE, et al. Modelling human development and disease in pluripotent stem-cell-derived gastric organoids. *Nature* (2014) **516**(7531):400-4. Epub 2014/11/05. doi: 10.1038/nature13863. PubMed PMID: 25363776; PubMed Central PMCID: PMCPMC4270898.

511. Schwank G, Koo BK, Sasselli V, Dekkers JF, Heo I, Demircan T, et al. Functional repair of CFTR by CRISPR/Cas9 in intestinal stem cell organoids of cystic fibrosis patients. *Cell Stem Cell* (2013) **13**(6):653-8. Epub 2013/12/10. doi: 10.1016/j.stem.2013.11.002. PubMed PMID: 24315439.

512. Boj SF, Hwang CI, Baker LA, Chio, II, Engle DD, Corbo V, et al. Organoid models of human and mouse ductal pancreatic cancer. *Cell* (2015) **160**(1-2):324-38. Epub 2015/01/06. doi: 10.1016/j.cell.2014.12.021. PubMed PMID: 25557080; PubMed Central PMCID: PMCPMC4334572.

513. Huch M, Dorrell C, Boj SF, van Es JH, Li VS, van de Wetering M, et al. In vitro expansion of single Lgr5+ liver stem cells induced by Wnt-driven regeneration. *Nature* (2013) **494**(7436):247-50. Epub 2013/01/29. doi: 10.1038/nature11826. PubMed PMID: 23354049; PubMed Central PMCID: PMCPMC3634804.

514. Huch M, Gehart H, van Boxtel R, Hamer K, Blokzijl F, Verstegen MM, et al. Long-term culture of genome-stable bipotent stem cells from adult human liver. *Cell* (2015) **160**(1-2):299-312. Epub 2014/12/24. doi: 10.1016/j.cell.2014.11.050. PubMed PMID: 25533785; PubMed Central PMCID: PMCPMC4313365.

515. Fujii M, Matano M, Nanki K, Sato T. Efficient genetic engineering of human intestinal organoids using electroporation. *Nat Protoc* (2015) **10**(10):1474-85. Epub 2015/09/04. doi: 10.1038/nprot.2015.088. PubMed PMID: 26334867.

516. Dedhia PH, Bertaux-Skeirik N, Zavros Y, Spence JR. Organoid Models of Human Gastrointestinal Development and Disease. *Gastroenterology* (2016) **150**(5):1098-112. Epub 2016/01/18. doi: 10.1053/j.gastro.2015.12.042. PubMed PMID: 26774180; PubMed Central PMCID: PMCPMC4842135.

517. Dutta D, Heo I, Clevers H. Disease Modeling in Stem Cell-Derived 3D Organoid Systems. *Trends Mol Med* (2017) **23**(5):393-410. Epub 2017/03/28. doi: 10.1016/j.molmed.2017.02.007. PubMed PMID: 28341301.

518. Clevers H. Modeling Development and Disease with Organoids. *Cell* (2016) **165**(7):1586-97. Epub 2016/06/18. doi: 10.1016/j.cell.2016.05.082. PubMed PMID: 27315476.

519. Leslie JL, Huang S, Opp JS, Nagy MS, Kobayashi M, Young VB, et al. Persistence and toxin production by Clostridium difficile within human intestinal organoids result in disruption of epithelial paracellular barrier function. *Infect Immun* (2015) **83**(1):138-45. Epub 2014/10/15. doi: 10.1128/IAI.02561-14. PubMed PMID: 25312952; PubMed Central PMCID: PMCPMC4288864.

520. Wilson SS, Tocchi A, Holly MK, Parks WC, Smith JG. A small intestinal organoid model of non-invasive enteric pathogen-epithelial cell interactions. *Mucosal Immunol* (2015) **8**(2):352-61. Epub 2014/08/15. doi: 10.1038/mi.2014.72. PubMed PMID: 25118165; PubMed Central PMCID: PMCPMC4326599.

521. In JG, Foulke-Abel J, Estes MK, Zachos NC, Kovbasnjuk O, Donowitz M. Human mini-guts: new insights into intestinal physiology and host-pathogen interactions. *Nat Rev Gastroenterol Hepatol* (2016) **13**(11):633-42. Epub 2016/10/26. doi: 10.1038/nrgastro.2016.142. PubMed PMID: 27677718; PubMed Central PMCID: PMCPMC5079760.

522. Zhang YG, Wu S, Xia Y, Sun J. Salmonella-infected crypt-derived intestinal organoid culture system for host-bacterial interactions. *Physiol Rep* (2014) **2**(9). Epub 2014/09/13. doi: 10.14814/phy2.12147. PubMed PMID: 25214524; PubMed Central PMCID: PMCPMC4270227.

523. VanDussen KL, Marinshaw JM, Shaikh N, Miyoshi H, Moon C, Tarr PI, et al. Development of an enhanced human gastrointestinal epithelial culture system to facilitate patient-based assays. *Gut* (2015) **64**(6):911-20. Epub 2014/07/11. doi: 10.1136/gutjnl-2013-306651. PubMed PMID: 25007816; PubMed Central PMCID: PMCPMC4305344.

524. Sasaki T, Giltay R, Talts U, Timpl R, Talts JF. Expression and distribution of laminin alpha1 and alpha2 chains in embryonic and adult mouse tissues: an immunochemical approach. *Exp Cell Res* (2002) **275**(2):185-99. Epub 2002/04/24. doi: 10.1006/excr.2002.5499. PubMed PMID: 11969289.

525. Dignass AU, Sturm A. Peptide growth factors in the intestine. *European journal of gastroenterology & hepatology* (2001) **13**(7):763-70. Epub 2001/07/28. PubMed PMID: 11474304.

526. Hardwick JCH, Van Den Brink GR, Bleuming SA, Ballester I, Van Den Brande JMH, Keller JJ, et al. Bone morphogenetic protein 2 is expressed by, and acts upon, mature epithelial cells in the colon. *Gastroenterology* (2004) **126**(1):111-21. doi: 10.1053/j.gastro.2003.10.067. PubMed PMID: WOS:000187803300018.

527. Haramis AP, Begthel H, van den Born M, van Es J, Jonkheer S, Offerhaus GJ, et al. De novo crypt formation and juvenile polyposis on BMP inhibition in mouse intestine. *Science (New York, NY)* (2004) **303**(5664):1684-6. Epub 2004/03/16. doi: 10.1126/science.1093587. PubMed PMID: 15017003.

528. Pinto D, Gregorieff A, Begthel H, Clevers H. Canonical Wnt signals are essential for homeostasis of the intestinal epithelium. *Genes Dev* (2003) **17**(14):1709-13. Epub 2003/07/17. doi: 10.1101/gad.267103. PubMed PMID: 12865297; PubMed Central PMCID: PMCPMC196179.

529. Kuhnert F, Davis CR, Wang HT, Chu P, Lee M, Yuan J, et al. Essential requirement for Wnt signaling in proliferation of adult small intestine and colon revealed by adenoviral expression of Dickkopf-1. *Proceedings of the National Academy of Sciences of the United States of America* (2004) **101**(1):266-71. Epub 2003/12/30. doi: 10.1073/pnas.2536800100. PubMed PMID: 14695885; PubMed Central PMCID: PMCPMC314174.

530. Kim KA, Kakitani M, Zhao J, Oshima T, Tang T, Binnerts M, et al. Mitogenic influence of human R-spondin1 on the intestinal epithelium. *Science (New York, NY)* (2005) **309**(5738):1256-9. Epub 2005/08/20. doi: 10.1126/science.1112521. PubMed PMID: 16109882.

531. Watanabe K, Ueno M, Kamiya D, Nishiyama A, Matsumura M, Wataya T, et al. A ROCK inhibitor permits survival of dissociated human embryonic stem cells. *Nat Biotechnol* (2007) **25**(6):681-6. Epub 2007/05/29. doi: 10.1038/nbt1310. PubMed PMID: 17529971.

532. In J, Foulke-Abel J, Zachos NC, Hansen AM, Kaper JB, Bernstein HD, et al. Enterohemorrhagic Escherichia coli reduce mucus and intermicrovillar bridges in human stem cell-derived colonoids. *Cellular and molecular gastroenterology and hepatology* (2016) **2**(1):48-62 e3. Epub 2016/02/09. doi: 10.1016/j.jcmgh.2015.10.001. PubMed PMID: 26855967; PubMed Central PMCID: PMCPMC4740923.

533. Ettayebi K, Crawford SE, Murakami K, Broughman JR, Karandikar U, Tenge VR, et al. Replication of human noroviruses in stem cell-derived human enteroids. *Science (New York, NY)* (2016) **353**(6306):1387-93. Epub 2016/08/27. doi: 10.1126/science.aaf5211. PubMed PMID: 27562956; PubMed Central PMCID: PMCPMC5305121.

534. Yin Y, Bijvelds M, Dang W, Xu L, van der Eijk AA, Knipping K, et al. Modeling rotavirus infection and antiviral therapy using primary intestinal organoids. *Antiviral Res* (2015) **123**:120-31. Epub 2015/09/27. doi: 10.1016/j.antiviral.2015.09.010. PubMed PMID: 26408355.

535. Finkbeiner SR, Zeng XL, Utama B, Atmar RL, Shroyer NF, Estes MK. Stem cell-derived human intestinal organoids as an infection model for rotaviruses. *mBio* (2012) **3**(4):e00159-12. Epub 2012/07/05. doi: 10.1128/mBio.00159-12. PubMed PMID: 22761392; PubMed Central PMCID: PMCPMC3398537.

536. Siegmund B. Interleukin-18 in intestinal inflammation: friend and foe? *Immunity* (2010) **32**(3):300-2. Epub 2010/03/30. doi: 10.1016/j.immuni.2010.03.010. PubMed PMID: 20346770.

537. Yamamoto M, Yaginuma K, Tsutsui H, Sagara J, Guan X, Seki E, et al. ASC is essential for LPS-induced activation of procaspase-1 independently of TLR-associated signal adaptor molecules. *Genes Cells* (2004) **9**(11):1055-67. Epub 2004/10/28. doi: 10.1111/j.1365-2443.2004.00789.x. PubMed PMID: 15507117.

538. Mariathasan S, Weiss DS, Newton K, McBride J, O'Rourke K, Roose-Girma M, et al. Cryopyrin activates the inflammasome in response to toxins and ATP. *Nature* (2006) **440**(7081):228-32. Epub 2006/01/13. doi: 10.1038/nature04515. PubMed PMID: 16407890.

539. Hwang S, Maloney NS, Bruinsma MW, Goel G, Duan E, Zhang L, et al. Nondegradative role of Atg5-Atg12/ Atg16L1 autophagy protein complex in antiviral activity of interferon gamma. *Cell Host Microbe* (2012) **11**(4):397-409. Epub 2012/04/24. doi: 10.1016/j.chom.2012.03.002. PubMed PMID: 22520467; PubMed Central PMCID: PMCPMC3348177.

540. Kamada N, Sakamoto K, Seo SU, Zeng MY, Kim YG, Cascalho M, et al. Humoral Immunity in the Gut Selectively Targets Phenotypically Virulent Attaching-and-Effacing Bacteria for Intraluminal Elimination. *Cell Host Microbe* (2015) **17**(5):617-27. Epub 2015/05/06. doi: 10.1016/j.chom.2015.04.001. PubMed PMID: 25936799; PubMed Central PMCID: PMCPMC4433422.

541. Gurung P, Li B, Subbarao Malireddi RK, Lamkanfi M, Geiger TL, Kanneganti TD. Chronic TLR Stimulation Controls NLRP3 Inflammasome Activation through IL-10 Mediated Regulation of NLRP3 Expression and Caspase-8 Activation. *Sci Rep* (2015) **5**:14488. Epub 2015/09/29. doi: 10.1038/srep14488. PubMed PMID: 26412089; PubMed Central PMCID: PMCPMC4585974.

542. Pfaffl MW. Quantification strategies in real-time PCR. *AZ of quantitative PCR* (2004).

543. Fukata M, Arditi M. The role of pattern recognition receptors in intestinal inflammation. *Mucosal Immunol* (2013) **6**(3):451-63. Epub 2013/03/22. doi: 10.1038/mi.2013.13. PubMed PMID: 23515136; PubMed Central PMCID: PMCPMC3730813.

544. Walsh D, McCarthy J, O'Driscoll C, Melgar S. Pattern recognition receptors--molecular orchestrators of inflammation in inflammatory bowel disease. *Cytokine & growth factor reviews* (2013) **24**(2):91-104. Epub 2012/10/30. doi: 10.1016/j.cytogfr.2012.09.003. PubMed PMID: 23102645.

545. Nunes T, de Souza HS. Inflammasome in intestinal inflammation and cancer. *Mediators Inflamm* (2013) **2013**:654963. Epub 2013/04/23. doi: 10.1155/2013/654963. PubMed PMID: 23606794; PubMed Central PMCID: PMCPMC3625567.

546. Groß O, Yazdi AS, Thomas CJ, Masin M, Heinz LX, Guarda G, et al. Inflammasome activators induce interleukin-1 secretion via distinct pathways with differential requirement for the protease function of caspase-1. *Immunity* (2012) **36**(3):388-400.

547. Di Paolo NC, Shayakhmetov DM. Interleukin 1alpha and the inflammatory process. *Nat Immunol* (2016) **17**(8):906-13. Epub 2016/07/21. doi: 10.1038/ni.3503. PubMed PMID: 27434011; PubMed Central PMCID: PMCPMC5152572.

548. Ouyang W, Rutz S, Crellin NK, Valdez PA, Hymowitz SG. Regulation and functions of the IL-10 family of cytokines in inflammation and disease. *Annual review of immunology* (2011) **29**:71-109. Epub 2010/12/21. doi: 10.1146/annurev-immunol-031210-101312. PubMed PMID: 21166540.

549. Sagulenko V, Thygesen SJ, Sester DP, Idris A, Cridland JA, Vajjhala PR, et al. AIM2 and NLRP3 inflammasomes activate both apoptotic and pyroptotic death pathways via ASC. *Cell Death Differ* (2013) **20**(9):1149-60. Epub 2013/05/07. doi: 10.1038/cdd.2013.37. PubMed PMID: 23645208; PubMed Central PMCID: PMCPMC3741496.

550. Perez-Lopez A, Behnsen J, Nuccio SP, Raffatellu M. Mucosal immunity to pathogenic intestinal bacteria. *Nat Rev Immunol* (2016) **16**(3):135-48. Epub 2016/02/24. doi: 10.1038/nri.2015.17. PubMed PMID: 26898110.

551. Huber S, Gagliani N, Zenewicz LA, Huber FJ, Bosurgi L, Hu B, et al. IL-22BP is regulated by the inflammasome and modulates tumorigenesis in the intestine. *Nature* (2012) **491**(7423):259.

552. Yao X, Zhang C, Xing Y, Xue G, Zhang Q, Pan F, et al. Remodelling of the gut microbiota by hyperactive NLRP3 induces regulatory T cells to maintain homeostasis. *Nat Commun* (2017) **8**(1):1896. Epub 2017/12/03. doi: 10.1038/s41467-017-01917-2. PubMed PMID: 29196621; PubMed Central PMCID: PMCPMC5711854.

553. Ghosh S, Dai C, Brown K, Rajendiran E, Makarenko S, Baker J, et al. Colonic microbiota alters host susceptibility to infectious colitis by modulating inflammation, redox status, and ion transporter gene expression. *Am J Physiol Gastrointest Liver Physiol* (2011) **301**(1):G39-49. Epub 2011/04/02. doi: 10.1152/ajpgi.00509.2010. PubMed PMID: 21454446.

554. Willing BP, Vacharaksa A, Croxen M, Thanachayanont T, Finlay BB. Altering host resistance to infections through microbial transplantation. *PLoS One* (2011) **6**(10):e26988. Epub 2011/11/03. doi: 10.1371/journal.pone.0026988. PubMed PMID: 22046427; PubMed Central PMCID: PMCPMC3203939.

555. Zaki MH, Vogel P, Body-Malapel M, Lamkanfi M, Kanneganti TD. IL-18 production downstream of the Nlrp3 inflammasome confers protection against colorectal tumor formation. *Journal of immunology (Baltimore, Md : 1950)* (2010) **185**(8):4912-20. Epub 2010/09/22. doi: 10.4049/jimmunol.1002046. PubMed PMID: 20855874; PubMed Central PMCID: PMCPMC3104023.

556. Fritz JH, Le Bourhis L, Magalhaes JG, Philpott DJ. Innate immune recognition at the epithelial barrier drives adaptive immunity: APCs take the back seat. *Trends Immunol* (2008) **29**(1):41-9. Epub 2007/12/07. doi: 10.1016/j.it.2007.10.002. PubMed PMID: 18054284.

557. Prabhakara R, Harro JM, Leid JG, Keegan AD, Prior ML, Shirtliff ME. Suppression of the inflammatory immune response prevents the development of chronic biofilm infection due to methicillin-resistant Staphylococcus aureus. *Infect Immun* (2011) **79**(12):5010-8. Epub 2011/09/29. doi: 10.1128/IAI.05571-11. PubMed PMID: 21947772; PubMed Central PMCID: PMCPMC3232664.

558. Joshi A, Pancari G, Cope L, Bowman EP, Cua D, Proctor RA, et al. Immunization with Staphylococcus aureus iron regulated surface determinant B (IsdB) confers protection via Th17/IL17 pathway in a murine sepsis model. *Hum Vaccin Immunother* (2012) **8**(3):336-46. Epub 2012/02/14. doi: 10.4161/hv.18946. PubMed PMID: 22327491; PubMed Central PMCID: PMCPMC3426080.

559. Taylor PR, Roy S, Leal SM, Jr., Sun Y, Howell SJ, Cobb BA, et al. Activation of neutrophils by autocrine IL-17A-IL-17RC interactions during fungal infection is regulated by IL-6, IL-23, RORgammat and dectin-2. *Nat Immunol* (2014) **15**(2):143-51. Epub 2013/12/24. doi: 10.1038/ni.2797. PubMed PMID: 24362892; PubMed Central PMCID: PMCPMC3972892.

560. Kim YG, Kamada N, Shaw MH, Warner N, Chen GY, Franchi L, et al. The Nod2 sensor promotes intestinal pathogen eradication via the chemokine CCL2-dependent recruitment of inflammatory monocytes. *Immunity* (2011)

34(5):769-80. Epub 2011/05/14. doi: 10.1016/j.immuni.2011.04.013. PubMed PMID: 21565531; PubMed Central PMCID: PMCPMC3103637.

561. Jarchum I, Liu M, Shi C, Equinda M, Pamer EG. Critical role for MyD88-mediated neutrophil recruitment during Clostridium difficile colitis. *Infect Immun* (2012) **80**(9):2989-96. Epub 2012/06/13. doi: 10.1128/IAI.00448-12. PubMed PMID: 22689818; PubMed Central PMCID: PMCPMC3418725.

562. Broderick L, De Nardo D, Franklin BS, Hoffman HM, Latz E. The inflammasomes and autoinflammatory syndromes. *Annu Rev Pathol* (2015) **10**:395-424. Epub 2014/11/26. doi: 10.1146/annurev-pathol-012414-040431. PubMed PMID: 25423351.

563. Progatzky F, Sangha NJ, Yoshida N, McBrien M, Cheung J, Shia A, et al. Dietary cholesterol directly induces acute inflammasome-dependent intestinal inflammation. *Nat Commun* (2014) **5**:5864. Epub 2014/12/24. doi: 10.1038/ncomms6864. PubMed PMID: 25536194; PubMed Central PMCID: PMCPMC4284652.

564. Sellin ME, Maslowski KM, Maloy KJ, Hardt WD. Inflammasomes of the intestinal epithelium. *Trends Immunol* (2015) **36**(8):442-50. Epub 2015/07/15. doi: 10.1016/j.it.2015.06.002. PubMed PMID: 26166583.

565. Sato T, Clevers H. Growing self-organizing mini-guts from a single intestinal stem cell: mechanism and applications. *Science (New York, NY)* (2013) **340**(6137):1190-4. Epub 2013/06/08. doi: 10.1126/science.1234852. PubMed PMID: 23744940.

566. Sato T, Vries RG, Snippert HJ, van de Wetering M, Barker N, Stange DE, et al. Single Lgr5 stem cells build crypt villus structures in vitro without a mesenchymal niche. *Nature* (2009) **459**(7244):262-5.

567. Elia PP, Tolentino YF, Bernardazzi C, de Souza HS. The role of innate immunity receptors in the pathogenesis of inflammatory bowel disease. *Mediators Inflamm* (2015) **2015**:936193. Epub 2015/03/31. doi: 10.1155/2015/936193. PubMed PMID: 25821356; PubMed Central PMCID: PMCPMC4364059.

568. Gross O. Measuring the inflammasome. *Methods in molecular biology (Clifton, NJ)* (2012) **844**:199-222. Epub 2012/01/21. doi: 10.1007/978-1-61779-527-5_15. PubMed PMID: 22262445.

569. Qu Y, Misaghi S, Newton K, Maltzman A, Izrael-Tomasevic A, Arnott D, et al. NLRP3 recruitment by NLRC4 during Salmonella infection. *J Exp Med* (2016) **213**(6):877-85. Epub 2016/05/04. doi: 10.1084/jem.20132234. PubMed PMID: 27139490; PubMed Central PMCID: PMCPMC4886354.

570. Stutz A, Horvath GL, Monks BG, Latz E. ASC speck formation as a readout for inflammasome activation. *The Inflammasome: Methods and Protocols* (2013):91-101.

571. Dick MS, Sborgi L, Ruhl S, Hiller S, Broz P. ASC filament formation serves as a signal amplification mechanism for inflammasomes. *Nat Commun* (2016) **7**:11929. Epub 2016/06/23. doi: 10.1038/ncomms11929. PubMed PMID: 27329339; PubMed Central PMCID: PMCPMC4917984.

572. Satoh T, Kambe N, Matsue H. NLRP3 activation induces ASC-dependent programmed necrotic cell death, which leads to neutrophilic inflammation. *Cell Death Dis* (2013) **4**:e644. Epub 2013/05/25. doi: 10.1038/cddis.2013.169. PubMed PMID: 23703389; PubMed Central PMCID: PMCPMC3674376.

573. Yang J, Tauschek M, Hart E, Hartland EL, Robins-Browne RM. Virulence regulation in Citrobacter rodentium: the art of timing. *Microb Biotechnol* (2010) **3**(3):259-68. Epub 2011/01/25. doi: 10.1111/j.1751-7915.2009.00114.x. PubMed PMID: 21255326; PubMed Central PMCID: PMCPMC3815369.

574. Bustamante VH, Villalba MI, Garcia-Angulo VA, Vazquez A, Martinez LC, Jimenez R, et al. PerC and GrlA independently regulate Ler expression in enteropathogenic Escherichia coli. *Mol Microbiol* (2011) **82**(2):398-415. Epub 2011/09/08. doi: 10.1111/j.1365-2958.2011.07819.x. PubMed PMID: 21895790.

575. Crepin VF, Girard F, Schuller S, Phillips AD, Mousnier A, Frankel G. Dissecting the role of the Tir:Nck and Tir:IRTKS/IRSp53 signalling pathways in vivo. *Mol Microbiol* (2010) **75**(2):308-23. Epub 2009/11/06. doi: 10.1111/j.1365-2958.2009.06938.x. PubMed PMID: 19889090; PubMed Central PMCID: PMCPMC2814079.

576. Hu J, Jacinto R, McCall C, Li L. Regulation of IL-1 receptor-associated kinases by lipopolysaccharide. *Journal of immunology (Baltimore, Md : 1950)* (2002) **168**(8):3910-4. Epub 2002/04/09. PubMed PMID: 11937546.

577. Abreu MT, Arnold ET, Thomas LS, Gonsky R, Zhou Y, Hu B, et al. TLR4 and MD-2 expression is regulated by immune-mediated signals in human intestinal epithelial cells. *J Biol Chem* (2002) **277**(23):20431-7. Epub 2002/03/30. doi: 10.1074/jbc.M110333200. PubMed PMID: 11923281.

578. Mullineaux-Sanders C, Collins JW, Ruano-Gallego D, Levy M, Pevsner-Fischer M, Glegola-Madejska IT, et al. Citrobacter rodentium Relies on Commensals for Colonization of the Colonic Mucosa. *Cell Rep* (2017)

21(12):3381-9. Epub 2017/12/21. doi: 10.1016/j.celrep.2017.11.086. PubMed PMID: 29262319; PubMed Central PMCID: PMCPMC5746604.

579. Fang FC, Rimsky S. New insights into transcriptional regulation by H-NS. *Curr Opin Microbiol* (2008) **11**(2):113-20. Epub 2008/04/05. doi: 10.1016/j.mib.2008.02.011. PubMed PMID: 18387844; PubMed Central PMCID: PMCPMC2394665.

580. Lai Y, Rosenshine I, Leong JM, Frankel G. Intimate host attachment: enteropathogenic and enterohaemorrhagic Escherichia coli. *Cell Microbiol* (2013) **15**(11):1796-808. Epub 2013/08/10. doi: 10.1111/cmi.12179. PubMed PMID: 23927593; PubMed Central PMCID: PMCPMC4036124.

581. Celli J, Deng W, Finlay BB. Enteropathogenic Escherichia coli (EPEC) attachment to epithelial cells: exploiting the host cell cytoskeleton from the outside. *Cell Microbiol* (2000) **2**(1):1-9. Epub 2001/02/24. PubMed PMID: 11207558.

582. Vaishnava S, Yamamoto M, Severson KM, Ruhn KA, Yu X, Koren O, et al. The antibacterial lectin RegIIIgamma promotes the spatial segregation of microbiota and host in the intestine. *Science (New York, NY)* (2011) **334**(6053):255-8. Epub 2011/10/15. doi: 10.1126/science.1209791. PubMed PMID: 21998396; PubMed Central PMCID: PMCPMC3321924.

583. Round JL, Mazmanian SK. The gut microbiota shapes intestinal immune responses during health and disease. *Nat Rev Immunol* (2009) **9**(5):313-23. Epub 2009/04/04. doi: 10.1038/nri2515. PubMed PMID: 19343057; PubMed Central PMCID: PMCPMC4095778.

584. Liu J, Qian C, Cao X. Post-Translational Modification Control of Innate Immunity. *Immunity* (2016) **45**(1):15-30. Epub 2016/07/22. doi: 10.1016/j.immuni.2016.06.020. PubMed PMID: 27438764.

585. Diamond CE, Leong KWK, Vacca M, Rivers-Auty J, Brough D, Mortellaro A. Salmonella typhimurium-induced IL-1 release from primary human monocytes requires NLRP3 and can occur in the absence of pyroptosis. *Sci Rep* (2017) **7**(1):6861. Epub 2017/08/02. doi: 10.1038/s41598-017-07081-3. PubMed PMID: 28761045; PubMed Central PMCID: PMCPMC5537352.

586. Chen KW, Bezbradica JS, Gross CJ, Wall AA, Sweet MJ, Stow JL, et al. The murine neutrophil NLRP3 inflammasome is activated by soluble but not particulate or crystalline agonists. *European journal of immunology* (2016) **46**(4):1004-10. Epub 2016/04/12. doi: 10.1002/eji.201545943. PubMed PMID: 27062120.

587. Karmakar M, Katsnelson M, Malak HA, Greene NG, Howell SJ, Hise AG, et al. Neutrophil IL-1β processing induced by pneumolysin is mediated by the NLRP3/ASC inflammasome and caspase-1 activation and is dependent on K+ efflux. *The Journal of Immunology* (2015) **194**(4):1763-75.

588. Cho JS, Guo Y, Ramos RI, Hebroni F, Plaisier SB, Xuan C, et al. Neutrophil-derived IL-1β is sufficient for abscess formation in immunity against Staphylococcus aureus in mice. *PLoS pathogens* (2012) **8**(11):e1003047.

589. Gremel G, Wanders A, Cedernaes J, Fagerberg L, Hallstrom B, Edlund K, et al. The human gastrointestinal tract-specific transcriptome and proteome as defined by RNA sequencing and antibody-based profiling. *J Gastroenterol* (2015) **50**(1):46-57. Epub 2014/05/03. doi: 10.1007/s00535-014-0958-7. PubMed PMID: 24789573.

590. Broz P, Newton K, Lamkanfi M, Mariathasan S, Dixit VM, Monack DM. Redundant roles for inflammasome receptors NLRP3 and NLRC4 in host defense against Salmonella. *J Exp Med* (2010) **207**(8):1745-55. Epub 2010/07/07. doi: 10.1084/jem.20100257. PubMed PMID: 20603313; PubMed Central PMCID: PMCPMC2916133.

591. Rakoff-Nahoum S, Paglino J, Eslami-Varzaneh F, Edberg S, Medzhitov R. Recognition of commensal microflora by toll-like receptors is required for intestinal homeostasis. *Cell* (2004) **118**(2):229-41.

592. Nenci A, Becker C, Wullaert A, Gareus R, van Loo G, Danese S, et al. Epithelial NEMO links innate immunity to chronic intestinal inflammation. *Nature* (2007) **446**(7135):557-61. Epub 2007/03/16. doi: 10.1038/nature05698. PubMed PMID: 17361131.

593. Powrie F, Leach MW, Mauze S, Caddle LB, Coffman RL. Phenotypically distinct subsets of CD4+ T cells induce or protect from chronic intestinal inflammation in C. B-17 scid mice. *Int Immunol* (1993) **5**(11):1461-71. Epub 1993/11/01. PubMed PMID: 7903159.

594. Wilson RK, Shaw RK, Daniell S, Knutton S, Frankel G. Role of EscF, a putative needle complex protein, in the type III protein translocation system of enteropathogenic Escherichia coli. *Cell Microbiol* (2001) **3**(11):753-62. Epub 2001/11/07. PubMed PMID: 11696035.

595. Hoytema van Konijnenburg DP, Reis BS, Pedicord VA, Farache J, Victora GD, Mucida D. Intestinal Epithelial and Intraepithelial T Cell Crosstalk Mediates a Dynamic Response to Infection. *Cell* (2017) **171**(4):783-94

e13. Epub 2017/09/26. doi: 10.1016/j.cell.2017.08.046. PubMed PMID: 28942917; PubMed Central PMCID: PMCPMC5670000.

596. Nozaki K, Mochizuki W, Matsumoto Y, Matsumoto T, Fukuda M, Mizutani T, et al. Co-culture with intestinal epithelial organoids allows efficient expansion and motility analysis of intraepithelial lymphocytes. *J Gastroenterol* (2016) **51**(3):206-13. Epub 2016/01/24. doi: 10.1007/s00535-016-1170-8. PubMed PMID: 26800996; PubMed Central PMCID: PMCPMC4771822.

597. Harrison OJ, Powrie FM. Regulatory T cells and immune tolerance in the intestine. *Cold Spring Harb Perspect Biol* (2013) **5**(7). Epub 2013/07/03. doi: 10.1101/cshperspect.a018341. PubMed PMID: 23818502; PubMed Central PMCID: PMCPMC3685893.

598. Gaidt MM, Hornung V. Pore formation by GSDMD is the effector mechanism of pyroptosis. *EMBO J* (2016) **35**(20):2167-9. Epub 2016/11/01. doi: 10.15252/embj.201695415. PubMed PMID: 27572465; PubMed Central PMCID: PMCPMC5069554.

599. Gringhuis SI, Kaptein TM, Wevers BA, Theelen B, van der Vlist M, Boekhout T, et al. Dectin-1 is an extracellular pathogen sensor for the induction and processing of IL-1beta via a noncanonical caspase-8 inflammasome. *Nat Immunol* (2012) **13**(3):246-54. Epub 2012/01/24. doi: 10.1038/ni.2222. PubMed PMID: 22267217.

600. Kumar Y, Radha V, Swarup G. Interaction with Sug1 enables Ipaf ubiquitination leading to caspase 8 activation and cell death. *Biochem J* (2010) **427**(1):91-104. Epub 2010/01/21. doi: 10.1042/BJ20091349. PubMed PMID: 20085538.

601. Schwank G, Koo B-K, Sasselli V, Dekkers JF, Heo I, Demircan T, et al. Functional repair of CFTR by CRISPR/Cas9 in intestinal stem cell organoids of cystic fibrosis patients. *Cell stem cell* (2013) **13**(6):653-8.

602. Bezbradica JS, Coll RC, Schroder K. Sterile signals generate weaker and delayed macrophage NLRP3 inflammasome responses relative to microbial signals. *Cell Mol Immunol* (2017) **14**(1):118-26. Epub 2016/03/22. doi: 10.1038/cmi.2016.11. PubMed PMID: 26996064; PubMed Central PMCID: PMCPMC5214936.

603. Chudnovskiy A, Mortha A, Kana V, Kennard A, Ramirez JD, Rahman A, et al. Host-Protozoan Interactions Protect from Mucosal Infections through Activation of the Inflammasome. *Cell* (2016) **167**(2):444-56 e14. Epub 2016/10/08. doi: 10.1016/j.cell.2016.08.076. PubMed PMID: 27716507; PubMed Central PMCID: PMCPMC5129837.

604. Wlodarska M, Willing B, Keeney KM, Menendez A, Bergstrom KS, Gill N, et al. Antibiotic treatment alters the colonic mucus layer and predisposes the host to exacerbated Citrobacter rodentium-induced colitis. *Infect Immun* (2011) **79**(4):1536-45. Epub 2011/02/16. doi: 10.1128/IAI.01104-10. PubMed PMID: 21321077; PubMed Central PMCID: PMCPMC3067531.